

Resolving Central Nervous System
Inflammation in Acquired
Immunodeficiency Syndrome:
The Impact of Antiretroviral Therapy on
Macrophage In and Traffic Out of the
Central Nervous System

Zoey Kathryn Wallis

A dissertation
submitted to the Faculty of
the department of Biology
in partial fulfillment
of the requirements for the degree of
Doctor of Philosophy

Boston College
Morrissey College of Arts and Sciences
Graduate School

November 2024

Resolving Central Nervous System Inflammation in Acquired Immunodeficiency Syndrome: The Impact of Antiretroviral Therapy on Macrophage in and Traffic Out of the Central Nervous System

Author: Zoey Kathryn Wallis

Advisor: Kenneth C. Williams, Ph.D.

Abstract

Understanding the persistence of viral reservoirs despite durable antiretroviral therapy (ART) is essential to addressing the challenge of viral clearance and chronic immune activation with human immunodeficiency virus (HIV) and simian immunodeficiency virus (SIV). It had not previously been demonstrated that HIV or SIV-infected macrophage traffic out of the CNS to reseed the periphery, potentially contributing to viral recrudescence. This thesis proposes the central hypothesis that persistent traffic of monocytes and macrophages out of the CNS and subsequent viral reseeding of the periphery plays a key role in viral dissemination, particularly in the context of acquired immunodeficiency syndrome (AIDS), with ART, and following ART interruption.

In Chapter 2, utilizing Superparamagnetic iron oxide nanoparticles (SPION) as a novel *in vivo* method to label CNS macrophages, we demonstrate that under normal conditions, CNS macrophages migrate out to the deep cervical lymph nodes. However, during SIV infection, we observe an accumulation of macrophages within the CNS and a reduction in traffic out to the periphery. Importantly, with SIV-infection, we found that SIV-infected macrophages traffic out to deep cervical lymph nodes. From these, we find that under normal conditions, macrophages traffic out of the CNS. However, during SIV

infection, macrophages are retained within the CNS, contributing to inflammation in the brain, and those that do migrate out are virally infected.

In Chapter 3, we hypothesized that ART restores CNS macrophage traffic and prevents viral dissemination from the CNS reservoir by eliminating the traffic of virally infected macrophage out of the CNS, as seen with AIDS and SIV-induced encephalitis (SIVE). We also hypothesized that following four weeks of ART interruption there would be expansion of the CNS viral reservoir with traffic out of virally infected macrophages to the deep cervical lymph node. Utilizing a rapid AIDS model with CD8 depletion to induce a high incidence of SIVE and intracisternal injection of SPION, we found that SIV-infected macrophages accumulate in the perivascular space, meninges, choroid plexus, and traffic out at a low rate to the deep cervical lymph node, spleen, and even to the dorsal root ganglia (DRG). With ART, we found clearance of virally infected macrophages in the brain perivascular space but not in the meninges or choroid plexus. Importantly following four weeks of ART interruption, the perivascular space remained clear of virus but there was a rebound in the meninges and scattered virally infected macrophages in the choroid plexus. With ART and following a brief ART interruption, there was no traffic of CNS virally infected macrophages out to the deep cervical lymph node, spleen, or DRGs. These data demonstrate that ART effectively clears virus-infected perivascular macrophages and eliminates the traffic of virus-infected macrophages out of the CNS to the deep cervical lymph node and spleen but does not eliminate virally infected macrophages in the meninges or choroid plexus. By using two differently colored SPION injected early and late, we observed an increase in early SPION+ macrophages within and outside the CNS with SIVE, ART, and ART interruption, indicating that SIV-infected perivascular macrophages

establish an early viral reservoir with ongoing seeding in the meninges and choroid plexus throughout infection. These findings are consistent with the retention of CNS macrophages in the presence of inflammation and viral infection, as well as the potential for viral rebound in the CNS from sources such as the blood, meninges, and choroid plexus with ART and following ART interruption.

In Chapter 4, we propose a novel pathway for virus-infected macrophages to traffic out of the CNS via cranial and spinal nerves. Due to the persistence of virally infected macrophages in the meninges with durable ART and continuity of the CNS meninges with peripheral nerves, we hypothesize that virally infected macrophage traffic out of the CNS via cranial and peripheral nerves with AIDS and SIVE, on ART, and following ART interruption. To test this hypothesis, we tracked SPION⁺ macrophages by quantifying them at central (spinal cord and cranial nerves) and peripheral sites (dorsal root ganglia, DRG). Similar to our previous findings in the brain, SIV infection increased the numbers of macrophages in the spinal cord and decreased them in peripheral sites. Staining for viral RNA and GP41 identified virus-infected SPION⁺ macrophages in cranial nerves and DRG, which were significantly reduced but not eliminated by ART. In animals with AIDS, late- and dual-labeled SPION⁺ macrophages decreased, suggesting reduced macrophage trafficking late in infection. ART appeared to restore traffic, as higher numbers of late- and dual-labeled macrophages were observed, though this reversed to levels seen in AIDS/SIVE upon ART interruption. Our findings reveal a previously understudied pathway that allows CNS macrophage viral reservoirs to reseed virus to the periphery, a process that persists despite ART.

In Chapter 5, we performed a literature review to better understand the effects of HIV

infection on aging, as age is a primary risk factor for the development of HIV-associated neurocognitive disorders and HIV-associated sensory neuropathy. With ART extending the lifespan of people living with HIV, they now also experience accelerated aging, leading to earlier onset of age-related conditions like cardiovascular disease and neurocognitive disorders. Evidence suggests this is due to chronic immune activation, co-infections, and possibly ART itself. HIV and aging both alter immune cell populations, increasing inflammatory markers and contributing to "inflamm-aging." While ART slows this acceleration, it cannot prevent aging or related comorbidities.

This thesis explores the role of macrophage traffic from the CNS and its contribution to the spread of the virus to peripheral tissues. To investigate this, we utilized a novel *in vivo* labeling method to track CNS macrophages, identify migration out of the CNS, and evaluate how ART and ART interruption influence the traffic of virally infected macrophages to peripheral tissues. Our findings underscore the role of CNS macrophages in the resolution of inflammation by trafficking out of the CNS, viral rebound from blood-derived sources following ART interruption, and the role of perineural pathways in viral dissemination even with durable ART.

TABLE OF CONTENTS

Table of Contents	vii
List of Figures and Tables	x
Abbreviations.....	xiii
Acknowledgments	xv
1.0 Literature Review	1
1.1 Human Immunodeficiency Virus, Acquired Immunodeficiency Syndrome (AIDS), and Rapid AIDS Simian Model.....	1
A. HIV and AIDS in the ART Era.....	1
B. Rapid AIDS Model	6
1.2 Immune Privilege in the CNS	8
A. CNS Immune Privilege: The Role of Protective Barriers.....	8
i. Blood-Brain Barrier	8
ii. Blood-CSF Barrier.....	9
iii. Blood-Nerve Barrier	10
iv. Meninges of the CNS and PNS	11
B. Macrophages in the CNS	15
i. Microglia.....	15
ii. Perivascular Macrophages.....	16
iii. Meningeal Macrophages	16
iv. Choroid Plexus Macrophages.....	17
C. Other Immune Cells in the CNS.....	19
i. Myeloid-DCs	19
ii. T Cells.....	19
iii. Natural Killer Cells.....	20
iv. MAC387+ Macrophages	20
1.3 CNS as a Viral Reservoir	20
A. Viral Infection of the CNS.....	20
B. Monocytes and Macrophages in the CNS as a Viral Reservoir.....	22
1.4 Fluid Within and Out of the CNS	25
A. Cerebrospinal Fluid within the CNS.....	25
B. Glymphatic System.....	26
C. Traditional View of CSF Drainage Out of the CNS.....	26

D.	Perineural Drainage of CSF	27
E.	Meningeal Lymphatics and CSF Drainage	28
F.	Spinal Drainage of CSF	29
1.5	Immune Cell Entry Into the CNS.....	31
A.	Migration from the Blood and Entry to the CNS.....	31
B.	Increased Monocyte Traffic to the CNS with HIV and SIV.....	32
1.6	Immune Cell Traffic out of the CNS.....	33
A.	Potential Pathways of Monocytes and Macrophages Out of the Brain	34
B.	Potential Pathways of Monocytes and Macrophages Out of the Spinal Cord	37
1.7	Superparamagnetic Iron Oxide Nanoparticles to Track Immune Cell Migration out of the CNS.....	38
A.	Superparamagnetic Iron Oxide Nanoparticles (SPION).....	38
B.	SPION to Label Macrophage <i>in vivo</i>	39
1.8	References.....	41
2.0	Chapter 2.....	62
	Simian Immunodeficiency Virus-Infected Macrophages Traffic Out of the Central Nervous System	
2.1	Author Contributions.....	63
2.2	Abstract	64
2.3	Introduction.....	66
2.4	Results.....	69
2.5	Discussion	72
2.6	Experimental Procedures.....	76
2.7	Tables, Figures, and Figure Legends	80
2.8	References.....	98
2.9	Chapter Overview and Next Steps	103
3.0	Chapter 3.....	104
	Resolving Inflammation: The Impact of Antiretroviral Therapy on Macrophage Traffic In and Out of the CNS	
3.1	Author Contributions.....	105
3.2	Abstract	106
3.3	Introduction.....	108
3.4	Results.....	112
3.5	Discussion	120
3.6	Experimental Procedures.....	128
3.7	Tables, Figures, and Figure Legends	135
3.8	References.....	153
3.9	Chapter Overview and Next Steps	161
4.0	Chapter 4.....	162
	Perineural Pathways Allow Simian Immunodeficiency Virus-Infected Macrophages to Traffic Out of the Central Nervous System	
4.1	Author Contributions.....	163
4.2	Abstract	164

4.3	Introduction.....	165
4.4	Results	169
4.5	Discussion	176
4.6	Experimental Procedures.....	181
4.7	Tables, Figures, and Figure Legends	187
4.8	References.....	209
4.9	Chapter Overview and Next Steps	213
5.0	Chapter 5.....	214
	Monocytes in HIV, SIV Infection and Aging: Implications for Inflammaging and Accelerated Aging	
5.1	Author Contributions	215
5.2	Abstract	216
5.3	Introduction.....	217
5.4	Monocytes and Macrophage in HIV and SIV	220
5.5	Chronic Monocyte/Macrophage Activation, Inflammation, and "Inflammaging".....	224
5.6	Monocytes and Macrophage Traffic to Tissues with HIV, SIV, and Aging.....	227
5.7	Immunosenescence and Aging.....	229
5.8	Myeloid Mitochondria Dysfunction and Contribution to Immunosenescence.....	230
5.9	Accelerated Aging with HIV Infection	232
5.10	Conclusions.....	234
5.11	Figure and Figure Legend.....	235
5.12	References.....	237
6.0	Chapter 6.....	245
	Discussion and Summary	
6.1	Discussion	245
6.2	What immune cells can traffic out of the CNS?.....	246
6.3	What evidence supports viral traffic out of the CNS?	247
6.4	What is the effect of ART on CNS macropahge and rebound following ART interruption?	250
6.5	What is the effect of CNS macrophage traffic on immune activation, tolerance, and pathogenesis?.....	252
6.6	Can macrophage traffic out of the CNS play a role in neurodegenerative diseases such as HAND, HIV-SN, Multiple sclerosis, Alzheimer’s disease, and normal aging?... 	254
6.7	Signals that could initiate or prevent macrophage traffic out of the CNS.....	259
6.8	How to target macrophage activation and traffic out of the CNS?.....	260
6.9	Summary	264
6.10	References.....	265

LIST OF FIGURES AND TABLES

Figure 1.1	HIV Infection and Progression to AIDS Reproduced with permission from Springer Nature	2
Figure 1.2	HIV Replication and Effects of ART Reproduced with permission from Springer Nature	4
Figure 1.3	Advances in ART have reduced severity but not the prevalence of HAND Reproduced with permission from Springer Nature	6
Figure 1.4	CNS Protective Barriers Reproduced with permission from Springer Nature	10
Figure 1.5	Blood Nerve Barrier Reproduced with permission and licensed under CC BY 4.0	13
Figure 1.6	Connection between the CNS and PNS Figure adapted and reproduced with permission from John Wiley and Sons	14
Figure 1.7	Macrophages in the CNS Figure Created in BioRender. Wallis, Z. (2024) https://BioRender.com/q50i134	18
Figure 1.8	Monocyte and Macrophage HIV Reservoir Reproduced with permission and licensed under CC BY 4.0	24
Figure 1.9	CSF Drainage from the CNS Reprinted with permission from The Lancet Neurology	30
Figure 1.10	Pathways of Immune Cells Out of the CNS Reproduced with permission and licensed under CC BY 4.0	36
Figure 2.1	Study Design Created in BioRender. Wallis, Z. (2024) https://BioRender.com/a42e272	80
Figure 2.2	Distribution of SPION after i.c. injection	82
Figure 2.3	SPION localizes to CNS macrophage	84
Table 2.1	Accumulation of SPION+ macrophage in the CNS over time	86
Figure 2.4	SPION+ Macrophage outside of the CNS over time	88
Figure 2.5	Traffic of SPION+ macrophage out of the CNS to the dCLN over time	90
Table 2.2	SPION+ macrophage outside of the CNS over time	92
Figure 2.6	SPION localized to CD163+ gp41+ productively macrophage in the dCLN	94

Figure 2.7	SIV-RNA+ SPION+ macrophage in the dCLN with AIDS	96
Table 3.1	Animals used in the study	135
Figure 3.1	Study design and plasma viral load <small>Created in BioRender. Wallis, Z. (2024)</small>	137
	https://BioRender.com/a42e272	
Figure 3.2	ART reduces the number of SPION+ perivascular macrophages and increases traffic out	139
Figure 3.3	SPION+ SIV-RNA+ macrophages in the parenchyma, meninges, choroid plexus, dCLN, spleen, and DRG of animals with AIDS and SIVE	141
Table 3.2	SPION+ SIV-RNA+ macrophages and gp41+ cells are reduced with ART but not in the meninges and choroid plexus which rebound following ART interruption	144
Figure 3.4	GP41+ SPION+ MNGC in the CNS of an animal with AIDS and SIVE	145
Figure 3.5	SPION-containing macrophages in and outside of the CNS are primarily labeled with SPION from early injection	147
Table 3.3	Distribution of early, late, and dual SPION+ macrophage in the CNS and periphery	149
Table 3.4	ART eliminates SPION+SIV-RNA CNS perivascular macrophages and SPION+SIV-RNA macrophages outside of the CNS but SPION+SIV-RNA+ meningeal and choroid plexus macrophages persist	151
Figure 4.1	ART and CNS Inflammation Resolution: The Role of Macrophage Traffic <small>Created in BioRender. Wallis, Z. (2024)</small> https://BioRender.com/f671783	187
Table 4.1	Animals used in the study	189

Figure 4.2	Accumulation of SPION in the spinal cord is similar to accumulation in the brain <small>Created in BioRender. Wallis, Z. (2024) https://BioRender.com/p44b504</small>	191
Figure 4.3	SPION+macrophage in the DRG and cranial nerves following i.c. injection	193
Figure 4.4	SPION+ macrophage accumulates in the DRG over time and is unchanged with ART	195
Figure 4.5	Accumulation of SPION+ macrophage in cranial nerves	197
Figure 4.6	ART does not eliminate virally infected SPION+ macrophages in cranial nerves	199
Table 4.2	ART eliminates virally infected SPION+ macrophages within the DRG but not cranial nerves	201
Figure 4.7	Macrophage accumulation in the spinal cord	203
Figure 4.8	SPION+ Macrophage accumulation in each level of the DRG over time	205
Figure 4.9	Macrophage accumulation in the DRG	207
Figure 5.1	Altered myeloid production with aging and HIV infection contributes to chronic inflammation <small>Reproduced with permission and licensed under CC BY</small>	235

[4.0](#)

ABBREVIATIONS

AIDS	Acquired Immunodeficiency Syndrome
ANI	Asymptomatic Neurocognitive Impairment
APC	Antigen Presenting Cells
AQP4	Aquaporin-4
ART	Antiretroviral Therapy
ATN	Antiretroviral Toxic Neuropathy
BBB	Blood Brain Barrier
BCSF	Blood CSF Barrier
BNB	Blood-Nerve Barrier
BrdU	Bromodeoxyuridine
CCR	C-C Chemokine Receptor
CD	Cluster of Differentiation
CNS	Central Nervous System
CSF	Cerebrospinal Fluid
CXCR	C-X-C Chemokine Receptor
dCLN	Deep Cervical Lymph Node
DCs	Dendritic Cells
DNA	Deoxyribonucleic acid
dpi	Days Post Infection
DRG	Dorsal Root Ganglia
EGFP	Enhanced Green Fluorescent Protein
Env	Envelope Glycoprotein
FTC	Emtricitabine
HAD	HIV-Associated Dementia
HAND	HIV-Associated Neurocognitive Disorders
HIV	Human Immunodeficiency Virus
HIV-DSP	HIV-Associated Distal Sensory Polyneuropathy

HIV-SN	HIV-Associated Sensory Neuropathy
I.c.	Intracisternal
Iba1	Ionized Calcium-Binding Adapter Molecule 1
ICAM-1	Intercellular Adhesion Molecule
INSTI	Integrase Strand Transfer Inhibitor
ISF	Interstitial Fluid
MGBG	Methyl-bis-guanylhydrazone
MHC	Major Histocompatibility Complex
MND	Mild Neurocognitive Disorder
MNGC	Multinucleated Giant Cell
MRI	Magnetic Resonance Imaging
NNRTI	Non-Nucleoside Reverse Transcriptase Inhibitor
NRTI	Nucleoside Reverse-Transcriptase Inhibitors
PLHIV	People Living with HIV
PNS	Peripheral Nervous System
PVM	Perivascular Macrophage
RNA	Ribonucleic Acid
ROS	Reactive Oxygen Species
SAS	Subarachnoid Space
sCD163	soluble CD163
SIV	Simian Immunodeficiency virus
SIVE	SIV Encephalitis
SPION	Superparamagnetic Iron Oxide Nanoparticles
TDF	Tenofovir Disoproxil Fumarate
VCAM-1	Vascular Cell Adhesion Molecule 1
VLA-4	Very Late Antigen-4

ACKNOWLEDGEMENTS

I am truly grateful to have had the opportunity to work under Dr. Ken Williams during my time at Boston College. His encouragement to explore my own ideas has been instrumental in shaping me into a better scientist. I truly appreciate the opportunities he provided for me to mentor undergraduate students, rotation students, and fellow Ph.D. candidates, recognizing my passion for teaching, even when it meant diverting my focus from my research. Although there were tough times, he adapted his approach to offer the support I needed to navigate challenges both within and outside of the lab. I am incredibly fortunate to have had such a dedicated mentor who believed in my potential and fostered my growth as a scientist and an educator.

I would like to express my heartfelt gratitude to Cecily Midkiff, Robert Blair, and the entire veterinary staff at TNPRC. Cecily's invaluable guidance was instrumental throughout my Ph.D. journey. Her expertise, advice, and encouragement helped me navigate complex experiments and data analysis, and I could not have completed this work without her and her incredible team. I would also like to express my deepest gratitude to Dr. Robert Blair for his outstanding mentorship. He is an exceptional pathologist who was always willing to answer my questions and spend hours discussing the data. This thesis was greatly dependent on histological analysis and his expertise was crucial in making these experiments possible. I am deeply grateful to the veterinary staff for their compassionate care of the animals involved in these studies. Their dedication and exceptional attention were essential to the success of this work.

I want to thank my entire thesis committee—Dr. Welkin Johnson, Dr. Ken Williams, Dr. Josh Rappoport, Dr. Maitreyi Das, and Dr. Robert Blair—for their support and valuable guidance during our meetings. I would also like to thank Dr. Patrick Autissier for his support with flow cytometry. His guidance not only strengthened my technical abilities but also made a significant impact on my experiments. I am truly thankful for his consistent help and support in the lab.

I am deeply grateful to my parents for their unwavering support throughout my Ph.D. journey. From encouraging my passions to embracing my endless questions, they have always been there for me and supported my pursuit of science. Despite the distance, we made it a priority to stay connected and their willingness to travel to watch me present at conferences means more to me than words can express. Their love and encouragement have been a constant source of strength. I am incredibly thankful to my sister for her unwavering support throughout my Ph.D. Her patience and selflessness inspire me to be a better person every day. I would also like to express my gratitude to my husband for being the reason I followed my dreams to research in Boston. I can't imagine how different my life would be if you hadn't taken me to that Red Sox game. Although you're not a scientist, your support and eagerness to learn about HIV and immunology truly reflect your dedication to my journey.

I dedicate my Ph.D. journey to my Papa—Wayne Wallis—who sadly lost his life to COVID-19 during my first semester. This loss had a profound effect on me and ignited a passion to make the world a better place. Your support meant everything to me, and I promise to make an impact that would make you proud.

1.0 Literature Review

1.1 Human Immunodeficiency Virus (HIV), Acquired Immunodeficiency Syndrome (AIDS), and Rapid AIDS Simian Model

A. HIV and AIDS in the ART Era

With over 40 million people worldwide infected with human immunodeficiency virus (HIV), the virus remains a global pandemic and poses profound difficulties in healthcare and disease prevention efforts [1]. The virus spread largely unnoticed in the 1960s for two decades until reports from the United States of *Pneumocystis carinii* pneumonia and Kaposi's Sarcoma in young, previously healthy individuals [2]. It was not until 1983 that researchers isolated a retrovirus—now known as human immunodeficiency virus type 1 (HIV-1)—as the cause of what has since become one of the most devastating infectious diseases in modern history [2]. Since the discovery, genetic analysis identified that both HIV types (HIV-1 and HIV-2) arose from multiple cross-species transmissions from simian immunodeficiency viruses (SIVs) naturally infecting African primates [2-4]. HIV-2 originated from SIV in sooty mangabeys, while HIV-1, the primary cause of the pandemic, arose from SIV transmitted by chimpanzees [2-4]. HIV infects T cells, macrophages, and dendritic cells (DCs) by binding the envelope glycoprotein (Env, gp120) to the CD4 receptor on the cell surface [5-7]. After binding, there is interaction with a co-receptor—primarily CCR5 on macrophages or CXCR4 on T cells—which results in fusion of the viral envelope with the host cell membrane [5-7]. Fusion of the HIV envelope with the host membrane is mediated by the Env glycoprotein, gp41, binding to CD4, resulting in a conformational change to produce a coiled-coil, anchoring the virus to the host membrane [8]. The coiled-coil has grooves that fit other gp41

subunits and essentially folds back on itself, forming a stable six-helix bundle that brings the virus membrane closer to the host membrane [8]. Once inside, viral RNA and enzymes are maintained in the capsid core while reverse transcription occurs and traffics into the nucleus for DNA integration [5-7]. The virus then hijacks the host cell's machinery to produce and release virions that can infect other cells [5-7]. Activated CD4+ T cells are the primary producers of virions, but they are short-lived, surviving only about a day after infection due to the cytopathic effects of HIV, which rapidly destroys these cells [9]. In contrast, HIV infection is non-lytic in monocytes and macrophages enabling these cells to produce virions and maintain provirus for long periods of time [10-12]. HIV is primarily transmitted through mucosal membranes, and infection progresses through several phases: an initial asymptomatic phase of viral spread, acute infection with high viremia within 2-4 weeks, a decade-long period of viral latency, and eventually development of acquired immunodeficiency syndrome (AIDS) in the absence of effective treatment (**Figure 1.1, Reproduced with permission from Springer Nature**) [2].

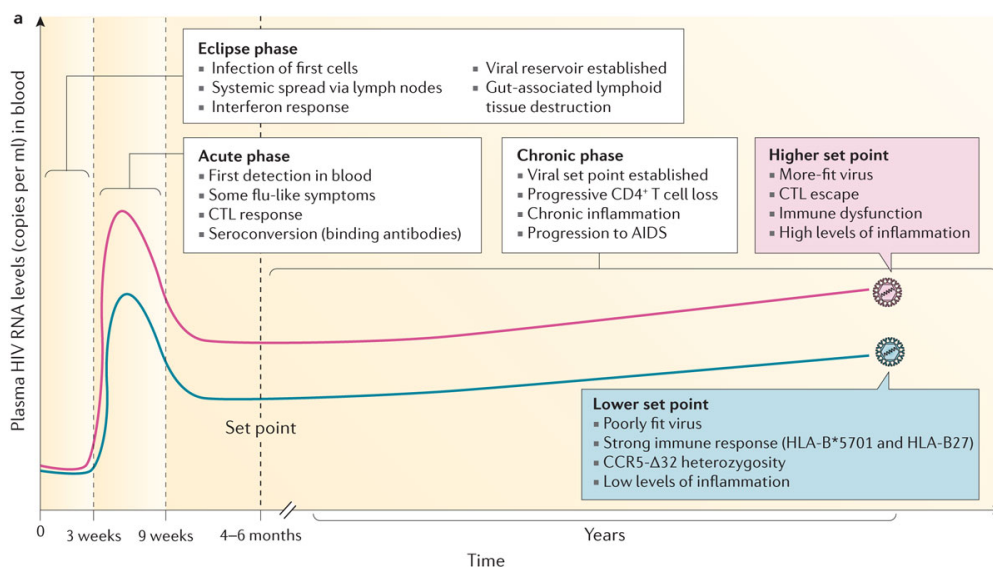


Figure 1.1 HIV Infection and Progression to AIDS. In the early stages of HIV infection, the virus infects T cells and macrophages within mucosal tissues and spreads throughout the lymphoid system (Eclipse phase). Within days, HIV RNA is detectable and exponentially rises to a peak within weeks until partial control by the adaptive immune response (Acute phase). Rapid viral escape renders antibody responses primarily ineffective. A set point level of viremia is established, driven by virus-host interactions, with some individuals experiencing a lower set point due to poor viral fitness, strong host immune response, low levels of CCR5 coreceptor, and low levels of inflammation. Over years, HIV-driven CD4⁺ T cell loss leads to immunodeficiency, chronic inflammation, and myeloid immune activation, contributing to HIV-associated comorbidities such as HIV-associated neurocognitive disorders (Chronic phase). *Reproduced with permission from Springer Nature (5916061484462).* Deeks, S., Overbaugh, J., Phillips, A. *et al.*, HIV Infection, Nature Reviews Disease Primers, 1, 1-22, 2015, Springer Nature.

HIV and SIV infection initially results in rapid depletion of CD4⁺ T cells in the gut associate lymphoid tissue followed by body-wide CD4⁺ T cell depletion inducing systemic immune activation (**Figure 1.1, [Reproduced with permission from Springer Nature](#)**) [2]. Antiretroviral therapy (ART) blocks HIV (and SIV) replication by targeting critical steps in the virus life cycle (**Figure 1.2, [Reproduced with permission from Springer Nature](#)**) [5, 13, 14]. ART medications such as reverse transcriptase inhibitors (Tenofovir disoproxil fumarate (TDF) and Emtricitabine (FTC)) prevent the conversion of viral RNA into DNA, while integrase inhibitors (Raltegravir and Dolutegravir) block the integration of viral DNA into the host genome, and protease inhibitors (Darunavir) stop the maturation of new viral proteins (**Figure 1.2, [Reproduced with permission from Springer Nature](#)**) [5, 13, 14]. However, ART does not kill infected cells or eliminate viral reservoirs; it limits viral replication, reduces viral load, and prevents further viral spread [15].

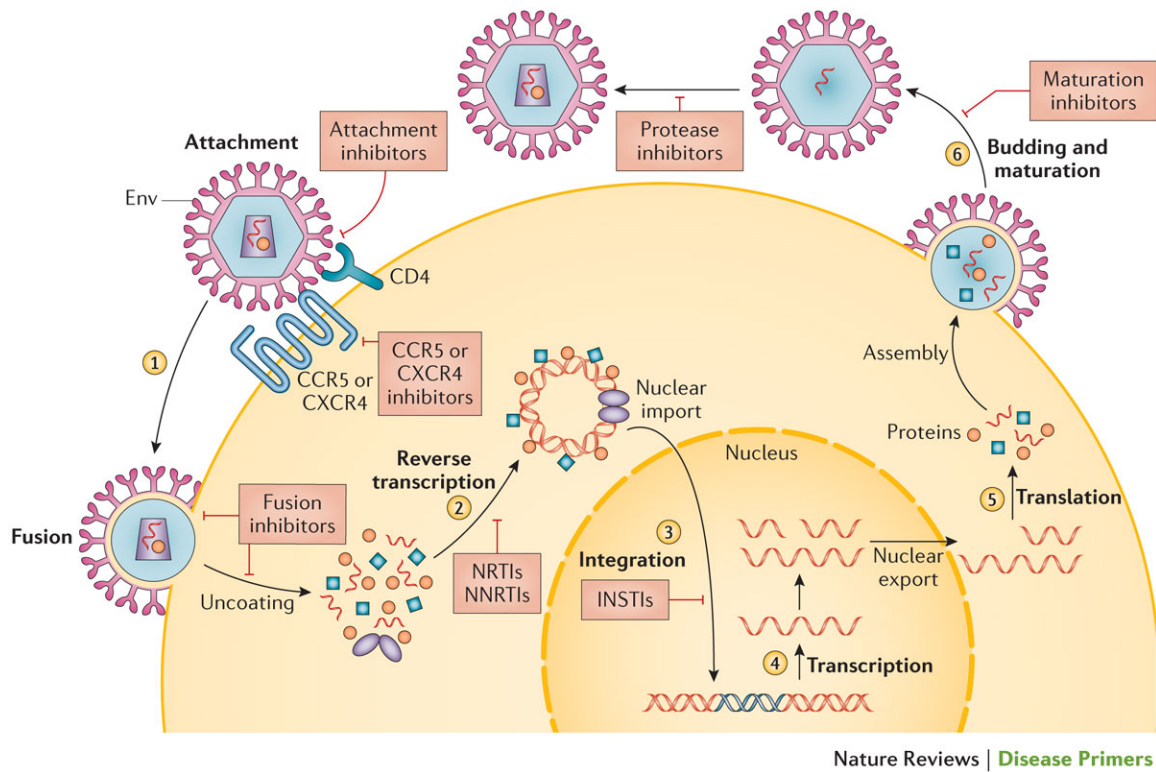


Figure 1.2 HIV Replication and Effects of ART. HIV infects monocytes, macrophages, and T cells by binding to CD4 and either CCR5 or CXCR4 through its envelope (Env) glycoprotein (step 1). After the virus fuses with the cell membrane, its RNA is reverse-transcribed into DNA (step 2). This pre-integration complex enters the nucleus, where the viral DNA integrates into the host genome (step 3). Subsequently, host enzymes transcribe the integrated viral DNA into mRNAs (step 4), which are transported to the cytoplasm for translation (step 5) into viral proteins and virions mature after budding from the host cell membrane (step 6). Each step of the HIV life cycle—entry, reverse transcription, integration, and protein maturation—serves as a crucial target for ART to effectively inhibit viral replication. Abbreviations: INSTI (integrase strand transfer inhibitor), NNRTI (non-nucleoside reverse transcriptase inhibitor), NRTI (nucleoside reverse transcriptase inhibitor). *Reproduced with permission from Springer Nature (5916061484462).* Deeks, S., Overbaugh, J., Phillips, A. *et al.*, HIV Infection, *Nature Reviews Disease Primers*, 1, 1-22, 2015, Springer Nature. *Original figure adapted from and reproduced with permission from Springer Nature (5916500315550).* Brenchley, J., Price, D. & Douek, D. HIV disease: fallout from a mucosal catastrophe? *Nature Immunology*, 7, 235–239, 2006, Springer Nature.

HIV-associated neurocognitive disorders (HAND) remain a challenge to eliminate despite effective ART due to the persistence of viral reservoirs and chronic macrophage activation [5, 10, 16-18]. The proportion of people living with HIV (PLHIV) affected by HAND has not changed in the ART era, with roughly 60% of people experiencing neurocognitive impairment (**Figure 1.3, Reproduced with permission from Springer Nature**) [19]. However, the severity has decreased in the ART era, where the prevalence of the most severe form of HIV-associated dementia (HAD) is less frequent, and asymptomatic neurocognitive impairment (ANI) represents the majority of cases (**Figure 1.3, Reproduced with permission from Springer Nature**) [19]. Additionally, roughly 33% of PLHIV on ART experience sensory neuropathy (HIV-SN), which is linked to chronic macrophage activation and potential toxicity from ART, resulting in numbness, tingling, reduced sensation to temperature, and pain, all of which significantly reduce the quality of life of PLHIV [20-27]. HIV-SN includes two main types: HIV-associated distal sensory polyneuropathy (HIV-DSP), caused by the virus itself, and antiretroviral toxic neuropathy (ATN), which is mainly linked to specific nucleoside reverse-transcriptase inhibitors (NRTIs) that are no longer used [22, 23]. Since the introduction of ART in 1996, there have been significant improvements in both the quality of life and lifespan of individuals living with HIV. Improvements to ART regimens, including increasing drug half-life, lower toxicity, and increasing tissue penetration, have fallen short of eliminating HAND and HIV-SN because they are not addressing immune activation or eliminating viral reservoirs.

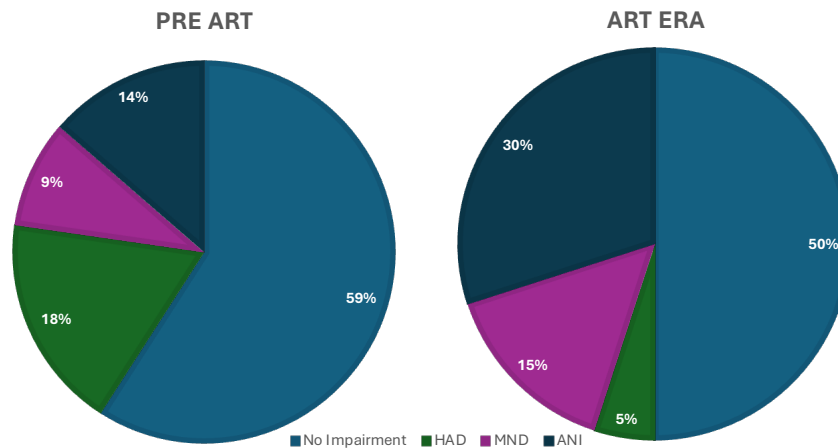


Figure 1.3 Advances in ART have reduced severity but not the prevalence of HAND. Following the introduction of ART, the overall rate of neurocognitive symptoms among HIV+ individuals has increased. However, cases with severe symptoms have declined, leading to a reduced prevalence of HIV-associated dementia (HAD). As a result, asymptomatic neurocognitive impairment (ANI) and mild neurocognitive disorder (MND) now comprise most cases. *Reproduced with permission from Springer Nature (5916510234532).* Saylor, D., Dickens, A., Sacktor, N. *et al.*, HIV-associated neurocognitive disorder — pathogenesis and prospects for treatment, *Nature Reviews Neurology*, 12, 234-248, 2016, Springer Nature. *Original figure adapted and reproduced with permission from John Wiley and Sons (5916501170110).* McArthur, J.C., Steiner, J., Sacktor, N. and Nath, A., Human immunodeficiency virus-associated neurocognitive disorders: Mind the gap. *Ann Neurol.*, 67, 699-714, 2010, John Wiley and Sons.

B. Rapid AIDS Model

SIV native to the Old-world monkey—*Sooty mangabey* (SIVmac)—is non-pathogenic to the *mangabey*, yet infection with SIVmac of the *Macaca mulatta* (Rhesus macaque) leads to the development of AIDS within 1-3 years, and roughly 30-40% of animals develop SIV-induced encephalitis (SIVE) [4, 16, 28]. SIVE is characterized by lymphocytic infiltration, microglial activation, myeloid accumulation, multinucleated giant cells (MNGCs), and viral RNA within the brain [29-33]. SIV infection, with intravenous inoculation of SIVmac251 in the rhesus macaques, is a well-established

model to study HIV pathology due to its close homology in viral targets, host immune response, and capability to monitor the animal throughout infection closely [16, 28]. CD8⁺ T cells are essential for the immune defense against viral infections in humans and non-human primates, including rhesus macaques [34-36]. Administering a chimeric humanized mouse anti-CD8 monoclonal antibody on days 6, 8, and 12 post-infection (dpi) depletes CD8⁺ lymphocytes and natural killer cells, significantly increasing plasma viremia and resulting in a high incidence of SIVE (>75% of animals) [16, 34-37]. These macaques exhibit cognitive, motor, and behavioral impairments due to central nervous system (CNS, composed of the brain and spinal cord) infection, closely mirroring the neuropsychological changes in individuals affected by HAND [38, 39]. The associated neuropathology is strikingly similar to PLHIV pre-ART with HIV encephalitis, including cerebral atrophy, neuronal damage, microglial nodules, MNGCs, macrophage infection, and white matter disease [16, 19, 38, 40]. This accelerated CNS disease in macaques infected with SIVmac251, and CD8-depleted makes them a valuable model for studying potential therapies to treat and target viral reservoirs in the CNS.

While SIV is a valuable and well-established model to study HIV pathology, there are some key differences in infection, genetics, and pathology. With SIV infection, generally, a viral clone is intravenously injected to inoculate the non-human primate, whereas HIV infection is typically a result of sexual contact or injection of a viral swarm, which can vary genetically [28, 41]. SIVmac251 is a common viral strain used to study HIV pathogenesis but has a different accessory protein than HIV-1 that makes viral replication more efficient: vpx is a cytoplasmic protein in SIVmac251 and makes dNTPs readily available for reverse transcription, while HIV-1 lacks this protein [42]. HIV-1 has vpu

which can mediate the downregulation of CD4 and promote virion release [42]. Due to these slight differences between HIV-1 and SIVmac251, there are minor differences in pathology, primarily in the time to progress to AIDS, where humans progress in usually 10-15 years while the disease is more rapid and severe in non-human primates with AIDS progression in 1-3 years [4, 16, 28, 41]. Despite these minor differences, SIV is a well-established model to study HIV pathogenesis in a shortened timeline.

1.2 Immune Privilege in the CNS

A. CNS Immune Privilege: The Role of Protective Barriers

i. Blood-Brain Barrier

The CNS has been historically regarded as immune privileged due to prolonged graft survival, the lack of obvious draining lymphatics, and protective barriers [43-45]. Immune privilege of the CNS has been increasingly challenged due to the rediscovery of meningeal lymphatics [46-48]. Traditionally, the brain was thought to be isolated from systemic immune surveillance due to the blood-brain barrier (BBB) and the absence of classical lymphatic drainage [43-45]. The discovery of the BBB traces back to the 1880s when Paul Ehrlich observed that high molecular weight dye (Evans blue) injected into the vascular system was promptly absorbed by all organs except the brain and spinal cord [49, 50]. Shortly after, Edwin E. Goldman, an associate of Ehrlich, demonstrated that the same dye (Evans blue), when injected into the CSF, stained nervous tissue exclusively, indicating that the CNS is restricted from the bloodstream [49, 50]. These early dye studies established the foundation that the CNS is anatomically and immunologically segregated from the rest of the body [51]. The BBB exerts stringent control over the

passage of soluble molecules and immune cells into the CNS by specialized endothelial cells, astrocyte end processes, and the intricate network of cadherins, adhesion molecules, occludin, and claudins at tight junctions envelops the entire surface of brain capillaries, controlling and limiting the passage of cells and macromolecules across (**Figure 1.4, [Reproduced with permission from Springer Nature](#)**) [43, 50-57]. The BBB covers the entire surface of brain capillaries that supply the brain and spinal cord, acting as a selective filter to regulate the exchange of nutrients, ions, and immune cells between the blood and neural tissue [43, 50-57].

ii. Blood-CSF Barrier

The choroid plexus—situated in the brain's ventricular system—comprises a sophisticated network of fenestrated capillaries and epithelial cells produce and secrete CSF [58-60]. This epithelial monolayer—particularly in the 4th ventricle—undergoes extensive folding, forming villi that extend from the ependyma lining of the brain's ventricles [56, 61-63]. The choroid plexus is pivotal in maintaining and regulating exchange between the blood-CSF barrier (BCSFB) (**Figure 1.4, [Reproduced with permission from Springer Nature](#)**) [49, 56, 63, 64]. Integral to its function, the epithelial layer expresses integrins and junctional complexes, establishing a barrier that separates the vascularized stroma from the CSF in the ventricles [63]. Protein complexes—desmosomes, tight, adherent, and gap junctions—lining the choroid plexus create a regulated barrier, controlling paracellular diffusion and cellular movement [56, 65-67]. The choroid plexus has a leaky CSF-brain interface as these junctions are connected loosely by desmosomes, and tight junctions are discontinuous [63, 68]. However, this

tightly regulated exchange between the CNS and the blood can be disrupted by viral infection and disease, which compromise the integrity of the BCSFB, leading to altered permeability, neuroinflammation, and the infiltration of immune cells, allowing pathogens and potentially harmful substances to access the CNS [49, 54, 57, 69].

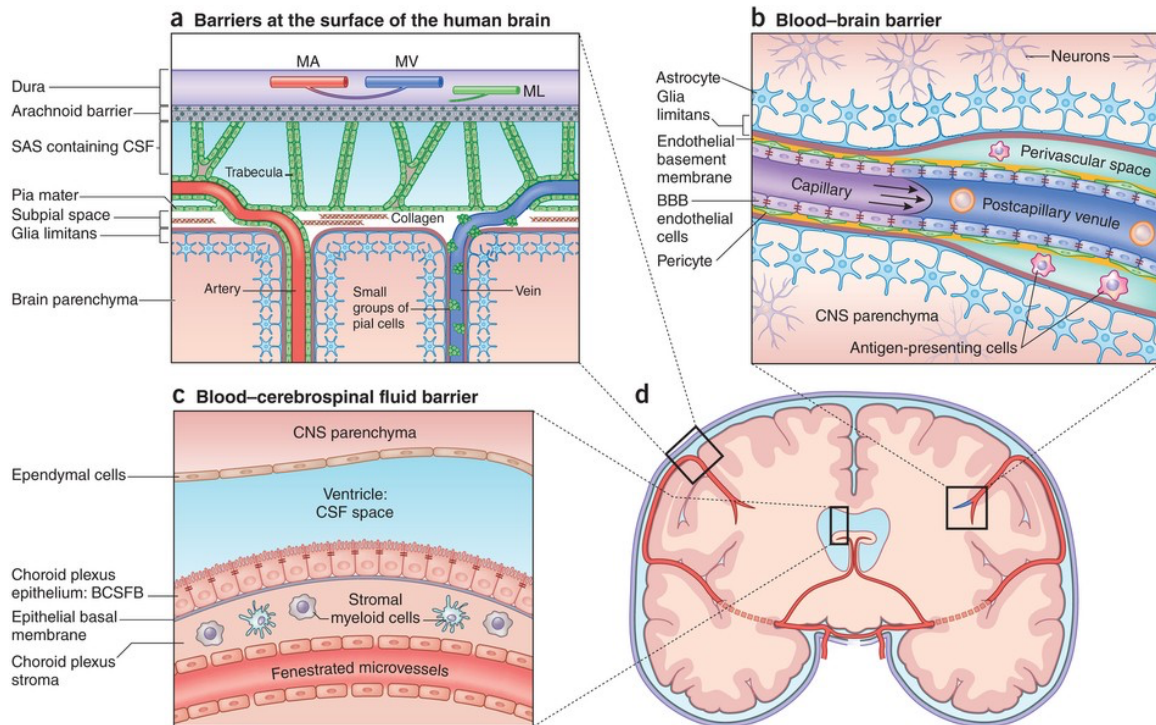


Figure 1.4 CNS Protective Barriers. (A) Barriers at the brain's surface include the dura, arachnoid, and pia mater, with the CSF-filled subarachnoid space between the arachnoid and pia. (B) The BBB lines all capillaries that innervate the brain parenchyma. (C) The choroid plexus epithelium forms the BCSFB. *Reproduced with permission from Springer Nature (5916070113309).* Engelhardt, B., Vajkoczy, P. & Weller, R, The movers and shapers in immune privilege of the CNS. *Nature Immunology*, 18, 123-131, 2017, Springer Nature.

iii. Blood-Nerve Barrier

Similarly to the BBB and BCSFB, the blood-nerve barrier (BNB) plays a critical role in maintaining the specialized environment of the peripheral nervous system

(PNS)—comprised of cranial and peripheral nerves—by limiting the passage of molecules and immune cells from the blood [43, 56, 70, 71]. The BNB restricts the transfer of substances and immune cells—including monocytes and macrophages—from surrounding tissue and blood to the nerve (also called the blood-nerve interface, BNI) **(Figure 1.5, *reproduced with permission and licensed under CC BY 4.0*)** [72, 73].

Because of the absence of astrocytes in the PNS, the BNB is relatively leakier than the BBB surrounding the CNS and is not considered immune privileged [73]. Immune cells and macromolecules move between blood and nerves in two main ways: primarily through the small blood vessels in nerves or indirectly through the epineurial extracellular space (the leaky BNB interface to blood) [72, 73]. Dye studies estimate that about 30% of endoneurial fluid is replaced daily [73], compared to the turnover of CSF, which is replaced roughly four times daily [74].

iv. Meninges of the CNS and PNS

The meninges consist of three protective layers surrounding the brain and spinal cord: the dura mater, arachnoid mater, and pia mater **(Figure 1.4A, *Reproduced with permission from Springer Nature*)** [75]. The dura mater—the outermost layer—is a dense, fibrous membrane that provides protection and structural support [75-78]. The arachnoid mater—beneath the dura—is a delicate, web-like structure [70, 75, 77, 79]. The pia mater—the innermost layer—closely adheres to the brain and spinal cord [70, 75, 77, 79]. The subarachnoid space (SAS) is located between the arachnoid and pia mater, where CSF surrounds and cushions the brain and spinal cord [70, 80, 81]. Collectively, the meninges and CSF are integral to the homeostasis and protection of the CNS.

The meninges of the CNS (dura, arachnoid, and pia) are continuous with connective tissues ensheathing the peripheral nerves (PNS) [72, 73, 82, 83]. The dura mater is continuous with the epineurium, the outer layer of peripheral nerves that binds nerve bundles together (**Figure 1.5, [reproduced with permission and licensed under CC BY 4.0](#)**) [72, 73, 82, 83]. Meanwhile, the arachnoid layer combines with the outer layers of the perineurium, the multiple layers of cells surrounding nerve bundles, and enclosing the inner nerve space (**Figure 1.5, [reproduced with permission and licensed under CC BY 4.0](#)**) [72, 73, 82, 83]. The inner layers of the perineurium are mirrored onto the nerve roots, forming the root sheath [83], while the outer root sheath—similar to the pia mater—comprises loosely organized cell layers with occasional connections (collagen) between them (**Figure 1.5, [reproduced with permission and licensed under CC BY 4.0](#)**) [83]. The inner layers of the root sheath originate from part of the perineurium, forming a direct connection where the nerve roots attach, connecting the fluid-filled SAS surrounding the brain and spinal cord and the space inside the nerve roots and is delineated at the subarachnoid angle (**Figure 1.6, [Figure adapted and reproduced with permission from John Wiley and Sons](#)**) [73, 83]. This direct connection allows fluid from the subarachnoid space—CSF—to flow into the endoneurial space due to pressure, serving as a source of fluid for the nerves [73, 83]. The subarachnoid angle crucially defines the boundary of the BBB, distinguishing the CNS from the PNS (**Figure 1.6, [Figure adapted and reproduced with permission from John Wiley and Sons](#)**) [84]. The BBB, BCSFB, BNB, and constitutive meningeal layers maintain a tightly regulated exchange between the CNS, PNS, and surrounding tissues; however, regulated entry of

immune cells is essential for monitoring the CNS environment and initiating appropriate immune responses.

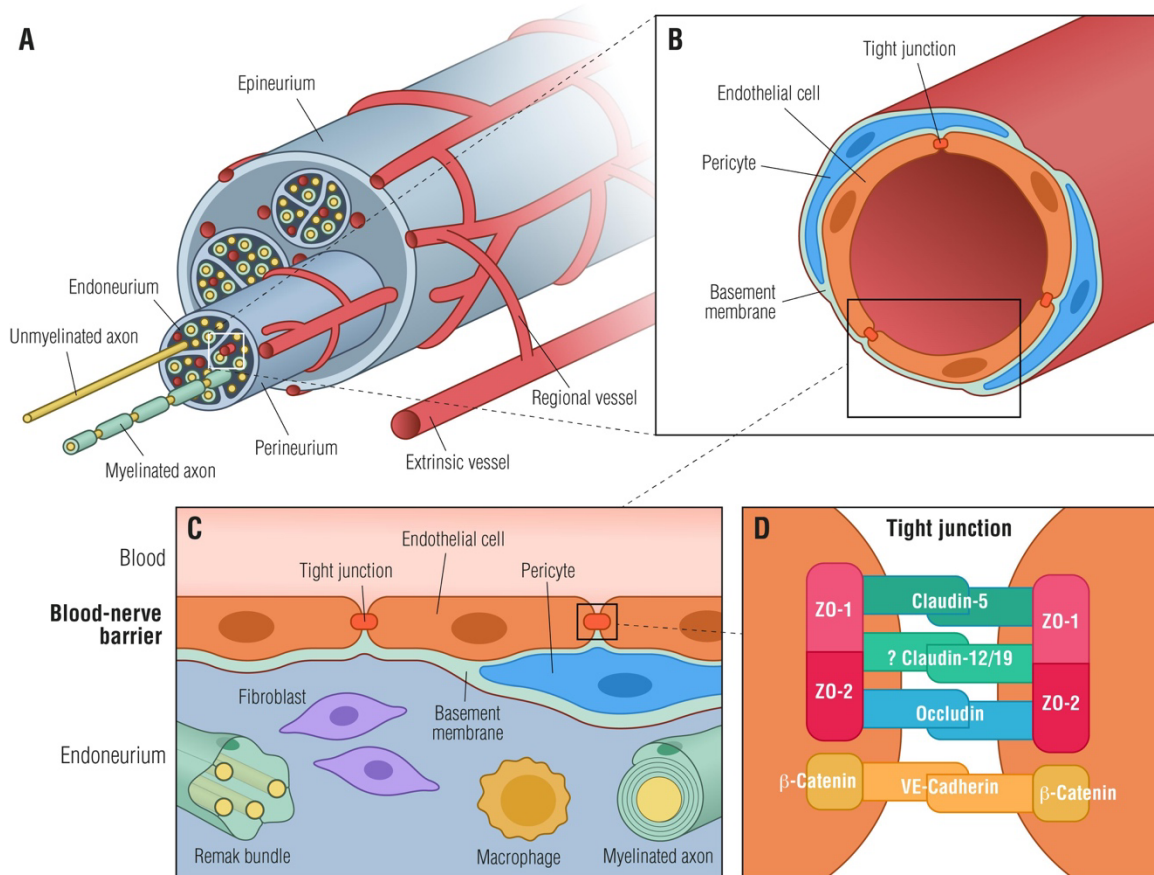


Figure 1.5 Blood Nerve Barrier. (A) A cross-section of a peripheral nerve surrounded by the epineurium contains collagen fibrils and blood vessels. Each nerve fascicle, containing unmyelinated and myelinated axons and small blood vessels, is enclosed by the perineurium, creating the endoneurial microenvironment. (B) An endoneurial blood vessel surrounded by endothelial cells, pericytes, and the basement membrane. (C) The structure of the blood-nerve barrier is formed by endothelial cells connected by tight junctions, pericytes, and the basement membrane, protecting the endoneurium from blood-borne toxins. (D) Endothelial cells form a barrier with tight and adherens junctions involving ZO-1/2, claudin-5, occludin, and β -catenin. Figure reproduced with permission from [Functional and Structural Changes of the Blood-Nerve-Barrier in Diabetic Neuropathy](#) by [Richner M](#), Ferreira N, Dudele A, Jensen TS, Vaegter CB and Gonçalves NP (2019) Neuropathy. *Front. Neurosci.* 12:1038 and is licensed under [CC BY 4.0](#).

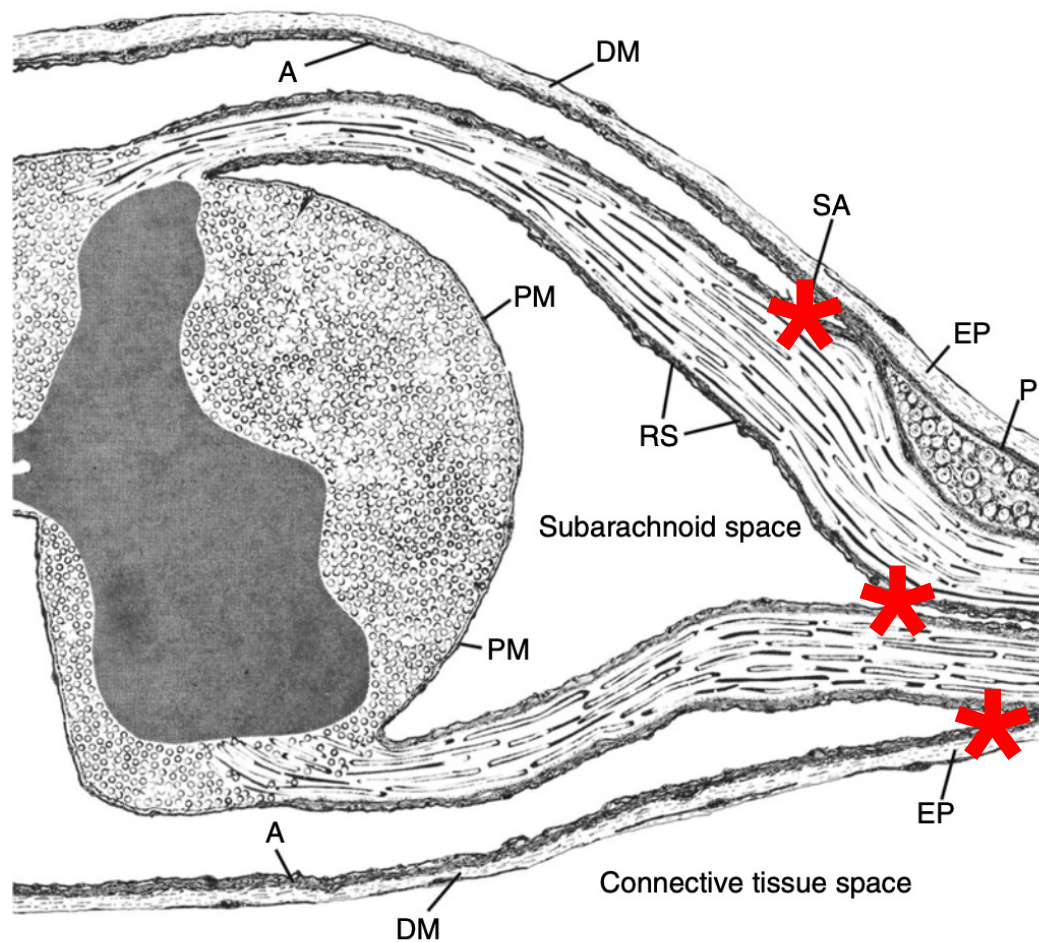


Figure 1.6 Connection between the CNS and PNS. Diagram illustrating the connections between the spinal cord meninges and connective tissue layers of the peripheral nerve. The subarachnoid angle (*) delineates the CNS from the PNS. Critical structures: A = arachnoid; DM = dura mater; EP = epineurium; En = endoneurium; P = pia mater; RS = root sheath. *Figure adapted and reproduced with permission from John Wiley and Sons (5916070401589). Haller, F. R., & Low, F. N., The fine structure of the peripheral nerve root sheath in the subarachnoid space in the rat and other laboratory animals. The American journal of anatomy, 131(1), 1-19, 1971, John Wiley and Sons.*

B. Macrophages in the CNS

i. Microglia

Mononuclear phagocytes—including monocytes and macrophages—play a central role in the CNS normally and in the pathogenesis of neuroinflammatory and neurodegenerative disorders, such as HAND [10, 85-87]. Macrophages within the brain are a heterogeneous population with diverse origins, phenotypes, and functions (**Figure 1.7, Created in BioRender**) [86, 87]. Parenchymal microglia are stationary, resident CNS macrophages that survey and maintain neural tissue by retracting and extending their processes, scanning their surroundings while their cell bodies remain stationary (**Figure 1.7, Created in BioRender**) [86, 88, 89]. Microglia are derived from the yolk sac, where a single embryonic wave of progenitors engrafts in the CNS during early embryonic development [90-94]. Early after conception (>9 days), microglia are found in the developing CNS (neuroectoderm) of the mouse embryo and are self-maintained at a low rate as a stable population [92-97]. Microglia express many macrophage-associated markers (antigen recognition, presentation, and pathogen-associated molecular patterns) such as ionized calcium-binding adapter molecule 1 (Iba1+), CD11b, MHC II, CD68—a pan macrophage marker—and have low to undetectable hemoglobin-haptoglobin scavenger receptor CD163 [CD68+CD163-] [98]. Microglia have inflammatory responses essential for identifying pathogens and promoting tissue repair; their chronic activation can lead to sustained neuroinflammation, which is implicated in neurodegenerative disorders such as HAND, Alzheimer's disease, and Parkinson's disease [99-101].

ii. Perivascular Macrophages

Perivascular macrophages (PVM) represent a specialized group of bone marrow-derived macrophages that are distinguished by their proximity to cerebral vasculature and localized to the compartment surrounding arteries and veins that extend deep into the brain, known as the perivascular space (or Virchow-Robin space) (**Figure 1.7, Created in BioRender**) [102-106]. The perivascular space is bordered by the vascular basement membrane on the side away from the lumen of the vessel and by the glia limitans basement membrane (astrocyte foot processes) on the parenchymal side [106, 107]. PVM migrate from the bone marrow to the perivascular space normally [86, 107-110] and at a rate that increases with HIV and SIV infection [32, 111-113]. Importantly, PVM are the primary cell type in the CNS infected with HIV and SIV [32, 113, 114]. Rodent studies using bone marrow chimeras indicate that 10% of PVM are replenished from bone marrow monthly, [110] while in non-human primates, our lab has found that almost all PVM are replaced from bone marrow progenitors in four years [108]. PVM express the hemoglobin-haptoglobin scavenger receptor CD163, MHC II+, and varying levels of other co-stimulatory molecules, including CD86 and Iba1, implying their involvement in antigen recognition and presentation [98, 103, 109, 110]. Some PVM also express with the mannose receptor, CD206, involved in pathogen recognition and receptor-mediated endocytosis and may have the capacity for self-renewal [115-118].

iii. Meningeal Macrophages

Meningeal macrophages (also referred to as border associated macrophages), reside within the meninges and play critical roles in maintaining CNS homeostasis and

responding to pathogens (**Figure 1.7, Created in BioRender**) [77, 79, 104, 119, 120]. Each meningeal layer—dura, arachnoid, and pia—is populated by immune cells, including macrophages and lymphocytes [70, 75, 76, 105, 121-123]. These specialized meningeal macrophages (with varying expression of Iba1, CD68, CD163, and CD206) originate from diverse sources, including embryonic yolk sac progenitors and from the bone marrow [77, 86, 104, 120]. Meningeal macrophages are involved in immune surveillance, antigen presentation, and tissue repair within the CNS [77, 79]. However, dysregulated turnover and recruitment of meningeal macrophages (and lymphocytes) have been implicated in the pathogenesis of neurological disorders, including HAND [77, 79, 104]. Meningeal macrophages are important for bringing HIV and SIV into the brain from the blood, sharing similar Env and Pol sequences (including protease (PR), reverse transcriptase (RT), and integrase (IN)) [124, 125]. Importantly, it has been suggested that HIV and SIV could potentially migrate into the brain via infected macrophages through meningeal lymphatics, even during ART when plasma and CSF viral loads are undetectable [126]. However, this has not been directly observed.

iv. Choroid plexus Macrophages

Macrophages in the choroid plexus include stromal and Epiplexus/Kolmer macrophages (**Figure 1.7, Created in BioRender**) [64, 77, 119, 127]. Stromal macrophages are located within the choroid plexus stroma, and Kolmer cells (Kolmer macrophages) attach to the apical side of the epithelial barrier and ventricular wall [61, 63, 105, 119]. Circulating monocytes infiltrate the choroid plexus stroma and can migrate across the epithelial barrier to become Kolmer macrophages [63, 128]. Stromal and

Kolmer macrophages share functional traits, such as phagocytic activity and antigen presentation, and have often been grouped in studies due to a lack of distinguishing markers (both expressing varying levels of Iba1, CD68, CD163, and CD206) [63, 128-131]. While both originate from the yolk sac, stromal macrophages are continuously replaced by circulating monocytes, while Kolmer cells can repopulate independently of bone marrow progenitors [86, 104, 132, 133]. Importantly, stromal and Kolmer macrophages are HIV and SIV-infected and may also be a viral reservoir [134-136].

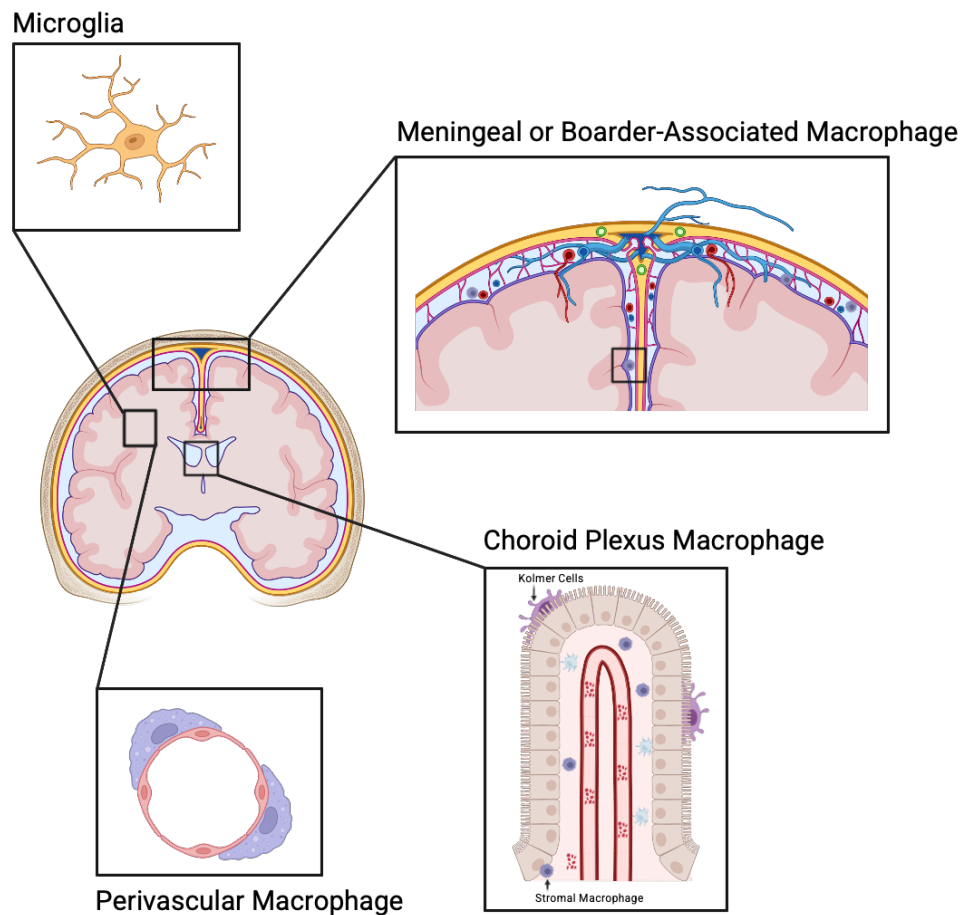


Figure 1.7 Macrophages in the CNS. Macrophages in the CNS are a heterogeneous population, including microglia, meningeal macrophages, perivascular macrophages, and choroid plexus macrophages (stromal and Kolmer macrophages). Created in BioRender. Wallis, Z. (2024) <https://BioRender.com/q50i134>

C. Other Immune Cells in the CNS

Neurons are not directly infected by HIV or SIV in the CNS; however, other immune cells, including DCs and T cells, represent a small proportion of cells in the healthy CNS and can become infected with HIV and SIV, potentially contributing to neuronal damage.

i. Myeloid Derived-Dendritic Cells (DCs)

In a healthy CNS, DCs are not found in the parenchyma [137] but are present in all three layers of meninges, in the choroid plexus, scattered in perivascular spaces, and in CSF [135, 138, 139]. DCs in the meninges play essential roles in immune surveillance and antigen presentation and are primarily found with CNS inflammation from a peripheral source of origin (bone marrow) [140-144].

ii. T Cells

T cells originate from hematopoietic stem cells in the bone marrow, undergo maturation and selection processes in the thymus, and play critical roles in adaptive immunity by recognizing and responding to specific antigens, thereby contributing to immune surveillance, regulation, and effector functions throughout the body [145, 146]. T cells play a significant role in immune surveillance of the CNS; however, they can also trigger significant immune responses with viral infections and autoimmunity [147]. There are CD4⁺ T cells in the healthy CNS and a few CD8⁺ T cells in the parenchyma, meninges, choroid plexus, and CSF [148, 149]. With viral infection, there is accumulation and persistence of CD8⁺ T cells, particularly within perivascular spaces, meninges, and the choroid plexus [149-152].

iii. Natural Killer Cells (NK Cells)

In the healthy mouse brain, NK cells (CD56⁺CD3⁻ and varying levels of CD16) are present in the CNS but constitute a small fraction ($1.1 \pm 0.14\%$) of the total immune cells and primarily reside in boundary regions such as the meninges and choroid plexus, rather than the parenchyma [122, 123]. As NK cells do not express the CD4 receptor required for HIV and SIV infection, they are not directly infected by the virus but play a key role in the immune response against HIV infection [153].

iv. MAC387⁺

Lastly, MAC387⁺ macrophages are bone-marrow derived [48-50] and rarely found in normal or noninflamed CNS tissue but are present in large numbers with CNS inflammation [46]. These macrophages are newly produced from the bone marrow and are rarely found to be infected with HIV and SIV [5, 19, 39, 46, 51]. Recent evidence suggests that skull bone marrow can serve as a reservoir for immune cells—including myeloid and lymphocytes—to migrate into the CNS [154]. These peripheral-derived immune cells play a significant role in maintaining neural integrity and homeostasis but also can drive CNS inflammation and neuropathogenesis.

1.3 CNS as a Viral Reservoir

A. Viral Infection of the CNS

In SIV-infected macaques, SIV enters the brain early in infection and is detectable in the frontal and temporal lobes and white matter within 3-7 days post-infection [155, 156]. SIV-RNA is only detectable during acute infection and with severe disease (SIVE),

while viral DNA persists in the brain [113]. This suggests that while active viral replication occurs early and during severe CNS involvement, the brain remains a long-term reservoir for viral DNA. One model for HIV and SIV to enter the brain is the “Trojan Horse” model where virally infected macrophages and lymphocytes cross the BBB early in infection (3-7 days) [33, 44]. Latent HIV infection persists during the asymptomatic phase and can reactivate with AIDS progression supported by viral sequencing data showing that quasispecies evolve independently in the CNS and are distinct from those in plasma, spleen, and lymph nodes [136, 157-159]. Furthermore, viral RNA in CNS lesions of patients with HAD is traced back to early brain infection [157]. These support the early establishment of virus in the CNS that contribute to the development of HAND in the later stages of AIDS. Meanwhile, the "Late Invasion" model suggests that CNS disease arises from late-stage viral entry rather than the virus already in the brain [160, 161]. This model is supported by evidence showing that distinct viral variants from the periphery continuously seed the CNS throughout the course of the disease [162, 163], indicating ongoing transmigration of virally infected monocytes into the brain during HIV and SIV infection. Other mechanisms of viral infection of the CNS include the infection of (or transcytosis through) endothelium cells and direct transmission of free virus from the blood to CSF [164-166]. Despite the early entry of HIV and SIV into the CNS, neurological disease occurs during the chronic phase, indicating that sustained innate immune activation, rather than initial viral infiltration, is the primary driver of CNS pathology.

It is generally accepted that HIV and SIV enter the CNS early after infection, establishing a viral reservoir prior to the initiation of ART [155, 156]. Without ART,

CNS infection is rapid and causes indirect neuronal damage primarily through immune activation, proinflammatory cytokines, and toxicity of viral proteins (such as tat) [33, 44, 167, 168]. Prior to ART, individuals with HIV often succumbed to AIDS and opportunistic infections before the development of neurocognitive disorders [19] (**Figure 1.3, Reproduced with permission from Springer Nature**). However, those who did develop neurocognitive disorders were often severe [19] (**Figure 1.3, Reproduced with permission from Springer Nature**). With ART, virus replication is inhibited, resulting in a reduced plasma and cerebrospinal fluid viral load, yet the tissue reservoir is less well-defined. With ART, there is less productive virus in the brain and spinal cord, but virus persists in a latent state that is not eradicated by ART [19, 169-171]. In addition, PLHIV are living longer on ART and more frequently experiencing a range of neurocognitive disorders primarily to monocyte and macrophage activation [19, 85, 164, 169-172] (**Figure 1.3, Reproduced with permission from Springer Nature**). Despite the use of ART to reduce productive virus, monocyte and macrophage activation are the main drivers of CNS disease and persistent reservoirs of virus in the brain and spinal cord.

B. Monocytes and Macrophages in the CNS as a Viral Reservoir

HIV reservoirs persist in numerous anatomical and cellular reservoirs in the body in three states: equilibrated, compartmentalized, and clonal [17]. By the time an individual exhibits symptoms and tests positive for HIV, latently infected cells have already been established in key reservoirs—such as the CNS and lymphoid tissues—rendering complete viral eradication through ART alone unfeasible [173, 174]. Anatomical reservoirs—such as the brain and gut—act as 'sanctuaries,' where virions

remain sequestered in tissue, enabling ongoing viral replication that remains undetected in blood for prolonged periods [175-177]. With ART interruption, plasma viral rebound occurs within as little as two weeks and from various tissue origins, underscoring the challenges posed by latent reservoirs [178, 179]. Macrophages play a pivotal role in HIV and SIV persistence in the CNS (**Figure 1.8, *reproduced with permission and licensed under [CC BY 4.0](#)***), as they harbor the virus long-term without cytopathic effects [10-12]. Distinct viral populations between CSF and blood have been well documented even with durable ART [17, 158, 180-182], and is suggestive of ongoing replication in the CNS [170, 183]. Importantly, replication-competent HIV and SIV are found in monocytes and T cells in PLHIV on ART from both the brain and peripheral tissues [114, 184, 185], indicating that these cells can harbor a virus throughout the disease despite suppression of viral load. The CNS viral reservoir presents a significant challenge to HIV eradication, as it facilitates ongoing viral replication despite ART, influenced by various factors including the BBB.

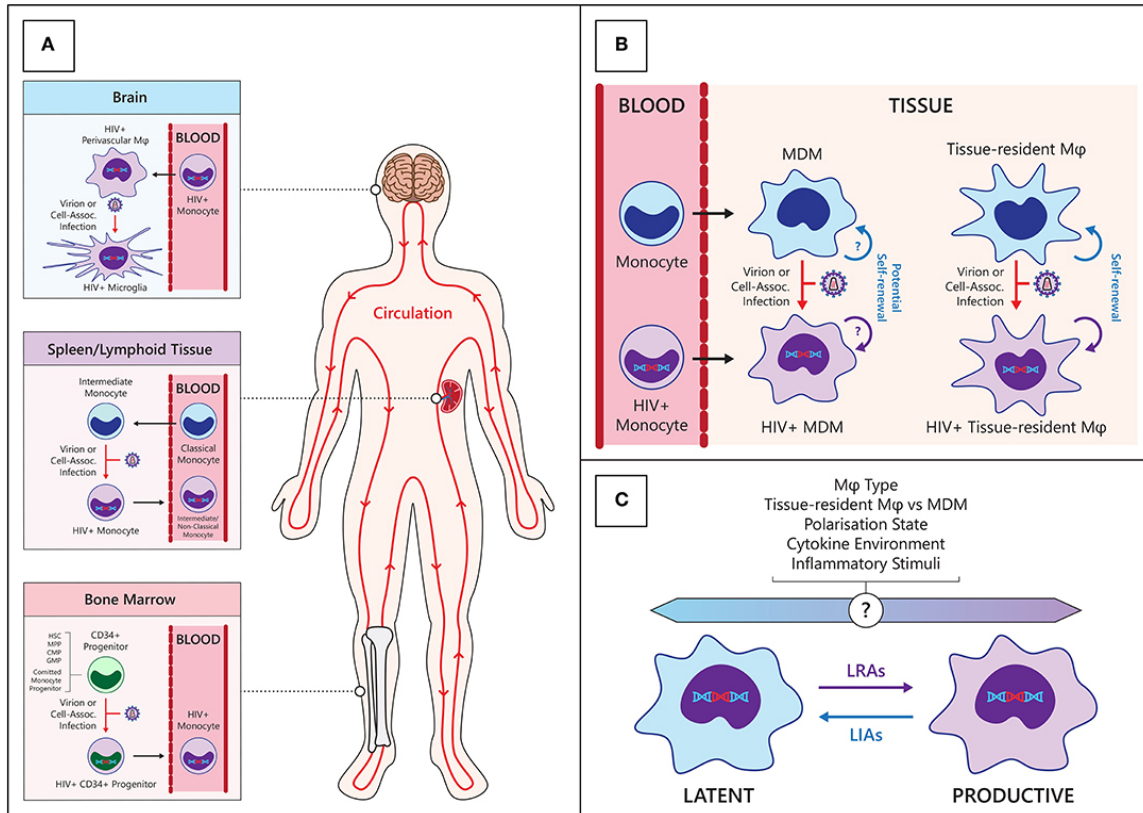


Figure 1.8 Monocyte and Macrophage HIV Reservoir. (A) CD34⁺ progenitors, including hematopoietic stem cells (HSC), multipotent progenitors (MPP), committed myeloid progenitors (CMP), Granulocyte-monocyte progenitors (GMP), and monocyte progenitors in the bone marrow, may become infected with HIV and differentiate into circulating monocytes (bottom panel). Classical monocytes (CD14⁺CD16^{dim}) mature into intermediate monocytes (CD14⁺CD16⁺), entering tissues like the spleen, where they may acquire HIV and re-enter circulation (center panel). Infected monocytes can travel to sanctuary sites, such as the brain, where they differentiate into macrophages (φ), forming viral reservoirs in tissues (top panel). (B) Macrophage HIV reservoirs are maintained by infected monocyte infiltration, new infections of monocyte-derived macrophages (MDMs), and less often, self-renewal of infected tissue-resident macrophages. (C) The HIV state within macrophages is affected by various endogenous and external factors, such as latency-reversing agents (LRAs) and latency-inducing agents (LIAs). Figure reproduced with permission from [The HIV Reservoir in Monocytes and Macrophages](#) by [Wong, M. E., Jaworowski, A., & Hearps, A. C. \(2019\) *Frontiers in immunology*, 10, 1435](#), and is licensed under [CC BY 4.0](#).

1.4 Fluid Within and Out of the CNS

A. Cerebrospinal Fluid (CSF) Within the CNS

Understanding the pathways of fluid movement within and out of the CNS is critical for uncovering how immune cells—particularly HIV and SIV-infected monocytes and macrophages—and antigens travel within the brain and spinal cord. Cerebrospinal fluid (CSF)—primarily produced by the choroid plexus—bathes the entire brain and plays a pivotal role as a medium for delivering essential nutrients, removing metabolic waste, regulating the extracellular environment, providing mechanical support, and maintaining neuronal function and overall brain health [62, 186-188]. On average, roughly 150 mL of CSF circulates within the ventricles and SAS [186, 188]. CSF moves from the lateral ventricles through the foramina of Monro, into the third ventricle and then continues through the aqueduct of Sylvius into the fourth ventricle [186-190]. From the fourth ventricle, CSF can leave laterally through the foramina of Lushka or medially through the foramen of Magendie to fill the subarachnoid space in the cranium or spinal cord [186-190]. CSF exits through the foramina of Lushka and disperses into the SAS surrounding the cisterns and cerebral cortex [186-190]. The conventional understanding is that CSF moves because of the forces produced by cardiac pulsations and breathing [187-189]. Surprisingly, CSF is replaced roughly four times daily [74], indicating the need for constant replenishment to remove waste and potentially immune cells from the CNS.

B. Glymphatic System

The paravascular pathway—also referred to as the “glymphatic system”—has recently been described as a potential pathway for waste clearance from the brain [191]. The glymphatic system transports interstitial fluid (ISF) to the CSF to remove soluble waste from the CNS [192-194]. Recent research has shown a continuous interchange between CSF and ISF, facilitated by the convective influx of CSF along the periarterial space [191]. Using fluorescent tracers injected into the cisterna magna, Iliff *et al.* demonstrated that CSF rapidly penetrates the brain via the cortical pial arteries [191]. This penetration is succeeded by an influx into the Virchow-Robin spaces through penetrating arterioles [191]. Instead of random diffusion, CSF tracers enter via periarterial pathways surrounding vascular smooth muscle cells and are confined by astrocytic end feet [191]. Subsequent analyses revealed that the convective flow of periarterial CSF into and across the brain parenchyma supports the removal of interstitial solutes via perivenous drainage pathways [191]. It has been suggested that the paravascular glymphatic pathway, facilitated by water channels (Aquaporin-4 (AQP4), is a significant route for clearing ISF solutes from the brain parenchyma [191, 193, 195-198]. The combined circulation of CSF and the glymphatic pathway plays a crucial role in clearing waste from the brain, yet the understanding of the impact of fluid drainage and traffic out of the CNS on immune activation is limited.

C. Traditional View of CSF Drainage Out of the CNS

The lack of obvious draining lymphatics in the brain limits the sites for immune cells, fluid, and macromolecules to exit the CNS [51]. The traditional view was that CSF drains

directly into the blood of the superior sagittal sinus through arachnoid villi and granulations (**Figure 1.9, [Reprinted with permission from The Lancet Neurology](#)**) [74]. Arachnoid granulations are clusters of arachnoid membranes that protrude into the dural sinuses and the superior sagittal sinus [186-190], serving as entry points for CSF into the venous system. This reabsorption occurs via a pressure-dependent gradient, with arachnoid granulations serving as conduits for CSF return into the circulation when the subarachnoid pressure exceeds venous sinus pressure [186-190]. Using injections of macromolecular tracers into the lateral ventricle or cisterna magna, Ma *et al.* found that the majority of CSF proceeds through the basal cisterns to the lymphatic outflow pathways from the skull involving arachnoid granulations and cranial nerves to reach extracranial lymphatic vessels [199-201]. Recent studies have found changes in morphology and a reduction in the number of arachnoid granulations with age, contributing to a buildup of metabolic waste and reduced solute clearance as seen with Alzheimer's disease [202-204]. The efficient function of CSF and ISF outflow is crucial for maintaining proper intracranial pressure, waste clearance, and CNS homeostasis, underscoring its significance in neurological health.

D. Perineural Drainage of CSF

In addition to arachnoid granulations, multiple pathways exist for CSF to exit across the cribriform plate but the most widely accepted is the perineural pathways along olfactory nerve sheaths to reach lymphatic vessels of the submucosa (**Figure 1.9, [Reprinted with permission from The Lancet Neurology](#)**) [62, 205, 206]. Weller *et al.* and others have used intracisternal injection of a water-soluble dye and Mircofil tracers to

map CSF drainage from the SAS across the cribriform plate to the nasal lymphatics and accumulation in the deep cervical lymph node [80, 207, 208]. Others found a direct connection between the SAS and the lymphatic network that passes through the cribriform plate—alongside the olfactory nerves—and into the nasal submucosa [80, 208]. Less well described is traffic out of the CNS via other cranial nerves, including the optic nerve, which outflow along this route and tracks along angular and facial veins to reach the submandibular or superficial cervical lymph node [200, 201]. CSF drainage along the cribriform plate involves distinct pathways, with one route accumulating in the deep cervical lymph node via olfactory nerve sheaths and another associated with the optic nerve draining primarily to the superficial cervical lymph node, highlighting the complexity of fluid dynamics in CNS and potential contributions to immune surveillance.

E. Meningeal Lymphatics and CSF Drainage

The discovery of lymphatic vessels in the meninges has revealed a new pathway of fluid movement and how immune surveillance works in the CNS. Recently, Louveau and colleagues used fluorescent dyes to identify and analyze these lymphatic vessels in the meninges (**Figure 1.9, [Reprinted with permission from The Lancet Neurology](#)**) [209]. These meningeal lymphatic vessels run parallel to dural venous sinuses, superior sagittal, and straight sinuses along branches of the meningeal artery [47, 78, 209]. Others have described these meningeal lymphatic vessels as leaving the skull at the cribriform plate, transverse sinuses, or with the middle meningeal artery [210]. It remains unclear whether, in humans and nonhuman primates, these lymphatic vessels in the meninges are draining immune cells, CSF, other macromolecules from the brain, or both.

F. Spinal Drainage of CSF

Despite the extensive work to define fluid drainage pathways from the brain, less is known regarding fluid drainage and the lymphatic networks in the spinal cord. Chen *et al.* and others have suggested that there are several different CSF drainage pathways in the spine, including through arachnoid villi to spinal veins [190, 196, 211-214], along spinal nerve roots to epidural lymphatics [215, 216], and routes through the arachnoid layer to the spinal meninges to dural lymphatics (**Figure 1.9, [Reprinted with permission from The Lancet Neurology](#)**) [217, 218]. Importantly, it has been suggested that roughly 16-25% of CSF drainage and outflow occurs through the spine [219-221]. Recently using intracisternal injection of tracers, near-infrared, and magnetic resonance imaging (MRI), Ma *et al.* identified there is a directional flow of CSF through the central canal from the fourth ventricle to the caudal end of the spine and a cranial-to-caudal movement within the spinal subarachnoid space [199]. In the sacral region of the spine, lymphatic-like vessels were filled with the i.c. injected tracer that emerged from the dorsal sacral spine and tracked caudally to the tail of the mouse [199]. On the ventral side of the spinal cord, lymphatic vessels were found along the axis from the sacral efflux sites, draining CSF in a rostral direction towards the caudal mesenteric and iliac lymph nodes [199]. CSF drainage pathways in the spinal cord underscore the complexity of CSF drainage to other lymphoid tissues in the body, contributing to immune surveillance and neurological health.

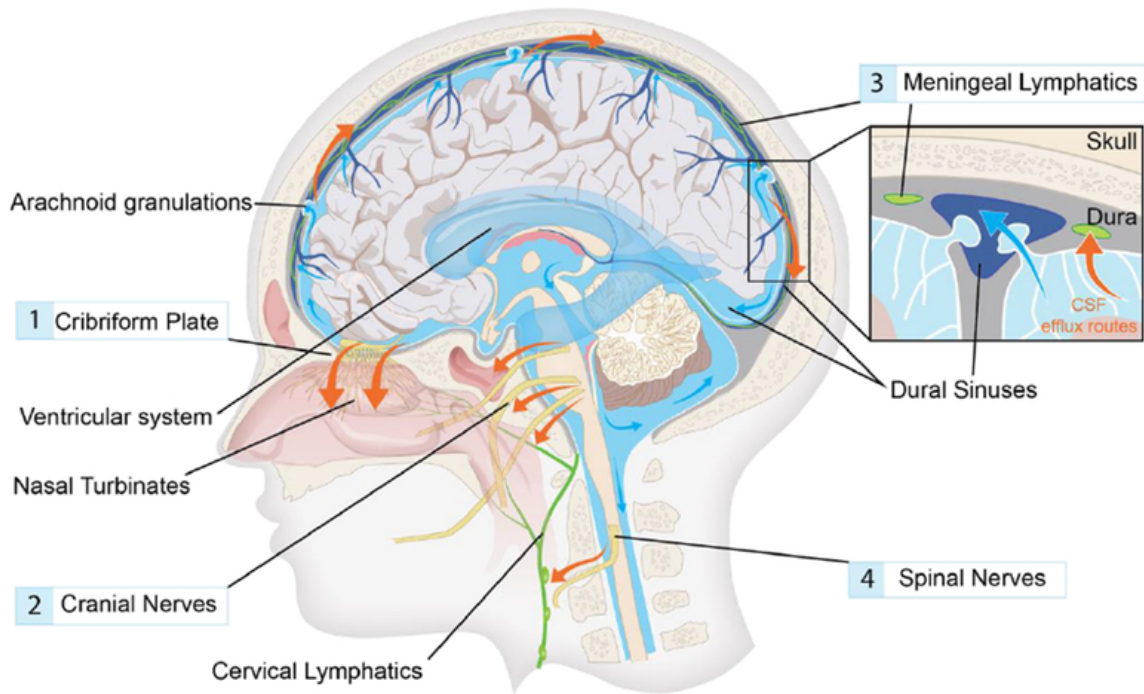


Figure 1.9 CSF Drainage from the CNS. CSF moves from the brain’s ventricles into the SAS, surrounding the brain and spinal cord. CSF exits the skull (red arrows) through three main pathways: perineural sheaths around cranial and spinal nerves, dural lymphatic vessels, and arachnoid granulations. A primary perineural exit site in humans and rodents is along the olfactory nerve through the cribriform plate (1) towards nasal mucosal lymphatic vessels, which drain into the CLNs. Additional pathways include other cranial nerves, such as the trigeminal, glossopharyngeal, vagal, and spinal accessory nerves (2). Dural (meningeal) lymphatics also direct CSF to cervical lymphatics (3) via exits near arteries and veins. Meningeal lymphatics are visualized in humans with MRI around the dural sinuses and the cribriform plate. Arachnoid granulations allow CSF drainage through the sagittal sinus, though little CSF enters the bloodstream at normal pressure. In the spinal cord, CSF exits primarily along spinal nerves (4). Reprinted with permission (5916070636568) from *The Lancet Neurology*, Volume 17 Issue 11, Rasmussen MK, Mestre H, Nedergaard M., *The glymphatic pathway in neurological disorders*, 1016-1024, Copyright (2018), with permission from Elsevier. Also *Lancet* special credit: Reprinted from *The Lancet*, Volume 17 Issue 11, Rasmussen MK, Mestre H, Nedergaard M., *The glymphatic pathway in neurological disorders*, 1016-1024, Copyright (2018), with permission from Elsevier.

1.5 Immune Cell Entry Into the CNS

A. Migration from the Blood and Entry to the CNS

Due to barriers restricting entry, monocyte and macrophage migration from the periphery to the CNS is tightly regulated. The migration of immune cells across the BBB is a multi-step process essential for CNS immune surveillance, but it can be dysregulated during inflammation and viral infection due to altered barrier integrity [56, 57, 69, 222]. Migration of immune cells across the BBB is a well-established process that begins with selectin-mediated vascular rolling, facilitating the initial contact between immune cells and the endothelium [53, 223, 224]. Rolling of immune cells reduces the speed and allows for the recognition of endothelial chemokines with their subsequent receptor [53, 223, 224]. This leads to the activation of adhesion molecules and results in firm arrestment of the immune cell on the luminal surface of endothelial cells, allowing the migration across the endothelial cells at endothelial junctions referred to as diapedesis [53, 223, 224]. Integrins, chemokine receptors, and adhesion molecules—such as vascular cell adhesion molecule 1 (VCAM-1) and intercellular adhesion molecule (ICAM-1) bind to very late antigen-4 (VLA-4, also known as $\alpha 4\beta 1$ integrin)—found on immune cells in the blood and cells within the CNS enable immune cells to move across the BBB. Peripheral immune cells can enter the CNS by: (i) migration directly from the blood via postcapillary venules in the parenchyma, (ii) postcapillary venules in the meninges, and (iii) migration through the choroid plexus into the SAS and subsequent CSF [51, 52, 225]. To traverse postcapillary venules in the parenchyma, immune cells must migrate across inner and outer basement membranes, whereas meninges vasculature

is a simple, one-layer structure [52, 53, 55, 225]. Unlike the rest of the CNS, the endothelial cells of the choroid plexus allow immune cell entry into the CSF due to the lack of continuous tight junctions [51, 56, 64, 225, 226], resulting in a leaky interphase between the choroid plexus stroma and vasculature [64, 225-227]. However, the epithelium of the choroid plexus is composed of a dense network of tight junctions and restricts the entry of cells and molecules from the stroma into the CSF (the BCSFB) [224]. Importantly, inflammation and viral infection can disrupt the expression of integrins, chemokine receptors, and adhesion molecules on both immune cells circulating in the blood, and the activation of astrocytes and endothelial cells within the CNS results in reduced integrity of the BBB [51, 57, 69, 228].

B. Increased Monocyte Traffic to the CNS with HIV and SIV Infection

Although increased viral load in plasma and CSF correlates with viral infiltration to the brain [229], HAND persists with ART-suppressed viremia, indicating that myeloid activation is driving CNS pathology and HIV-SN [183]. We and others have shown that with HIV and SIV infection, there is increased traffic of monocytes to the CNS and subsequent accumulation in the brain [108]. CD34+ myeloid progenitor cells in the bone marrow differentiate into CD14+ monocytes, which circulate in the blood for 3-5 days before entering tissues to become macrophages and myeloid dendritic cells (**Figure 1.8, *reproduced with permission and licensed under CC BY 4.0***) [230]. Importantly, these progenitors in the bone marrow can become infected with HIV and SIV, resulting in the production of virally infected monocytes (**Figure 1.8, *reproduced with permission and licensed under CC BY 4.0***) [231, 232]. Using autologous transfer of enhanced green

fluorescent protein (EGFP) CD34⁺ hemopoietic stem cells, we found a correlation between the percentage of EGFP⁺ monocytes in the blood and the percentage of EGFP⁺ PVM in the CNS, suggesting that perivascular macrophage turnover is directly influenced by peripheral immune activation and viral infection [108]. Using intravenous injection of bromodeoxyuridine (BrdU⁺)—incorporated into DNA during S phase—we have found that increased monocyte production from the bone marrow (BrdU⁺ Monocytes) is directly correlated with HIV and SIV disease progression [29]. Furthermore, BrdU⁺ monocyte turnover and plasma soluble CD163 (sCD163⁺)—a biomarker of macrophage activation—is a more accurate indicator of AIDS progression than plasma viral load or CD4⁺ T cell count [29, 233-235], underscoring the role of monocyte and macrophage activation in HIV and SIV pathogenesis. While the traffic of blood-derived immune cells to the CNS is well-documented and increased during inflammation and viral infection [107, 112, 236, 237], the fate of these cells within the CNS remains understudied.

1.6 Immune Cell Traffic out of the CNS

Drainage of fluid out of the CNS is well established, less known is the traffic of immune cells out of the CNS and implications for immune activation and tolerance. CNS antigens have been found in the deep cervical lymph node [192, 238] and even the lumbar lymph nodes [239], but whether these are drained from the CNS with fluid or traffic out via APCs has not been well defined. It is well known that there is drainage of CNS antigens out to the cervical lymph nodes; however, in the context of HIV infection, it raises significant concerns about whether virally infected immune cells can traffic out

and reseed the periphery, potentially contributing to ongoing viral dissemination and chronic immune activation.

A. Potential Pathways of Monocytes and Macrophages Out of the Brain

Monocytes and macrophages in the CNS may utilize various pathways to exit, many of which are similarly associated with fluid drainage (**Figure 1.10, *reproduced with permission and licensed under [CC BY 4.0](#)***). The basal and dorsal dural lymphatics (meningeal lymphatics) is a network of lymphatic vessels located in the basal dura mater and are proposed to play a crucial role in the egress of immune cells from the brain [76]. These lymphatic vessels are part of a broader dural lymphatic system to drain immune cells and interstitial fluid from the CNS [47, 76, 240]. In this context, the glymphatic system facilitates the flow of CSF along perivascular spaces, promoting the movement of fluids through the brain tissue and into the SAS [47, 241]. Monocytes, macrophages, and T cells could use these perivascular routes to migrate to dorsal leptomeningeal regions [48, 241-245]. Once immune cells reach the SAS, they are hypothesized to traverse the arachnoid mater and move into lymphatic vessels in the dura mater [48, 241-245]. This migration is thought to occur particularly at "hotspots" where the arachnoid barrier is more permeable or potentially incomplete [246-248]. The olfactory bulb-cribriform lymphatic axis also represents a unique pathway for immune cells to migrate from the CNS to the periphery. The olfactory nerves extend from the olfactory bulb through the foramina in the cribriform plate of the skull [80, 205, 206, 208, 249]. Notably, the meningeal layers surrounding these nerves are discontinuous, with possible gaps in the arachnoid mater [80, 205]. Lymphatic vessels are closely associated with these nerve bundles near the cribriform plate, and in mice, these lymphatic vessels extend through the

cribriform plate into the CNS side of the skull, potentially aligning with the discontinuities in the meningeal layers [80, 206, 250]. Immune cell migration along spinal nerves may allow immune cells to leave the CNS from the SAS and migrate into peripheral tissues [80, 205, 206, 208, 249].

The lack of clear lymphatic drainage pathways in the brain limits pathways that immune cells and fluid can exit the CNS underscoring the complex process of waste removal and immune surveillance within the brain. Goldman *et al.* and others have found that T cells can exit the CNS via the cribriform plate, a bone sieve-like structure at the base of the skull that separates the nasal cavity from the brain [251]. This process involves the migration of T cells from the CNS into CSF, where they can then travel along the olfactory nerve pathways [251]. As T cells traverse the cribriform plate, they follow chemotactic signals (CCR7) [202, 239] that guide them to the deep cervical lymph node [251]. This pathway is significant for immune surveillance and the regulation of inflammatory responses, as it enables T cells to move from the CNS to the deep cervical lymph nodes, resulting in activation and proliferation in response to antigens or induce tolerance [43, 45, 147, 192, 252]. Importantly, whether there is cellular traffic out of the CNS has not been studied in humans, non-human primates, and particularly in the context of AIDS and with ART.

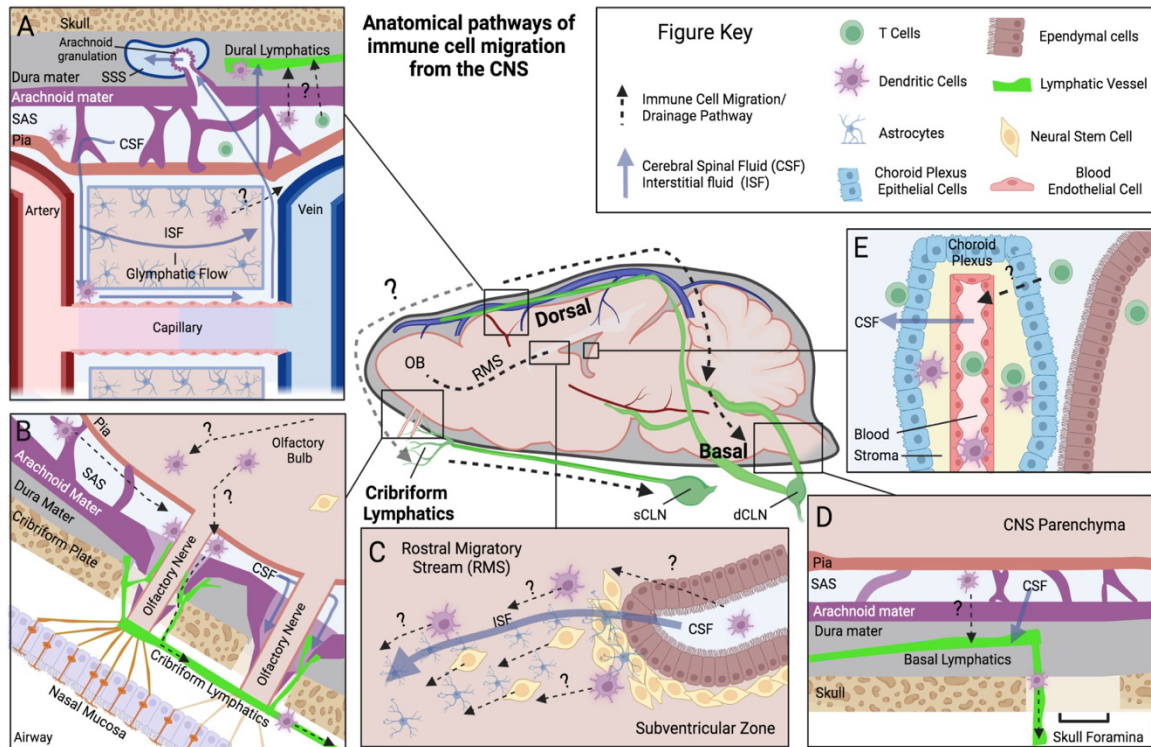


Figure 1.10 Pathways of Immune Cells Out of the CNS. Schematic showing proposed immune cell migration pathways (dotted lines) and common fluid movement pathways (solid blue lines) within the brain and meningeal compartments, based on rodent studies. Each panel highlights a different anatomical site for potential immune migration: **(A)** Dorsal dural lymphatics and glymphatic system, where perivascular glymphatic flow may transport immune cells to leptomeningeal spaces (Pia, SAS, Arachnoid), possibly crossing into dural lymphatics. **(B)** Olfactory bulb-cribriform lymphatic axis, where immune cells and CSF may move along the olfactory nerves through gaps in the arachnoid and exit to nasal mucosa. **(C)** Rostral migratory stream (RMS), an intra-parenchymal path for neural stem cells and DCs moving from the subventricular zone to the olfactory bulb (Note: not a pathway discussed in this thesis because this pathway is more commonly referred to for neuronal precursors to establish in the brain, and less likely a pathway of exit to the periphery). **(D)** Basal dural lymphatics, where immune cells exit from the skull through basal dura lymphatics. **(E)** Choroid plexus may facilitate immune cell egress back to the bloodstream. Acronyms: CSF = cerebrospinal fluid; ISF = interstitial fluid; SAS = subarachnoid space; OB = olfactory bulb; sCLN = superficial cervical lymph node; dCLN = deep cervical lymph node. Figure reproduced with permission from [Immune cells as messengers from the CNS to the periphery: the role of the meningeal lymphatic system in immune cell migration from the CNS](#) by [Laaker, C., Baenen, C., Kovács, K. G., Sandor, M., & Fabry, Z. \(2023\) *Frontiers in immunology*, 14, 1233908](#) and is licensed under [CC BY 4.0](#).

B. Potential Pathways of Monocytes and Macrophages Out of the Spinal Cord

Not only could immune cells leave the brain, but they could also leave via the spinal cord. The spinal lymphatic system, comprising lymphatic vessels along the dura mater of the spinal cord, plays a crucial role in maintaining fluid homeostasis and immune surveillance within the CNS [253]. These vessels, extending the length of the spine, facilitate the drainage of excess CSF and ISF [253]; they also may remove immune cells from the CNS to larger lymphatic ducts like the thoracic duct that return these fluids and cells to the blood [253]. In addition, spinal nerve root sheaths envelop the spinal nerve roots as they leave the spinal cord through the intervertebral foramina [199, 253-257]. These sheaths consist of layers of connective tissue (dura, arachnoid, and pia mater) which are continuous with the meninges surrounding the spinal cord. The interface between the SAS and the spinal nerve root sheaths is relatively permeable, facilitating the exchange of fluid and solutes between the CSF and the perineural space surrounding the spinal nerves [257, 258]. In response to inflammation or injury, the permeability of the spinal nerve root sheaths may increase [253]. This environment facilitates the movement of immune cells, cytokines, and other inflammatory mediators from the CSF into the perineural space and vice versa [253, 258]. Immune cells, including macrophages, T Cells, and DCs, can traffic along the spinal nerve root sheaths [257, 258]. They may enter the perineural space from the CSF within the subarachnoid space or migrate from the surrounding tissues [257, 258]. Once in the perineural space and exiting from the CNS, immune cells may access nearby lymphatic vessels or lymph nodes [253, 257, 258].

1.7 Superparamagnetic Iron Oxide Nanoparticles to Track Immune Cell Migration out of the CNS

A. Superparamagnetic Iron Oxide Nanoparticles (SPION)

Superparamagnetic Iron Oxide Nanoparticles (SPION) are nanoparticles with an iron core coated with a biocompatible polymer [259]. SPION cores, made of iron oxides, can be directed to specific areas using external magnets and exhibit superparamagnetism and high saturation field, resulting in the absence of residual magnetism after the external field is removed [259-261]. The SPION coating protects the magnetic particle from its environment and can be functionalized by attaching carboxyl groups, biotin, avidin, carbodiimide, and other molecules [259]. SPION have been widely used for *in vivo* biomedical applications, such as contrast enhancement in MRI, drug delivery, and magnetic hyperthermia [259-262]. SPION are generally viewed as biologically inert; however, their toxicity varies based on size, concentration, surface charge, and coatings [259-262]. In some cases, it has been shown that excess iron can promote reactive oxygen species production, which leads to oxidative stress and potentially cell death, also known as ferroptosis caused by excess iron [263-265]. However, other studies did not find that SPION dissolves at low pH, and colocalization in lysosomal colocalization was not reduced, but some dissolution in artificial lysosomal fluid was observed and could cause stress in the endoplasmic reticulum [266]. Other studies have observed SPIONs induce macrophage polarization towards the “pro-inflammatory M1 phenotype”, which has been repurposed in cancer research to target tumors [267, 268]. In addition, iron oxide nanoparticles can break down and be cleared in the spleen and liver, but it usually takes more than 100 days, depending on their size and coating [269].

B. SPION to Label Macrophage *in vivo*

The Bangs Laboratory encapsulated microspheres can be taken up by macrophages and are coated in a proprietary material made up of polystyrene divinylbenzene, which is more resistant to thermal degradation [270]. Within 30 minutes to 1 hour, SPION are quickly taken up by human macrophages, and after 24 hours, confocal microscopy showed they were mainly found in the lysosomes [265]. Factors such as size and flow rate can influence the uptake of nanoparticles by macrophages where the optimal size for macrophage uptake is around 1-2 μm , while smaller particles (0.4-1 μm) are primarily internalized by leukocytes [271]. For smaller particles (200-500 nm), internalization was similar at low flow rates (0.1 and 1 mL/min) but increased significantly at higher flow rates (10 mL/min) [272]. Using polystyrene particles of various sizes, ranging from 2.9 nm, others have shown that the majority of particles were internalized (RAW 264.7, HL-60, and human PBMCs) within 30 minutes under both static and flow conditions [272]. For larger particles, internalized did not differ between static and flow conditions [272]. This suggests that nanoparticles, including polystyrene and SPIONs ($\sim 1 \mu\text{m}$), are efficiently internalized by macrophages within a specific size range unchanged by flow rate. Macrophage uptake capacity remains consistent under static and flow conditions, but higher flow rates may enhance the uptake efficiency of smaller particles ($< 0.5 \mu\text{m}$). In macrophages, when the concentration of SPIONs exceeds 50 $\mu\text{g/ml}$, SPION can cause increased toxicity, leading to reduced cell activity, higher ROS levels, and cell damage [273, 274]. In our study, we used a lower concentration of SPION (30 $\mu\text{g/ml}$) to reduce potential toxicity. Importantly, using the Bangs Laboratory

encapsulated microspheres, others have reported low toxicity within a 28-day examination period [275, 276].

1.8 References

1. *Global HIV & AIDS statistics — Fact sheet*. 2024 [cited 2024; Available from: <https://www.unaids.org/en/resources/fact-sheet>].
2. Sharp, P.M. and B.H. Hahn, *Origins of HIV and the AIDS pandemic*. Cold Spring Harb Perspect Med, 2011. **1**(1): p. a006841.
3. Apetrei, C., et al., *Molecular epidemiology of simian immunodeficiency virus SIVsm in U.S. primate centers unravels the origin of SIVmac and SIVstm*. J Virol, 2005. **79**(14): p. 8991-9005.
4. Gao, F., et al., *Origin of HIV-1 in the chimpanzee Pan troglodytes troglodytes*. Nature, 1999. **397**(6718): p. 436-41.
5. Cohn, L.B., N. Chomont, and S.G. Deeks, *The Biology of the HIV-1 Latent Reservoir and Implications for Cure Strategies*. Cell Host Microbe, 2020. **27**(4): p. 519-530.
6. Deeks, S.G., R. Tracy, and D.C. Douek, *Systemic effects of inflammation on health during chronic HIV infection*. Immunity, 2013. **39**(4): p. 633-45.
7. Moir, S., T.W. Chun, and A.S. Fauci, *Pathogenic mechanisms of HIV disease*. Annu Rev Pathol, 2011. **6**: p. 223-48.
8. Doms, R.W. and J.P. Moore, *HIV-1 membrane fusion: targets of opportunity*. J Cell Biol, 2000. **151**(2): p. F9-14.
9. Markowitz, M., et al., *A novel antiviral intervention results in more accurate assessment of human immunodeficiency virus type 1 replication dynamics and T-cell decay in vivo*. J Virol, 2003. **77**(8): p. 5037-8.
10. Kruize, Z. and N.A. Kootstra, *The Role of Macrophages in HIV-1 Persistence and Pathogenesis*. Frontiers in Microbiology, 2019. **10**.
11. Clayton, K.L., et al., *HIV Infection of Macrophages: Implications for Pathogenesis and Cure*. Pathog Immun, 2017. **2**(2): p. 179-192.
12. Venzke, S. and O.T. Keppler, *Role of macrophages in HIV infection and persistence*. Expert Rev Clin Immunol, 2006. **2**(4): p. 613-26.
13. Gannon, P., M.Z. Khan, and D.L. Kolson, *Current understanding of HIV-associated neurocognitive disorders pathogenesis*. Curr Opin Neurol, 2011. **24**(3): p. 275-83.
14. Price, R.W. and S. Spudich, *Antiretroviral therapy and central nervous system HIV type 1 infection*. The Journal of infectious diseases, 2008. **197** Suppl 3(Suppl 3): p. S294-S306.

15. Achappa, B., et al., *Adherence to Antiretroviral Therapy Among People Living with HIV*. N Am J Med Sci, 2013. **5**(3): p. 220-3.
16. Williams, K., A. Lackner, and J. Mallard, *Non-human primate models of SIV infection and CNS neuropathology*. Curr Opin Virol, 2016. **19**: p. 92-8.
17. Bednar, M.M., et al., *Compartmentalization, Viral Evolution, and Viral Latency of HIV in the CNS*. Curr HIV/AIDS Rep, 2015. **12**(2): p. 262-71.
18. Wang, Y., et al., *Global prevalence and burden of HIV-associated neurocognitive disorder: A meta-analysis*. Neurology, 2020. **95**(19): p. e2610-e2621.
19. Saylor, D., et al., *HIV-associated neurocognitive disorder — pathogenesis and prospects for treatment*. Nature Reviews Neurology, 2016. **12**(4): p. 234-248.
20. Burdo, T.H. and A.D. Miller, *Animal models of HIV peripheral neuropathy*. Future Virology, 2014. **9**(5): p. 465-474.
21. Burdo, T.H., et al., *Dorsal root ganglia damage in SIV-infected rhesus macaques: an animal model of HIV-induced sensory neuropathy*. Am J Pathol, 2012. **180**(4): p. 1362-9.
22. Gabbai, A.A., A. Castelo, and A.S. Oliveira, *HIV peripheral neuropathy*. Handb Clin Neurol, 2013. **115**: p. 515-29.
23. Keswani, S.C., et al., *HIV-associated sensory neuropathies*. AIDS, 2002. **16**(16): p. 2105-2117.
24. Laast, V.A., et al., *Macrophage-mediated dorsal root ganglion damage precedes altered nerve conduction in SIV-infected macaques*. Am J Pathol, 2011. **179**(5): p. 2337-45.
25. Morgello, S., et al., *HIV-associated distal sensory polyneuropathy in the era of highly active antiretroviral therapy: the Manhattan HIV Brain Bank*. Arch Neurol, 2004. **61**(4): p. 546-51.
26. Pandya, R., et al., *HIV-related neurological syndromes reduce health-related quality of life*. Can J Neurol Sci, 2005. **32**(2): p. 201-4.
27. Schifitto, G., et al., *Incidence of and risk factors for HIV-associated distal sensory polyneuropathy*. Neurology, 2002. **58**(12): p. 1764-8.
28. Hatzioannou, T. and D.T. Evans, *Animal models for HIV/AIDS research*. Nature Reviews Microbiology, 2012. **10**(12): p. 852-867.
29. Burdo, T.H., et al., *Increased monocyte turnover from bone marrow correlates with severity of SIV encephalitis and CD163 levels in plasma*. PLoS Pathog, 2010. **6**(4): p. e1000842.

30. Nowlin, B.T., et al., *Monocyte subsets exhibit transcriptional plasticity and a shared response to interferon in SIV-infected rhesus macaques*. J Leukoc Biol, 2018. **103**(1): p. 141-155.
31. Williams, K., et al., *Proliferating cellular nuclear antigen expression as a marker of perivascular macrophages in simian immunodeficiency virus encephalitis*. Am J Pathol, 2002. **161**(2): p. 575-85.
32. Nowlin, B.T., et al., *SIV encephalitis lesions are composed of CD163(+) macrophages present in the central nervous system during early SIV infection and SIV-positive macrophages recruited terminally with AIDS*. Am J Pathol, 2015. **185**(6): p. 1649-65.
33. Beck, S.E., et al., *An SIV/macaque model targeted to study HIV-associated neurocognitive disorders*. Journal of neurovirology, 2018. **24**(2): p. 204-212.
34. Cartwright, E.K., et al., *CD8(+) Lymphocytes Are Required for Maintaining Viral Suppression in SIV-Infected Macaques Treated with Short-Term Antiretroviral Therapy*. Immunity, 2016. **45**(3): p. 656-668.
35. Ratai, E.M., et al., *CD8+ lymphocyte depletion without SIV infection does not produce metabolic changes or pathological abnormalities in the rhesus macaque brain*. J Med Primatol, 2011. **40**(5): p. 300-9.
36. Rife Magalis, B., et al., *Insights into the Impact of CD8(+) Immune Modulation on Human Immunodeficiency Virus Evolutionary Dynamics in Distinct Anatomical Compartments by Using Simian Immunodeficiency Virus-Infected Macaque Models of AIDS Progression*. J Virol, 2017. **91**(23).
37. Westmoreland, S.V., E. Halpern, and A.A. Lackner, *Simian immunodeficiency virus encephalitis in rhesus macaques is associated with rapid disease progression*. J Neurovirol, 1998. **4**(3): p. 260-8.
38. Crews, L., et al., *Neuronal injury in simian immunodeficiency virus and other animal models of neuroAIDS*. J Neurovirol, 2008. **14**(4): p. 327-39.
39. Fox, H.S., et al., *Simian Immunodeficiency Virus: A Model for NeuroAIDS*. Neurobiology of Disease, 1997. **4**(3): p. 265-274.
40. Kleihues, P., et al., *HIV encephalopathy: incidence, definition and pathogenesis. Results of a Swiss collaborative study*. Acta Pathol Jpn, 1991. **41**(3): p. 197-205.
41. Shaw, G.M. and E. Hunter, *HIV transmission*. Cold Spring Harb Perspect Med, 2012. **2**(11).
42. Andrew, A. and K. Strebel, *HIV-1 accessory proteins: Vpu and Vif*. Methods Mol Biol, 2014. **1087**: p. 135-58.

43. Carson, M.J., et al., *CNS immune privilege: hiding in plain sight*. Immunol Rev, 2006. **213**: p. 48-65.
44. Forrester, J.V., P.G. McMenamin, and S.J. Dando, *CNS infection and immune privilege*. Nat Rev Neurosci, 2018. **19**(11): p. 655-671.
45. Engelhardt, B., P. Vajkoczy, and R.O. Weller, *The movers and shapers in immune privilege of the CNS*. Nat Immunol, 2017. **18**(2): p. 123-131.
46. Raper, D., A. Louveau, and J. Kipnis, *How Do Meningeal Lymphatic Vessels Drain the CNS?* Trends Neurosci, 2016. **39**(9): p. 581-586.
47. Absinta, M., et al., *Human and nonhuman primate meninges harbor lymphatic vessels that can be visualized noninvasively by MRI*. eLife, 2017. **6**: p. e29738.
48. Da Mesquita, S., Z. Fu, and J. Kipnis, *The Meningeal Lymphatic System: A New Player in Neurophysiology*. Neuron, 2018. **100**(2): p. 375-388.
49. Engelhardt, B. and L. Sorokin, *The blood-brain and the blood-cerebrospinal fluid barriers: function and dysfunction*. Semin Immunopathol, 2009. **31**(4): p. 497-511.
50. Rubin, L.L. and J.M. Staddon, *The cell biology of the blood-brain barrier*. Annu Rev Neurosci, 1999. **22**: p. 11-28.
51. Wilson, E.H., W. Weninger, and C.A. Hunter, *Trafficking of immune cells in the central nervous system*. J Clin Invest, 2010. **120**(5): p. 1368-79.
52. Mrass, P. and W. Weninger, *Immune cell migration as a means to control immune privilege: lessons from the CNS and tumors*. Immunological Reviews, 2006. **213**(1): p. 195-212.
53. Engelhardt, B. and R.M. Ransohoff, *The ins and outs of T-lymphocyte trafficking to the CNS: anatomical sites and molecular mechanisms*. Trends Immunol, 2005. **26**(9): p. 485-95.
54. Stamatovic, S.M., R.F. Keep, and A.V. Andjelkovic, *Brain endothelial cell-cell junctions: how to "open" the blood brain barrier*. Curr Neuropharmacol, 2008. **6**(3): p. 179-92.
55. Bechmann, I., I. Galea, and V.H. Perry, *What is the blood-brain barrier (not)?* Trends Immunol, 2007. **28**(1): p. 5-11.
56. Tietz, S. and B. Engelhardt, *Brain barriers: Crosstalk between complex tight junctions and adherens junctions*. J Cell Biol, 2015. **209**(4): p. 493-506.

57. Kadry, H., B. Noorani, and L. Cucullo, *A blood–brain barrier overview on structure, function, impairment, and biomarkers of integrity*. Fluids and Barriers of the CNS, 2020. **17**(1): p. 69.
58. Redzic, Z.B. and M.B. Segal, *The structure of the choroid plexus and the physiology of the choroid plexus epithelium*. Advanced Drug Delivery Reviews, 2004. **56**(12): p. 1695-1716.
59. Schmidley, J.W. and S.L. Wissig, *Anionic sites on the luminal surface of fenestrated and continuous capillaries of the CNS*. Brain Res, 1986. **363**(2): p. 265-71.
60. Sakka, L., G. Coll, and J. Chazal, *Anatomy and physiology of cerebrospinal fluid*. Eur Ann Otorhinolaryngol Head Neck Dis, 2011. **128**(6): p. 309-16.
61. Cui, J., H. Xu, and M.K. Lehtinen, *Macrophages on the margin: choroid plexus immune responses*. Trends Neurosci, 2021. **44**(11): p. 864-875.
62. Proulx, S.T., *Cerebrospinal fluid outflow: a review of the historical and contemporary evidence for arachnoid villi, perineural routes, and dural lymphatics*. Cellular and Molecular Life Sciences, 2021. **78**(6): p. 2429-2457.
63. Thompson, D., C.A. Brissette, and J.A. Watt, *The choroid plexus and its role in the pathogenesis of neurological infections*. Fluids and Barriers of the CNS, 2022. **19**(1): p. 75.
64. Meeker, R.B., et al., *Cell trafficking through the choroid plexus*. Cell Adh Migr, 2012. **6**(5): p. 390-6.
65. Sarnat, H.B., *Histochemistry and immunocytochemistry of the developing ependyma and choroid plexus*. Microsc Res Tech, 1998. **41**(1): p. 14-28.
66. Liddelow, S.A., et al., *Mechanisms that determine the internal environment of the developing brain: a transcriptomic, functional and ultrastructural approach*. PLoS One, 2013. **8**(7): p. e65629.
67. Liddelow, S.A., *Development of the choroid plexus and blood-CSF barrier*. Front Neurosci, 2015. **9**: p. 32.
68. Del Bigio, M.R., *Ependymal cells: biology and pathology*. Acta Neuropathol, 2010. **119**(1): p. 55-73.
69. Hernández-Parra, H., et al., *Alteration of the blood-brain barrier by COVID-19 and its implication in the permeation of drugs into the brain*. Front Cell Neurosci, 2023. **17**: p. 1125109.

70. Weller, R.O., et al., *The meninges as barriers and facilitators for the movement of fluid, cells and pathogens related to the rodent and human CNS*. Acta Neuropathol, 2018. **135**(3): p. 363-385.
71. Klarica, M., M. Radoš, and D. Orešković, *The Movement of Cerebrospinal Fluid and Its Relationship with Substances Behavior in Cerebrospinal and Interstitial Fluid*. Neuroscience, 2019. **414**: p. 28-48.
72. Weerasuriya, A. and A.P. Mizisin, *The blood-nerve barrier: structure and functional significance*. Methods Mol Biol, 2011. **686**: p. 149-73.
73. Liu, Q., X. Wang, and S. Yi, *Pathophysiological Changes of Physical Barriers of Peripheral Nerves After Injury*. Frontiers in Neuroscience, 2018. **12**.
74. Johanson, C.E., et al., *Multiplicity of cerebrospinal fluid functions: New challenges in health and disease*. Cerebrospinal Fluid Research, 2008. **5**(1): p. 10.
75. Rua, R. and D.B. McGavern, *Advances in Meningeal Immunity*. Trends Mol Med, 2018. **24**(6): p. 542-559.
76. Rustenhoven, J., et al., *Functional characterization of the dural sinuses as a neuroimmune interface*. Cell, 2021. **184**(4): p. 1000-1016.e27.
77. Alves de Lima, K., J. Rustenhoven, and J. Kipnis, *Meningeal Immunity and Its Function in Maintenance of the Central Nervous System in Health and Disease*. Annu Rev Immunol, 2020. **38**: p. 597-620.
78. Louveau, A., *Meningeal Immunity, Drainage, and Tertiary Lymphoid Structure Formation*. Methods Mol Biol, 2018. **1845**: p. 31-45.
79. Rebejac, J., et al., *Meningeal macrophages protect against viral neuroinfection*. Immunity, 2022. **55**(11): p. 2103-2117.e10.
80. Kida, S., A. Pantazis, and R.O. Weller, *CSF drains directly from the subarachnoid space into nasal lymphatics in the rat. Anatomy, histology and immunological significance*. Neuropathol Appl Neurobiol, 1993. **19**(6): p. 480-8.
81. Smyth, L.C.D., et al., *Identification of direct connections between the dura and the brain*. Nature, 2024. **627**(8002): p. 165-173.
82. Haller, F.R. and F.N. Low, *The fine structure of the peripheral nerve root sheath in the subarachnoid space in the rat and other laboratory animals*. Am J Anat, 1971. **131**(1): p. 1-19.
83. Shanthaveerappa, T.R. and G.H. Bourne, *The 'perineural epithelium', a metabolically active, continuous, protoplasmic cell barrier surrounding peripheral nerve fasciculi*. J Anat, 1962. **96**(Pt 4): p. 527-37.

84. McCabe, J.S. and F.N. Low, *The subarachnoid angle: An area of transition in peripheral nerve*. The Anatomical Record, 1969. **164**(1): p. 15-33.
85. Fischer-Smith, T., et al., *Monocyte/macrophage trafficking in acquired immunodeficiency syndrome encephalitis: lessons from human and nonhuman primate studies*. J Neurovirol, 2008. **14**(4): p. 318-26.
86. Herz, J., et al., *Myeloid Cells in the Central Nervous System*. Immunity, 2017. **46**(6): p. 943-956.
87. Quintana, F.J., *Myeloid cells in the central nervous system: So similar, yet so different*. Science Immunology, 2019. **4**(32): p. eaaw2841.
88. Kierdorf, K. and M. Prinz, *Microglia in steady state*. J Clin Invest, 2017. **127**(9): p. 3201-3209.
89. Li, Q. and B.A. Barres, *Microglia and macrophages in brain homeostasis and disease*. Nat Rev Immunol, 2018. **18**(4): p. 225-242.
90. Barron, K.D., *The microglial cell. A historical review*. J Neurol Sci, 1995. **134 Suppl**: p. 57-68.
91. Ransohoff, R.M. and V.H. Perry, *Microglial physiology: unique stimuli, specialized responses*. Annu Rev Immunol, 2009. **27**: p. 119-45.
92. Alliot, F., I. Godin, and B. Pessac, *Microglia derive from progenitors, originating from the yolk sac, and which proliferate in the brain*. Brain Res Dev Brain Res, 1999. **117**(2): p. 145-52.
93. Ginhoux, F., et al., *Fate mapping analysis reveals that adult microglia derive from primitive macrophages*. Science, 2010. **330**(6005): p. 841-5.
94. Ginhoux, F., et al., *Origin and differentiation of microglia*. Frontiers in cellular neuroscience, 2013. **7**: p. 45.
95. Ajami, B., et al., *Local self-renewal can sustain CNS microglia maintenance and function throughout adult life*. Nat Neurosci, 2007. **10**(12): p. 1538-43.
96. Kierdorf, K., et al., *Microglia emerge from erythromyeloid precursors via *Pu.1*- and *Irf8*-dependent pathways*. Nat Neurosci, 2013. **16**(3): p. 273-80.
97. Nayak, D., T.L. Roth, and D.B. McGavern, *Microglia development and function*. Annual review of immunology, 2014. **32**: p. 367-402.
98. Kim, W.K., et al., *CD163 identifies perivascular macrophages in normal and viral encephalitic brains and potential precursors to perivascular macrophages in blood*. Am J Pathol, 2006. **168**(3): p. 822-34.

99. Hansen, D.V., J.E. Hanson, and M. Sheng, *Microglia in Alzheimer's disease*. Journal of Cell Biology, 2017. **217**(2): p. 459-472.
100. Cheng, J., et al., *Microglial autophagy defect causes parkinson disease-like symptoms by accelerating inflammasome activation in mice*. Autophagy, 2020. **16**(12): p. 2193-2205.
101. Wang, Z., et al., *Microglial autophagy in Alzheimer's disease and Parkinson's disease*. Front Aging Neurosci, 2022. **14**: p. 1065183.
102. Silvin, A., J. Qian, and F. Ginhoux, *Brain macrophage development, diversity and dysregulation in health and disease*. Cellular & Molecular Immunology, 2023.
103. Faraco, G., et al., *Brain perivascular macrophages: characterization and functional roles in health and disease*. J Mol Med (Berl), 2017. **95**(11): p. 1143-1152.
104. Kierdorf, K., et al., *Macrophages at CNS interfaces: ontogeny and function in health and disease*. Nat Rev Neurosci, 2019. **20**(9): p. 547-562.
105. Goldmann, T., et al., *Origin, fate and dynamics of macrophages at central nervous system interfaces*. Nat Immunol, 2016. **17**(7): p. 797-805.
106. Faraco, G., et al., *Perivascular macrophages mediate the neurovascular and cognitive dysfunction associated with hypertension*. J Clin Invest, 2016. **126**(12): p. 4674-4689.
107. Bechmann, I., et al., *Immune surveillance of mouse brain perivascular spaces by blood-borne macrophages*. Eur J Neurosci, 2001. **14**(10): p. 1651-8.
108. Soulas, C., et al., *Genetically modified CD34+ hematopoietic stem cells contribute to turnover of brain perivascular macrophages in long-term repopulated primates*. Am J Pathol, 2009. **174**(5): p. 1808-17.
109. Lassmann, H., et al., *Bone marrow derived elements and resident microglia in brain inflammation*. Glia, 1993. **7**(1): p. 19-24.
110. Hickey, W.F., K. Vass, and H. Lassmann, *Bone marrow-derived elements in the central nervous system: an immunohistochemical and ultrastructural survey of rat chimeras*. J Neuropathol Exp Neurol, 1992. **51**(3): p. 246-56.
111. Burdo, T.H., A. Lackner, and K.C. Williams, *Monocyte/macrophages and their role in HIV neuropathogenesis*. Immunological Reviews, 2013. **254**(1): p. 102-113.
112. Kim, W.K., et al., *Monocyte/macrophage traffic in HIV and SIV encephalitis*. J Leukoc Biol, 2003. **74**(5): p. 650-6.

113. Williams, K.C., et al., *Perivascular Macrophages Are the Primary Cell Type Productively Infected by Simian Immunodeficiency Virus in the Brains of Macaques: Implications for the Neuropathogenesis of AIDS*. *Journal of Experimental Medicine*, 2001. **193**(8): p. 905-916.
114. Abreu, C., et al., *Brain macrophages harbor latent, infectious simian immunodeficiency virus*. *Aids*, 2019. **33 Suppl 2**(Suppl 2): p. S181-s188.
115. Fabrick, B.O., et al., *CD163-positive perivascular macrophages in the human CNS express molecules for antigen recognition and presentation*. *Glia*, 2005. **51**(4): p. 297-305.
116. Linehan, S.A., et al., *Mannose receptor and its putative ligands in normal murine lymphoid and nonlymphoid organs: In situ expression of mannose receptor by selected macrophages, endothelial cells, perivascular microglia, and mesangial cells, but not dendritic cells*. *J Exp Med*, 1999. **189**(12): p. 1961-72.
117. Linehan, S.A., L. Martinez-Pomares, and S. Gordon, *Mannose receptor and scavenger receptor: two macrophage pattern recognition receptors with diverse functions in tissue homeostasis and host defense*. *Adv Exp Med Biol*, 2000. **479**: p. 1-14.
118. Galea, I., et al., *Mannose receptor expression specifically reveals perivascular macrophages in normal, injured, and diseased mouse brain*. *Glia*, 2005. **49**(3): p. 375-84.
119. Chinnery, H.R., M.J. Ruitenberg, and P.G. McMenamin, *Novel characterization of monocyte-derived cell populations in the meninges and choroid plexus and their rates of replenishment in bone marrow chimeric mice*. *J Neuropathol Exp Neurol*, 2010. **69**(9): p. 896-909.
120. Song, E. and A. Iwasaki, *Monocytes Inadequately Fill In for Meningeal Macrophages*. *Trends Immunol*, 2019. **40**(6): p. 463-465.
121. Brioschi, S., et al., *Heterogeneity of meningeal B cells reveals a lymphopoietic niche at the CNS borders*. *Science*, 2021. **373**(6553).
122. Mrdjen, D., et al., *High-Dimensional Single-Cell Mapping of Central Nervous System Immune Cells Reveals Distinct Myeloid Subsets in Health, Aging, and Disease*. *Immunity*, 2018. **48**(2): p. 380-395.e6.
123. Korin, B., et al., *High-dimensional, single-cell characterization of the brain's immune compartment*. *Nature Neuroscience*, 2017. **20**(9): p. 1300-1309.
124. Rose, R., et al., *Distinct HIV-1 Population Structure across Meningeal and Peripheral T Cells and Macrophage Lineage Cells*. *Microbiol Spectr*, 2022. **10**(5): p. e0250822.

125. Lamers, S.L., et al., *HIV-1 phylogenetic analysis shows HIV-1 transits through the meninges to brain and peripheral tissues*. *Infect Genet Evol*, 2011. **11**(1): p. 31-7.
126. Lamers, S.L., et al., *The meningeal lymphatic system: a route for HIV brain migration?* *J Neurovirol*, 2016. **22**(3): p. 275-81.
127. Strominger, I., et al., *The Choroid Plexus Functions as a Niche for T-Cell Stimulation Within the Central Nervous System*. *Front Immunol*, 2018. **9**: p. 1066.
128. Ling, E.A., C. Kaur, and J. Lu, *Origin, nature, and some functional considerations of intraventricular macrophages, with special reference to the epiplexus cells*. *Microsc Res Tech*, 1998. **41**(1): p. 43-56.
129. Lu, J., C. Kaur, and E.A. Ling, *Up-regulation of surface antigens on epiplexus cells in postnatal rats following intraperitoneal injections of lipopolysaccharide*. *Neuroscience*, 1994. **63**(4): p. 1169-78.
130. Carpenter, S.J., L.E. McCarthy, and H.L. Borison, *Electron microscopic study of the epiplexus (Kolmer) cells of the cat choroid plexus*. *Z Zellforsch Mikrosk Anat*, 1970. **110**(4): p. 471-86.
131. Lu, J., C. Kaur, and E.A. Ling, *Intraventricular macrophages in the lateral ventricles with special reference to epiplexus cells: a quantitative analysis and their uptake of fluorescent tracer injected intraperitoneally in rats of different ages*. *J Anat*, 1993. **183 (Pt 2)**(Pt 2): p. 405-14.
132. Goldmann, T., et al., *Origin, fate and dynamics of macrophages at central nervous system interfaces*. *Nature Immunology*, 2016. **17**(7): p. 797-805.
133. Van Hove, H., et al., *A single-cell atlas of mouse brain macrophages reveals unique transcriptional identities shaped by ontogeny and tissue environment*. *Nat Neurosci*, 2019. **22**(6): p. 1021-1035.
134. Falangola, M.F., B.G. Castro-Filho, and C.K. Petito, *Immune complex deposition in the choroid plexus of patients with acquired immunodeficiency syndrome*. *Ann Neurol*, 1994. **36**(3): p. 437-40.
135. Hanly, A. and C.K. Petito, *HLA-DR-positive dendritic cells of the normal human choroid plexus: a potential reservoir of HIV in the central nervous system*. *Hum Pathol*, 1998. **29**(1): p. 88-93.
136. Chen, H., C. Wood, and C.K. Petito, *Comparisons of HIV-1 viral sequences in brain, choroid plexus and spleen: potential role of choroid plexus in the pathogenesis of HIV encephalitis*. *J Neurovirol*, 2000. **6**(6): p. 498-506.
137. Hart, D.N., et al., *Localization of HLA-ABC and DR antigens in human kidney*. *Transplantation*, 1981. **31**(6): p. 428-33.

138. Matyszak, M.K. and V.H. Perry, *A comparison of leucocyte responses to heat-killed bacillus Calmette-Guérin in different CNS compartments*. *Neuropathology and Applied Neurobiology*, 1996. **22**(1): p. 44-53.
139. Pashenkov, M., et al., *Two subsets of dendritic cells are present in human cerebrospinal fluid*. *Brain*, 2001. **124**(3): p. 480-492.
140. Miller, S.D., et al., *Antigen presentation in the CNS by myeloid dendritic cells drives progression of relapsing experimental autoimmune encephalomyelitis*. *Annals of the New York Academy of Sciences*, 2007. **1103**(1): p. 179-191.
141. Fischer, H.-G. and G. Reichmann, *Brain dendritic cells and macrophages/microglia in central nervous system inflammation*. *The Journal of Immunology*, 2001. **166**(4): p. 2717-2726.
142. Hatterer, E., et al., *Cerebrospinal fluid dendritic cells infiltrate the brain parenchyma and target the cervical lymph nodes under neuroinflammatory conditions*. *PLoS One*, 2008. **3**(10): p. e3321.
143. McMahon, E.J., S.L. Bailey, and S.D. Miller, *CNS dendritic cells: critical participants in CNS inflammation?* *Neurochemistry international*, 2006. **49**(2): p. 195-203.
144. Karman, J., et al., *Initiation of immune responses in brain is promoted by local dendritic cells*. *J Immunol*, 2004. **173**(4): p. 2353-61.
145. Kumar, B.V., T.J. Connors, and D.L. Farber, *Human T Cell Development, Localization, and Function throughout Life*. *Immunity*, 2018. **48**(2): p. 202-213.
146. Murphy, K., et al., *Janeway's immunobiology*. Tenth edition. / Kenneth Murphy, Casey Weaver, Leslie J. Berg. ed. *Immunobiology*. 2022, New York: W.W. Norton and Company.
147. Korn, T. and A. Kallies, *T cell responses in the central nervous system*. *Nature Reviews Immunology*, 2017. **17**(3): p. 179-194.
148. Ellwardt, E., et al., *Understanding the Role of T Cells in CNS Homeostasis*. *Trends Immunol*, 2016. **37**(2): p. 154-165.
149. Baruch, K., et al., *CNS-specific immunity at the choroid plexus shifts toward destructive Th2 inflammation in brain aging*. *Proc Natl Acad Sci U S A*, 2013. **110**(6): p. 2264-9.
150. Steinbach, K., et al., *Brain-resident memory T cells represent an autonomous cytotoxic barrier to viral infection*. *J Exp Med*, 2016. **213**(8): p. 1571-87.
151. Wakim, L.M., A. Woodward-Davis, and M.J. Bevan, *Memory T cells persisting within the brain after local infection show functional adaptations to their tissue of*

- residence*. Proceedings of the National Academy of Sciences, 2010. **107**(42): p. 17872-17879.
152. Wakim, L.M., et al., *The molecular signature of tissue resident memory CD8 T cells isolated from the brain*. J Immunol, 2012. **189**(7): p. 3462-71.
 153. Mavilio, D., et al., *Natural killer cells in HIV-1 infection: Dichotomous effects of viremia on inhibitory and activating receptors and their functional correlates*. Proceedings of the National Academy of Sciences, 2003. **100**(25): p. 15011-15016.
 154. Cugurra, A., et al., *Skull and vertebral bone marrow are myeloid cell reservoirs for the meninges and CNS parenchyma*. Science, 2021. **373**(6553).
 155. Clay, C.C., et al., *Neuroinvasion of fluorescein-positive monocytes in acute simian immunodeficiency virus infection*. J Virol, 2007. **81**(21): p. 12040-8.
 156. Chakrabarti, L., et al., *Early viral replication in the brain of SIV-infected rhesus monkeys*. The American journal of pathology, 1991. **139**(6): p. 1273-1280.
 157. Schnell, G., et al., *Compartmentalized human immunodeficiency virus type 1 originates from long-lived cells in some subjects with HIV-1-associated dementia*. PLoS Pathog, 2009. **5**(4): p. e1000395.
 158. Schnell, G., et al., *Compartmentalization and clonal amplification of HIV-1 variants in the cerebrospinal fluid during primary infection*. J Virol, 2010. **84**(5): p. 2395-407.
 159. Stingele, K., et al., *Independent HIV replication in paired CSF and blood viral isolates during antiretroviral therapy*. Neurology, 2001. **56**(3): p. 355-61.
 160. Lackner, A.A., et al., *Early events in tissues during infection with pathogenic (SIVmac239) and nonpathogenic (SIVmac1A11) molecular clones of simian immunodeficiency virus*. Am J Pathol, 1994. **145**(2): p. 428-39.
 161. Gartner, S., *HIV Infection and Dementia*. Science, 2000. **287**(5453): p. 602-604.
 162. Salemi, M., et al., *Phylogenetic analysis of human immunodeficiency virus type 1 in distinct brain compartments provides a model for the neuropathogenesis of AIDS*. J Virol, 2005. **79**(17): p. 11343-52.
 163. Strickland, S.L., et al., *Efficient transmission and persistence of low-frequency SIVmac251 variants in CD8-depleted rhesus macaques with different neuropathology*. J Gen Virol, 2012. **93**(Pt 5): p. 925-938.
 164. Williams, K.C. and W.F. Hickey, *Central nervous system damage, monocytes and macrophages, and neurological disorders in AIDS*. Annu Rev Neurosci, 2002. **25**: p. 537-62.

165. Yadav, A. and R.G. Collman, *CNS inflammation and macrophage/microglial biology associated with HIV-1 infection*. J Neuroimmune Pharmacol, 2009. **4**(4): p. 430-47.
166. Davis, L.E., et al., *Early viral brain invasion in iatrogenic human immunodeficiency virus infection*. Neurology, 1992. **42**(9): p. 1736-9.
167. Borrajo, A., et al., *Important role of microglia in HIV-1 associated neurocognitive disorders and the molecular pathways implicated in its pathogenesis*. Ann Med, 2021. **53**(1): p. 43-69.
168. Marino, J., et al., *Functional impact of HIV-1 Tat on cells of the CNS and its role in HAND*. Cell Mol Life Sci, 2020. **77**(24): p. 5079-5099.
169. Chan, P. and S. Spudich, *HIV Compartmentalization in the CNS and Its Impact in Treatment Outcomes and Cure Strategies*. Curr HIV/AIDS Rep, 2022. **19**(3): p. 207-216.
170. Clements, J.E., et al., *A simian immunodeficiency virus macaque model of highly active antiretroviral treatment: viral latency in the periphery and the central nervous system*. Curr Opin HIV AIDS, 2011. **6**(1): p. 37-42.
171. Kranick, S.M. and A. Nath, *Neurologic complications of HIV-1 infection and its treatment in the era of antiretroviral therapy*. Continuum (Minneapolis, Minn.), 2012. **18**(6 Infectious Disease): p. 1319-1337.
172. Williams, K., et al., *Magnetic resonance spectroscopy reveals that activated monocytes contribute to neuronal injury in SIV neuroAIDS*. J Clin Invest, 2005. **115**(9): p. 2534-45.
173. Schacker, T., et al., *Rapid accumulation of human immunodeficiency virus (HIV) in lymphatic tissue reservoirs during acute and early HIV infection: implications for timing of antiretroviral therapy*. J Infect Dis, 2000. **181**(1): p. 354-7.
174. Maldarelli, F., et al., *ART suppresses plasma HIV-1 RNA to a stable set point predicted by pretherapy viremia*. PLoS Pathog, 2007. **3**(4): p. e46.
175. Ling, B., et al., *Classic AIDS in a sooty mangabey after an 18-year natural infection*. J Virol, 2004. **78**(16): p. 8902-8.
176. Garbuglia, A.R., et al., *Dynamics of viral load in plasma and HIV DNA in lymphocytes during highly active antiretroviral therapy (HAART): high viral burden in macrophages after 1 year of treatment*. J Chemother, 2001. **13**(2): p. 188-94.
177. Sahu, G.K., et al., *Low-level plasma HIVs in patients on prolonged suppressive highly active antiretroviral therapy are produced mostly by cells other than CD4 T-cells*. J Med Virol, 2009. **81**(1): p. 9-15.

178. Solis-Leal, A., et al., *Lymphoid tissues contribute to plasma viral clonotypes early after antiretroviral therapy interruption in SIV-infected rhesus macaques*. *Sci Transl Med*, 2023. **15**(726): p. eadi9867.
179. Rothenberger, M.K., et al., *Large number of rebounding/founder HIV variants emerge from multifocal infection in lymphatic tissues after treatment interruption*. *Proc Natl Acad Sci U S A*, 2015. **112**(10): p. E1126-34.
180. Pillai, S.K., et al., *Genetic attributes of cerebrospinal fluid-derived HIV-1 env*. *Brain*, 2006. **129**(Pt 7): p. 1872-83.
181. Tang, Y.W., et al., *Comparison of human immunodeficiency virus type 1 RNA sequence heterogeneity in cerebrospinal fluid and plasma*. *J Clin Microbiol*, 2000. **38**(12): p. 4637-9.
182. Lanier, E.R., et al., *HIV-1 reverse transcriptase sequence in plasma and cerebrospinal fluid of patients with AIDS dementia complex treated with Abacavir*. *Aids*, 2001. **15**(6): p. 747-51.
183. Zink, M.C., et al., *Simian Immunodeficiency Virus-Infected Macaques Treated with Highly Active Antiretroviral Therapy Have Reduced Central Nervous System Viral Replication and Inflammation but Persistence of Viral DNA*. *The Journal of Infectious Diseases*, 2010. **202**(1): p. 161-170.
184. Avalos, C.R., et al., *Quantitation of Productively Infected Monocytes and Macrophages of Simian Immunodeficiency Virus-Infected Macaques*. *Journal of virology*, 2016. **90**(12): p. 5643-5656.
185. Veenhuis, R.T., et al., *Monocyte-derived macrophages contain persistent latent HIV reservoirs*. *Nature Microbiology*, 2023. **8**(5): p. 833-844.
186. Brown, P.D., et al., *Molecular mechanisms of cerebrospinal fluid production*. *Neuroscience*, 2004. **129**(4): p. 957-70.
187. Bulat, M. and M. Klarica, *Recent insights into a new hydrodynamics of the cerebrospinal fluid*. *Brain Res Rev*, 2011. **65**(2): p. 99-112.
188. Khasawneh, A.H., R.J. Garling, and C.A. Harris, *Cerebrospinal fluid circulation: What do we know and how do we know it?* *Brain Circ*, 2018. **4**(1): p. 14-18.
189. Rasmussen, M.K., H. Mestre, and M. Nedergaard, *Fluid transport in the brain*. *Physiol Rev*, 2022. **102**(2): p. 1025-1151.
190. Wichmann, T.O., H.H. Damkier, and M. Pedersen, *A Brief Overview of the Cerebrospinal Fluid System and Its Implications for Brain and Spinal Cord Diseases*. *Front Hum Neurosci*, 2021. **15**: p. 737217.

191. Iliff, J.J., et al., *A paravascular pathway facilitates CSF flow through the brain parenchyma and the clearance of interstitial solutes, including amyloid β* . *Sci Transl Med*, 2012. **4**(147): p. 147ra111.
192. Laman, J.D. and R.O. Weller, *Drainage of cells and soluble antigen from the CNS to regional lymph nodes*. *J Neuroimmune Pharmacol*, 2013. **8**(4): p. 840-56.
193. Mestre, H., Y. Mori, and M. Nedergaard, *The Brain's Glymphatic System: Current Controversies*. *Trends Neurosci*, 2020. **43**(7): p. 458-466.
194. Bolte, A.C., et al., *Meningeal lymphatic dysfunction exacerbates traumatic brain injury pathogenesis*. *Nat Commun*, 2020. **11**(1): p. 4524.
195. Bacynski, A., et al., *The Paravascular Pathway for Brain Waste Clearance: Current Understanding, Significance and Controversy*. *Frontiers in Neuroanatomy*, 2017. **11**.
196. Benveniste, H., H. Lee, and N.D. Volkow, *The Glymphatic Pathway: Waste Removal from the CNS via Cerebrospinal Fluid Transport*. *Neuroscientist*, 2017. **23**(5): p. 454-465.
197. Plog, B.A. and M. Nedergaard, *The Glymphatic System in Central Nervous System Health and Disease: Past, Present, and Future*. *Annu Rev Pathol*, 2018. **13**: p. 379-394.
198. Zhou, Y., et al., *Impairment of the Glymphatic Pathway and Putative Meningeal Lymphatic Vessels in the Aging Human*. *Ann Neurol*, 2020. **87**(3): p. 357-369.
199. Ma, Q., et al., *Clearance of cerebrospinal fluid from the sacral spine through lymphatic vessels*. *Journal of Experimental Medicine*, 2019. **216**(11): p. 2492-2502.
200. Ma, Q., et al., *Outflow of cerebrospinal fluid is predominantly through lymphatic vessels and is reduced in aged mice*. *Nat Commun*, 2017. **8**(1): p. 1434.
201. Ma, Q., et al., *Rapid lymphatic efflux limits cerebrospinal fluid flow to the brain*. *Acta Neuropathol*, 2019. **137**(1): p. 151-165.
202. Da Mesquita, S., et al., *Aging-associated deficit in CCR7 is linked to worsened glymphatic function, cognition, neuroinflammation, and β -amyloid pathology*. *Sci Adv*, 2021. **7**(21).
203. Da Mesquita, S., et al., *Meningeal lymphatics affect microglia responses and anti- $A\beta$ immunotherapy*. *Nature*, 2021. **593**(7858): p. 255-260.
204. das Neves, S.P., N. Delivanoglou, and S. Da Mesquita, *CNS-Draining Meningeal Lymphatic Vasculature: Roles, Conundrums and Future Challenges*. *Front Pharmacol*, 2021. **12**: p. 655052.

205. Murtha, L.A., et al., *Cerebrospinal fluid is drained primarily via the spinal canal and olfactory route in young and aged spontaneously hypertensive rats*. *Fluids Barriers CNS*, 2014. **11**: p. 12.
206. Walter, B.A., et al., *The olfactory route for cerebrospinal fluid drainage into the peripheral lymphatic system*. *Neuropathology and Applied Neurobiology*, 2006. **32**(4): p. 388-396.
207. Weller, R.O., et al., *Lymphatic drainage of the brain and the pathophysiology of neurological disease*. *Acta Neuropathol*, 2009. **117**(1): p. 1-14.
208. Johnston, M., et al., *Evidence of connections between cerebrospinal fluid and nasal lymphatic vessels in humans, non-human primates and other mammalian species*. *Cerebrospinal Fluid Res*, 2004. **1**(1): p. 2.
209. Louveau, A., et al., *Structural and functional features of central nervous system lymphatic vessels*. *Nature*, 2015. **523**(7560): p. 337-41.
210. Andres, K.H., et al., *Nerve fibres and their terminals of the dura mater encephali of the rat*. *Anat Embryol (Berl)*, 1987. **175**(3): p. 289-301.
211. Elman, R., *Spinal arachnoid granulations with special reference to the cerebrospinal fluid*. *Johns Hopkins Hospital Bull*, 1923.
212. Kido, D., et al., *Human spinal arachnoid villi and granulations*. *Neuroradiology*, 1976. **11**(5): p. 221-228.
213. Welch, K. and M. Pollay, *The spinal arachnoid villi of the monkeys *Cercopithecus aethiops sabaeus* and *Macaca irus**. *The Anatomical Record*, 1963. **145**(1): p. 43-48.
214. Chen, L., et al., *Pathways of cerebrospinal fluid outflow: a deeper understanding of resorption*. *Neuroradiology*, 2015. **57**(2): p. 139-47.
215. Brierley, J. and E. Field, *The connexions of the spinal sub-arachnoid space with the lymphatic system*. *Journal of anatomy*, 1948. **82**(Pt 3): p. 153.
216. Iwanow, G., *Über die Abflußwege aus den submeningealen Räumen des Rückenmarks*. *Zeitschrift für die gesamte experimentelle Medizin*, 1928. **58**(1): p. 1-21.
217. Antila, S., et al., *Development and plasticity of meningeal lymphatic vessels*. *Journal of Experimental Medicine*, 2017. **214**(12): p. 3645-3667.
218. Zenker, W., S. Bankoul, and J.S. Braun, *Morphological indications for considerable diffuse reabsorption of cerebrospinal fluid in spinal meninges particularly in the areas of meningeal funnels*. *Anatomy and embryology*, 1994. **189**(3): p. 243-258.

219. Asgari, M., D.A. de Zélicourt, and V. Kurtcuoglu, *Barrier dysfunction or drainage reduction: differentiating causes of CSF protein increase*. *Fluids and Barriers of the CNS*, 2017. **14**(1): p. 1-11.
220. Bozanovic-Sosic, R., R. Mollanji, and M. Johnston, *Spinal and cranial contributions to total cerebrospinal fluid transport*. *American Journal of Physiology-Regulatory, Integrative and Comparative Physiology*, 2001. **281**(3): p. R909-R916.
221. Marmarou, A., K. Shulman, and J. Lamorgese, *Compartmental analysis of compliance and outflow resistance of the cerebrospinal fluid system*. *Journal of neurosurgery*, 1975. **43**(5): p. 523-534.
222. Atluri, V.S., et al., *Effect of human immunodeficiency virus on blood-brain barrier integrity and function: an update*. *Front Cell Neurosci*, 2015. **9**: p. 212.
223. Kubes, P. and P.A. Ward, *Leukocyte recruitment and the acute inflammatory response*. *Brain Pathol*, 2000. **10**(1): p. 127-35.
224. Greiner, T. and M. Kipp, *What Guides Peripheral Immune Cells into the Central Nervous System?* *Cells*, 2021. **10**(8): p. 2041.
225. Ransohoff, R.M., P. Kivisäkk, and G. Kidd, *Three or more routes for leukocyte migration into the central nervous system*. *Nature Reviews Immunology*, 2003. **3**(7): p. 569-581.
226. Engelhardt, B., *Regulation of immune cell entry into the central nervous system*. *Results Probl Cell Differ*, 2006. **43**: p. 259-80.
227. Kivisäkk, P., et al., *Human cerebrospinal fluid central memory CD4+ T cells: evidence for trafficking through choroid plexus and meninges via P-selectin*. *Proc Natl Acad Sci U S A*, 2003. **100**(14): p. 8389-94.
228. Zhang, L., et al., *SARS-CoV-2 crosses the blood–brain barrier accompanied with basement membrane disruption without tight junctions alteration*. *Signal Transduction and Targeted Therapy*, 2021. **6**(1): p. 337.
229. Zink, M.C., et al., *High viral load in the cerebrospinal fluid and brain correlates with severity of simian immunodeficiency virus encephalitis*. *J Virol*, 1999. **73**(12): p. 10480-8.
230. Patel, A.A., et al., *The fate and lifespan of human monocyte subsets in steady state and systemic inflammation*. *J Exp Med*, 2017. **214**(7): p. 1913-1923.
231. Campbell, J.H., et al., *The importance of monocytes and macrophages in HIV pathogenesis, treatment, and cure*. *AIDS*, 2014. **28**(15): p. 2175-87.

232. Wong, M.E., A. Jaworowski, and A.C. Hearps, *The HIV Reservoir in Monocytes and Macrophages*. Front Immunol, 2019. **10**: p. 1435.
233. Burdo, T.H., et al., *Soluble CD163 made by monocyte/macrophages is a novel marker of HIV activity in early and chronic infection prior to and after anti-retroviral therapy*. J Infect Dis, 2011. **204**(1): p. 154-63.
234. Burdo, T.H., et al., *Soluble CD163, a novel marker of activated macrophages, is elevated and associated with noncalcified coronary plaque in HIV-infected patients*. J Infect Dis, 2011. **204**(8): p. 1227-36.
235. Burdo, T.H., et al., *Elevated sCD163 in plasma but not cerebrospinal fluid is a marker of neurocognitive impairment in HIV infection*. AIDS, 2013. **27**(9): p. 1387-95.
236. Bechmann, I., et al., *Turnover of rat brain perivascular cells*. Exp Neurol, 2001. **168**(2): p. 242-9.
237. Crowe, S., T. Zhu, and W.A. Muller, *The contribution of monocyte infection and trafficking to viral persistence, and maintenance of the viral reservoir in HIV infection*. J Leukoc Biol, 2003. **74**(5): p. 635-41.
238. de Vos, A.F., et al., *Transfer of central nervous system autoantigens and presentation in secondary lymphoid organs*. J Immunol, 2002. **169**(10): p. 5415-23.
239. van Zwam, M., et al., *Brain antigens in functionally distinct antigen-presenting cell populations in cervical lymph nodes in MS and EAE*. J Mol Med (Berl), 2009. **87**(3): p. 273-86.
240. Aspelund, A., et al., *A dural lymphatic vascular system that drains brain interstitial fluid and macromolecules*. J Exp Med, 2015. **212**(7): p. 991-9.
241. Louveau, A., et al., *Understanding the functions and relationships of the glymphatic system and meningeal lymphatics*. J Clin Invest, 2017. **127**(9): p. 3210-3219.
242. Kanamori, M. and J. Kipnis, *Meningeal lymphatics "drain" brain tumors*. Cell Res, 2020. **30**(3): p. 191-192.
243. Frederick, N. and A. Louveau, *Meningeal lymphatics, immunity and neuroinflammation*. Curr Opin Neurobiol, 2020. **62**: p. 41-47.
244. Semyachkina-Glushkovskaya, O., et al., *Meningeal Lymphatic Pathway of Brain Clearing From the Blood After Haemorrhagic Injuries*. Adv Exp Med Biol, 2020. **1232**: p. 63-68.

245. Louveau, A., et al., *CNS lymphatic drainage and neuroinflammation are regulated by meningeal lymphatic vasculature*. Nat Neurosci, 2018. **21**(10): p. 1380-1391.
246. Herz, J., et al., *Morphological and Functional Analysis of CNS-Associated Lymphatics*. Methods Mol Biol, 2018. **1846**: p. 141-151.
247. Da Mesquita, S., et al., *Functional aspects of meningeal lymphatics in ageing and Alzheimer's disease*. Nature, 2018. **560**(7717): p. 185-191.
248. Absinta, M., et al., *Human and nonhuman primate meninges harbor lymphatic vessels that can be visualized noninvasively by MRI*. Elife, 2017. **6**.
249. Laaker, C., et al., *Immune cells as messengers from the CNS to the periphery: the role of the meningeal lymphatic system in immune cell migration from the CNS*. Front Immunol, 2023. **14**: p. 1233908.
250. Kaminski, M., et al., *Migration of monocytes after intracerebral injection*. Cell Adh Migr, 2012. **6**(3): p. 164-7.
251. Goldmann, J., et al., *T cells traffic from brain to cervical lymph nodes via the cribriform plate and the nasal mucosa*. J Leukoc Biol, 2006. **80**(4): p. 797-801.
252. Mohammad, M.G., et al., *Immune cell trafficking from the brain maintains CNS immune tolerance*. J Clin Invest, 2014. **124**(3): p. 1228-41.
253. Jacob, L., et al., *Anatomy and function of the vertebral column lymphatic network in mice*. Nature Communications, 2019. **10**(1): p. 4594.
254. Ahn, J.H., et al., *Meningeal lymphatic vessels at the skull base drain cerebrospinal fluid*. Nature, 2019. **572**(7767): p. 62-66.
255. Haller, F.R., C. Haller, and F.N. Low, *The fine structure of cellular layers and connective tissue space at spinal nerve root attachments in the rat*. Am J Anat, 1972. **133**(1): p. 109-23.
256. Kitamura, K., et al., *Cervical nerve roots and the dural sheath: a histological study using human fetuses near term*. Anat Cell Biol, 2020. **53**(4): p. 451-459.
257. Pettersson, C.A., *Drainage of molecules from subarachnoid space to spinal nerve roots and peripheral nerve of the rat. A study based on Evans blue-albumin and lanthanum as tracers*. Acta Neuropathol, 1993. **86**(6): p. 636-44.
258. Miura, M., S. Kato, and M. von Lüdinghausen, *Lymphatic drainage of the cerebrospinal fluid from monkey spinal meninges with special reference to the distribution of the epidural lymphatics*. Arch Histol Cytol, 1998. **61**(3): p. 277-86.

259. Mahmoudi, M., et al., *Superparamagnetic iron oxide nanoparticles (SPIONs): Development, surface modification and applications in chemotherapy*. *Advanced Drug Delivery Reviews*, 2011. **63**(1): p. 24-46.
260. Dulińska-Litewka, J., et al., *Superparamagnetic Iron Oxide Nanoparticles- Current and Prospective Medical Applications*. *Materials* (Basel), 2019. **12**(4).
261. Janko, C., et al., *Functionalized Superparamagnetic Iron Oxide Nanoparticles (SPIONs) as Platform for the Targeted Multimodal Tumor Therapy*. *Frontiers in Oncology*, 2019. **9**.
262. Chen, Y. and S. Hou, *Recent progress in the effect of magnetic iron oxide nanoparticles on cells and extracellular vesicles*. *Cell Death Discovery*, 2023. **9**(1): p. 195.
263. Wang, S., et al., *Ferroptosis: A double-edged sword*. *Cell Death Discovery*, 2024. **10**(1): p. 265.
264. Wu, C., et al., *p53 Promotes Ferroptosis in Macrophages Treated with Fe(3)O(4) Nanoparticles*. *ACS Appl Mater Interfaces*, 2022. **14**(38): p. 42791-42803.
265. Lunov, O., et al., *The effect of carboxydextran-coated superparamagnetic iron oxide nanoparticles on c-Jun N-terminal kinase-mediated apoptosis in human macrophages*. *Biomaterials*, 2010. **31**(19): p. 5063-71.
266. Guggenheim, E.J., J.Z. Rappoport, and I. Lynch, *Mechanisms for cellular uptake of nanosized clinical MRI contrast agents*. *Nanotoxicology*, 2020. **14**(4): p. 504-532.
267. Laskar, A., et al., *SPION primes THP1 derived M2 macrophages towards M1-like macrophages*. *Biochem Biophys Res Commun*, 2013. **441**(4): p. 737-42.
268. Rojas, J.M., et al., *Superparamagnetic iron oxide nanoparticle uptake alters M2 macrophage phenotype, iron metabolism, migration and invasion*. *Nanomedicine*, 2016. **12**(4): p. 1127-1138.
269. Tate, J.A., et al., *In vivo biodistribution of iron oxide nanoparticles: an overview*. *Proc SPIE Int Soc Opt Eng*, 2011. **7901**: p. 790117.
270. Straus, S. and S.L. Madorsky, *Thermal Stability of Polydivinylbenzene and of Copolymers of Styrene With Divinylbenzene and With Trivinylbenzene*. *J Res Natl Bur Stand A Phys Chem*, 1961. **65a**(3): p. 243-248.
271. Tabata, Y. and Y. Ikada, *Effect of the size and surface charge of polymer microspheres on their phagocytosis by macrophage*. *Biomaterials*, 1988. **9**(4): p. 356-62.

272. Srinivas, M., P. Sharma, and S. Jhunjhunwala, *Phagocytic Uptake of Polymeric Particles by Immune Cells under Flow Conditions*. *Molecular Pharmaceutics*, 2021. **18**(12): p. 4501-4510.
273. Ghosh, S., et al., *Genotoxicity and biocompatibility of superparamagnetic iron oxide nanoparticles: Influence of surface modification on biodistribution, retention, DNA damage and oxidative stress*. *Food Chem Toxicol*, 2020. **136**: p. 110989.
274. Singh, N., et al., *Potential toxicity of superparamagnetic iron oxide nanoparticles (SPION)*. *Nano Rev*, 2010. **1**.
275. Trost, A., et al., *Time-dependent retinal ganglion cell loss, microglial activation and blood-retina-barrier tightness in an acute model of ocular hypertension*. *Exp Eye Res*, 2015. **136**: p. 59-71.
276. Ebert, S.N., et al., *Noninvasive Tracking of Cardiac Embryonic Stem Cells In Vivo Using Magnetic Resonance Imaging Techniques*. *STEM CELLS*, 2007. **25**(11): p. 2936-2944.

2.0 Chapter 2

Simian Immunodeficiency Virus-Infected Macrophages Traffic Out of the Central Nervous System

Xavier Alvarez¹

Zoey K. Wallis²

Cecily C. Midkiff³

Jaclyn Mallard¹

Pete J. Didier³

Kenneth C. Williams²

¹ Imaging PET-CT and OIL Core, Southwest National Primate Research Center, San Antonio, TX, USA.

² Morrissey College of Arts and Sciences, Biology Department, Boston College, Chestnut Hill, MA, USA.

³ Tulane National Primate Research Center, Covington, LA, USA.

2.1 Author Contributions

Conceptualization, K.C.W., and X.A.; Obtained and analyzed data and images, X.A., Z.K.W. J.M., and C.C.M.; writing—original draft preparation, X.A., and Z.K.W.; writing—review and editing, K.C.W., Z.K.W., and P.J.D.; funding acquisition, K.C.W.

Manuscript in preparation as of November 2024.

2.2 Abstract

Studies have highlighted the significance of monocyte/macrophage traffic to the central nervous system and accumulation within the CNS infection during HIV infection. We asked whether CNS macrophages can leave the CNS under normal conditions, during inflammation, or when lesions resolve. Pathways and mechanisms for this have been suggested but are not well-defined. Less well-known is whether CNS-derived HIV produced in the CNS can exit with such traffic. We use intracisternal (ic) injection of fluorescent- superparamagnetic iron oxide nanoparticles (SPION) in non-infected and SIV-infected monkeys that label CNS macrophages and measure macrophage accumulation and exit from the CNS. SPION are readily taken up by CD68-CD163-CD206 and Iba1 perivascular, meningeal, and choroid plexus macrophages. CD163+ SPION+ macrophages are also found within the optic nerve, nasal septum, and cribriform plate that are potential sites of macrophage exit, and outside the CNS in deep cervical lymph node (dCLN), spleen, dorsal root ganglia (DRG), and bone marrow. CD163+ SPION+ macrophages are most abundant within 24 hours after i.c. injection in non-infected monkeys, and decrease over time at 7, 14, and 28 days post-injection, consistent with cell traffic out of the CNS. I.c. injected, soluble fluorescent-dextran are found outside the CNS in dCLN an hour after injection, but SPION+ macrophage are detected in dCLN 24 hours post i.c injection, consistent with active uptake and traffic of SPION-labelled cells. With SIV infection, there are increased numbers of SPION-labeled CD163+ macrophages in the CNS as expected in inflammation but decreased numbers of SPION+ macrophages than expected outside the CNS. SPION+ SIV-p28 and SIV-RNA+ macrophages are found within the CNS, and outside the CNS in the dCLN,

spleen, DRG 7-14 days post SPION i.c. injection. These data are consistent with populations of perivascular, meningeal, and choroid plexus macrophages that readily take up SPION, can leave the CNS normally, and are slower to leave during SIV infection. These data demonstrate macrophage populations traffic out of the CNS to the peripheral circulation and are virally infected. These observations support the notion that populations of CNS macrophages can leave the CNS via meningeal and perivascular lymphatics and can be a source of CNS virus that reseeds the body.

Keywords: HIV, SIV, CNS macrophages, SPION, Traffic

2.3 Introduction

The central nervous system (CNS) and CNS macrophage are known targets of HIV infection early and late, in the pre-ART era and even with ART [1, 2]. HIV is found early in the CNS and is associated with perivascular cuffs of macrophages and later in CNS lesions that also consist of macrophage accumulation [1, 3, 4]. We and others have shown that HIV and SIV are found within CNS perivascular macrophages, meningeal macrophages, and choroid plexus macrophages [1, 5]. The biology of these macrophages, including origin from bone marrow and traffic to the CNS normally or sourced from embryonic stem cells (yolk sac-derived) and repopulate by cell division within the CNS, is critical when considering the CNS as a reservoir of HIV [6-9]. Moreover, the biology of inflammation in the CNS and macrophage traffic in and out of the CNS before and after HIV infection are of high interest.

The majority of HIV and SIV-infected cells in the CNS are blood-derived perivascular macrophages that are located at the blood-CSF interface [1]. These macrophages are a key component of the CNS immune defense and, when infected, can become reservoirs for SIV and HIV [1, 10]. Once infected, CNS macrophages can facilitate viral persistence and dissemination, contributing to neuroinflammation and the development of neurocognitive disorders [11, 12]. The cerebrospinal fluid (CSF) serves as another route for viral dissemination where infected cells originate from the bloodstream, migrating into the CNS either as part of repopulation or in response to infection [3, 13, 14]. The trafficking of SIV or HIV-infected macrophages into the CNS is well-documented, but whether these cells can traffic out has significant implications for understanding HIV and SIV persistence and latency, as well as the challenges in eradicating these infections.

It is now well established that CNS fluids—and in some instances cells—drain or exit [15-21] but that was counter to dogma that the CNS lacked or had limited draining lymphatics [21]. Radiolabeled proteins and fluorescence dyes injected intracisternally (i.c) and fluorescent-labeled antigen-presenting cells (APCs) transplanted into the CNS have been demonstrated in deep cervical lymph nodes (dCLN) [22] likely trafficking via meningeal lymphatics. These studies were done in normal, non-inflamed, or infected animals and in brain injury or autoimmune models [23-25]. Importantly, studies in rodents and non-human primates have demonstrated CNS myelin antigens-presenting macrophages and dendritic cells (APC) in lymph nodes LN with CNS myelin protein, suggesting such cell traffic out is important in the maintenance of tolerance to CNS antigens and perhaps autoimmune responses in experimental allergic encephalomyelitis and multiple sclerosis [26-28]. Indeed, ablation of the meningeal lymphatics reduced clinical symptoms in EAE [24]. An alternative route for cells to exit the CNS is via the central canal and the meninges of the spinal cord, where they connect with the inner layers of the peripheral nerve root sheaths as they leave the spinal cord [29]. This forms a direct connection near the root attachment, known as the subarachnoid angle, which creates a continuous passage linking the cerebrospinal fluid-filled subarachnoid space (SAS) surrounding the brain and spinal cord with the perineural space of the nerve roots [29, 30]. This path communicates with the dorsal root ganglia (DRG) at the interface of the CNS, the peripheral nervous system (PNS), and immune organs outside the CNS [30-32]. The study of transplanted and injected fluorescent-labeled cells leaving the CNS is important and informative, but they have the caveat of inducing CNS injury, breach of the blood-brain barrier (BBB), or both, which can facilitate CNS inflammation.

Importantly, such studies have not been done to date in humans or non-human primates with HIV- or SIV- infection or using SPION injected into the CSF that are normally taken up by cells at the blood-brain-CNS interface.

We injected superparamagnetic iron oxide (SPION) particles i.c. with internal fluorescence in non-infected and SIV-infected monkeys and studied their uptake and distribution in the CNS over time and cell-associated traffic out of the CNS. Because of their size (0.86 μ m diameter), SPION cannot diffuse out of the CNS into the periphery but are taken up by CNS macrophages in perivascular spaces, the meninges, and the choroid plexus. These studies, for the first time, demonstrate labeling of macrophage populations by SPION injected i.c., the traffic of SPION+ macrophages out, and their CNS accumulation in infected animals. They underscore the ability of SPION+ macrophages labeled in the CNS to traffic out to peripheral lymph organs and the peripheral nervous system, where some of these macrophages are SIV-infected. These data are discussed in the context of CNS inflammation and resolution of infection, and HIV viral reservoirs.

2.4 Results

We injected SPIONs (30 ug/ml) intracisternally (i.c.) into normal non-infected and SIV-infected animals and studied their uptake within CNS macrophages one hour (dextran and SPION), 1 day (dextran and SPION) and 7, 14 and 28 days post injection (**Figure 2.1**). SPION-labeled cells were detected by bright-field microscopy, Prussian blue iron stain, or using the internal fluorescence of the SPION (data not shown) (**Figure 2.2**). Multiple SPION were taken up per labeled cells that are distributed within perivascular spaces, the meninges, and the choroid plexus (**Figure 2.2**). We do not find free (non-cell-associated) SPION in the CNS, likely due to their size (0.86 μ m diameter), but free SPION are found around meninges and the DRG in the subarachnoid space contiguous with the central canal of the spinal cord and CSF (data below).

Immunohistochemical (Prussian blue) and fluorescence (Dragon green) SPION consistently labeled CD68, CD163, and CD206 perivascular macrophages, meningeal macrophages, and choroid plexus macrophages (**Figure 2.3**). There is a consistent >2-fold increase in the number of meningeal versus perivascular macrophages that are SPION+, consistent with the greater number of total meningeal versus perivascular macrophages in each respective compartment (**Table 2.1**). In non-infected animals, over time there are decreased numbers of SPION+ perivascular (p=0.06) and meningeal macrophages (p=0.09) consistent with SPION-labeled cells leaving the CNS (**Table 2.1**): In contrast, in SIV-infected animals, there are increased numbers of SPION+ macrophages with CNS inflammation and macrophage accumulation (**Table 2.1**).

Next, we studied SPION+ macrophages exiting the CNS. We find SPION+ macrophages examined in the optic nerve, nasal septum, cribriform plate, at the interface

border of the CNS (border associated macrophages, BAM), and outside the CNS in the superficial and dCLN, spleen, and dorsal root ganglia (cervical, thoracic and lumbar, DRG) 1, 7, 14 and 28 days post SPION inoculation in non-infected and SIV infected animals (**Figure 2.4**). To assess the movement of cells and fluid outside the CNS we injected (n=2) soluble fluorescence-labeled dextran and SPION together (i.c.).

Fluorescently labeled dextran dye is found in the dCLN 1 hour after i.c. inoculation in the medullary sinuses, but SPION+ macrophages are not detected in the paracortex until 24 hr (**Figure 2.5**). SPION+ macrophages are found in the dCLN 24 hr. post dextran and SPOIN i.c. they are differently located (**Figure 2.5**). The delay (24 hr) for traffic of SPION+ macrophages out of the CNS is consistent with the time required for uptake of SPION in the CNS and macrophage traffic out (**Figure 2.5**). In addition to dCLN, SPION+ positive macrophages are found in the optic nerve, cribriform plate, axillary LN, spleen, and DRG (cervical, thoracic, lumber) between 7 - 28 days post-inoculation in non-infected animals and SIV infected animals (**Table 2.2**). With SIV infection there are decreased numbers of SPION+ macrophages in peripheral sites (**Table 2.2**). Overall, these data, similar to the observation in the CNS suggest that SPION-labeled macrophages leave the CNS at a higher rate in non-infected animals but accumulate in the CNS with SIV infection.

Using fluorescence of SPION and SIVp28 and SIV-RNA, we find SPION+ SIVp28+ and SIV-RNA+ macrophages in the CNS and outside the CNS in dCLN (**Figure 2.6**). Serial section, double-label IF, SIV-gp41 show these are CD163+ SIVp28+ (**Figure 2.6**). In AIDS animals with SIVE, we find SPION+ SIV-RNA+ macrophages (20 to 50 SPION+ SIV-RNA+ cells per dcLN section, 1.0 ± 1.7 SPION+SIV-RNA+/mm²) inside

of the CNS and in the dcLN (**Figure 2.7**). These data are consistent with SPION-labeled macrophages that were in the CNS that are productively SIV-infected. Whether these are SIV-infected in the CNS and carried SIV-RNA and DNA out or if they were infected upon leaving the CNS was not determined in this study.

2.5 Discussion

In this study we injected SPION ic and assessed their distribution within the CNS over time in normal and SIV infected animals. We found SPIONS in perivascular macrophages, macrophages in the meninges, and choroid plexus macrophages. Macrophage populations were identified based on their location and co-localization with CD163, CD206, CD68, and in some cases Iba1. There were a greater number of SPION-labeled macrophages within the meninges than the perivascular macrophages, likely a consequence of a greater number of total macrophages in the meninges. This may be due both to the fluid speed and SPION interaction with macrophages in the meninges versus the perivascular space. Also, macrophages in the meninges had much larger numbers of SPIONS per macrophage than the perivascular macrophages, which may alter the ability of the meningeal macrophage to traffic [33, 34]. We found that the ratio of total macrophages and SPION+ macrophages in each compartment is relatively fixed in non-infected and SIV-infected animals. Outside the CNS, we found SPION+ macrophages in dCLN, far fewer in superficial LN, and found them in the spleen and DRG with the greatest numbers in the DRG, consistent with parts of the DRG being continuous with the subarachnoid space of the spinal cord and in contact with CSF into which the SPION were injected. In non-infected animals, there were higher numbers of SPION+ macrophages early after injection that normalized. With SIV infection, the number of SPION+ macrophages in the CNS increased, and fewer SPION+ macrophages were found that trafficked out. Importantly, almost all of the SPION in the CNS and outside were cell-associated within macrophages and not ones that simply diffused out. Others using SPION injected ic have similar findings [17, 22]. Our findings suggest that with

SIV infection and macrophage accumulation in the CNS, there is an accumulation of SPION+ macrophages. In contrast, in non-infected animals, the SPION+ macrophages seem less likely to accumulate in the CNS and are found trafficking out. Interestingly, with ART we find more SPION+ macrophages outside the CNS and fewer inside, consistent with ART resolving CNS inflammation and more SPION+ cells trafficking out (Wallis *et al.*, submitted).

In SIV-infected animals, we found SPION+ macrophages in the CNS and, importantly, outside the CNS in dCLN. The fact that the SPION+ macrophages in the dCLN have SPION is strong evidence that they have trafficked out of the CNS. We cannot ascertain whether they were infected within the CNS or outside. Work by our group and others use gene flow analysis and SIV sequencing to demonstrate viral traffic from the CNS to tissues outside late in infection [35, 36]. Such analysis would need to be done on a single cell level, comparing CNS to peripheral viral sequences.

Studies in rodents using transplanted or injected (CSF) cells and dyes into the CNS support the notion that immune cells, including DC, T cells, and B cells and, in some cases, monocytes, can leave the CNS [17, 19, 22, 37-39]. Those studies, by the nature of injection and injury, somewhat compromise the BBB and activate the brain [17, 22]. Our study reported here is the first to study cells out in the periphery with SIV infection. Pathways by which cells can traffic out are many and have been described and reviewed by others [23, 39-44]. These include meningeal lymphatics and perineural pathways via the cribriform plate. It is interesting in this study that i.c. injected dextrans are readily found outside the CNS in dCLN hours after administration but SPION+ macrophages are not detected until 24 hours post i.c. inoculation. This is likely because of the size

restriction of the SPION that do not readily leak out [18, 45, 46] but are instead taken up by macrophage before they leave in contrast to dextran dyes that readily leak out. Also, the location of the SPION in the dCLN is different than that of dextran dye, suggesting differential fluid pathways versus myeloid cell traffic [17, 26, 47].

We and others have previously demonstrated in HIV-infected humans and SIV-infected monkeys that perivascular macrophages are a major site in the CNS of productive lentiviral infection [1, 5, 48]. In other work (Wallis *et al.*, submitted), we find ART effectively clears the CNS perivascular macrophage SIV infection and somewhat also CNS meninges and choroid plexus macrophages, and with 4 weeks of ART interruption, CNS perivascular macrophages remain SIV-RNA negative, but there is a rebound in the meningeal macrophage and choroid plexus. Similarly, in the periphery, plasma virus is decreased, as it is in the spleen and dCLN, but not the DRG.

In this study, we now also show the macrophages in the choroid plexus also are targets. Others have previously noted early CP macrophage infected by HIV and SIV with aseptic meningitis but have generally not considered this to be a reservoir site [49-51]. This, however, seems to be the case and might be a source of CSF virus as macrophages in the choroid plexus are close to both blood and CSF production, which subsequently bathes the brain [4, 49-52]. Another site of interest is the DRG part of which is at the interface of the CNS and the PNS. SPION are abundant in the DRG, which is in communication with the subarachnoid space of the spinal cord and the subarachnoid angle surrounding the nerve sheath [32, 53]. We also find SPION within macrophages in the epineurium and with fascicles of the nerve, suggesting a novel route of possible traffic of macrophages (Wallis *et al.*, submitted). Importantly, macrophages with SIV in the peripheral nerve

and DRG are less affected by ART, unlike the spleen and dCLN. Thus, the DRG and peripheral and cranial nerves, which are still affected with HIV in PLWH on durable ART, deserve more investigation with regard to viral reservoirs and macrophages. It is important to note that Clements *et al.*, show evidence of replication-competent virus in monocytes of PLWH on ART [48, 54].

Possible shortcomings of our work include our use of CD8 depletion for a rapid AIDS model with high tissue pathology. Because of the CD8 depletion ART in this model, this 3-4-month time period does not lower plasma virus to non-detectable levels. That said, many of the observations made in this model, including sCD163 correlating with CNS and CVD pathology, SIV productive infection of PV macrophage in the CNS and CNS tissues, and neuronal injury of the CNS with SIV infection, as well as the ability to clear CNS infection with ART have been confirmed in humans prior to the advent of ART and also in individuals on ART.

This study investigates the distribution of SPION-labeled macrophages within the CNS of normal and SIV-infected animals over time. We found SPION-labeled macrophages primarily in the perivascular space (perivascular macrophages), meninges, and choroid plexus, identifying that meningeal macrophages had a greater accumulation of SPION than PVM. The data suggest that SIV infection leads to increased accumulation of SPION+ macrophages in the CNS, while in non-infected animals, these macrophages traffic out of the CNS. We highlight the significance of SPION-labeled macrophages found in the dCLN, indicating traffic from the CNS, and underscore the need for further investigation into the role of macrophages in viral reservoirs and the impact of ART on CNS inflammation and reseeding of the viral reservoir in the periphery.

2.6 Experimental Procedures

Ethics Statement: All animal work was approved by the Tulane National Primate Research Center Care and Animal Use Committee. The TNRPC protocol number is 3497 and the animal welfare assurance number is A4499-01.

Animals and Viral Infection: Fourteen rhesus macaques (*Macaca mulatta*) born and housed at the Tulane National Primate Research Center in strict adherence to the "Guide for the Care and Use of Laboratory Animals" were used (Figure 1). Of these, 6 are non-infected macaques and 8 are SIV-infected. Animals were experimentally infected i.v with a bolus of SIVmac251 viral swarm (20 ng of SIV p28) over 5 minutes. Two animals received i.c. SPION and fluorescent dextran, and the remaining 12 macaques were inoculated with i.c. SPION. Animals were euthanized at 2 hrs. and 1-day post dextran and SPION injection, and 7, 14, and 28 days post SPION injection.

SPION and Dextran: Superparamagnetic iron oxide nanoparticles (SPION) were obtained from Bang Laboratories Inc (Fishers, IN) (PSCOOHMag/Encapsulated, MEDG001). SPION are iron oxide nanospheres encapsulated in an inert polymer with inherent fluorescence. SPION used have an average particle size of 0.86 μ m diameter and internal fluorescence (Dragon Green [480/520]). SPION were under sterile conditions using a 3 mL stock solution and 7 mL of sterile, low endotoxin 1XPBS. A magnet was used to separate the SPION from liquid and 7 - 10 additional washes were done. SPION were resuspended 1mL of sterile 1XPBS for a final concentration of 33 mg/mL. Select animals (n=2) also received fluorescent dextran (RITC-Dextran, 10 KD, Invitrogen, CA) i.c at a concentration of 33 mg/mL.

Intracisternal Inoculation: To avoid an increase in intracranial pressure, 1 mL of cerebrospinal fluid (CSF) was removed from the cisterna magna prior to the inoculation of SPION or RITC-Dextran. Dragon Green [480/520] SPION (33mg/mL) were injected at 1 hour, 24 hours, and 7, 14, or 28 days prior to euthanasia.

Tissue Collection and Processing: Animals were anesthetized with ketamine-HCl and euthanized with i.v. pentobarbital overdose and exsanguinated. Blood was collected and Heparin Sulfate was administered i.v. and allowed 5 minutes to diffuse. Sodium pentobarbital was administered via intracardiac stick and CSF was collected. Following CSF collection, animals underwent perfusion with 3L of chilled 1XPBS. Postmortem examination was performed by a veterinary pathologist as previously described [33, 34, 52, 85]. Brain (frontal, temporal, occipital, parietal, and choroid plexus) and peripheral tissues (cranial nerves, cribriform plate, nasal septum, brachial plexus, spleen, deep cervical lymph nodes, superficial lymph nodes, axillary lymph nodes) were: i) collected in zinc-buffered formalin and embedded in paraffin, ii) fixed with 2% paraformaldehyde for 4-48 hours, sucrose protected and embedded in optimal cutting temperature (OCT) compound for SPION analysis, or iii) snap frozen in OCT without fixation.

Immunohistochemistry: IHC was performed as previously described using antibodies targeting CD163 (1:250, Leica (Deer Park, IL)), CD68 (1:100, DAKO (Carpinteria, CA)), CD206 (1:1000, R&D Systems (Minneapolis, MN)), and IBA1+ macrophages (1:100, Wako (Osaka, Japan)) [33, 34, 85]. Briefly, formalin-fixed paraffin-embedded sections were de-paraffinised and rehydrated followed by antigen retrieval with a citrate-based Antigen Unmasking Solution (Vector Laboratories, Burlingame, CA) in a microwave (900 W) for 20 min. After cooling for 20 min, sections were washed with

Tris-buffered saline (TBS) containing 0.05% Tween-20 for 5 minutes before incubation with peroxidase block (DAKO, Carpinteria, CA) followed by protein block (DAKO, Carpinteria, CA) for 30 minutes and incubation with primary antibody. Following incubation with a peroxidase-conjugated polymer, slides were developed using a diaminobenzidine chromogen (DAKO, Carpinteria, CA) with Harris Hematoxylin (StatLab, McKinney, TX).

Immunofluorescence: Antibodies targeting CD163 (NCL-CD163 CE, AF568, Invitrogen (Carlsbad, CA)) and gp41+ (KK41+, 1:100, NIH (Manassas, VA)) cells was performed on 2% paraformaldehyde (PFA) fixed frozen sections as previously described [5, 55, 56]. 2% PFA, fixed frozen sections were thawed for 20 minutes at room temperature, unwrapped, submerged in a citrate-based Antigen Unmasking Solution, and microwaved for one minute and forty-five seconds and cooled to room temperature. Slides were permeabilized in a solution of phosphate-buffered saline with 0.01% Triton X-100 and 0.02% fish skin gelatin (PBS-FSG-TX100) followed by a PBS-FSG wash, transferred to a humidified chamber and blocked with 10% normal goat serum (NGS) diluted in PBS-FSG for 40 minutes, followed by a 60-minute primary antibody incubation, washes, and 40-minute secondary antibody incubation. Routine washes were performed and DAPI nuclear stain added for 10 minutes. Slides were mounted using a custom-formulated anti-bleaching mounting media containing Mowiol (#475904, Calbiochem; San Diego, CA) and DABCO (#D2522, Sigma: St. Louis, MO) and allowed to dry overnight before being digitally imaged with a Zeiss Axio Scan.Z1. HALO software (HALO v3.4, Indica Labs; Albuquerque, NM) was used for quantification and analysis.

Detection and quantification of SPION+ macrophages in tissues: SPIONs were detected in the central nervous system (CNS) and peripheral tissues by 1) light microscopy by morphology of the amber SPION beads, 2) Prussian blue iron staining (Sigma Aldrich Iron Stain, St. Louis, MO), and 3) internal fluorescence of Dragon Green. SPION+ cells in whole tissue sections were counted manually at 20x by light microscopy (Plan-Apochromat 620/0.7, Olympus; Japan) in a blinded fashion. Whole section tiling, and stitching was done using a Zeiss Axio Imager M1 microscope (Zeiss;Oberkochen, Germany) with AxioVision (Version 4.8, Zeiss; Oberkochen, Germany) using Plan-Apochromat 620/0.8 and 640/0.95 Korr objectives followed by manual annotation of the parenchyma from the meninges into separate regions of interest (ROIs) and tissue area reported as mm².

Viral RNA and Detection: Ultrasensitive SIV-RNAscope with probes for SIVmac251 was used to detect SPION-containing SIV-RNA positive cells within and outside of the CNS as previously described [56]. Tissue sections were placed in a target antigen retrieval solution, heated, and treated with protease plus, and a hydrogen peroxide blocker according to the manufacturer's protocol (Advanced Cell Diagnostics, Newark, CA). SIVmac239 RNAscope probes (Advanced Cell Diagnostics, Newark, CA) were hybridized at 40°C in the HybEZ II Hybridization System. The RNAscope 2.5 HD Assay amplification steps were applied according to the manufacturer's protocol. Target RNA was visualized through the addition of chromogenic Fast Red A and Fast Red B (Advanced Cell Diagnostics, Newark, CA), and sections were counterstained with hematoxylin (Sigma-Aldrich) and mounted using Vectamount (Vector Laboratories).

2.7 Tables, Figures, and Figure Legends

Figure 2.1

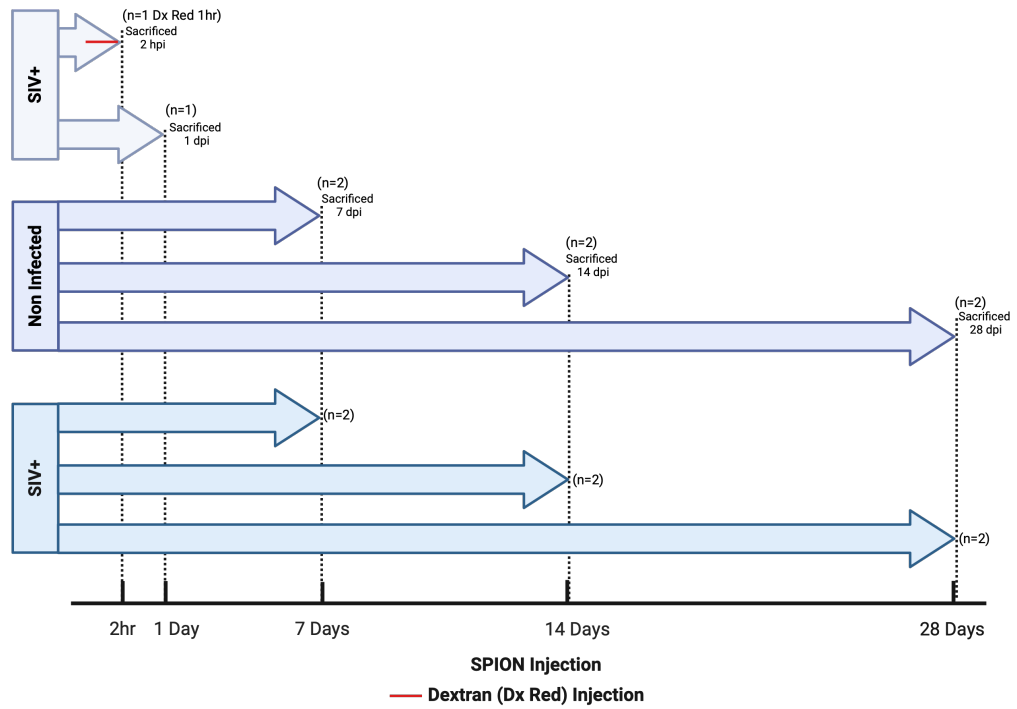


Figure 2.1 Study Design. Fourteen Indian rhesus macaques were used in this study. Six were non-infected and eight were infected with SIVmac251. Macaques received i.c. SPION injection and serial sacrifices with or without dextran dye 1 hour, 1 day, 7-, 14-, or 28- days post-injection. Created in BioRender. Wallis, Z. (2024)

<https://BioRender.com/a42e272>

Figure 2.2

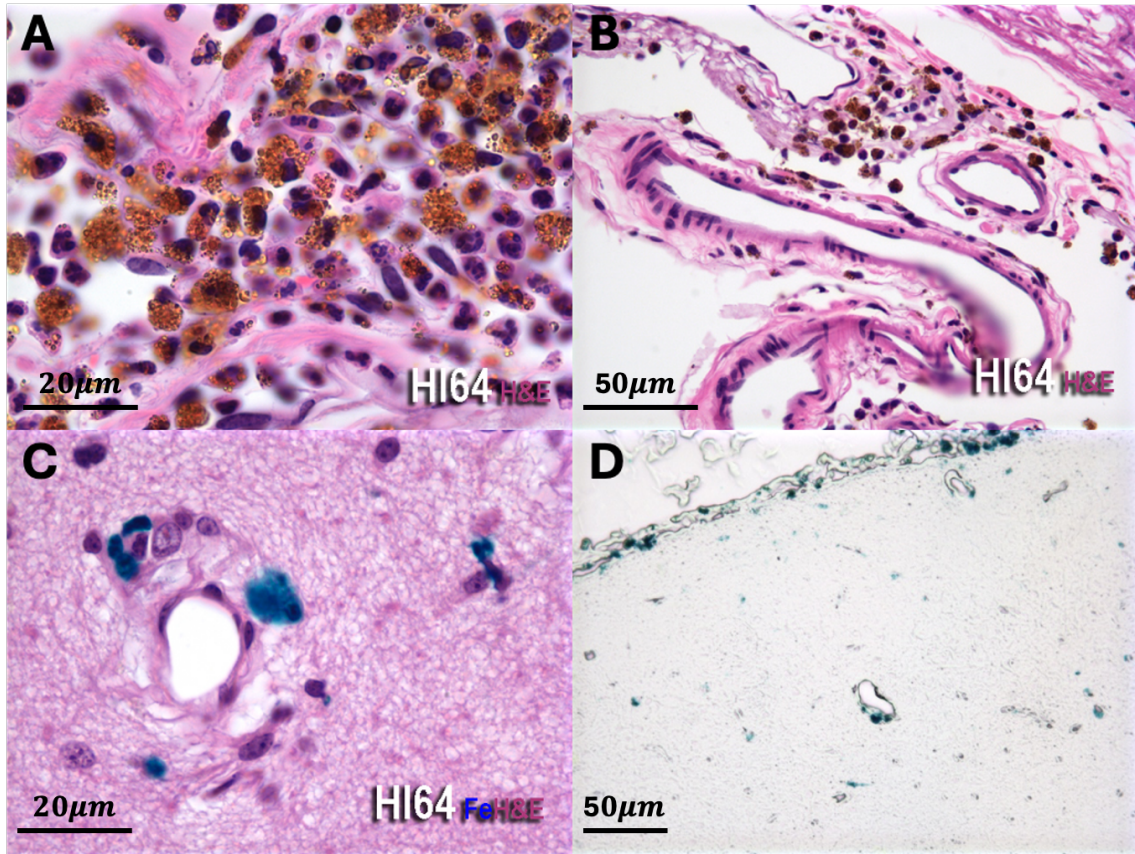


Figure 2.2 Distribution of SPION after i.c. injection. Following i.c. SPION injection, SPION (amber beads) are cell-associated in the CNS (A&B) cerebellum meninges using hematoxylin and eosin to stain the cell nuclei (purple) and the cytoplasm (pink), (C) perivascular space identifying SPION-containing cells with a Prussian blue stain (blue) and hematoxylin and eosin to stain the cell nuclei (purple) and the cytoplasm (pink), and (D) cerebrum meninges and perivascular space identifying SPION-containing cells with a Prussian blue stain (blue).

Figure 2.3

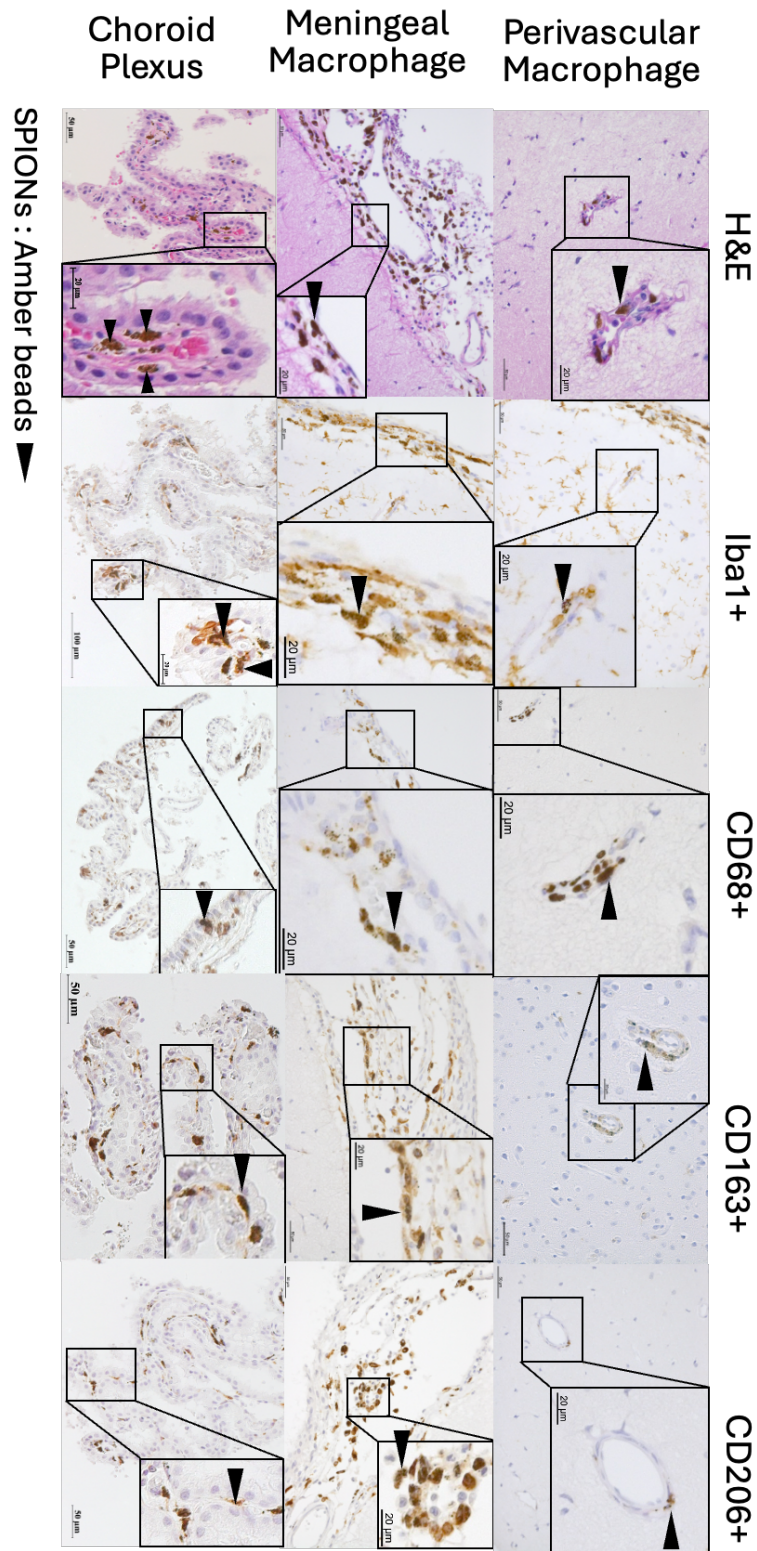


Figure 2.3 SPION localizes to CNS macrophage. SPION (amber beads) localize to Iba1+, CD68+, CD163+, and CD206+ perivascular, meningeal, and choroid plexus macrophages in the CNS using immunohistochemistry to stain macrophages with diaminobenzidine (DAB) forming a brown deposit.

Table 2.1

Time with SPION	Non-Infected	SIV+
Perivascular Macrophages		
7 Days	0.3 ± 0.3 A= 652 mm ² (155)	1.6 ± 0.7 A= 608 mm ² (936)
14 Days	0.6 ± 0.8 A= 675 mm ² (122)	1.8 ± 1.9 A= 792 mm ² (916)
28 Days	0.2 ± 0.1 A=252 mm ² (51)	0.6 ± 0.5 A= 558 mm ² (302)
Meningeal Macrophages		
7 Days	81 ± 43 A= 18 mm ² (1331)	63 ± 63 A= 15 mm ² (1362)
14 Days	36 ± 33 A= 12 mm ² (420)	25 ± 14 A= 32 mm ² (538)
28 Days	50 ± 47 A= 7 mm ² (85)	125 ± 111 A= 6 mm ² (868)

*

Table 2.1 Accumulation of SPION+ macrophage in the CNS over time. Data are cell numbers (average \pm StDev) counted in whole tissue sections and expressed as cells per mm². The total area examined is indicated and expressed as tissue area per mm². The area of the meninges and parenchyma were obtained by tiling and hand-drawing around each ROI. The total number of SPION+ macrophages counted is shown in parentheses. A minimum of 4 sections per animal were examined. Prism was used for graphing and statistical analysis Kruskal-Wallis nonparametric test. Non-infected perivascular macropahge, p=0.61. SIV-infected perivascular macropahge, p=0.19. Non-infected to SIV-infected perivascular macropahge, p<0.005. Non-infected meningeal macropahge, p=0.10. SIV-infected meningeal macropahge, p<0.05. Non-infected to SIV-infected meningeal macropahge, p=0.053.

Figure 2.4

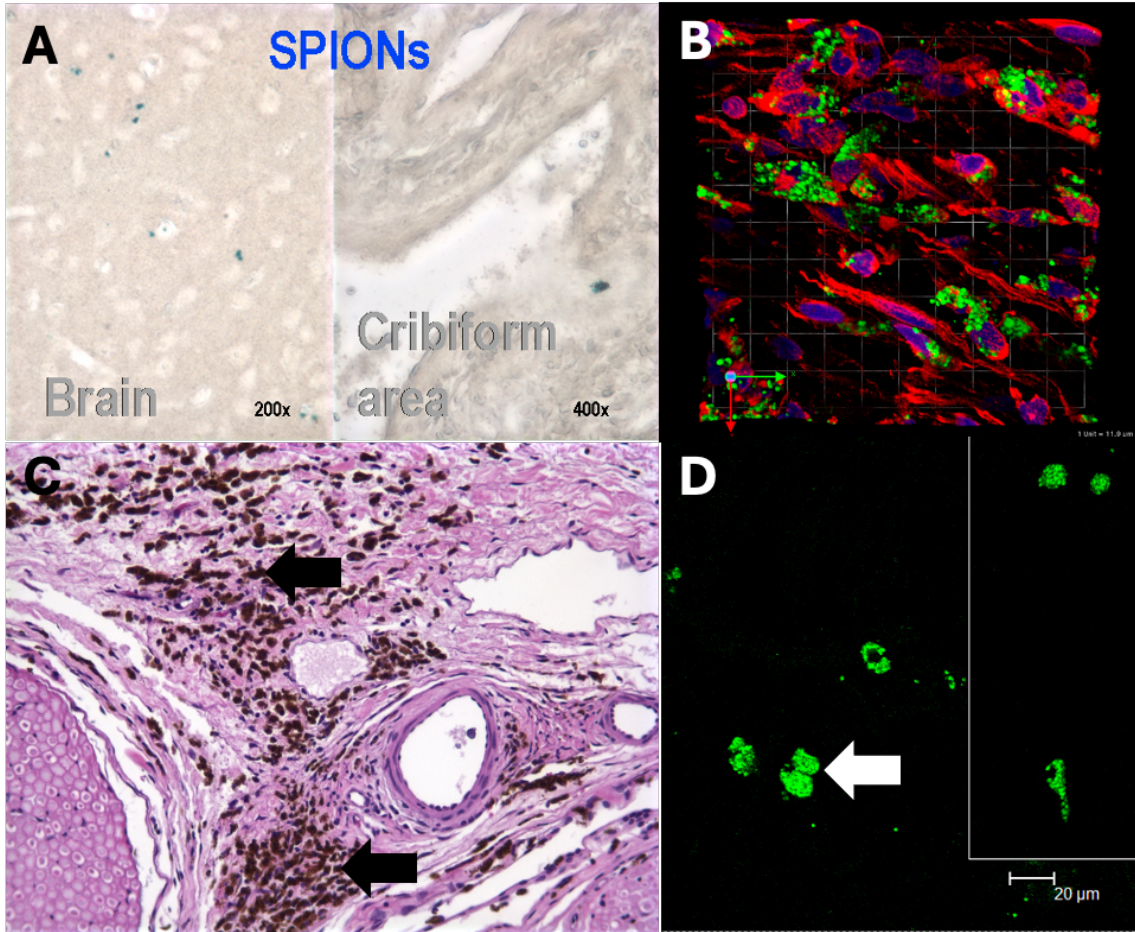


Figure 2.4 SPION+ Macrophage outside of the CNS over time. (A) SPION (Prussian blue) in the brain and cribriform plate area, (B) SPION (green) localized to CD163+ macrophage (Red) in cranial nerves, (C) SPION (amber beads) clustered in the DRGs, and (D) SPION (green) in the tonsils.

Figure 2.5

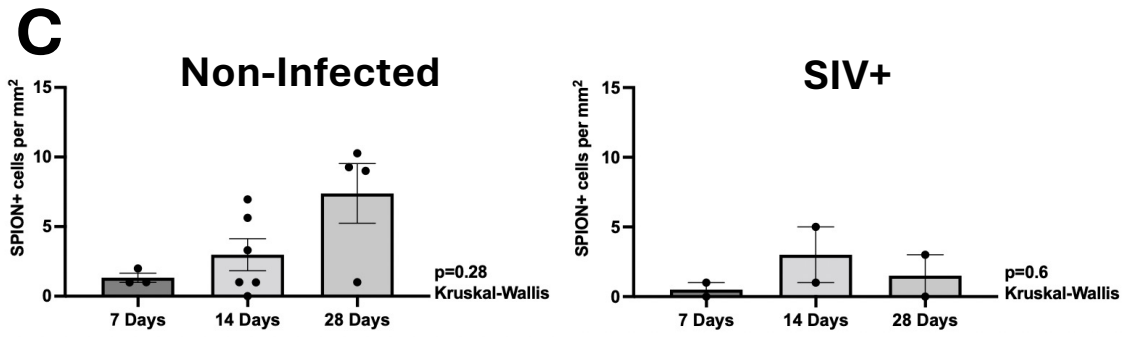
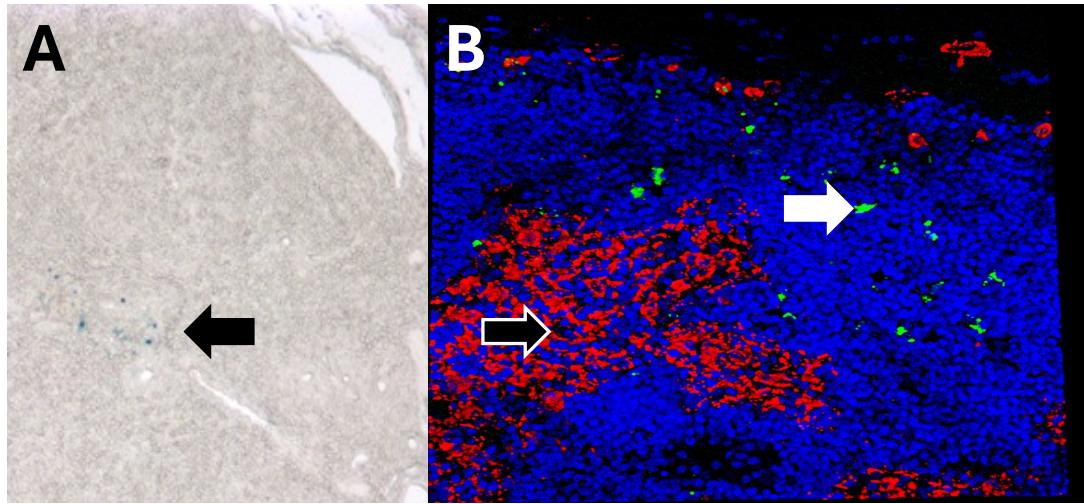


Figure 2.5 Traffic of SPION+ macrophage out of the CNS to the dCLN over time.

(A) SPION (Prussian blue) located in the deep CLN 7 days post i.c. SPION injection. (B) Dextran dye (Red, white border arrow) and SPION (green, black arrow) in different regions of the deep CLN post i.c. injection. (C) Number of SPION+ macrophages in the deep CLN post i.c. injection in non-infected and SIV-infected macaques. Each data point represents the cell count from the tissue section examined and is expressed as the number of positive cells per mm². Prism was used for graphing and statistical analysis Kruskal-Wallis nonparametric test.

Table 2.2

Tissue Outside of the CNS	Days after SPIONs Injection in the Cisterna Magna				
	0.4	1	7	14	28
Non-Infected Animals					
Optic Nerve+Eye	nd	nd	20 ± 6.6	2.7 ± 2.8	49 ± 18
Cervical Lymph Node	nd	nd	24 ± 2.3**	0.35 ± 0.63	4.8 ± 4.1
Nasal Septum	nd	nd	147 ± 12**	nd	1.3 ± 1.4
Cribiform Plate	nd	nd	6.0 ± 2.5	nd	49 ± 41
Spleen	nd	nd	73 ± 48**	66 ± 38	49 ± 18
SIV+ Animals					
Optic Nerve+Eye	0	0	nd	0.67 ± 0.92	3.3 ± 3.8
Cervical Lymph Node	0	0	0.43 ± 0.06**	2.8 ± 2.9	1.1 ± 0.22
Nasal Septum	0	0	2.5 ± 0.51**	0.33 ± 2.7	0
Axiliar Lymph Node	0	0	0	1.7 ± 2.1	1.1 ± 0.77
Spleen	0	0	0.26 ± 0.27**	58 ± 43	12 ± 10

Table 2.2 SPION+ macrophage outside of the CNS over time. Data are cell numbers (average \pm StDev) counted in 10 fields of view at 40x and expressed as the number of cells per mm². Prism was used for graphing and statistical analysis Kruskal-Wallis nonparametric test, $p < 0.005$. ** $P < 0.01$

Figure 2.6

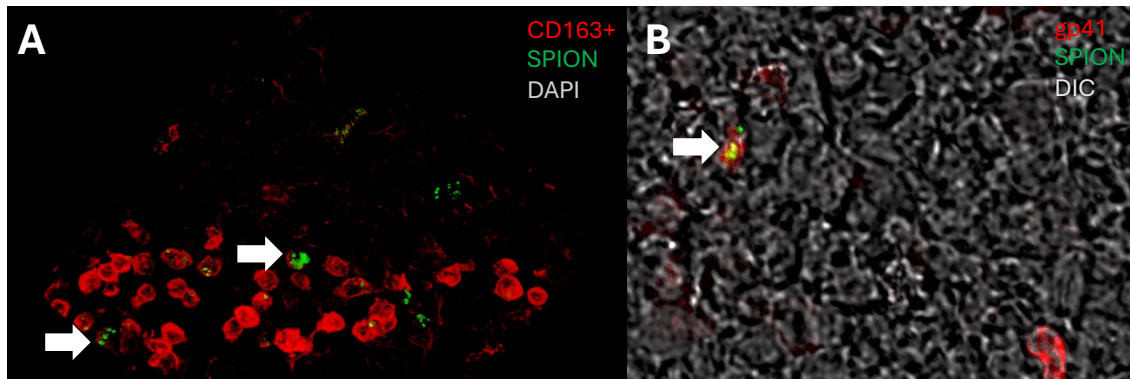


Figure 2.6 SPION localized to CD163+ gp41+ productively macrophage in the dCLN. (A) SPION (Green) are localized to CD163+ macrophage (Red) in the dCLN following i.c. injection and (B) serial section with SPION+ (green) gp41+ (red).

Figure 2.7

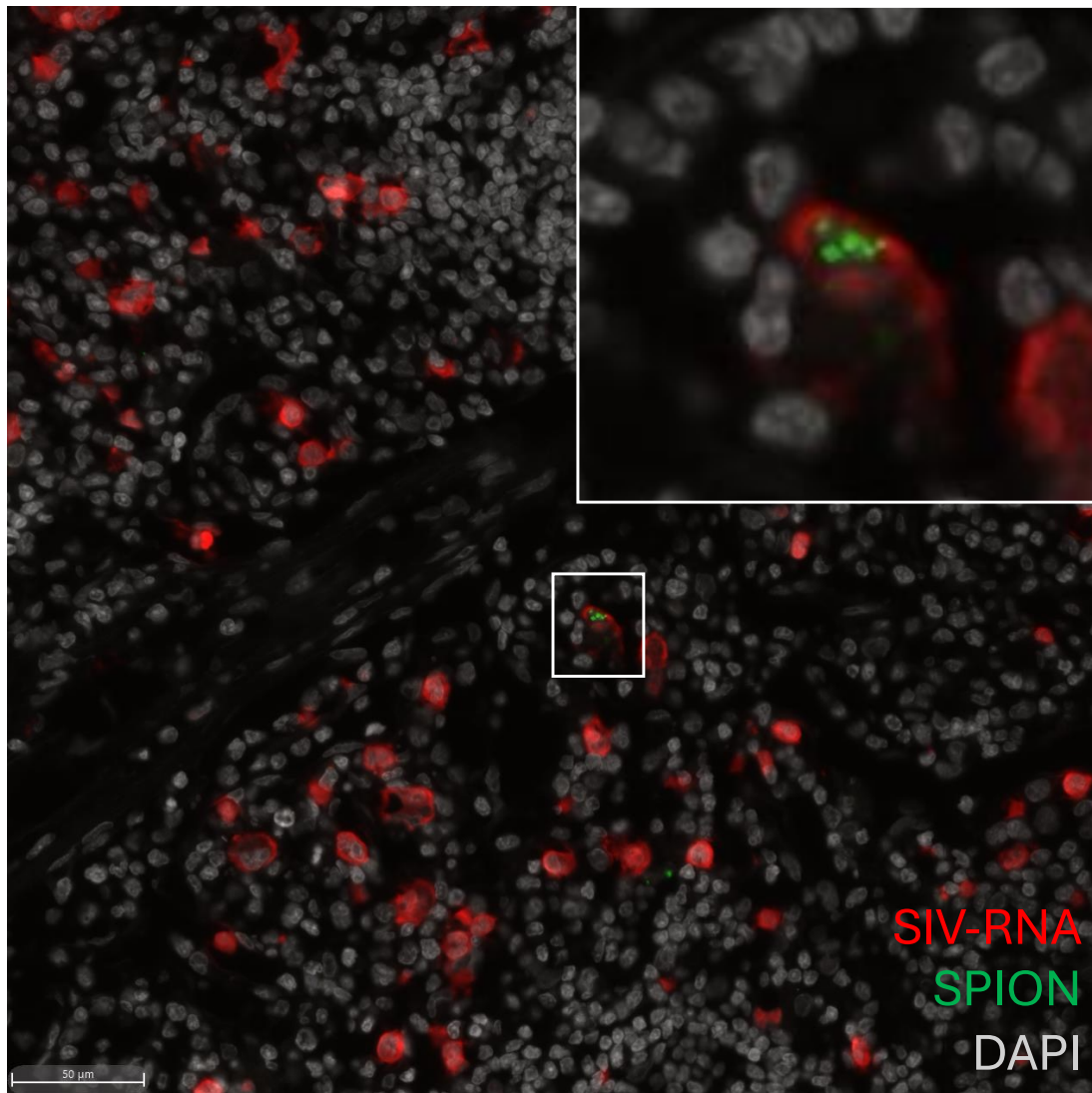


Figure 2.7 SIV-RNA+ SPION+ macrophage in the dCLN with AIDS. SPION((green) localized to SIV-RNA+ (red) macrophage in the dCLN. Image captured from scanned dCLN section.

2.8 References

1. Williams, K.C., et al., *Perivascular Macrophages Are the Primary Cell Type Productively Infected by Simian Immunodeficiency Virus in the Brains of Macaques: Implications for the Neuropathogenesis of AIDS*. Journal of Experimental Medicine, 2001. **193**(8): p. 905-916.
2. Zink, M.C., et al., *Simian Immunodeficiency Virus-Infected Macaques Treated with Highly Active Antiretroviral Therapy Have Reduced Central Nervous System Viral Replication and Inflammation but Persistence of Viral DNA*. The Journal of Infectious Diseases, 2010. **202**(1): p. 161-170.
3. Bednar, M.M., et al., *Compartmentalization, Viral Evolution, and Viral Latency of HIV in the CNS*. Curr HIV/AIDS Rep, 2015. **12**(2): p. 262-71.
4. Lackner, A.A., et al., *Localization of simian immunodeficiency virus in the central nervous system of rhesus monkeys*. Am J Pathol, 1991. **139**(3): p. 609-21.
5. Nowlin, B.T., et al., *SIV encephalitis lesions are composed of CD163(+) macrophages present in the central nervous system during early SIV infection and SIV-positive macrophages recruited terminally with AIDS*. Am J Pathol, 2015. **185**(6): p. 1649-65.
6. Bechmann, I., et al., *Turnover of rat brain perivascular cells*. Exp Neurol, 2001. **168**(2): p. 242-9.
7. Goldmann, T., et al., *Origin, fate and dynamics of macrophages at central nervous system interfaces*. Nat Immunol, 2016. **17**(7): p. 797-805.
8. Lassmann, H., et al., *Bone marrow derived elements and resident microglia in brain inflammation*. Glia, 1993. **7**(1): p. 19-24.
9. Hickey, W.F., K. Vass, and H. Lassmann, *Bone marrow-derived elements in the central nervous system: an immunohistochemical and ultrastructural survey of rat chimeras*. J Neuropathol Exp Neurol, 1992. **51**(3): p. 246-56.
10. Kierdorf, K., et al., *Macrophages at CNS interfaces: ontogeny and function in health and disease*. Nat Rev Neurosci, 2019. **20**(9): p. 547-562.
11. Saylor, D., et al., *HIV-associated neurocognitive disorder — pathogenesis and prospects for treatment*. Nature Reviews Neurology, 2016. **12**(4): p. 234-248.
12. Williams, K.C. and W.F. Hickey, *Central nervous system damage, monocytes and macrophages, and neurological disorders in AIDS*. Annu Rev Neurosci, 2002. **25**: p. 537-62.
13. Clements, J.E., et al., *The central nervous system is a viral reservoir in simian immunodeficiency virus--infected macaques on combined antiretroviral therapy:*

- a model for human immunodeficiency virus patients on highly active antiretroviral therapy.* J Neurovirol, 2005. **11**(2): p. 180-9.
14. Zink, M.C., et al., *High viral load in the cerebrospinal fluid and brain correlates with severity of simian immunodeficiency virus encephalitis.* J Virol, 1999. **73**(12): p. 10480-8.
 15. Aspelund, A., et al., *A dural lymphatic vascular system that drains brain interstitial fluid and macromolecules.* J Exp Med, 2015. **212**(7): p. 991-9.
 16. Engelhardt, B., et al., *Vascular, glial, and lymphatic immune gateways of the central nervous system.* Acta Neuropathol, 2016. **132**(3): p. 317-38.
 17. Hatterer, E., et al., *How to drain without lymphatics? Dendritic cells migrate from the cerebrospinal fluid to the B-cell follicles of cervical lymph nodes.* Blood, 2006. **107**(2): p. 806-12.
 18. Iliff, J.J., et al., *A paravascular pathway facilitates CSF flow through the brain parenchyma and the clearance of interstitial solutes, including amyloid β .* Sci Transl Med, 2012. **4**(147): p. 147ra111.
 19. Kida, S., A. Pantazis, and R.O. Weller, *CSF drains directly from the subarachnoid space into nasal lymphatics in the rat. Anatomy, histology and immunological significance.* Neuropathol Appl Neurobiol, 1993. **19**(6): p. 480-8.
 20. Ma, Q., et al., *Outflow of cerebrospinal fluid is predominantly through lymphatic vessels and is reduced in aged mice.* Nat Commun, 2017. **8**(1): p. 1434.
 21. Proulx, S.T., *Cerebrospinal fluid outflow: a review of the historical and contemporary evidence for arachnoid villi, perineural routes, and dural lymphatics.* Cellular and Molecular Life Sciences, 2021. **78**(6): p. 2429-2457.
 22. Hatterer, E., et al., *Cerebrospinal fluid dendritic cells infiltrate the brain parenchyma and target the cervical lymph nodes under neuroinflammatory conditions.* PLoS One, 2008. **3**(10): p. e3321.
 23. Da Mesquita, S., et al., *Functional aspects of meningeal lymphatics in ageing and Alzheimer's disease.* Nature, 2018. **560**(7717): p. 185-191.
 24. Louveau, A., et al., *CNS lymphatic drainage and neuroinflammation are regulated by meningeal lymphatic vasculature.* Nat Neurosci, 2018. **21**(10): p. 1380-1391.
 25. Louveau, A., et al., *Understanding the functions and relationships of the glymphatic system and meningeal lymphatics.* J Clin Invest, 2017. **127**(9): p. 3210-3219.

26. Laman, J.D. and R.O. Weller, *Drainage of cells and soluble antigen from the CNS to regional lymph nodes*. J Neuroimmune Pharmacol, 2013. **8**(4): p. 840-56.
27. van Zwam, M., et al., *Brain antigens in functionally distinct antigen-presenting cell populations in cervical lymph nodes in MS and EAE*. J Mol Med (Berl), 2009. **87**(3): p. 273-86.
28. de Vos, A.F., et al., *Transfer of central nervous system autoantigens and presentation in secondary lymphoid organs*. J Immunol, 2002. **169**(10): p. 5415-23.
29. Ma, Q., et al., *Clearance of cerebrospinal fluid from the sacral spine through lymphatic vessels*. Journal of Experimental Medicine, 2019. **216**(11): p. 2492-2502.
30. Jacob, L., et al., *Anatomy and function of the vertebral column lymphatic network in mice*. Nature Communications, 2019. **10**(1): p. 4594.
31. Miura, M., S. Kato, and M. von Lüdinghausen, *Lymphatic drainage of the cerebrospinal fluid from monkey spinal meninges with special reference to the distribution of the epidural lymphatics*. Arch Histol Cytol, 1998. **61**(3): p. 277-86.
32. Hu, P. and E.M. McLachlan, *Macrophage and lymphocyte invasion of dorsal root ganglia after peripheral nerve lesions in the rat*. Neuroscience, 2002. **112**(1): p. 23-38.
33. Delcroix, G.J., et al., *Mesenchymal and neural stem cells labeled with HEDP-coated SPIO nanoparticles: in vitro characterization and migration potential in rat brain*. Brain Res, 2009. **1255**: p. 18-31.
34. Jendelová, P., et al., *Magnetic resonance tracking of transplanted bone marrow and embryonic stem cells labeled by iron oxide nanoparticles in rat brain and spinal cord*. J Neurosci Res, 2004. **76**(2): p. 232-43.
35. Salemi, M., et al., *Phylogenetic analysis of human immunodeficiency virus type 1 in distinct brain compartments provides a model for the neuropathogenesis of AIDS*. J Virol, 2005. **79**(17): p. 11343-52.
36. Lamers, S.L., et al., *HIV-1 phylogenetic analysis shows HIV-1 transits through the meninges to brain and peripheral tissues*. Infect Genet Evol, 2011. **11**(1): p. 31-7.
37. Goldmann, J., et al., *T cells traffic from brain to cervical lymph nodes via the cribriform plate and the nasal mucosa*. J Leukoc Biol, 2006. **80**(4): p. 797-801.
38. Karman, J., et al., *Initiation of immune responses in brain is promoted by local dendritic cells*. J Immunol, 2004. **173**(4): p. 2353-61.

39. Laaker, C., et al., *Immune cells as messengers from the CNS to the periphery: the role of the meningeal lymphatic system in immune cell migration from the CNS*. Front Immunol, 2023. **14**: p. 1233908.
40. Raper, D., A. Louveau, and J. Kipnis, *How Do Meningeal Lymphatic Vessels Drain the CNS?* Trends Neurosci, 2016. **39**(9): p. 581-586.
41. Lamers, S.L., et al., *The meningeal lymphatic system: a route for HIV brain migration?* J Neurovirol, 2016. **22**(3): p. 275-81.
42. Frederick, N. and A. Louveau, *Meningeal lymphatics, immunity and neuroinflammation*. Curr Opin Neurobiol, 2020. **62**: p. 41-47.
43. Kanamori, M. and J. Kipnis, *Meningeal lymphatics "drain" brain tumors*. Cell Res, 2020. **30**(3): p. 191-192.
44. das Neves, S.P., N. Delivanoglou, and S. Da Mesquita, *CNS-Draining Meningeal Lymphatic Vasculature: Roles, Conundrums and Future Challenges*. Front Pharmacol, 2021. **12**: p. 655052.
45. Daneman, R. and A. Prat, *The blood-brain barrier*. Cold Spring Harb Perspect Biol, 2015. **7**(1): p. a020412.
46. Chen, H. and E.E. Konofagou, *The size of blood-brain barrier opening induced by focused ultrasound is dictated by the acoustic pressure*. J Cereb Blood Flow Metab, 2014. **34**(7): p. 1197-204.
47. Girard, J.-P., C. Moussion, and R. Förster, *HEVs, lymphatics and homeostatic immune cell trafficking in lymph nodes*. Nature Reviews Immunology, 2012. **12**(11): p. 762-773.
48. Abreu, C., et al., *Brain macrophages harbor latent, infectious simian immunodeficiency virus*. Aids, 2019. **33 Suppl 2**(Suppl 2): p. S181-s188.
49. Falangola, M.F., B.G. Castro-Filho, and C.K. Petito, *Immune complex deposition in the choroid plexus of patients with acquired immunodeficiency syndrome*. Ann Neurol, 1994. **36**(3): p. 437-40.
50. Hanly, A. and C.K. Petito, *HLA-DR-positive dendritic cells of the normal human choroid plexus: a potential reservoir of HIV in the central nervous system*. Hum Pathol, 1998. **29**(1): p. 88-93.
51. Chen, H., C. Wood, and C.K. Petito, *Comparisons of HIV-1 viral sequences in brain, choroid plexus and spleen: potential role of choroid plexus in the pathogenesis of HIV encephalitis*. J Neurovirol, 2000. **6**(6): p. 498-506.

52. Liu, Y., et al., *Analysis of human immunodeficiency virus type 1 gp160 sequences from a patient with HIV dementia: evidence for monocyte trafficking into brain.* J Neurovirol, 2000. **6 Suppl 1**: p. S70-81.
53. McCabe, J.S. and F.N. Low, *The subarachnoid angle: An area of transition in peripheral nerve.* The Anatomical Record, 1969. **164**(1): p. 15-33.
54. Veenhuis, R.T., et al., *Monocyte-derived macrophages contain persistent latent HIV reservoirs.* Nature Microbiology, 2023. **8**(5): p. 833-844.
55. Soulas, C., et al., *Recently infiltrating MAC387(+) monocytes/macrophages a third macrophage population involved in SIV and HIV encephalitic lesion formation.* Am J Pathol, 2011. **178**(5): p. 2121-35.
56. White, K.S., et al., *Simian immunodeficiency virus-infected rhesus macaques with AIDS co-develop cardiovascular pathology and encephalitis.* Front Immunol, 2023. **14**: p. 1240946.

2.9 Chapter Overview and Next Steps

Our study investigated whether CNS macrophages can exit the CNS under normal conditions and with SIV infection to examine their potential for CNS virus dissemination. Using intracisternal injection of fluorescent-SPION in both non-infected and SIV-infected macaques, we found that CNS macrophages exit the CNS to draining lymphatics including the dCLN, spleen, and DRG. Notably, in SIV-infected animals, we observed an increase in CNS macrophages and reduced traffic to peripheral sites, whereas there was traffic out over time in non-infected macaques. SPION-labeled macrophages outside the CNS contained SIV-RNA and gp41+ in SIV-infected macaques, indicating that CNS-derived virally infected macrophages can exit and reseed the periphery. Our next steps were to determine the effects of AIDS, ART, and following ART interruption on macrophage traffic out of the CNS (Chapter 3).

3.0 Chapter 3

Resolving Inflammation: The Impact of Antiretroviral Therapy on Macrophage Traffic In and Out of the CNS.

Zoey K. Wallis¹

Cecily C. Midkiff²

Miaoyun Zhao³

Soon Ok Kim¹

Addison Amadeck¹

Yiwei Wang¹

Maia Jakubowski¹

Tricia Burdo⁴

Andrew D. Miller⁵

Qingsheng Li³

Xavier Alvarez⁶

Robert V. Blair²

Kenneth C. Williams¹

¹ Morrissey College of Arts and Sciences, Biology Department, Boston College, Chestnut Hill, MA, USA.

² Tulane National Primate Research Center, Covington, LA, USA.

³ Nebraska Center for Virology, School of Biological Sciences, University of Nebraska-Lincoln, Lincoln, NE, USA.

⁴ Department of Medicine, Rutgers Institute for Translational Medicine and Science, Robert Wood Johnson School of Medicine, New Brunswick, NJ, USA.

⁵ Department of Population Medicine and Diagnostic Sciences, Section of Anatomic Pathology, College of Veterinary Medicine, Cornell University, Ithaca, NY, USA.

⁶ Imaging PET-CT and OIL Core, Southwest National Primate Research Center, San Antonio, TX, USA.

3.1 Author Contributions

Conceptualization, K.C.W., Z.K.W., and X.A.; Obtained and analyzed data and images, Z.K.W., C.C.M., M.Z., S.O.K, A.A., Y.W., and M.J.; writing—original draft preparation, Z.K.W., C.C.M., and K.C.W; writing—review and editing, K.C.W., Z.K.W., T.B., A.D.M, Q.L., X.A., and R.V.B.; funding acquisition, K.C.W.

Manuscript in preparation as of November 2024.

3.2 Abstract

The effects of antiretroviral therapy (ART) and therapy interruption on myeloid traffic out of the central nervous system (CNS) with human immunodeficiency virus (HIV) and simian immunodeficiency virus (SIV) infection are understudied. Using intracisternal (i.c.) injection of dual-colored fluorescent superparamagnetic iron oxide nanoparticles (SPION) in SIV-infected macaques early (12-14 dpi) and late (30 days before sacrifice) we studied CNS macrophage viral reservoirs, turnover, and traffic out. SPION are preferentially taken up by perivascular, meningeal, and choroid plexus macrophages. In non-infected macaques, SPION+ macrophages traffic out of the CNS to the periphery (deep cervical lymph node (dCLN), spleen, and dorsal root ganglia (DRG)) but accumulate in the CNS with SIV infection. ART reduces the accumulation of CNS SPION+ perivascular macrophages but not meningeal or choroid plexus macrophages. Four weeks after ART interruption, SPION+ perivascular and choroid plexus macrophage numbers remain the same, but the numbers of SPION+ meningeal macrophages increase. ART eliminates SIV-RNA perivascular macrophages, but few scattered SIV-RNA macrophages remain in the meninges and choroid plexus. Four weeks after ART interruption, perivascular macrophages remain SIV- and scattered SIV+ meningeal and choroid plexus macrophages remain. Normally, SPION+ macrophages leave the CNS trafficking to dCLN, spleen, and DRG at a rate that is decreased with SIV infection and AIDS. SIV-RNA+ SPION+ macrophages that traffic out of the CNS are eliminated by ART and do not rebound with ART interruption. Using two different colored SPION to study the establishment of CNS SIV viral reservoirs, we find greater numbers of early SPION+ macrophages within and outside of the CNS with SIVE, ART,

and ART interruption. These data are consistent with SIV-infected perivascular macrophages establishing an early viral reservoir and continual viral seeding of the meninges and choroid plexus during infection. They are consistent with ART reducing the CNS perivascular macrophage viral reservoir, preventing traffic of infected macrophages out of the CNS, but less so SIV-RNA macrophages in meninges and choroid plexus that can rebound following ART interruption.

Keywords: HIV, SIV, AIDS, SIVE, ART, ART Interruption, Traffic, CNS Macrophages

3.3 Introduction

Antiretroviral therapy (ART) has reduced the incidence of severe human immunodeficiency virus (HIV)-associated neurocognitive disorders (HAND), yet the prevalence of mild and asymptomatic HAND and HIV-associated neuropathy has increased [1]. While durable ART diminishes HIV and simian immunodeficiency virus (SIV) infection, latently infected myeloid cells persist in the CNS and may be a source of viral recrudescence where macrophage traffic out of the CNS could result in viral redistribution [2-8]. Distinct CNS macrophages, some of which originate from bone marrow derived monocytes, can be infected by HIV and SIV and establish the CNS viral reservoir [9-11]. These include perivascular macrophages, meningeal macrophages, and macrophages in the choroid plexus. CNS perivascular macrophages monitor the interface between cerebrospinal fluid (CSF) and blood [12-15], are HIV and SIV-RNA+ and DNA+ as early as 3-7 days post-infection the periphery [16, 17], and make up the CNS viral reservoir [6, 9, 10, 16]. Resident meningeal macrophages, derived from mesodermal precursors in the yolk sac, are repopulated from the bone marrow at a slow, consistent rate [13, 18-21]. Whereas, the choroid plexus contains bone marrow-derived stromal and Kolmer macrophages that turnover continuously [22, 23] and are HIV and SIV-RNA+ and DNA+ [24-28]. The resident CNS macrophage—microglia—with a minimal capacity for self-renewal are thought to be a viral reservoir less so than perivascular macrophages [13, 29, 30]. In normal and HIV-infected humans and SIV-infected non-human primates, there is CNS inflammation and both turnover and an accumulation of bone marrow-derived perivascular, meningeal, and choroid plexus macrophages [31-34]. Less well-studied and more pressing is the effect of ART and ART interruption on CNS

macrophage with HIV and SIV infection, accumulation, and their potential to traffic out of the CNS.

Minimally, there are three entry routes of bone marrow and blood-derived monocytes/macrophage into the CNS, including (i) migration directly from the blood via postcapillary venules in the parenchyma (perivascular macrophage), (ii) migration from postcapillary venules in the meninges (meningeal macrophage), and (iii) migration to and through the choroid plexus (stromal and Kolmer macrophage) into the CSF and subarachnoid space (SAS) (meningeal and perivascular macrophage) [35-37]. Using CD34⁺ autologous hematopoietic stem cell transplant in rhesus macaques, we found perivascular macrophages are continuously renewed from the bone marrow, similar to what others have shown in humans [12, 14, 15, 38-42]. We and others have shown early traffic (3-7 days) of virally infected monocytes into the CNS seeds the brain with HIV and SIV [43-45] and blocking traffic with the anti- $\alpha 4\beta 1$ antibody (Natalizumab) alone blocks CNS virus and resolves neuronal injury [43-45]. While previous efforts have focused on blocking the migration of bone marrow-monocytes/macrophages to the CNS, whether macrophages leave the brain and traffic out to the periphery normally and with HIV and SIV infection has not been determined. That CNS macrophage populations are reservoirs of HIV and SIV is established; their ability to reseed the periphery with CNS-derived virus has been suggested but, to date, not investigated.

Potential pathways, effects of immune cells and fluid leaving the CNS, the dynamics of viral infection and ART, and the resolution of inflammation are understudied. Historically, this was in part due to the belief in a lack of CNS-draining lymphatics [35]. Using intracisternal and intraparenchymal injection (i.c.) of dyes and fluorescently

labeled antigen-presenting cells (APCs), traffic of APCs and drainage of CSF to the deep cervical lymph nodes (dCLN) is documented to occur normally and at a rate that is increased with inflammation [19, 46-51]. Importantly, ablation of meningeal lymphatics and the dCLN reduces such traffic and effectively reduces clinical symptoms in experimental autoimmune encephalomyelitis (EAE) [19, 46-51]. In addition, CSF flows from the fourth ventricle into the central canal and through the lateral and median apertures to the SAS along the entirety of the spinal cord. This pathway also allows for the exchange between the CSF in the central canal, the CSF enveloping the spinal cord in the SAS via perivascular spaces, and is crucial for the traffic of cells out of the CNS [52]. While eloquent, experimental injection or transplantation of labeled cells and fluid into the CNS parenchymal can result in CNS injury and/or disruption of the blood-brain barrier (BBB) and CNS parenchymal immune cell activation. Additionally, these studies have largely been done in rodents. To date, it is unknown whether macrophages leave the CNS in humans or non-human primates normally and with HIV or SIV infection. Similarly, the effects of ART on CNS macrophage viral reservoirs, macrophage traffic out, CNS inflammation, viral recrudescence, and CNS viral redistribution to the periphery are not known.

We used i.c. injection of fluorescently labeled superparamagnetic iron oxide nanoparticles (SPION) to study perivascular, meningeal, and choroid plexus macrophages accumulation, traffic, and infection with acquired immunodeficiency syndrome (AIDS) and SIV-encephalitis (SIVE), ART, and ART interruption. We previously showed SPION preferentially labeled these macrophages in non-infected macaques in the CNS and can migrate out to secondary lymphoid organs including the

dCLN, spleen, and DRG (Alvarez *et al.*, in prep). With SIV infection, there was an accumulation of SPION+ macrophage in the CNS, which reduced traffic out (Alvarez *et al.*, in prep). In the current study, we analyzed CNS macrophage accumulation, traffic out with SIV infection in animals with AIDS and SIVE, on ART, and 4 weeks post ART interruption. We find retention of SPION+ macrophages in the CNS with AIDS and SIVE and decreased traffic out. ART reduces SPION+ macrophages in the CNS and increases their numbers in the periphery. We find SIV-RNA+ SPION+ macrophages in the CNS and periphery (dCLN, spleen, and DRG) that are eliminated with ART. ART clears SIV-RNA+SPION+ perivascular macrophages but not SIV-RNA+SPION+ meningeal and choroid plexus macrophages. There is a rebound of plasma virus, SIV-RNA+SPION+ meningeal, and choroid plexus macrophages, but not CNS perivascular macrophages with ART interruption. These findings are discussed in the context of CNS macrophage inflammation, accumulation, infection, and a viral rebound with ART interruption.

3.4 Results

ART reduces SPION+ perivascular macrophages but not meningeal or choroid plexus macrophages.

We analyzed SIV-infected animals that were untreated and developed AIDS and SIVE (n=5), that were on ART and did not develop AIDS or SIVE (SIVnoE) (n=10) and had ART interruption for four weeks and were sacrificed (n=4) (**Table 3.1, Figure 3.1**). We analyzed the number of SPION+ perivascular, meningeal, and choroid plexus macrophages in SIVE, ART, and ART interruption (ART Off) animals (**Figure 3.1A**). Overall, there are reduced numbers of SPION+ perivascular macrophages than SPION+ meningeal macrophages (50-195x) and SPION+ choroid plexus macrophages (1-5x) (**Figure 3.2A-C**). Because there are greater numbers of total macrophages in the meninges than perivascular macrophages in the parenchyma that could take up SPION, we determined the ratio of total CD163+ and CD68+ SPION+ macrophages to the total number of CD163+ and CD68+ macrophages for perivascular, meningeal, and choroid plexus macrophages to compare the ratio in each compartment and importantly the ratio did not change (**Figure 3.2**). Animals with AIDS and SIVE have 0.66 ± 0.13 SPION+/mm² SPION+ perivascular macrophages that were reduced (p=0.054) to 0.18 ± 0.02 SPION+/mm² with ART and did not change with ART interruption (0.21 ± 0.20 SPION+/mm²) (**Figure 3.2A**). SIVE animals had 28 ± 5.8 SPION+/mm² SPION+ meningeal macrophages and no decrease with ART (22 ± 4.9 SPION+/mm²) and significantly (p<0.05) increased numbers with ART interruption compared to ART (ART Off: 39 ± 8.6 SPION+/mm²) (**Figure 3.2B**). There were 18 ± 13 SPION+/mm² SPION+ macrophages in the choroid plexus of SIVE animals that slightly increased with

ART (26 ± 25 SPION⁺/mm²) and a significant decrease with ART interruption (8.0 ± 3.7 SPION⁺/mm²) ($p < 0.05$) (**Figure 3.2C**). This decrease in the number of SPION⁺ macrophages in the choroid plexus following ART interruption may correspond with the increase in the number of SPION⁺ macrophages in the meninges, indicative of macrophage traffic into the CNS. These data are consistent with the accumulation of perivascular macrophages with SIVE that is reduced with ART and an accumulation of SPION⁺ meningeal and choroid plexus macrophages that are unaffected by ART.

ART decreases perivascular, meningeal, and choroid plexus macrophages.

We next assessed the effects of ART and ART interruption on the accumulation of CNS macrophage. SIVE animals have 13 ± 1.5 CD163⁺/mm² CD163⁺ perivascular macrophages that significantly decrease with ART (4 ± 0.26 CD163⁺/mm², $p < 0.0001$) and significantly increase compared to ART after ART interruption (7.7 ± 0.66 CD163⁺/mm², $p < 0.001$) (**Figure 3.2A**). Similarly, ART significantly ($p < 0.0001$) decreases meningeal and choroid plexus macrophages (2-fold) (Meninges SIVE: 91 ± 12 CD163⁺/mm²; ART: 54 ± 3.3 CD163⁺/mm²) (Choroid plexus SIVE: 622 ± 441 CD68⁺/mm²; ART: 246 ± 192 CD68⁺/mm²) (**Figure 3.2B-C**). There is a 1.5-fold increase in the number of meningeal macrophages compared to ART that did not reach statistical significance and no increase in the numbers of choroid plexus macrophages (meninges ART: 54 ± 3.3 CD163⁺/mm²; ART Off: 70 ± 5.5 CD163⁺/mm²) (choroid plexus ART: 246 ± 192 CD68⁺/mm²; ART Off: 293 ± 167 CD68⁺/mm²) (**Figure 3.2B-C**). Our data suggest there is an increased accumulation of perivascular, meningeal, and choroid plexus macrophages with SIV infection and AIDS that is reduced with ART and does not significantly change in the

meninges and choroid plexus but increases in perivascular macrophages following 4 weeks of ART interruption.

There is increased traffic of SPION+ macrophages out of the CNS with ART.

Following i.c. SPION inoculation, we found SPION+ macrophage in the optic nerve and eye, nasal septum, cribriform plate, and in peripheral draining lymphatics, including dCLN, spleen, and DRG (Alvarez *et al.*, submitted). In contrast to the CNS and consistent with our previous findings, animals with AIDS and SIVE have fewer numbers of SPION+ macrophages in the periphery and increased numbers with ART (dCLN SIVE: 0.28 ± 0.15 SPION+/mm²; ART: 1.3 ± 0.39 SPION+/mm²) (spleen SIVE: 0.95 ± 3.5 SPION+/mm²; ART: 3.0 ± 8.6 SPION+/mm²) (DRG SIVE: 420 ± 104 SPION+/mm²; ART: 947 ± 400 SPION+/mm²) (**Figure 3.2D-F**). With ART, there are significantly ($p < 0.005$) increased numbers of SPION+ macrophages in the dcLN and spleen that trended to decreases following ART interruption (dCLN ART: 1.3 ± 0.39 SPION+/mm²; ART Off: 0.53 ± 0.18 SPION+/mm²) (spleen ART: 3.0 ± 8.6 SPION+/mm²; ART Off: 0.051 ± 0.070 SPION+/mm²) (**Figure 3.2D&E**). Interestingly, the numbers of SPION+ macrophages in the DRG increase with ART (2.3x) and with ART interruption (3.5x) compared to animals with AIDS and SIVE but did not reach statistical significance (DRG ART: 947 ± 400 SPION+/mm²; ART Off: 1458 ± 398 SPION+/mm²) (**Figure 3.2F**). With ART interruption, the number of SPION+ macrophages did not significantly increase ($p = 0.06$) in the DRG, yet there was a reduced ratio of CD163+ to CD163+SPION+ macrophages in the DRG (SIVE 1:42, ART 1:213, ART Off 1:304), suggestive of an increased in SPION+ macrophage leaving the CNS via

the DRG with ART interruption. These data are consistent with SPION+ macrophages being retained in the CNS with viral infection and inflammation, and increased CNS macrophages trafficking out to the periphery with ART and resolution of CNS inflammation.

ART decreases the number of CNS macrophages in the periphery.

In parallel with studies of SPION+ macrophages in the periphery, we assessed numbers of macrophages in the same tissue with ART and ART interruption. In the dCLN, SIVE animals have 69 ± 4.8 CD163+/ mm^2 CD163+ macrophages significantly decrease with ART (45 ± 7.0 CD163+/ mm^2 , $p < 0.05$) and that are similar to ART after ART interruption (ART Off 45 ± 5.6 CD163+/ mm^2) (**Figure 3.2D**). Similarly, ART reduces macrophages in the spleen and significantly ($p < 0.005$) decreases macrophages in the DRG compared to animals with AIDS and SIVE (Spleen SIVE: 1190 ± 348 CD163+/ mm^2 ; ART: 1041 ± 40 CD163+/ mm^2) (DRG SIVE: 10 ± 0.89 CD163+/ mm^2 ; ART: 4.5 ± 0.45 CD163+/ mm^2) (**Figure 3.2E-F**). There are no differences in the number of macrophages in the spleen and DRG between ART and ART interruption (Spleen ART: 1041 ± 40 CD163+/ mm^2 ; ART Off 1008 ± 270 CD163+/ mm^2) (DRG ART: 4.5 ± 0.45 CD163+/ mm^2 ; ART Off 4.9 ± 0.51 CD163+/ mm^2) (**Figure 3.2E-F**). Our data demonstrate there is an increased accumulation of macrophages in the dCLN, spleen, and DRG with SIV infection and AIDS that is reduced with ART and does not rebound with ART interruption.

ART reduces SPION+ and total SIV-RNA+ macrophages and gp41+ cells in the CNS and periphery.

Using ultrasensitive SIV-RNAscope with IHC for macrophages and IHC for gp41+ cells we counted the number of viral RNA+ macrophage and gp41+ cells with and without SPION in the CNS and periphery to assess the effects of ART and ART interruption on virus in the CNS and the periphery (**Table 3.2, Figure 3.3**). Overall, animals with AIDS and SIVE have large numbers of SIV-RNA+ macrophages with and without SPION and gp41+ cells in the CNS and periphery that are significantly reduced with ART (**Table 3.2, Figure 3.3**). Within the CNS, there are greater numbers of SIV-RNA+SPION+ meningeal (25x) and choroid plexus macrophages (3.2x) versus SIV-RNA+SPION+ perivascular macrophages in animals with AIDS and SIVE (**Table 3.2, Figure 3.3**). There are large numbers of gp41+ cells, including MNGC, localized primarily in CNS lesions—some of which contain SPION—and scattered SIV-DNA+ cells that are also primarily localized to lesions (**Table 3.2, Figure 3.4**). With ART, there are few, scattered SIV-RNA+ macrophages and gp41+ perivascular macrophages (CD163+ $p < 0.005$; CD68+ $p < 0.0001$), meninges (CD163+ $p < 0.005$; CD68+ $p < 0.005$), and choroid plexus (CD68+ $p = 0.17$) that are significantly reduced compared to SIVE (**Table 3.2**). ART fully eliminates SIV-RNA+SPION+ perivascular macrophages while few scattered SIV-RNA+SPION+ meningeal (1 SPION+SIV-RNA+ macrophage) and choroid plexus macrophages (10 SPION+SIV-RNA+ macrophages) persist (**Figure 3.3, Table 3.2**). With ART interruption, there is a slight increase although not statically significant in the number of SPION+SIV-RNA+ macrophages (4 SPION+SIV-RNA+ macrophage) and gp41+ cells in the meninges, but not SPION+SIV-RNA+ or SIV-RNA+

perivascular macrophages or in the choroid plexus (**Table 3.2**). These data show ART reduces the number of infected CNS macrophages but there is a persistence of SPION+ macrophage with SIV-RNA in choroid plexus and a rebound in the meninges with ART interruption.

ART eliminates SPION+ SIV-RNA+ macrophages in the periphery with no rebound following ART interruption.

Outside the CNS, there are large numbers of SPION+ SIV-RNA+ and SIV-RNA+ macrophages with AIDS and SIVE that are significantly reduced with ART ($p < 0.05$) that not significantly rebound with ART interruption (**Table 3.2**). There are few scattered CD163+ and CD68+ SIV-RNA+ macrophages in the dCLN, spleen, and DRG in SIVE animals that are eliminated with ART and did not rebound with ART interruption. (**Table 3.2**). These data are consistent with ART reducing the number of virally infected macrophages in the CNS and periphery, where virus rebounds in the meninges, choroid plexus, dCLN, and spleen but not in CNS perivascular macrophages with ART interruption.

ART reduces early SPION+ perivascular macrophages in the CNS which corresponds to an increase in EARLY SPION+ macrophages in the periphery.

To better define the timing and establishment of CNS macrophage viral reservoirs and the effect of ART and ART interruption on CNS macrophage retention and traffic out, we injected two different colored SPION. Green, fluorescent SPION were injected 12-14 days post-infection (Early), and red fluorescent SPION were injected 30 days prior

to sacrifice (between 3-28 days prior to sacrifice, Late) (**Table 3.1, Figure 3.1**). Our preliminary studies and work by others demonstrated SPION are internalized by macrophages within 30 minutes and remain intact in animals for greater than 120 days or the duration our experiments [53, 54]. We analyze the labeled cells in terms of ones that have Early, Late, or Dual Labeled with both SPIONs. There are significantly ($p < 0.0001$) greater numbers of early versus late and dual-SPION+ perivascular macrophages in SIVE animals, ART, and with ART interruption (**Figure 3.5A, Table 3.3**). In contrast, there are equivalent numbers of early, late, and dual SPION+ meningeal macrophages in SIVE, ART, and ART interruption animals (**Figure 3.5A-B, Table 3.3**). The distribution of early and late SPION+ choroid plexus macrophages is similar to the meninges with equivalent numbers of early, late, and dual SPION+ macrophages. There are slightly greater numbers of early (SIVE: 3-fold, ART 4-fold, ART Off 4.6-fold) versus late or dual choroid plexus macrophages (**Table 3.3**). Overall, these data suggest the CNS perivascular macrophage viral reservoir is established early in infection. In contrast, these data suggest that meningeal and choroid plexus macrophages have ongoing recruitment that increases upon the development of AIDS and SIVE.

ART animals have increased Early SPION+ macrophage in the periphery compared to animals with SIVE.

Outside of the CNS in the dcLN, spleen, and DRG, there are greater numbers of early SPION+ macrophages than late or dual with SIVE, ART, and ART interruption, although these did not reach statistical significance (**Figure 3.5C, Table 3.3**). With ART, there are greater numbers of early SPION+ macrophages in the spleen and few to no late

or dual (**Figure 3.5D, Table 3.3**). In the DRG, there are greater numbers of early and dual SPION⁺ macrophages compared to late in animals with AIDS and SIVE, ART, and following ART interruption (**Figure 3.5E, Table 3.3**). These data support the early establishment of the CNS macrophage viral reservoir, ART resolving CNS inflammation by inducing traffic of macrophages out early, and increased traffic of virally infected macrophages out of the CNS occurs late during infection with AIDS and SIVE. The SPION⁺SIV-RNA⁺ perivascular macrophages in SIVE animals are primarily labeled with Early SPION, which are eliminated with ART, and do not rebound with ART interruption (**Table 3.4**). In contrast to perivascular macrophages, SIVE animals have greater numbers of Dual SPION⁺ SIV-RNA⁺ meningeal macrophages than Early or Late SPION (**Table 3.4**). SPION⁺ SIV-RNA⁺ choroid plexus macrophages are primarily labeled with Late SPION that are not eliminated with ART (**Table 3.4**).

SPION⁺ SIV-RNA⁺ macrophages that traffic out of the CNS to the periphery are eliminated with ART and do not rebound with ART interruption.

The majority of SPION in SIVE animals with SIV-RNA⁺ macrophages in the dcLN are Late (**Table 3.4**). The SPION⁺SIV-RNA⁺ macrophages in the dCLN are eliminated with ART and do not rebound with ART interruption (**Table 3.4**). In the spleen of SIVE animals, there are equivalent numbers of early and late injected SPION⁺SIV-RNA⁺ macrophages that are eliminated with ART and do not rebound following ART interruption (**Table 3.4**).

3.5 Discussion

Few studies have investigated CNS macrophage accumulation and traffic out normally, with HIV and SIV infection, or ART, and ART interruption. Using i.c. injection of SPION that labeled CNS perivascular, meningeal, and choroid plexus macrophages we found animals with AIDS and SIVE had increased CNS SPION+ macrophages. There was a differential distribution of SPION+ macrophages with 50 to 200-fold greater numbers of SPION+ meningeal macrophages than SPION+ perivascular macrophages and 1 to 5-fold greater numbers of meningeal than choroid plexus macrophages. These results are consistent with greater numbers of total meningeal versus perivascular macrophages, and interestingly, the ratio of total macrophages versus SPION+ macrophages in the two compartments did not change between SIVE, ART, and ART Off animals. ART reduced the numbers of SPION+ perivascular macrophages within the CNS, whereas macaques with SIVE have approximately 4x more SPION+ perivascular macrophages than ART animals. ART did not affect the numbers of SPION+ macrophages in the meninges and choroid plexus. Following ART interruption, there were increased numbers of SPION+ meningeal macrophages and decreased SPION+ choroid plexus macrophages. Increased numbers in the meninges may account for decreased choroid plexus macrophages, where increased traffic of BM macrophages from the choroid plexus to the CSF could result in a corresponding increase in the SPION+ meningeal macrophages. We note that SPION+ macrophages in the perivascular space, dCLN, and the spleen typically contain fewer SPION per cell compared to macrophages in the meninges and DRG that contain more SPION per macrophage (data not shown). The differential numbers are likely due to the fluid-SPION interface in the

different macrophage compartments [18, 55, 56]. Additionally, the kinetics of turnover of these cells normally, and once they have taken up SPION, is also likely a factor. It is possible that once a macrophage is sufficiently loaded with SPION, certain egress routes, such as passing through the cribriform plate, are less feasible. SPION uptake by macrophages could ultimately slow their exit from the CNS and potentially contribute to the accumulation of these cells in different compartments, for example, the meninges. Alternatively, macrophages that are more able to traffic out of the CNS might do so once they take up fewer SPION. An assumption of our studies, supported by the work of others, is that SPIONs, unlike dextrans, [33, 47, 57-59] do not leak out of the CNS. This is supported by the SPION size in our studies and also our lack of finding single, non-cell associated SPION inside and outside the CNS. These data are consistent with a differential turnover of CNS perivascular, meningeal, and choroid plexus macrophages and a reduction primarily in CNS perivascular macrophages with ART.

Macrophage turnover in the CNS has been shown to occur normally at a rate that increases with inflammation[38]. Less well known is the effect of ART and the contribution of early versus late macrophage accumulation with inflammation with regard to viral infection. Using two different colored SPION injected Early and Late, we found greater numbers of Early versus Late or Dual labeled macrophage in all tissues examined regardless of treatment. Perivascular macrophages are primarily labeled with early SPION, suggesting they are a resident, low-turnover macrophage population with SIV infection. A greater number of Early SPION-labeled macrophages may occur due to a limited capacity for SPION uptake. Regardless, this data is consistent with our previous reports of early recruitment of CD163+ bone marrow-derived perivascular macrophages

to the CNS with SIV infection [33, 60, 61] and that perivascular macrophage turnover occurs at a low rate that is increased with SIV infection [12, 38, 41, 60, 61]. In contrast, meningeal macrophages had equivalent numbers of Early and Late injected SPION+ macrophages in SIVE, ART, and following ART interruption suggesting these are a more static locally maintained macrophage population that is unchanged with ART or following ART interruption. Fluid dynamics in regions such as the meninges and even DRG may contribute to the even distribution of Early, Late, and Dual-labeled macrophages in these compartments, as these cells are continuously exposed to CSF-containing SPION. Choroid plexus macrophages also had equivalent numbers of Early and Late but few Dual SPION+ macrophages in SIVE, ART, and ART interruption animals, consistent with a high rate of traffic and turnover of monocytes/macrophages. The continuous turnover and exit of CNS macrophages to the periphery may occur with CNS lesion resolution and provide a mechanism to prevent chronic inflammation and tissue damage with SIV and HIV infection, similar to findings in recent rodent studies[62, 63]. Overall, our data using SPION to label CNS macrophages to investigate turnover shows the traffic of CNS macrophages out to the periphery (dCLN, spleen, and DRG). In the periphery, we typically observed more Early-labeled macrophages, which may indicate a delay in the clearance of SPION+ cells from the CNS rather than the rapid drainage of free SPION. It is a valid question whether SPIONs could be broken down and exit the CNS as others have previously shown [64, 65], though this is unlikely in our timeframe examined (<1 year) and beads used due to the stability of their encapsulated synthetic polymer coating [59, 66-68]. A more likely outcome in our study is the clearance of SPION through the kidneys or the induction of iron-programmed cell death

due to high levels of iron ions and reactive oxygen species, leading to lipid peroxidation and eventual cell death [59, 66-69]. In this study, we did not directly measure traffic of specific SPION+ CNS macrophage populations out of the CNS, nor did we define specific pathways of exit. Furthermore, specific studies would be required to better understand specific macrophage populations that can leave the CNS. Such future studies are likely critical to understanding CNS inflammation and the resolution of inflammation.

Pathways by which macrophages can exit the CNS have been proposed and described [19, 23, 46, 47, 51, 62, 63, 70-82] , including i) dorsal and basal dural lymphatics, ii) the olfactory bulb-cribriform lymphatic axis, ii) the choroid plexus, and ii) egress via spinal pathways [50, 74, 83]. More recently, discontinuities in the arachnoid barrier at bridging veins are another path underscoring immune cell and CSF drainage into the dura and egress via dural lymphatics [84]. Perivascular and meningeal macrophages could exit with CSF via meningeal lymphatics or cranial nerve routes to reach the dCLN [49, 50, 85]. We find increased numbers of SPION+ macrophages in the dCLN, which likely exited the CNS via nasal and meningeal routes rather than in the superficial cLN, which would likely be drainage for cranial nerve egress [49, 86]. Choroid plexus stromal macrophages exit via perivenous routes and/or migrate through the choroid plexus to the CSF and to the subarachnoid space. Choroid plexus Kolmer macrophages could likewise leave via pathways of CSF drainage [19, 47, 48, 73]. Additionally, immune cells could exit the CNS via CSF drainage pathways in the spine including arachnoid villi to spinal veins [87-89], along spinal nerve roots (DRG) to epidural lymphatics [90, 91] , and routes through the arachnoid layer to the spinal meninges to dural lymphatics [92, 93]. The egress of macrophages, some of which can be

infected, is crucial for understanding CNS reservoir resolution and possible redistribution of CNS virus.

An important consideration is whether CNS SIV or HIV virally infected macrophages can traffic out of the CNS to the periphery. We found SIVE animals had SIV-RNA+ SPION+ perivascular macrophages, meningeal, choroid plexus macrophages, and SIV-RNA+ SPION+ macrophages in the dCLN, spleen, and DRG. With ART, SIV-RNA+ SPION+ macrophages were eliminated in the CNS parenchyma (perivascular macrophages) and periphery, but not meninges and choroid plexus. With ART interruption, there was a rebound of SIV-RNA+ SPION+ and SIV-RNA+ meningeal macrophages, choroid plexus macrophages, macrophages in the spleen, and plasma virus but not SIV-RNA+SPION+ perivascular macrophages. We did not find any SIV-DNA+ macrophage with SPION within or outside the CNS with ART which is most likely due to the reduced sensitivity of the DNAscope assay compared to SIV-RNAscope. Clements *et al.* recently found that virologically suppressed people living with HIV have persistent, replication-competent virus in monocyte-derived macrophages in blood using a quantitative viral outgrowth assay [11]. Although we did not find SIV-RNA+SPION+ macrophages with ART in the peripheral tissue sections, Clements and colleagues recently showed despite low levels of viral DNA, replication-competent virus persists in monocyte-derived macrophages despite ART [11]. Importantly, with ART interruption, we find a rebound of virally infected macrophages in CNS meninges, choroid plexus, plasma virus, and spleen, but not in the CNS perivascular macrophages or cell-associated SIV-RNA and DNA in PBMCs (data not shown). These data suggest that with AIDS and SIVE, there is ongoing reseeding of the periphery from the CNS viral reservoir that is

eliminated with ART, and with ART interruption, virus rebounds from the plasma, meninges, and spleen. While the CNS has been historically regarded as an immune-privileged site with restricted immune cell trafficking and controlled egress of immune cells—particularly macrophages—is critical for controlling inflammation. Our data underscores the dynamic nature of macrophages in the CNS that can migrate from the bone marrow to the CNS and traffic antigens out with inflammation or viral infection. The egress of macrophages from the CNS with ART results in the resolution of inflammation and reduced macrophage infection. While macrophage traffic out of the CNS challenges the conventional notion of CNS immune privilege, it is critical for the regulation of neuroinflammation.

We used two different colored, fluorescently labeled SPION i.c. injected Early (12-14 days post-infection) and Late (30 days prior to sacrifice) to study CNS macrophage viral reservoir establishment, including the timing and location. We found significantly more Early SPION+ SIV-RNA+ perivascular macrophages compared to Late or Dual in AIDS and SIVE animals that were eliminated with ART and did not rebound with ART interruption. This suggests and agrees with our previous data [33] that the CNS perivascular macrophage viral reservoir is established during early infection. Conversely, in the meninges, we found equal distribution of SIV-RNA+ Early, Late, and Dual-labeled SPION+ macrophages in animals with AIDS and SIVE that were eliminated with ART but rebounded with ART interruption. This suggests ongoing recruitment of SIV-RNA+ macrophages in the meninges with AIDS and SIVE that is eliminated with ART and rebounds following ART interruption. In the choroid plexus, we found greater numbers of Late SPION+ SIV-RNA+ macrophages in SIVE animals that were not

eliminated with ART. This data is consistent with the choroid plexus being a site of entry for BM-derived monocytes to the CNS, which has a high rate of turnover that is increased with SIV infection [33, 38]. It is important to note in CD8-depleted macaques, we do not reduce plasma viral load to undetectable levels with ART ($1 \times 10^4 \log_{10}$ copies/mL). Thus, it would be expected to find viral RNA⁺ monocytes in the blood, possibly even containing SPION (not examined). These data support the early establishment of the CNS macrophage viral reservoir, ART resolving CNS inflammation by inducing traffic out early, differential rates of viral seeding in the parenchyma, meninges, and choroid plexus, and increased traffic of virally infected SPION⁺ macrophages out to the periphery with AIDS.

One site of particular interest to the CNS with regards to neuroimmune modulation is the choroid plexus, as it is viewed as an immune cell gateway to the brain [22, 26, 27, 36, 94]. HIV and SIV-infected cells have been found in the choroid plexus [26, 27, 95] but whether it is a viral reservoir has not been established. We found an accumulation of SPION⁺ macrophages within the choroid plexus, which could have been labeled via diffusion of SPION with CSF across the epiplaxus, recirculation of SPION or SPION⁺ monocytes/macrophage. Previously, we used an anti-A4B1 antibody to block the traffic of monocytes and macrophages to the CNS and prevent the establishment of the CNS viral reservoir, and reduce neuronal injury [43]. Because A4 integrin is expressed on both sides of the choroid plexus, anti-A4B1 treatment could prevent cellular traffic via both sides of the choroid plexus and determine if there is recirculation of monocytes/macrophages to the CNS. By blocking the traffic of immune cells out of the CNS by ablation of meningeal lymphatics, Louveau *et al.* found there is a

reduction in clinical symptoms from EAE while conversely improving the function of meningeal lymphatics and increasing traffic of immune cells out of the CNS in aged mice improved clinical symptoms [19, 46-51]. Our SPION data indicates that traffic of CNS macrophages out to the dcLN, spleen, and DRG occurs normally, with SIV infection, and is increased with ART with the resolution of CNS inflammation. Using anti-A4B1 antibody in conjunction with ART to block the accumulation of macrophages in the CNS could prevent viral recrudescence of SPION+ macrophages we found in the CNS meninges and choroid plexus with ART interruption.

The results of this study suggest myeloid traffic within and outside the CNS with HIV and SIV infection plays a major role in the resolution of CNS inflammation. Our study found that animals with SIVE had more SPION+ macrophages in the CNS compared to those without infection or those treated with ART. In contrast, the ART animals had fewer SPION+ CNS macrophages but more SPION+ macrophages that moved out of the CNS to the periphery, suggestive of inflammation resolution. This situation creates a paradox because historically, the CNS has been seen as a place where the immune system is restricted, and the movement of immune cells, especially macrophages, is tightly controlled to manage inflammation. Our findings emphasize how macrophages recruited into the CNS are dynamic as they migrate from the bone marrow and respond to CNS inflammation and viral infections.

3.6 Experimental Procedures

Ethics Statement: All animal work was approved by the Tulane National Primate Research Center Care and Animal Use Committee. The TNRPC protocol number is 3497 and the animal welfare assurance number is A4499-01.

Animals and Viral Infection: A total of 20 adult rhesus macaques (*Macaca mulatta*) born and housed at the Tulane National Primate Research Center in strict adherence to the "Guide for the Care and Use of Laboratory Animals" were used in this study (**Figure 3.1, Table 3.1**). CD8⁺ lymphocytes were depleted to achieve rapid AIDS (3 to 4 months) with >75% incidence of SIVE, as previously described [33, 34, 60, 96]. CD8⁺ T lymphocyte depletion was monitored longitudinally by flow cytometry and all macaques were persistently depleted (>28 days). Animals were experimentally infected intravenously (i.v) by inoculation with a bolus of SIVmac251 viral swarm (20 ng of SIV p28) provided by Dr. Ronald Desrosiers, over 5 minutes. At 21 days post-infection, n=14 macaques began a 12 - 15-week regimen of antiretroviral therapy (ART) consisting of Raltegravir (Merck, 22 mg/kg) given orally twice daily, and Tenofovir (Gilead, 30 mg/kg) and Emtricitabine (Gilead, 10 mg/kg) combined in a sterile solution given once-daily, s.c. Ten animals were euthanized on ART and 4 were removed from ART for 4 weeks to allow for viral rebound. Animals were euthanized based on the recommendations of the American Veterinary Medical Association Guidelines for the Euthanasia of Animals upon developing signs of AIDS, which included: a >15% decrease in body weight in 2 weeks or >30% decrease in body weight in 2 months; documented opportunistic infection; persistent anorexia>3 days without explicable cause; severe, intractable diarrhea; progressive neurological symptoms; or significant cardiac or

pulmonary symptoms. SIV encephalitis (SIVE) was defined by the presence of multinucleated giant cells (MNGC) and the accumulation of macrophages [60]. Longitudinal plasma viral load (PVL) was assessed as previously described [97-99] to monitor viral suppression during treatment and rebound following ART interruption (**Figure 3.1B**). For PVL, 500 μ L of EDTA plasma was collected and plasma virions were pelleted by centrifugation (20,000 x g for 1 hour). The sensitivity threshold of the assay was 100 copy Eq/mL with an average intra-assay coefficient variation of less than 25%. Log-transformed PVLs below the limit of detection were set to 0 for statistical analysis.

SPION: Superparamagnetic iron oxide nanoparticles (SPION) were obtained from Bang Laboratories Inc. (PS-COOH Mag/Encapsulated, MEDG001, and MEFR001, Fishers, IN). SPION have internal fluorescence (Dragon Green [480/520] and Flash Red [660/690]) and are iron oxide nanospheres encapsulated in an inert polymer with an average particle size of 0.86 μ m diameter. SPION were prepared in a class 2 biosafety cabinet. 3 mL of stock solution and 7 mL of sterile, low endotoxin 1XPBS were added to a 15 mL conical tube and gently mixed. A magnet was used to separate the SPION from the liquid and an additional 7 mL of 1XPBS was added for a second wash. This process was repeated 7 - 10 times to ensure all original buffer was removed and the SPION were resuspended in a sterile 1XPBS solution. SPION reconstituted in 1mL of sterile 1XPBS, at a final concentration of 33 mg/mL.

Intracisternal Inoculation Procedure: To avoid an increase in intracranial pressure, 1 mL of cerebrospinal fluid (CSF) was removed from the cisterna magna prior to the inoculation of SPION or RITC-Dextran. Dragon Green [480/520] SPION (33 mg/mL)

were administered 2 weeks post-inoculation at 12 or 14 dpi. Flash Red [660/690] SPION (33 mg/mL) were injected late during infection prior to euthanasia (Range 3-22 days).

Tissue Collection and Processing: Animals were anesthetized with ketamine-HCl and euthanized with i.v. pentobarbital overdose and exsanguinated. Blood was collected and Heparin Sulfate was administered i.v. and given 5 minutes to diffuse. Sodium pentobarbital was administered via intracardiac stick and CSF was collected. Following CSF collection, animals underwent perfusion with 3L of chilled 1XPBS. Postmortem examination was performed by a veterinary pathologist that confirmed the presence of AIDS-defining lesions as previously described [33, 34, 60, 96]. Brain (frontal, temporal, occipital, parietal, and choroid plexus) and peripheral tissues (cervical lymph nodes, spleen, and DRG) were: i) collected in zinc-buffered formalin and embedded in paraffin, ii) fixed with 2% paraformaldehyde for 4-48 hours, sucrose protected and embedded in optimal cutting temperature (OCT) compound for SPION analysis, or iii) snap frozen in OCT without fixation (spleen).

Immunohistochemistry: IHC was performed as previously described using the antibodies targeting CD163 (1:250, Leica (Deer Park, IL)), CD68 (1:100, DAKO (Carpinteria, CA)), CD206 (1:1000, R&D Systems (Minneapolis, MN)), and IBA1+ macrophages (1:100, Wako (Osaka, Japan)) [33, 34, 96]. Briefly, formalin-fixed paraffin-embedded sections were deparaffinized and rehydrated followed by antigen retrieval with a citrate-based Antigen Unmasking Solution (Vector Laboratories, Burlingame, CA) in a microwave (900 W) for 20 min. After cooling for 20 min, sections were washed with Tris-buffered saline (TBS) containing 0.05% Tween-20 for 5 minutes before incubation with peroxidase block (DAKO, Carpinteria, CA) followed by protein block (DAKO,

Carpinteria, CA) for 30 minutes and incubation with primary antibody. Following incubation with a peroxidase-conjugated polymer, slides were developed using a diaminobenzidine chromogen (DAKO, Carpinteria, CA) with Harris Hematoxylin (StatLab, McKinney, TX).

Immunofluorescence: Immunofluorescence for CD163+, CD68+, IBA1+, and gp41+ macrophages was performed using antibodies and fluorochromes using CD163 (NCL-CD163 CE, AF568, Invitrogen (Carlsbad, CA)), CD68 (DAKO, AF568 (Carpinteria, CA)), IBA1+ macrophages (Wako, DISCOVERY OmniMap Anti-Rb HRP (Osaka, Japan)), and gp41+ (KK41+, 1:100, NIH (Manassas, VA)) on 2% paraformaldehyde (PFA) fixed frozen sections. 2% PFA, fixed frozen sections were thawed for 20 minutes at room temperature, unwrapped, submerged in a citrate-based Antigen Unmasking Solution, and microwaved for one minute and forty-five seconds and cooled to room temperature. Slides were permeabilized in a solution of phosphate-buffered saline with 0.01% Triton X-100 and 0.02% fish skin gelatin (PBS-FSG-TX100) followed by a PBS-FSG wash, transferred to a humidified chamber and blocked with 10% normal goat serum (NGS) diluted in PBS-FSG for 40 minutes, followed by a 60-minute primary antibody incubation, washes, and 40-minute secondary antibody incubation. Routine washes were performed and DAPI nuclear stain added for 10 minutes. Slides were mounted using a custom-formulated anti-bleaching mounting media containing Mowiol (#475904, Calbiochem; San Diego, CA) and DABCO (#D2522, Sigma: St. Louis, MO) and allowed to dry overnight before being digitally imaged with a Zeiss Axio Scan.Z1. HALO software (HALO v3.4, Indica Labs; Albuquerque, NM) was used for quantification and analysis.

Viral RNA and DNA Detection: Ultrasensitive SIV-RNAscope with probes for SIVmac251 was used to detect SPION-containing SIV-RNA positive cells within and outside of the CNS as previously described [96]. Tissue sections were placed in a target antigen retrieval solution, heated, and treated with protease plus, and a hydrogen peroxide blocker according to the manufacturer's protocol (Advanced Cell Diagnostics, Newark, CA). SIVmac239 RNAscope probes (Advanced Cell Diagnostics, Newark, CA) were hybridized at 40°C in the HybEZ II Hybridization System. The RNAscope 2.5 HD Assay amplification steps were applied according to the manufacturer's protocol. Target RNA was visualized through the addition of chromogenic Fast Red A and Fast Red B (Advanced Cell Diagnostics, Newark, CA), and sections were counterstained with hematoxylin (Sigma-Aldrich) and mounted using Vectamount (Vector Laboratories). Viral RNA processed sections were subsequently stained for CD163+ or CD68+ macrophages using primary antibodies and IHC methods described above. Prussian blue iron staining and/or the internal fluorescence of SPION was used to detect vRNA+SPION-containing CD163+ macrophage. DNAscope was performed, as previously described [96, 100, 101]. SIV-DNA was detected in situ using an SIV-DNA sense probe (Advanced Cell Diagnostics, Newark, CA) for RNAscope® Assay on 3 – 4 CNS cortical sections and 1 peripheral tissue (dcLN, spleen, and DRG) per animal. To reduce non-specific signal, brain tissues were pre-treated with 2N HCL for 30 min at room temperature.

Detection and quantification of SPION-containing macrophages in tissues: SPION were detected in the central nervous system (CNS) and peripheral tissues by 1) light microscopy by morphology of the amber SPION beads, 2) Prussian blue iron staining

(Sigma Aldrich Iron Stain, St. Louis, MO), and 3) internal fluorescence of Dragon Green or Flash Red. The number of SPION-containing macrophages with IHC for macrophages with CD163+ or CD68+ was counted. SPION+ macrophages in whole tissue sections were counted manually at 20x by light microscopy (Plan-Apochromat 620/0.7, Olympus; Japan) in a blinded fashion. Whole section tiling and stitching was done using a Zeiss Axio Imager M1 microscope (Zeiss; Oberkochen, Germany) with AxioVision (Version 4.8, Zeiss; Oberkochen, Germany) using Plan-Apochromat 620/0.8 and 640/0.95 Korr objectives followed by manual annotation of the parenchyma from the meninges into separate regions of interest (ROI) and tissue area reported as mm².

For analysis of early versus late SPION+ macrophages and virally infected SPION+ macrophages, whole slide fluorescent images of stained sections were scanned using a Zeiss AxioScan Z.1 (Carl Zeiss MicroImaging, Inc., Thornwood, NY). Scanned sections were analyzed with HALO modular analysis software (HALO v3.4, Indica Labs; Albuquerque, NM). The parenchyma and meninges were first annotated into separate ROI/annotation layers and the number of early, late, and dual SPION-containing macrophages and vRNA-FISH early, late, and dual SPION-containing macrophages were counted using the FISH v.3.2.3 module (HALO v3.4, Indica Labs; Albuquerque, NM) and reported as the number of cells per mm².

Statistical Analysis: Statistical analyses were performed using Prism version 10.0 (GraphPad Software; San Diego, CA). Comparisons between animals with SIVE, ART, and following ART interruption were made using a nonparametric one-way analysis of variance (Kruskal-Wallis, GraphPad Software; San Diego, CA) with Dunn's multiple

comparisons. Statistical significance was accepted at $p < 0.05$ and all graphing was done using Prism (GraphPad Software; San Diego, CA).

Acknowledgments: We would like to acknowledge the Core staff at the Tulane National Primate Research Center (RRID:SCR_008167) that worked on this project including the Anatomic Pathology Core (RRID: SCR_024606) Clinical Pathology Core (RRID: SCR_024609) Confocal Microscopy and Molecular Pathology Core (RRID: SCR_024613) (RRID:SCR_008167), and Virus Characterization, Isolation, Production and Sequencing Core (RRID:SCR_024679).

Funding Sources: This work was supported by P51 OD011104

3.7 Tables, Figures, and Figure Legends

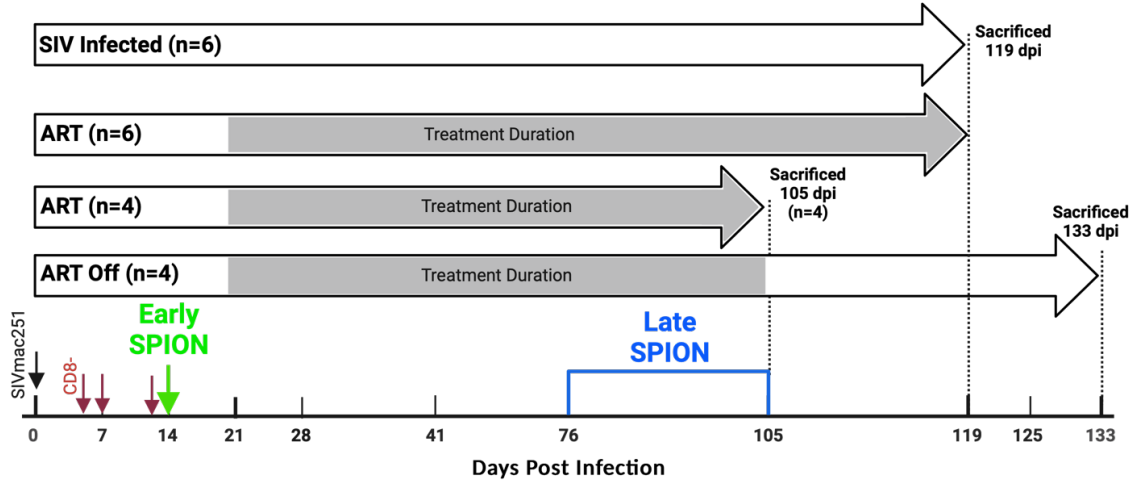
Table 3.1

Cohort	Animal ID	Treatment	DPI at Death	CNS Pathology	Days with Green SPIONs	Days with Red SPIONs
SIVE (n=6)	IK28	Untreated	100	SIVE	86	3
	JE87	Untreated	119	SIVE	105	14
	JD29	Untreated	126	SIVE	112	7
	KN69	Untreated	83	SIVE	69	6
	KT79	Untreated	119	SIVE	105	22
	LB12	Untreated	115	SIVE	101	10
ART (n=10)	JJ86	ART	105	SIVnoE	89	26
	KD67	ART	105	SIVnoE	89	26
	KM38	ART	105	SIVnoE	90	27
	LK25	ART	105	SIVnoE	93	28
	JH68	ART	118	SIVnoE	108	28
	JI15	ART	118	SIVnoE	108	28
	GI68	ART	119	SIVnoE	109	29
	JB07	ART	119	SIVnoE	109	29
	GH18	ART	120	SIVnoE	110	30
	JF58	ART	120	SIVnoE	110	30
ART Off (n=4)	KD12	ART Interruption	133	SIVnoE	119	28
	JV76	ART Interruption	132	SIVnoE	118	27
	JV78	ART Interruption	133	SIVnoE	119	28
	KE98	ART Interruption	133	SIVnoE	119	28

Table 3.1 Animals used in the study. Twenty SIV-infected, CD8+ T-lymphocyte-depleted rhesus macaques were used in this study. Sections of cortical CNS tissue were examined blindly by a veterinary pathologist, and the presence of SIV-induced encephalitis (SIVE) was defined by productive viral replication, the presence of MNGC, and macrophage accumulation or the presence of SIV with no encephalitis (SIVnoE). All macaques received i.c. SPION injection early (12-14 dpi, Green Early SPION) and late (26-30 days before sacrifice, Red Late SPION). ART animals began treatment daily at 21 dpi, and four animals had ART interrupted (ART Off) for 4 weeks prior to sacrifice.

Figure 3.1

A.



B.

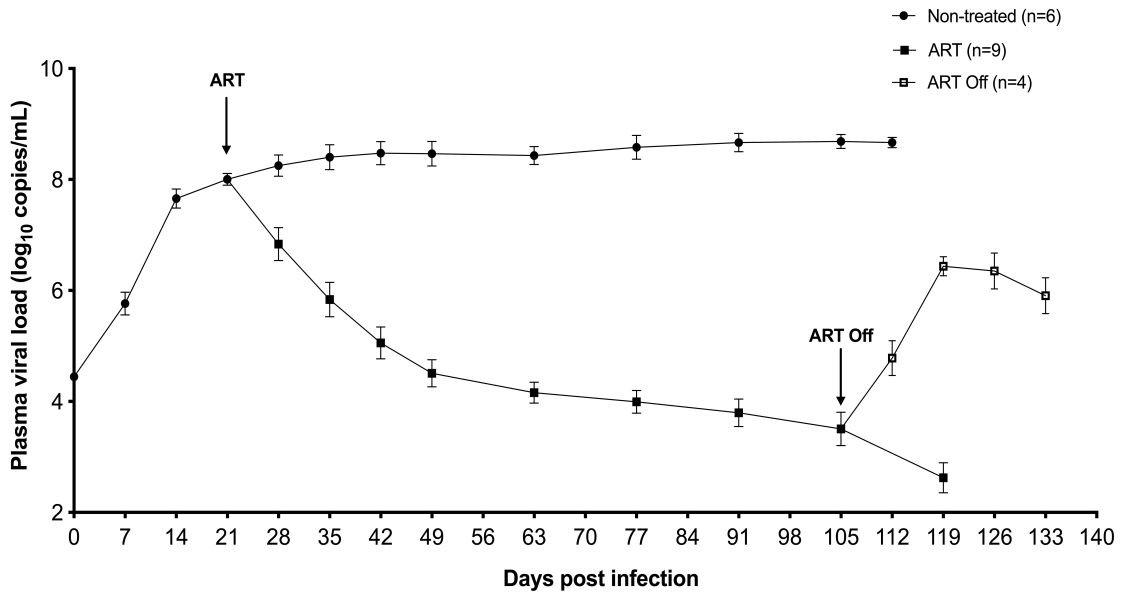


Figure 3.1 Study design and plasma viral load. (A) Nineteen rhesus macaques were infected with SIVmac251 (black arrow) and CD8 T lymphocytes depleted on 5, 7, and 12 dpi (red arrows). Fourteen macaques were treated with ART twice daily starting 21 dpi until 105 – 119 dpi where animals were sacrificed on ART treatment (n=10) or had ART interruption (n=4) for 4 weeks before sacrifice. Macaques received i.c. SPION injection early (12-14 dpi, Green Early SPION) and late (30 days prior to sacrifice, Late SPION). All untreated macaques were sacrificed upon progression to AIDS between 83–126 dpi. Created in BioRender. Wallis, Z. (2024) <https://BioRender.com/a42e272> **(B)** Plasma viral load was measured longitudinally in SIV-infected animals (n=6), SIV-infected animals with ART (n=9), and SIV-infected with ART and following ART Off (n=4). Prism was used for graphing and statistical analysis using Kruskal-Wallis nonparametric test followed by Dunn’s post-hoc test, with significance accepted at $p < 0.05$.

Figure 3.2

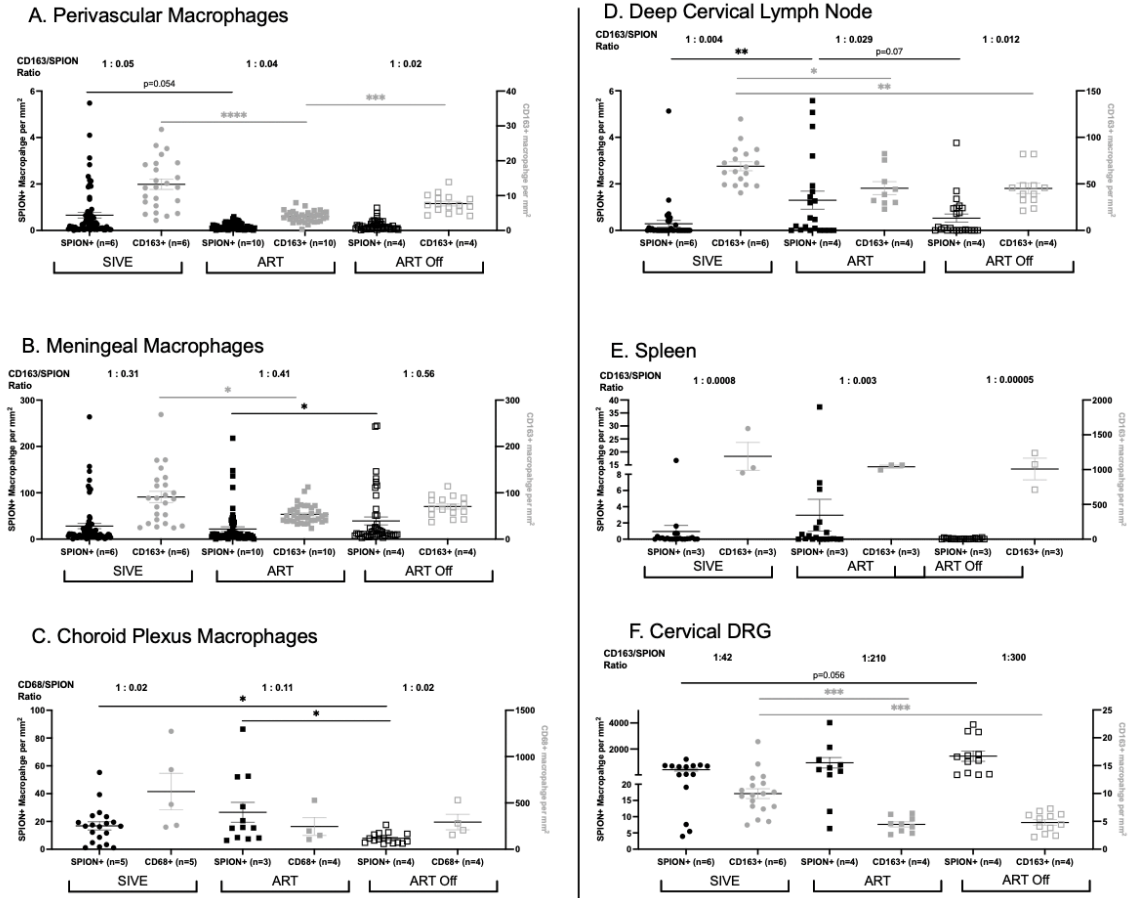


Figure 3.2 ART reduces the number of SPION+ perivascular macrophages and increases traffic out. Single-label immunohistochemistry for CD163 with Prussian Blue staining for SPION (black) or macrophage alone (grey) in non-treated SIV-infected animals with encephalitis (SIVE), SIV-infected macaques sacrificed on ART (ART), and SIV-infected macaques with 4 weeks of ART interruption (ART Off) in **(A)** perivascular space, **(B)** meninges, **(C)** choroid plexus, **(D)** dcLN, **(E)** spleen, and **(F)** DRG. Each data point represents the cell count from the cortical tissue section examined and is expressed as the number of positive cells per mm². The numbers above each graph are the average ratio of CD163+SPION+/ CD163+ macrophages or CD68+SPION+/CD68+ in the choroid plexus. Prism was used for graphing and statistical analysis Kruskal-Wallis nonparametric test was followed by Dunn's post-hoc test, *P < 0.05, **P < 0.01, and ****P < 0.0001.

Figure 3.3

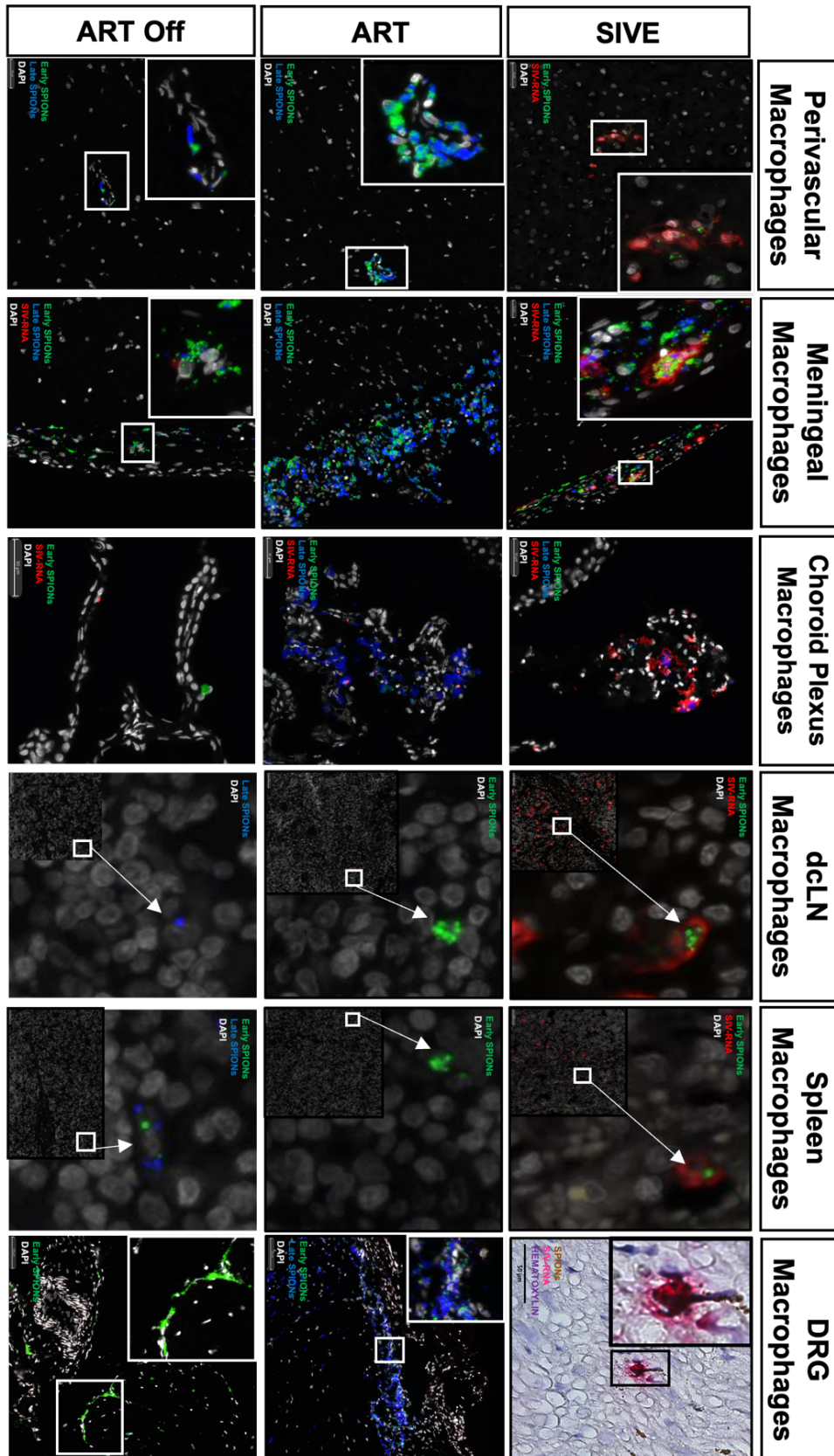


Figure 3.3 SPION+ SIV-RNA+ macrophages in the parenchyma, meninges, choroid plexus, dCLN, spleen, and DRG of animals with AIDS and SIVE. SIV-RNA (red) was detected in the CNS perivascular space, meninges, choroid plexus, and outside of the CNS in the dCLN, spleen, and DRG using RNAscope in situ hybridization. Early (green) SPION were i.c. injected 12-14 dpi and Late (pseudo-colored blue) SPION were i.c. injected 30 days prior to sacrifice. Images were captured from scanned sections. Nuclei are stained with Dapi (grey).

Table 3.2

A.

Tissue	Cohort	SIV-RNA+ Macrophage			gp41+ Cells	
		CD163+ vRNA+	CD68+ vRNA+	SPION+		
CNS	Parenchyma	Untreated (SIVE)	4.8 ± 1.9 [4784] 334 mm ²	9.5 ± 6.4 [4052] 452 mm ²	0.018 ± 0.033 [38] 1885 mm ²	0.32 ± 0.52 [7146] 3217 mm ²
		ART	0.01 ± 0.01 [10] 396 mm ²	0 [0] 539 mm ²	0 [0] 1308 mm ²	0.02 ± 0.01 [27] 1810 mm ²
		ART Off	0 [0] 199 mm ²	0.01 ± 0.01 [3] 892 mm ²	0 [0] 1843 mm ²	0.02 ± 0.02 [63] 2761 mm ²
	Meninges	Untreated (SIVE)	71 ± 48 [2683] 13 mm ²	38.3 ± 13.4 [313] 7.5 mm ²	12.0 ± 25.8 [965] 103 mm ²	11.8 ± 9.5 [1474] 122 mm ²
		ART	0.13 ± 0.14 [8] 19 mm ²	0 [0] 20 mm ²	0.004 ± 0.011 [1] 78 mm ²	0 [0] 68 mm ²
		ART Off	0 [0] 9 mm ²	0 [0] 17 mm ²	0.08 ± 0.13 [4] 71 mm ²	0.15 ± 0.24 [12] 78 mm ²
Choroid Plexus	Untreated (SIVE)	NA	7.1 ± 6.5 [55] 10 mm ²	3.0 ± 4.6 [120] 31 mm ²	NA	
	ART	NA	0 [0] 14 mm ²	0.40 ± 0.33 [10] 71 mm ²	NA	
	ART Off	NA	0 [0] 39 mm ²	0.04 ± 0.08 [1] 49 mm ²	NA	

B.

Tissue	Cohort	SIV-RNA+ Cells	SIV-RNA+ Macrophage			gp41+ Cells	
			CD163+ vRNA+	CD68+ vRNA+	SPION+		
Periphery	dcLN	Untreated (SIVE)	962 ± 819 [165,745] 343 mm ²	157 ± 47 [352] 0.75 mm ²	48.7 ± 22.5 [146] 3 mm ²	1.0 ± 1.7 [70] 172 mm ²	70.0 ± 74.0 [20382] 226 mm ²
		ART	0.80 ± 0.66 [116] 307 mm ²	3.3 ± 5.3 [22] 2.5 mm ²	0 [0] 2.5 mm ²	0 [0] 185 mm ²	0.14 ± 0.24 [22] 127 mm ²
		ART Off	12 ± 20.5 [2031] 567 mm ²	8.5 ± 6.6 [19] 0.75 mm ²	0 [0] 0.75 mm ²	0 [0] 323 mm ²	1.3 ± 2.5 [16] 223 mm ²
	Spleen	Untreated (SIVE)	1.04 ± 1.5 [665] 1717 mm ²	97 ± 38 [218] 0.75 mm ²	19.4 ± 28.6 [43] 2 mm ²	0.008 ± 0.02 [8] 610 mm ²	76.0 ± 68.0 [2745] 36 mm ²
		ART	0.31 ± 0.33 [17] 1611 mm ²	0 [0] 1.5 mm ²	0 [0] 4.5 mm ²	0 [0] 738 mm ²	0.72 ± 0.90 [13] 18 mm ²
		ART Off	2.3 ± 1.5 [44] 2168 mm ²	8.5 ± 12.4 [19] 0.75 mm ²	0.45 ± 0.77 [1] 2 mm ²	0 [0] 516 mm ²	16 ± 14 [394] 24 mm ²
DRG	Untreated (SIVE)	214 ± 53 [112,333] 128 mm ²	1.6 ± 1.7 [259] 36 mm ²	0.23 ± 0.11 [17] 73 mm ²	0.03 ± 0.08 [157] 110 mm ²	1.0 ± 1.0 [364] 303 mm ²	
	ART	0.1 ± 0.04 [37] 87 mm ²	0 [0] 99 mm ²	0 [0] 64 mm ²	0 [0] 79 mm ²	0 [0] 147 mm ²	
	ART Off	14 ± 21 [5273] 122 mm ²	0 [0] 48 mm ²	0 [0] 58 mm ²	0 [0] 107 mm ²	0 [0] 242 mm ²	

Table 3.2 SPION+ SIV-RNA+ macrophages and gp41+ cells are reduced with ART but not in the meninges and choroid plexus which rebound following ART

interruption. SIV-RNA+ macrophages and cells were detected using ultrasensitive SIV-RNAscope with double-labeled CD163+ and CD68+ and GP41+ was detected using IHC. Whole tissue sections were analyzed and the number of positive cells assessed using fluorescence. A minimum of 2 CNS cortical regions and an average of 3 peripheral tissue sections were analyzed per animal. Counts are the mean \pm SEM of the number of viral RNA+ cells, macrophages, SPION-labeled viral RNA+ macrophages, and gp41+ cells. Prism was used for graphing and statistical analysis Kruskal-Wallis nonparametric test was followed by Dunn's post-hoc test, *P < 0.05, **P < 0.01, and ****P < 0.0001.

Figure 3.4

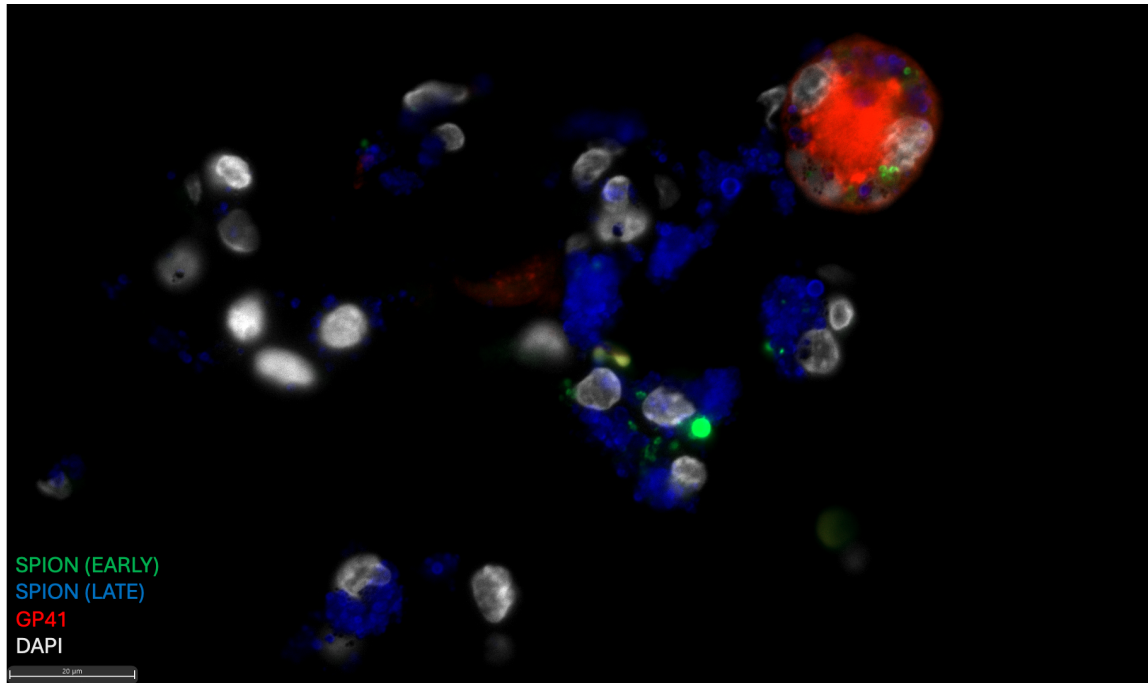
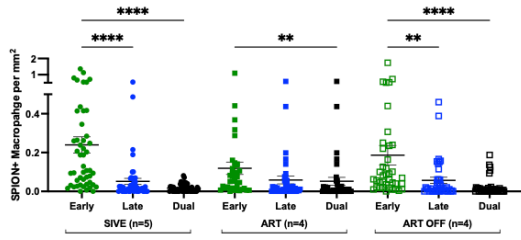


Figure 3.4 GP41+ SPION+ MNGC in the CNS of an animal with AIDS and SIVE.

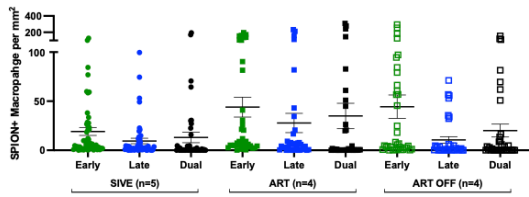
SPION (Green and Blue) localizes to a gp41+ (red) MNGC in the cerebellum. Nuclei are stained with Dapi (grey).

Figure 3.5

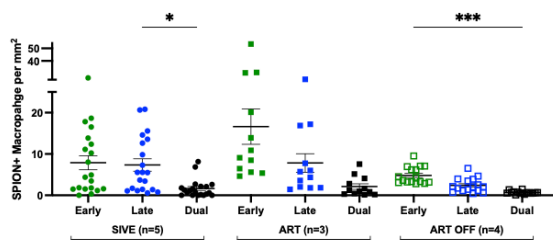
A. Perivascular Macrophages



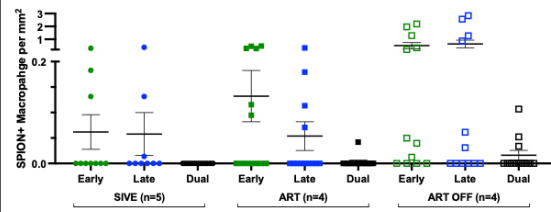
B. Meningeal Macrophages



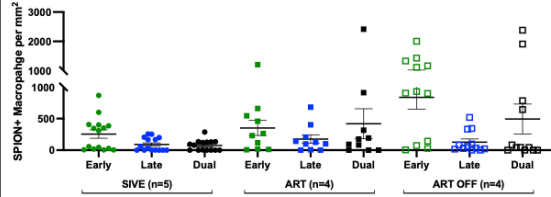
C. Choroid Plexus Macrophages



D. Cervical Lymph Node



F. Cervical DRG



E. Spleen

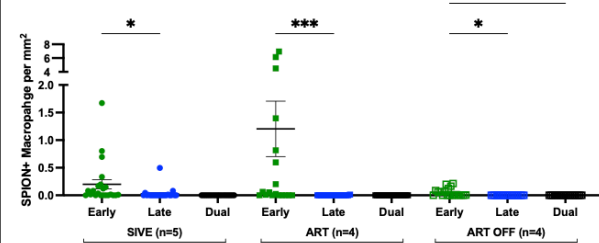


Figure 3.5 SPION-containing macrophages in and outside of the CNS are primarily labeled with SPION from early injection. Distribution of early, late, and dual-labeled SPION-labeled macrophage within the CNS (**A**) parenchyma, (**B**) meninges, (**C**) choroid plexus, and in the periphery including (**D**) dCLN, (**E**) spleen, and (**F**) DRG. Data points are the number of positive cells detected in one tissue section per animal and a minimum of 2 tissue sections were analyzed per animal. Prism was used for graphing and statistical analysis Kruskal-Wallis nonparametric test was followed by Dunn's post-hoc test, *P < 0.05, **P < 0.01, and ****P < 0.0001.

Table 3.3

	Tissue	Cohort	EARLY SPION+ Macrophage (mm ²)	LATE SPION+ Macrophage (mm ²)	DUAL SPION+ Macrophage (mm ²)	
	CNS	Parenchyma	Untreated (SIVE)	0.24 ± 0.04	0.05 ± 0.02	0.02 ± 0.003
ART			0.12 ± 0.03	0.06 ± 0.02	0.05 ± 0.02	
ART Off			0.19 ± 0.05	0.06 ± 0.02	0.02 ± 0.01	
Meninges		Untreated (SIVE)	19 ± 4.0	9.5 ± 2.6	13 ± 5.4	
		ART	44 ± 10	28 ± 9.8	35 ± 13	
		ART Off	44 ± 12	11 ± 3.3	20 ± 6.7	
Choroid Plexus		Untreated (SIVE)	7.9 ± 1.7	7.3 ± 1.5	1.6 ± 0.5	
		ART	17 ± 4.3	7.8 ± 2.3	2.1 ± 0.70	
		ART Off	4.8 ± 0.51	2.4 ± 0.42	0.67 ± 0.09	
Periphery		dcLN	Untreated (SIVE)	0.06 ± 0.03	0.06 ± 0.04	0
			ART	0.13 ± 0.05	0.05 ± 0.03	0.003 ± 0.003
			ART Off	0.51 ± 0.24	0.64 ± 0.30	0.02 ± 0.01
	Spleen	Untreated (SIVE)	0.2 ± 0.08	0.03 ± 0.02	0	
		ART	1.2 ± 3.0	0.0007 ± 0.0007	0	
		ART Off	0.05 ± 0.02	0	0	
	DRG	Untreated (SIVE)	255 ± 67	90 ± 27	352 ± 22	
		ART	352 ± 120	177 ± 68	419 ± 238	
		ART Off	836 ± 186	128 ± 50	494 ± 237	

Table 3.3 Distribution of early, late, and dual SPION+ macrophage in the CNS and periphery. Whole tissue sections were analyzed and the number of positive cells were identified using fluorescence. A minimum of 2 CNS cortical tissues were analyzed and an average of 3 peripheral sections were examined per animal, per tissue region. Counts are the mean \pm SEM of the number of SPION+ macrophages (Early, Late, or Dual (both early and late) SPION). SIVE, SIV encephalitis; dCLN, deep cervical lymph node; DRG, dorsal root ganglia.

Table 3.4

CNS	Cohort	Tissue	SIV-RNA+SPION+ Macrophage (mm ²)		
			EARLY	LATE	DUAL
	Untreated (SIVE)	Parenchyma	0.012 ± 0.027 [22]	0.005 ± 0.008 [13]	0.002 ± 0.003 [3]
Meninges		2.1 ± 3.0 [191]	3 ± 6 [250]	7 ± 17 [524]	
Choroid Plexus		0.61 ± 0.62 [23]	1.9 ± 3.5 [77]	0.50 ± 0.68 [20]	
ART	Parenchyma	0 [0]	0 [0]	0 [0]	
	Meninges	0 [0]	0.004 ± 0.01 [1]	0 [0]	
	Choroid Plexus	0 [0]	0.29 ± 0.52 [7]	0.18 ± 0.27 [3]	
ART OFF	Parenchyma	0 [0]	0 [0]	0 [0]	
	Meninges	0.01 ± 0.04 [1]	0.01 ± 0.04 [1]	0.03 ± 0.07 [2]	
	Choroid Plexus	0 [0]	0 [0]	0.042 ± 0.084 [1]	

Periphery	Cohort	Tissue	SIV-RNA+SPION+ Macrophage (mm ²)		
			EARLY	LATE	DUAL
	Untreated (SIVE)	dcLN	0.07 ± 0.14 [20]	0.9 ± 1.7 [50]	0 [0]
Spleen		0.0025 ± 0 [3]	0.004 ± 0.009 [5]	0 [0]	
DRG		NA	NA	* 0.03 ± 0.086 [157]	
ART	dcLN	0 [0]	0 [0]	0 [0]	
	Spleen	0 [0]	0 [0]	0 [0]	
	DRG	NA	NA	0 [0]	
ART OFF	dcLN	0 [0]	0 [0]	0 [0]	
	Spleen	0 [0]	0 [0]	0 [0]	
	DRG	NA	NA	* 0.0012 ± 0.008 [3]	

Table 3.4 ART eliminates SPION+SIV-RNA CNS perivascular macrophages and SPION+SIV-RNA macrophages outside of the CNS but SPION+SIV-RNA+ meningeal and choroid plexus macrophages persist. SIVE, SIV encephalitis; dCLN, deep cervical lymph node; DRG, dorsal root ganglia. Counts are the mean \pm SEM of the number of viral RNA+ cells and SPION-labeled viral RNA+ macrophages. Whole tissue sections were analyzed to obtain the number of positive cells based on the detection of fluorescence. A minimum of 2 cortical CNS tissues and an average of 3 peripheral sections were examined per animal, per tissue region.

3.8 References

1. Saylor, D., et al., *HIV-associated neurocognitive disorder — pathogenesis and prospects for treatment*. Nature Reviews Neurology, 2016. **12**(4): p. 234-248.
2. Furtado, M.R., et al., *Persistence of HIV-1 transcription in peripheral-blood mononuclear cells in patients receiving potent antiretroviral therapy*. N Engl J Med, 1999. **340**(21): p. 1614-22.
3. Sharkey, M.E., et al., *Persistence of episomal HIV-1 infection intermediates in patients on highly active anti-retroviral therapy*. Nat Med, 2000. **6**(1): p. 76-81.
4. Demeter, L.M., et al., *Detection of replication-competent human immunodeficiency virus type 1 (HIV-1) in cultures from patients with levels of HIV-1 RNA in plasma suppressed to less than 500 or 50 copies per milliliter*. J Clin Microbiol, 2002. **40**(6): p. 2089-94.
5. Cavert, W., et al., *Kinetics of response in lymphoid tissues to antiretroviral therapy of HIV-1 infection*. Science, 1997. **276**(5314): p. 960-4.
6. Crowe, S., T. Zhu, and W.A. Muller, *The contribution of monocyte infection and trafficking to viral persistence, and maintenance of the viral reservoir in HIV infection*. J Leukoc Biol, 2003. **74**(5): p. 635-41.
7. Salemi, M., et al., *Phylodynamic analysis of human immunodeficiency virus type 1 in distinct brain compartments provides a model for the neuropathogenesis of AIDS*. J Virol, 2005. **79**(17): p. 11343-52.
8. Salemi, M. and B. Rife, *Phylogenetics and Phyloanatomy of HIV/SIV Intra-Host Compartments and Reservoirs: The Key Role of the Central Nervous System*. Current HIV research, 2016. **14**(2): p. 110-120.
9. Clements, J.E., et al., *A simian immunodeficiency virus macaque model of highly active antiretroviral treatment: viral latency in the periphery and the central nervous system*. Curr Opin HIV AIDS, 2011. **6**(1): p. 37-42.
10. Clements, J.E., et al., *The central nervous system is a viral reservoir in simian immunodeficiency virus--infected macaques on combined antiretroviral therapy: a model for human immunodeficiency virus patients on highly active antiretroviral therapy*. J Neurovirol, 2005. **11**(2): p. 180-9.
11. Veenhuis, R.T., et al., *Monocyte-derived macrophages contain persistent latent HIV reservoirs*. Nature Microbiology, 2023. **8**(5): p. 833-844.
12. Bechmann, I., et al., *Turnover of rat brain perivascular cells*. Exp Neurol, 2001. **168**(2): p. 242-9.

13. Goldmann, T., et al., *Origin, fate and dynamics of macrophages at central nervous system interfaces*. Nat Immunol, 2016. **17**(7): p. 797-805.
14. Hickey, W.F. and H. Kimura, *Perivascular Microglial Cells of the CNS Are Bone Marrow-Derived and Present Antigen in Vivo*. Science, 1988. **239**(4837): p. 290-292.
15. Hickey, W.F., K. Vass, and H. Lassmann, *Bone marrow-derived elements in the central nervous system: an immunohistochemical and ultrastructural survey of rat chimeras*. J Neuropathol Exp Neurol, 1992. **51**(3): p. 246-56.
16. Williams, K.C., et al., *Perivascular Macrophages Are the Primary Cell Type Productively Infected by Simian Immunodeficiency Virus in the Brains of Macaques: Implications for the Neuropathogenesis of AIDS*. Journal of Experimental Medicine, 2001. **193**(8): p. 905-916.
17. Lane, J.H., et al., *Neuroinvasion by simian immunodeficiency virus coincides with increased numbers of perivascular macrophages/microglia and intrathecal immune activation*. J Neurovirol, 1996. **2**(6): p. 423-32.
18. Frederick, N. and A. Louveau, *Meningeal lymphatics, immunity and neuroinflammation*. Curr Opin Neurobiol, 2020. **62**: p. 41-47.
19. Louveau, A., et al., *Structural and functional features of central nervous system lymphatic vessels*. Nature, 2015. **523**(7560): p. 337-41.
20. Song, E. and A. Iwasaki, *Monocytes Inadequately Fill In for Meningeal Macrophages*. Trends Immunol, 2019. **40**(6): p. 463-465.
21. Lamers, S.L., et al., *HIV-1 phylogenetic analysis shows HIV-1 transits through the meninges to brain and peripheral tissues*. Infection, Genetics and Evolution, 2011. **11**(1): p. 31-37.
22. Cui, J., H. Xu, and M.K. Lehtinen, *Macrophages on the margin: choroid plexus immune responses*. Trends in Neurosciences, 2021. **44**(11): p. 864-875.
23. Proulx, S.T., *Cerebrospinal fluid outflow: a review of the historical and contemporary evidence for arachnoid villi, perineural routes, and dural lymphatics*. Cellular and Molecular Life Sciences, 2021. **78**(6): p. 2429-2457.
24. Lackner, A.A., et al., *Localization of simian immunodeficiency virus in the central nervous system of rhesus monkeys*. Am J Pathol, 1991. **139**(3): p. 609-21.
25. Burkala, E.J., et al., *Compartmentalization of HIV-1 in the central nervous system: role of the choroid plexus*. Aids, 2005. **19**(7): p. 675-84.

26. Falangola, M.F., et al., *HIV infection of human choroid plexus: a possible mechanism of viral entry into the CNS*. J Neuropathol Exp Neurol, 1995. **54**(4): p. 497-503.
27. Petito, C.K., et al., *HIV infection of choroid plexus in AIDS and asymptomatic HIV-infected patients suggests that the choroid plexus may be a reservoir of productive infection*. J Neurovirol, 1999. **5**(6): p. 670-7.
28. Harouse, J.M., et al., *Human choroid plexus cells can be latently infected with human immunodeficiency virus*. Ann Neurol, 1989. **25**(4): p. 406-11.
29. Herz, J., et al., *Myeloid Cells in the Central Nervous System*. Immunity, 2017. **46**(6): p. 943-956.
30. Norris, G.T. and J. Kipnis, *Immune cells and CNS physiology: Microglia and beyond*. J Exp Med, 2019. **216**(1): p. 60-70.
31. Filipowicz, A.R., et al., *Proliferation of Perivascular Macrophages Contributes to the Development of Encephalitic Lesions in HIV-Infected Humans and in SIV-Infected Macaques*. Sci Rep, 2016. **6**: p. 32900.
32. Fischer-Smith, T., et al., *CNS invasion by CD14+/CD16+ peripheral blood-derived monocytes in HIV dementia: perivascular accumulation and reservoir of HIV infection*. J Neurovirol, 2001. **7**(6): p. 528-41.
33. Nowlin, B.T., et al., *SIV encephalitis lesions are composed of CD163(+) macrophages present in the central nervous system during early SIV infection and SIV-positive macrophages recruited terminally with AIDS*. Am J Pathol, 2015. **185**(6): p. 1649-65.
34. Soulas, C., et al., *Recently infiltrating MAC387(+) monocytes/macrophages a third macrophage population involved in SIV and HIV encephalitic lesion formation*. Am J Pathol, 2011. **178**(5): p. 2121-35.
35. Wilson, E.H., W. Weninger, and C.A. Hunter, *Trafficking of immune cells in the central nervous system*. J Clin Invest, 2010. **120**(5): p. 1368-79.
36. Ransohoff, R.M., P. Kivisäkk, and G. Kidd, *Three or more routes for leukocyte migration into the central nervous system*. Nature Reviews Immunology, 2003. **3**(7): p. 569-581.
37. Mrass, P. and W. Weninger, *Immune cell migration as a means to control immune privilege: lessons from the CNS and tumors*. Immunological Reviews, 2006. **213**(1): p. 195-212.
38. Soulas, C., et al., *Genetically modified CD34+ hematopoietic stem cells contribute to turnover of brain perivascular macrophages in long-term repopulated primates*. Am J Pathol, 2009. **174**(5): p. 1808-17.

39. Bechmann, I., et al., *Immune surveillance of mouse brain perivascular spaces by blood-borne macrophages*. Eur J Neurosci, 2001. **14**(10): p. 1651-8.
40. Cronk, J.C., et al., *Peripherally derived macrophages can engraft the brain independent of irradiation and maintain an identity distinct from microglia*. J Exp Med, 2018. **215**(6): p. 1627-1647.
41. Cugurra, A., et al., *Skull and vertebral bone marrow are myeloid cell reservoirs for the meninges and CNS parenchyma*. Science, 2021. **373**(6553).
42. Lassmann, H., et al., *Bone marrow derived elements and resident microglia in brain inflammation*. Glia, 1993. **7**(1): p. 19-24.
43. Campbell, J.H., et al., *Anti-alpha4 antibody treatment blocks virus traffic to the brain and gut early, and stabilizes CNS injury late in infection*. PLoS Pathog, 2014. **10**(12): p. e1004533.
44. Lakritz, J.R., et al., *alpha4-Integrin Antibody Treatment Blocks Monocyte/Macrophage Traffic to, Vascular Cell Adhesion Molecule-1 Expression in, and Pathology of the Dorsal Root Ganglia in an SIV Macaque Model of HIV-Peripheral Neuropathy*. Am J Pathol, 2016. **186**(7): p. 1754-1761.
45. Walker, J.A., et al., *Anti-alpha4 Integrin Antibody Blocks Monocyte/Macrophage Traffic to the Heart and Decreases Cardiac Pathology in a SIV Infection Model of AIDS*. J Am Heart Assoc, 2015. **4**(7).
46. das Neves, S.P., N. Delivanoglou, and S. Da Mesquita, *CNS-Draining Meningeal Lymphatic Vasculature: Roles, Conundrums and Future Challenges*. Front Pharmacol, 2021. **12**: p. 655052.
47. Hatterer, E., et al., *How to drain without lymphatics? Dendritic cells migrate from the cerebrospinal fluid to the B-cell follicles of cervical lymph nodes*. Blood, 2006. **107**(2): p. 806-12.
48. Hatterer, E., et al., *Cerebrospinal fluid dendritic cells infiltrate the brain parenchyma and target the cervical lymph nodes under neuroinflammatory conditions*. PLoS One, 2008. **3**(10): p. e3321.
49. Kaminski, M., et al., *Migration of monocytes after intracerebral injection*. Cell Adh Migr, 2012. **6**(3): p. 164-7.
50. Kida, S., A. Pantazis, and R.O. Weller, *CSF drains directly from the subarachnoid space into nasal lymphatics in the rat. Anatomy, histology and immunological significance*. Neuropathol Appl Neurobiol, 1993. **19**(6): p. 480-8.
51. Louveau, A., *Meningeal Immunity, Drainage, and Tertiary Lymphoid Structure Formation*. Methods Mol Biol, 2018. **1845**: p. 31-45.

52. Bradbury, M.W. and W. Lathem, *A flow of cerebrospinal fluid along the central canal of the spinal cord of the rabbit and communications between this canal and the sacral subarachnoid space*. The Journal of Physiology, 1965. **181**(4): p. 785-800.
53. Srinivas, M., P. Sharma, and S. Jhunjhunwala, *Phagocytic Uptake of Polymeric Particles by Immune Cells under Flow Conditions*. Molecular Pharmaceutics, 2021. **18**(12): p. 4501-4510.
54. Tabata, Y. and Y. Ikada, *Effect of the size and surface charge of polymer microspheres on their phagocytosis by macrophage*. Biomaterials, 1988. **9**(4): p. 356-62.
55. Alves de Lima, K., J. Rustenhoven, and J. Kipnis, *Meningeal Immunity and Its Function in Maintenance of the Central Nervous System in Health and Disease*. Annu Rev Immunol, 2020. **38**: p. 597-620.
56. Kierdorf, K., et al., *Macrophages at CNS interfaces: ontogeny and function in health and disease*. Nat Rev Neurosci, 2019. **20**(9): p. 547-562.
57. Carare, R.O., et al., *Solutes, but not cells, drain from the brain parenchyma along basement membranes of capillaries and arteries: significance for cerebral amyloid angiopathy and neuroimmunology*. Neuropathol Appl Neurobiol, 2008. **34**(2): p. 131-44.
58. Hoffmann, A., et al., *High and Low Molecular Weight Fluorescein Isothiocyanate (FITC)-Dextrans to Assess Blood-Brain Barrier Disruption: Technical Considerations*. Translational Stroke Research, 2011. **2**(1): p. 106-111.
59. Muldoon, L.L., et al., *Trafficking of superparamagnetic iron oxide particles (Combidex) from brain to lymph nodes in the rat*. Neuropathology and Applied Neurobiology, 2004. **30**(1): p. 70-79.
60. Burdo, T.H., et al., *Increased monocyte turnover from bone marrow correlates with severity of SIV encephalitis and CD163 levels in plasma*. PLoS Pathog, 2010. **6**(4): p. e1000842.
61. Hasegawa, A., et al., *The level of monocyte turnover predicts disease progression in the macaque model of AIDS*. Blood, 2009. **114**(14): p. 2917-25.
62. Da Mesquita, S., et al., *Functional aspects of meningeal lymphatics in ageing and Alzheimer's disease*. Nature, 2018. **560**(7717): p. 185-191.
63. Louveau, A., et al., *CNS lymphatic drainage and neuroinflammation are regulated by meningeal lymphatic vasculature*. Nat Neurosci, 2018. **21**(10): p. 1380-1391.

64. Chen, Y. and S. Hou, *Recent progress in the effect of magnetic iron oxide nanoparticles on cells and extracellular vesicles*. Cell Death Discovery, 2023. **9**(1): p. 195.
65. Nkansah, M.K., D. Thakral, and E.M. Shapiro, *Magnetic poly(lactide-co-glycolide) and cellulose particles for MRI-based cell tracking*. Magn Reson Med, 2011. **65**(6): p. 1776-85.
66. Dadfar, S.M., et al., *Size-isolation of superparamagnetic iron oxide nanoparticles improves MRI, MPI and hyperthermia performance*. Journal of Nanobiotechnology, 2020. **18**(1): p. 22.
67. Dulińska-Litewka, J., et al., *Superparamagnetic Iron Oxide Nanoparticles- Current and Prospective Medical Applications*. Materials (Basel), 2019. **12**(4).
68. Janko, C., et al., *Functionalized Superparamagnetic Iron Oxide Nanoparticles (SPIONs) as Platform for the Targeted Multimodal Tumor Therapy*. Frontiers in Oncology, 2019. **9**.
69. Wang, S., et al., *Ferroptosis: A double-edged sword*. Cell Death Discovery, 2024. **10**(1): p. 265.
70. Absinta, M., et al., *Human and nonhuman primate meninges harbor lymphatic vessels that can be visualized noninvasively by MRI*. Elife, 2017. **6**.
71. Ahn, J.H., et al., *Meningeal lymphatic vessels at the skull base drain cerebrospinal fluid*. Nature, 2019. **572**(7767): p. 62-66.
72. Asgari, M., D.A. de Zélicourt, and V. Kurtcuoglu, *Barrier dysfunction or drainage reduction: differentiating causes of CSF protein increase*. Fluids and Barriers of the CNS, 2017. **14**(1): p. 1-11.
73. Aspelund, A., et al., *A dural lymphatic vascular system that drains brain interstitial fluid and macromolecules*. J Exp Med, 2015. **212**(7): p. 991-9.
74. Chen, L., et al., *Pathways of cerebrospinal fluid outflow: a deeper understanding of resorption*. Neuroradiology, 2015. **57**(2): p. 139-47.
75. Louveau, A., S. Da Mesquita, and J. Kipnis, *Lymphatics in Neurological Disorders: A Neuro-Lympho-Vascular Component of Multiple Sclerosis and Alzheimer's Disease?* Neuron, 2016. **91**(5): p. 957-973.
76. Louveau, A., T.H. Harris, and J. Kipnis, *Revisiting the Mechanisms of CNS Immune Privilege*. Trends Immunol, 2015. **36**(10): p. 569-577.
77. Louveau, A., et al., *Understanding the functions and relationships of the glymphatic system and meningeal lymphatics*. J Clin Invest, 2017. **127**(9): p. 3210-3219.

78. Ma, Q., et al., *Outflow of cerebrospinal fluid is predominantly through lymphatic vessels and is reduced in aged mice*. Nat Commun, 2017. **8**(1): p. 1434.
79. Papadopoulos, Z., J. Herz, and J. Kipnis, *Meningeal Lymphatics: From Anatomy to Central Nervous System Immune Surveillance*. J Immunol, 2020. **204**(2): p. 286-293.
80. Raper, D., A. Louveau, and J. Kipnis, *How Do Meningeal Lymphatic Vessels Drain the CNS?* Trends Neurosci, 2016. **39**(9): p. 581-586.
81. Schiefenhövel, F., et al., *Indications for cellular migration from the central nervous system to its draining lymph nodes in CD11c-GFP(+) bone-marrow chimeras following EAE*. Exp Brain Res, 2017. **235**(7): p. 2151-2166.
82. Laaker, C., et al., *Immune cells as messengers from the CNS to the periphery: the role of the meningeal lymphatic system in immune cell migration from the CNS*. Front Immunol, 2023. **14**: p. 1233908.
83. Murtha, L.A., et al., *Cerebrospinal fluid is drained primarily via the spinal canal and olfactory route in young and aged spontaneously hypertensive rats*. Fluids Barriers CNS, 2014. **11**: p. 12.
84. Smyth, L.C.D., et al., *Identification of direct connections between the dura and the brain*. Nature, 2024. **627**(8002): p. 165-173.
85. Johnston, M., et al., *Evidence of connections between cerebrospinal fluid and nasal lymphatic vessels in humans, non-human primates and other mammalian species*. Cerebrospinal Fluid Res, 2004. **1**(1): p. 2.
86. Walter, B.A., et al., *The olfactory route for cerebrospinal fluid drainage into the peripheral lymphatic system*. Neuropathology and Applied Neurobiology, 2006. **32**(4): p. 388-396.
87. Elman, R., *Spinal arachnoid granulations with special reference to the cerebrospinal fluid*. Johns Hopkins Hospital Bull, 1923.
88. Kido, D., et al., *Human spinal arachnoid villi and granulations*. Neuroradiology, 1976. **11**(5): p. 221-228.
89. Welch, K. and M. Pollay, *The spinal arachnoid villi of the monkeys Cercopithecus aethiops sabaeus and Macaca irus*. The Anatomical Record, 1963. **145**(1): p. 43-48.
90. Brierley, J. and E. Field, *The connexions of the spinal sub-arachnoid space with the lymphatic system*. Journal of anatomy, 1948. **82**(Pt 3): p. 153.

91. Iwanow, G., *Über die Abflußwege aus den submeningealen Räumen des Rückenmarks*. Zeitschrift für die gesamte experimentelle Medizin, 1928. **58**(1): p. 1-21.
92. Antila, S., et al., *Development and plasticity of meningeal lymphatic vessels*. Journal of Experimental Medicine, 2017. **214**(12): p. 3645-3667.
93. Zenker, W., S. Bankoul, and J.S. Braun, *Morphological indications for considerable diffuse reabsorption of cerebrospinal fluid in spinal meninges particularly in the areas of meningeal funnels*. Anatomy and embryology, 1994. **189**(3): p. 243-258.
94. Kivisäkk, P., et al., *Human cerebrospinal fluid central memory CD4+ T cells: evidence for trafficking through choroid plexus and meninges via P-selectin*. Proc Natl Acad Sci U S A, 2003. **100**(14): p. 8389-94.
95. Hanly, A. and C.K. Petito, *HLA-DR-positive dendritic cells of the normal human choroid plexus: a potential reservoir of HIV in the central nervous system*. Hum Pathol, 1998. **29**(1): p. 88-93.
96. White, K.S., et al., *Simian immunodeficiency virus-infected rhesus macaques with AIDS co-develop cardiovascular pathology and encephalitis*. Front Immunol, 2023. **14**: p. 1240946.
97. Hansen, S.G., et al., *Profound early control of highly pathogenic SIV by an effector memory T-cell vaccine*. Nature, 2011. **473**(7348): p. 523-7.
98. Hansen, S.G., et al., *Immune clearance of highly pathogenic SIV infection*. Nature, 2013. **502**(7469): p. 100-4.
99. Lifson, J.D., et al., *Role of CD8(+) lymphocytes in control of simian immunodeficiency virus infection and resistance to rechallenge after transient early antiretroviral treatment*. J Virol, 2001. **75**(21): p. 10187-99.
100. Ko, A., et al., *Macrophages but not Astrocytes Harbor HIV DNA in the Brains of HIV-1-Infected Aviremic Individuals on Suppressive Antiretroviral Therapy*. J Neuroimmune Pharmacol, 2019. **14**(1): p. 110-119.
101. Yuan, Z., et al., *Controlling Multicycle Replication of Live-Attenuated HIV-1 Using an Unnatural Genetic Switch*. ACS Synth Biol, 2017. **6**(4): p. 721-731.

3.9 Chapter Overview and Next Steps

In this study, we used i.c. injection of SPION to investigate the accumulation, traffic, and infection of perivascular, meningeal, and choroid plexus macrophages in animals with AIDS and SIVE, on ART, and following ART interruption. Our findings show that SPION-labeled macrophages are retained in the CNS with AIDS and SIVE, with limited traffic out to the dcLN, spleen, and DRGs. We found that ART reduced the number of SPION-labeled macrophages in the CNS while increasing traffic out to the dcLN, spleen, and DRG. Additionally, ART clears SIV-RNA⁺, SPION-labeled perivascular macrophages in the CNS but not in the meningeal and choroid plexus macrophages, which show a viral rebound—but not perivascular macrophages—after ART interruption. These results highlight the role of CNS macrophage in inflammation, infection, and the dynamics of viral rebound with ART interruption from a blood-derived source. Interestingly, some ART-treated animals did not show increased numbers of SPION-labeled macrophages in the dcLN, despite a reduction of macrophages in the brain, suggesting alternative, non-lymphatic routes of egress. Based on these findings, we sought to explore perineural pathways, particularly cranial and spinal nerves, as possible routes for macrophage migration from the CNS to the periphery.

4.0 Chapter 4

Perineural Pathways Allow Simian Immunodeficiency Virus-Infected Macrophages to Traffic Out of the Central Nervous System.

Zoey K. Wallis¹

Yingshan Wei¹

Lily Ceraso¹

Cecily C. Midkiff²

Addison Amadeck¹

Yiwei Wang¹

Andrew D. Miller³

Xavier Alvarez⁴

Robert V. Blair²

Kenneth C. Williams¹

¹ Morrissey College of Arts and Sciences, Biology Department, Boston College, Chestnut Hill, MA, USA.

² Tulane National Primate Research Center, Covington, LA, USA.

³ Department of Population Medicine and Diagnostic Science, Section of Anatomic Pathology, College of Veterinary Medicine, Cornell University, Ithaca, NY, USA.

⁴ Imaging PET-CT and OIL Core, Southwest National Primate Research Center, San Antonio, TX, USA.

4.1 Author Contributions

Conceptualization, K.C.W., Z.K.W., and X.A.; Obtained and analyzed data and images, Z.K.W., Y.Wei., L.C., and C.C.M.; Cut tissues, Z.K.W., A.A, Y.Wang., and L.C.; writing—original draft preparation, Z.K.W., K.C.W., and R.V.B; writing—review and editing, K.C.W., Z.K.W., R.V.B, and A.D.M.; funding acquisition, K.C.W.

Manuscript in preparation as of November 2024.

4.2 Abstract

One of the major challenges to the eradication of human immunodeficiency virus (HIV) and simian immunodeficiency virus (SIV) is the central nervous system (CNS) viral reservoir and our lack of understanding of the mechanisms by which it contributes to viral rebound and reseeding both on and off antiretroviral therapy (ART). To better understand the role macrophage traffic plays in reseeding the periphery both on and off ART, we used intracisternal (i.c.) injection of superparamagnetic iron oxide nanoparticles (SPION), to label CNS macrophage, early and late in macaques with acquired immunodeficiency syndrome (AIDS), on ART, and 4 weeks after ART interruption. We then tracked SPION+ macrophages by quantifying them at different central (spinal cord and cranial nerves) and peripheral (dorsal root ganglia, DRG) sites. Similar to our prior work in the brain, SIV infection resulted in increased numbers of macrophages in the CNS and a decrease in peripheral sites. Staining for viral RNA and GP41 identified virus-infected, SPION+ macrophages in cranial nerves and DRG that was significantly reduced, but not eliminated on ART. Animals with AIDS had reduced numbers of late- and dual-labeled SPION+ macrophages, indicating reduced macrophage trafficking late in infection. ART appeared to restore traffic with higher numbers of late- and dual-labeled macrophages, which, when ART was interrupted, returned to levels similar to AIDS/SIVE. Our findings reveal a newly discovered perineural pathway through which CNS macrophage viral reservoirs can redistribute virus, a process that persists despite ART.

Keywords: HIV, SIV, CNS macropahge, cranial nerves, DRG, perineural, traffic

4.3 Introduction

Human immunodeficiency virus (HIV) and simian immunodeficiency virus (SIV) persist in the central nervous system (CNS) [1-3] yet the extent to which virally infected macrophages can exit the CNS is unclear. Previous studies have elegantly detailed the pathways by which myeloid cells (monocyte-derived-dendritic cells and macrophages), T cells, and antigens drain from the CNS to the cervical lymph nodes (cLN) in rodents [4-10]; however, investigation in SIV-infected macaques, with acquired immunodeficiency syndrome (AIDS) and SIV-induced encephalitis (SIVE), and the impact of antiretroviral therapy (ART) have been limited. We recently used intracisternal (i.c.) injection of superparamagnetic iron oxide nanoparticles (SPION), which are internalized by and label CNS macrophages [11, 12], to study CNS macrophage kinetics and found traffic to the periphery in non-infected animals. SIV infection resulted in the accumulation of SPION+ macrophages in the CNS and reduced macrophage traffic to the periphery (Alvarez *et al.*, in prep) (**Figure 4.1**). ART reduced the number of SPION+ macrophages in the CNS and simultaneously increased the number of SPION+ macrophages detected in the periphery, consistent with macrophage traffic out of the CNS with resolution of inflammation (Wallis *et al.*, in prep). Importantly, SIV-RNA+ SPION+ macrophages could be found in the deep cervical lymph node (dCLN) of animals with AIDS, indicating traffic of virally infected macrophages from the CNS to peripheral lymph node, which was effectively eliminated with ART (Wallis *et al.*, in prep). Although our data indicated increased traffic of SPION-labeled macrophages out of the CNS in animals on ART, the dCLN did not contain increased numbers of SPION-labeled macrophages, implying an alternative egress pathway for these cells. Given these findings, we sought to investigate

macrophage trafficking in and around cranial and spinal nerves, which transverse the boundary between the CNS and PNS, providing another avenue for CNS egress.

The CNS has long been perceived as anatomically and immunologically segregated from the rest of the body, primarily due to tight junctions, lack of draining lymphatics, and the blood-brain barrier (BBB) [13, 14]. However, the connection between the CNS and the peripheral nervous system (PNS) is often disregarded and poorly understood. The meninges of the CNS merge with connective tissues ensheathing the peripheral nerves: the dura mater is continuous with the epineurium, the arachnoid layer combines with the outer layers of the perineurium, and the inner layers of the perineurium are mirrored onto the nerve roots, forming the root sheath [15-18]. The inner layers of the root sheath originate from a part of the perineurium, creating a continuous connection between the subarachnoid space surrounding the CNS and the space inside the nerve roots (the endoneurium) [19]. This connection allows fluid from the subarachnoid space—CSF—to flow into the endoneurial space due to pressure, serving as a source of fluid for the nerves potentially carrying immune cells (and antigens) out of the BBB, which is delineated by the subarachnoid angle [20, 21]. Given that the dorsal root ganglion (DRG) is located outside of the BBB [22], it is crucial to investigate whether CNS macrophages, particularly those infected with SIV, are trafficking from the CNS to the DRG and other peripheral nerves, including cranial nerves, to better understand the immune dynamics and viral spread at this critical interface.

Macrophage accumulation in the CNS, PNS, and DRG are associated with peripheral nerve damage and neuropathy [23, 24]. However, the origin of these macrophages—from the CNS or the periphery—has not been demonstrated. We have previously found that

SIV-infected macaques have increased macrophage accumulation (CD68, CD163, and MAC387) in the DRG, and therapy with methyl-bis-guanylhydrazone (MGBG) decreased accumulation and reduced myeloid activation of these cells [23, 24]. Warfield *et al.* found persistent inflammation in the DRG of SIV-infected macaques (elevated cytokine profile and macrophage accumulation) that was not reduced with ART [25]. However, neither we nor Warfield determined the origin (CNS versus peripheral) of these macrophages. This is of particular importance because potential migration of SIV-infected macrophages from the CNS to the PNS, particularly during and after ART interruption, is critical to better understand viral recrudescence. A direct connection between the CNS and the PNS has recently been described and supports the hypothesis that macrophages can exit the CNS, potentially facilitating the spread of HIV and SIV to peripheral tissues [19].

We used i.c. injection of two different-colored SPION in macaques to label macrophages within the CNS at the time of injection, once early (12-14 days post infection) and once late in infection (3-28 days prior to endpoint). We utilized three NHP cohorts: 1) AIDS and SIVE (SIVE, n=6), 2) ART (n=4), and 3) four weeks following ART interruption (n=4) to investigate the impact of SIV infection and ART on CNS macrophages traffic via cranial and spinal nerves to the DRG and periphery. In non-infected animals, we found CD163+ SPION+ macrophages accumulated in the DRGs and cranial nerves. This accumulation increases with SIV infection and persists despite ART, in contrast to the brain and spinal cord wherein ART effectively reduces the total number of macrophages. This persistence in the face of decreasing numbers at other CNS sites (brain and spinal cord) indicates redistribution from other CNS sites to the cranial

nerves and DRG, typical of a route of traffic. In animals with AIDS and SIVE, we found SIV-RNA+ and GP41+ SPION+ macrophages in cranial nerves, suggesting that infected macrophages can use cranial nerves as a pathway of egress from the CNS, a process that was not entirely eliminated by ART. Macrophages are labeled primarily with early SPION in animals with AIDS and SIVE compared to more equal early and late labeling with ART, indicating ongoing migration out of the CNS under ART and retention within the CNS during SIVE late in infection. Our findings underscore the potential for CNS macrophage viral reservoirs to redistribute virus to the periphery via perineural pathways around and within cranial and spinal nerves.

4.4 Results

ART and CNS inflammation resolution: the role of macrophage traffic.

We and others have shown that CSF and CNS macrophages can be labeled using dextran dye and SPIONs, respectively. This is due to physiochemical properties that prevent them from crossing the BBB. Instead, like CSF, dextran is absorbed by lymphatics and eventually joins systemic circulation, whereas SPIONs, due to their larger size, require trafficking in phagocytes to exit the CNS. Consistent with this, we have found that following a single i.c injection of dextran and SPIONs, dextran can be found in the dcLN within hours of injection, whereas the earliest SPION-containing cells are observed 1 day after injection (Alvarez *et al.*, in prep) (**Figure 4.1**). Using these tracers, we found SIV infection resulted in the accumulation of macrophages in the brain and that these macrophages were capable of trafficking out of the CNS to the dcLN (Alvarez *et al.*, in prep) (**Figure 4.1**). With ART, we found increased numbers of SPION-labeled macrophages in the deep cervical lymph node and a reduction in the number of macrophages within the brain, consistent with increased traffic out of the CNS with resolution of inflammation (Wallis *et al.*, in prep) (**Figure 4.1**). Interestingly, in some animals treated with ART, we were unable to find increased numbers of SPION-labeled macrophages in the dcLN despite a similar reduction of macrophages in the brain suggesting alternative (non-lymphatic) routes of egress from the CNS. Therefore, we sought to investigate perineural pathways as potential routes of macrophage traffic to the periphery, focusing on cranial and spinal nerves that provide a direct connection between the CNS and PNS.

Accumulation of SPION+ macrophage in the spinal cord is similar to the brain.

Our previous work showed an accumulation of macrophages within the meninges and brain parenchyma following SIV infection with resolution and increased trafficking following ART therapy. Therefore, we first sought to investigate if these macrophage kinetics could be explained by redistribution within the CNS, to the spinal cord (**Figure 4.2**). We quantified SPION+ macrophages in the spinal cord and compared it to the accumulation in the spinal cord meninges (**Figure 4.2B**). In agreement with our work in the brain, there is no difference in the number of SPION+ macrophages in the spinal cord in animals with AIDS and SIVE compared to ART (SIVE: 2.6 ± 2.8 SPION+/mm²; ART: 1.2 ± 0.83 SPION+/mm²; ART Off: 2.3 ± 3.3 SPION+/mm²) ($p=0.36$) (**Figure 4.2B**). In the spinal cord meninges, there is a decrease in the number of SPION+ macrophages with AIDS compared to ART and following ART interruption that was significant (SIVE: 275 ± 164 SPION+/mm²; ART: 441 ± 245 SPION+/mm²; ART Off: 210 ± 183 SPION+/mm²) ($p<0.05$) (**Figure 4.2B**). Due to the large accumulation of SPION+ macrophages in the meninges compared to the spinal cord (33 to 80-fold increase), we hypothesize that within the CNS SPION+ macrophage traffic primarily traffic within the subarachnoid space. The subarachnoid space along the spinal cord provides a potential pathway for egress of SPION+ macrophages to the DRG and distal nerve, through the subarachnoid angle, as others have suggested occurring in rodents [20]. Additionally, we quantified the total number of macrophages in the spinal cord and found a decrease with ART that did not reach statistical significance (**Figure 4.7**).

SPION localizes to macrophage in DRG and cranial nerves following i.c. injection.

Following i.c. SPION injection, we find SPION in the DRG primarily cell-associated to macrophage (CD163+) (**Figure 4.3A-C**). Likewise, within cranial nerves, we find SPION primarily cell-associated with macrophage (CD163+), and few free SPION in CSF-filled areas (**Figure 4.3D-E**). Localization of SPION+ macrophages within the DRG and cranial nerves indicates the potential trafficking of SPION+ macrophages and SPIONs out of the CNS through CSF outflow pathways.

SPION+ macrophages in DRG accumulate over time and are unchanged with ART.

SPION+ macrophage accumulates in the DRG over time.

We next assessed the kinetics of SPION+ macrophage accumulation within the DRG in non-infected macaques with serial sacrifices following i.c. inoculation of SPIONs at 7-, 14-, and 28 days (**Figure 4.4A**). In non-infected macaques, we found that SPION+ macrophages gradually accumulate within the DRG for the first 14 days following a single ic injection of SPIONs and appear to remain stable for 28 days post. (n=2, p=0.13) (7 days: 0.86 ± 0.37 SPION+/mm²; 14 days: 2.2 ± 0.64 SPION+/mm²; 28 days: 2.4 ± 0.75 SPION+/mm²) (**Figure 4.4A**). In addition, we analyzed the normal distribution of SPION+ macrophages at different levels of the spinal cord (cervical, thoracic, lumbar, and sacral) and found no statistical differences in the DRG between levels (p=0.14) (**Figure 4.8**). These findings suggest that following a single i.c. injection of SPION, SPION+ macrophages gradually and evenly distribute throughout all levels of the spinal cord with traffic out of the CNS to the DRG at all levels of the spinal cord under normal conditions (uninfected).

Accumulation of SPION+ macrophage in the DRG with SIV infection and on ART.

To better understand the impact of SIV infection on CNS macrophage dynamics and traffic out to the PNS at the DRG and the effect of ART and ART interruption, we injected two fluorescently labeled SPION, early (green, 12-14 days post-infection) and late (red, 3-28 days prior to sacrifice). In the DRG, SIVE animals had the lowest total number of SPION+ macrophages with higher numbers in ART and ART interruption, but these differences did not achieve statistical significance (SIVE: 420 ± 105 SPION+/mm²; ART: 947 ± 400 SPION+/mm²; ART Off: 1458 ± 399 SPION+/mm²). When comparing early- to late-labeled SPION+ macrophages, early-labeled SPION+ macrophages predominated in all three groups, but varied, non-significantly, in proportion (AIDS and SIVE: 2.8-fold, ART: 2-fold, and ART interruption: 6.5-fold) (**Figure 4.4B**). ART animals have increased numbers, although not statistically significant, of dual SPION+ macrophages in DRG compared to AIDS and SIVE animals and there is no change with ART interruption (Dual SIVE: 74 ± 84 SPION+/mm²; Dual ART: 419 ± 752 SPION+/mm²; Dual ART interruption: 494 ± 821 SPION+/mm²) (**Figure 4.4B**). Additionally, we examined the total number of macrophages in the DRG, and consistent with our previous work, we found a significant decrease with ART (**Figure 4.9**). These data suggest that there is continual traffic of SPION+ macrophages out of the CNS to the PNS with ART that is reduced with the development of AIDS and SIVE.

SPION+ macrophages accumulate in cranial nerves with SIV infection and is unchanged with ART.

With the identification of perineural trafficking to the DRG, we sought to investigate another potential pathway that transverses the junction between the CNS and PNS, the cranial nerves. we quantified the number of early, late, and dual-labeled SPION+ macrophages in SIV-infected animals with AIDS and SIVE (n=5), on ART (n=4), and following ART off (n=4) (**Figure 4.5**). AIDS and SIVE animals have significantly ($p<0.01$) higher numbers of early SPION+ macrophage compared to late and dual SPION+ macrophage in cranial nerves (Early: 23 ± 34 SPION+/mm²; Late: 2.1 ± 2.8 SPION+/mm²; Dual: 3.3 ± 5.5 SPION+/mm²) (**Figure 4.5**). Conversely, ART animals have significantly ($p<0.001$) increased numbers of late and dual SPION+ macrophages in cranial nerves compared to AIDS and SIVE animals (Late SIVE: 2.1 ± 2.8 SPION+/mm²; Late ART: 38 ± 60 SPION+/mm²; Dual SIVE: 5.7 ± 0.7 SPION+/mm²; Dual ART: 129 ± 74 SPION+/mm²) (**Figure 4.5**). Following ART interruption, there are significantly ($p<0.001$) fewer late- and dual-SPION-labeled macrophages compared to ART which is a shift towards the AIDS phenotype with fewer late and dual-labeled macrophages (Early: 29 ± 18 SPION+/mm²; Late: 5.2 ± 4.6 SPION+/mm²; Dual: 8.6 ± 6.0 SPION+/mm²). These macrophage kinetics mirror those observed in the DRG, but at the cranial nerves, achieved statistical significance. These kinetics suggest that with AIDS and SIVE, there is retention of macrophages with reduced trafficking, especially late in infection, whereas ART facilitates trafficking of macrophages, consistent with the resolution of inflammation.

Trafficking of virally infected SPION+ macrophages persists despite ART in cranial nerves, but not DRG.

ART eliminates virally infected SPION+ macrophages within the DRG.

To investigate whether SIV-infected macrophage are trafficking out of the CNS via perineural pathways, we performed ultrasensitive SIV-RNAscope and staining for GP41+ and quantified the number of SPION+ macrophages that were also positive for virus. Animals with AIDS and SIVE had scattered SIV-RNA+ macrophage (CD163+ and CD68+) with and without SPION in the DRG (data not shown). With ART, virally infected macrophages were no longer seen within the DRG nor did they rebound following 4 weeks of ART interruption (**Figure 4.6., Table 4.2**). Scattered SIV-RNA+ cells without SPIONs (possibly T cells) were noted in the DRG in animals on ART and none were found in animals following 4 weeks of ART cessation (**Figure 4.6., Table 4.2**). These data suggest virally infected macrophages traffic out of the CNS to the PNS at the DRG with AIDS and SIVE, and although ART effectively eliminates viral replication, it promotes macrophage trafficking which has the potential to redistribute virus especially if ART is interrupted.

Virally infected SPION+ macrophage traffic out to cranial nerves with AIDS and SIVE.

We found animals with AIDS and SIVE have early, late, and dual SPION+SIV-RNA+ macrophages SPION+GP41+ macrophages within cranial nerves that are not eliminated with ART and do not rebound following ART interruption (**Figure 4.6., Table 4.2**). The majority of SPION+SIV-RNA+ macrophages in cranial nerves in animals with AIDS and SIVE have dual-labeled SPION and equal numbers of SIV-RNA+ early and late SPION+ macrophages (**Figure 4.6., Table 4.2**). SPION+SIV-GP41+ macrophages in

cranial nerves of animals with AIDS and SIVE are primarily early and late, no dual SPION (Figure 4.6., Table 4.2). Our findings show that ART does not eliminate SIV-RNA+ and GP41+ SPION+ macrophages in cranial nerves and there is no immediate rebound following four weeks of ART interruption (Figure 4.6., Table 4.2).

4.5 Discussion

Traffic of immune cells and drainage of antigens out of the CNS to secondary lymphoid organs is critical for the initiation and regulation of immune responses in the CNS. Using i.c. SPION injection, we found macrophage traffic out of the CNS in non-infected animals. SIV infection results in a reduced rate of traffic out of the CNS leading to the accumulation of macrophages within and low numbers of CNS macrophages detected at peripheral sites; whereas, ART restores traffic following the resolution of inflammation characterized by a reduction in the number of macrophages in the CNS, and increased numbers of CNS macrophages detected in the periphery (dcLN, spleen, and DRG) (Wallis, *et al.*, 2024). We found large numbers of CNS macrophages within perineural pathways (cranial nerves, spinal nerves, and the DRG) in animals with AIDS and SIVE that either remained stable or increased following ART. In the current study, we found that animals with AIDS and SIVE have fewer late SPION+ macrophage in cranial nerves and the DRG than ART animals, suggestive of reduced trafficking late during AIDS and SIVE versus continual traffic out with ART. With ART interruption, we found a reduction of late SPION+ macrophages in cranial and spinal nerves compared to ART, suggesting a reduction in trafficking and a return to the SIVE phenotype with ART off. Importantly, with AIDS and SIVE, we found CNS macrophages in cranial and spinal nerves that were virally infected (SIV-RNA+ and GP41+) and persisted with ART. Our findings highlight that the perineural pathway, well known for CNS antigen drainage, remains active irrespective of SIV infection or ART, with significant macrophage accumulation in cranial and spinal nerves and DRG.

The CNS is well described as a critical reservoir for lentiviruses, with PVM being the primary HIV and SIV-infected cells in the CNS [1]. Our recent work (Wallis et al., in prep) demonstrates that ART clears SIV from PVM within the CNS and scattered virally infected meningeal and choroid plexus macrophages persist and infection returns in these latter sites following a four-week interruption in ART. While viral levels in peripheral tissues such as plasma, spleen, and dCLN decrease with ART, the DRGs and cranial nerves remain infected. In animals with AIDS and SIVE, infected macrophages (SIV-RNA+ and GP41+) containing SPION were found within cranial and spinal nerves, suggesting that virally infected macrophages may travel out of the CNS via perineural pathways. Although ART significantly reduces SIV-RNA+ cells in the CNS, it does not fully eliminate SIV-RNA+ SPION+ macrophages within cranial and spinal nerves. These findings underscore the role of myeloid cells as viral reservoirs within the CNS, with the potential to traffic virus out to peripheral sites even on ART.

Whether virally infected CNS macrophages could traffic out of the CNS had not previously been determined, and our study reveals a newly discovered pathway by which virus can be redistributed, a process that remains unaffected by ART. We found that ART did not reduce the number of SPION+ macrophages in cranial and spinal nerves or the DRG. Animals with AIDS and SIVE have fewer late SPION+ macrophages in the cranial nerves and DRG compared to those on ART, indicating reduced trafficking of macrophages during AIDS and SIVE, as opposed to continuous trafficking out of the CNS while on ART. Importantly, ART did not fully eliminate virally infected CNS macrophage in cranial nerves, potentially enabling viral redistribution to the periphery. Our study is not the first time that traffic out of the CNS along perineural pathways has been shown, as others have

eloquently described this pathway for fluid [26, 27], antigen [4, 6], T cells [10], and DCs [28, 29] to leave the CNS and initiate an immune response in the dcLN. These studies support our finding that macrophage can traffic out of the CNS within and along cranial and spinal nerves with the potential to traffic HIV and SIV out to the periphery with AIDS and SIVE and even on ART.

Macrophages that traffic out of the CNS via cranial and spinal nerves would likely migrate to lymph nodes and terminal sites associated with these nerves. For cranial nerves, macrophages would primarily drain into cervical lymph nodes, such as the deep (dcLN) and superficial cervical nodes, where they could interact with peripheral immune cells and initiate an immune response, similar to what others have shown with DCs [28, 30]. Similarly, macrophages exiting via spinal nerves would travel to lymphatic structures near the spinal cord, including the lumbar lymph nodes [7]. Additionally, these cells may reach terminal sites in peripheral tissues where nerves innervate target organs, allowing further immune signaling and possibly contributing to localized inflammation. Importantly, a reduction in clinical symptoms of EAE with surgical ligation of cervical and lumbar lymph nodes [31] further highlights the involvement of macrophage traffic out via perineural pathways in CNS immune modulation and inflammation. Although we did not perform electron microscopy (TEM or Cryo-EM) for detailed anatomical analysis for the exact location of SPION+ macrophages within nerves, it is clear from our H&E staining that there are SPION+ macrophages primarily within the perineurium and endoneurium (Figure 3). As the perineurium is continuous with arachnoid mater, it forms a direct connection with the subarachnoid space surrounding the CNS and merges at the subarachnoid angle in the spine where SPION and SPION+ macrophage could traffic directly from the CSF filled-

subarachnoid space to the endoneurial fluid filled perineurium. Alternatively, SPION+ macrophage within the endoneurium within nerve fascicles could traffic from i) the dorsal horn, ii) from the subarachnoid angle, or iii) transmigration from perineurium to endoneurium as previously shown with increased inflammation [16]. Regardless, the localization of SPION+ macrophages within cranial and spinal nerves suggests a direct path for macrophages to leave the CNS to the PNS and contribute to persistent inflammation.

Our results underscore the importance of the connection between central and peripheral nerves in immunity, particularly the impact of macrophage traffic on persistent myeloid activation in the DRGs and peripheral nerves. In SIV-infected rhesus macaques, increased numbers of CD68+, CD163+, and MAC387+ macrophages are observed in DRG compared to uninfected controls. Even with ART, Burdo et al. report persistent neuroinflammation in the DRGs and dorsal horn, marked by elevated IL-1 β levels and activated CD68+ macrophages. This chronic inflammation is linked to ongoing nociceptor sensitization, potentially explaining sustained neuropathic pain in treated animals. Our findings suggest that this inflammation may result from continued immune cell traffic from the CNS to the DRG via perineural pathways, promoting macrophage activation in the DRG. Importantly, it was recently found that macrophage expansion in the DRG, but not at the site of injury, was required for initiation of the nerve injury-induced mechanical hypersensitivity [32]. Our findings suggest that macrophage trafficking from the CNS and subsequent accumulation in the DRG may be a significant contributor to neuropathic pain, even in animals receiving ART.

Our findings show that in animals with AIDS and SIVE, CNS macrophages accumulate in perineural pathways (cranial and spinal nerves and the DRG), persisting and even increasing with ART. Animals on ART had more SPION+ macrophages in these pathways than those with AIDS, suggesting active macrophage traffic from the CNS to the periphery during ART. Even with ART, virally infected (SIV-RNA+ and GP41+) macrophages were found in cranial nerves, indicating macrophages have the potential to carry HIV and SIV from the CNS to peripheral sites, contributing to viral persistence. This study underscores that the perineural pathway facilitates continual macrophage migration from the CNS, reseeding virus and sustaining inflammation even on ART.

4.6 Experimental Procedures

Ethics Statement: All animal work was approved by the Tulane National Primate Research Center Care and Animal Use Committee. The TNRPC protocol number is 3497 and the animal welfare assurance number is A4499-01.

Animals and Viral Infection: A total of 21 adult rhesus macaques (*Macaca mulatta*) born and housed at the Tulane National Primate Research Center in strict adherence to the "Guide for the Care and Use of Laboratory Animals" were used (**Figure 1. Table 1**). SPION injection controls consisted of one SIV infected macaque that received SPION injection 2 hours prior to sacrifice and six, non-infected macaques that received SPION injection 7 (n=2), 14 (n=2), or 28 (n=2) days before sacrifice. For the SIV+ study cohorts, CD8+ lymphocytes were depleted to achieve rapid AIDS (3 to 4 months) with >75% incidence of SIVE, as previously described [2, 33-35]. CD8+ T lymphocyte depletion was monitored longitudinally by flow cytometry and all macaques were persistently depleted (>28 days). Animals were experimentally infected intravenously (i.v) with a bolus of SIVmac251 viral swarm (20 ng of SIV p28) over 5 minutes. At 21 days post-infection, n=8 macaques began a 12-week regimen of antiretroviral therapy (ART) consisting of Raltegravir (Merck, 22 mg/kg) given orally twice daily, and Tenofovir (Gilead, 30 mg/kg) and Emtricitabine (Gilead, 10 mg/kg) combined in a sterile solution given once-daily, s.c. Four animals were euthanized on ART and 4 were removed from ART for 4 weeks to allow for viral rebound. Animals were euthanized at the study completion or based on the recommendations of the American Veterinary Medical Association Guidelines for the Euthanasia of Animals upon developing signs of AIDS, which included: a >15% decrease in body weight in 2 weeks or >30% decrease in body weight

in 2 months; documented opportunistic infection; persistent anorexia > 3 days without explicable cause; severe, intractable diarrhea; progressive neurological symptoms; or significant cardiac or pulmonary symptoms. SIV encephalitis (SIVE) was defined by the presence of multinucleated giant cells (MNGC) and the accumulation of macrophages [33]. Longitudinal plasma viral load (PVL) was assessed as previously described [36-38] to monitor viral suppression during treatment and rebound following ART cessation (Data not shown).

SPION: Superparamagnetic iron oxide nanoparticles (SPION) were obtained from Bang Laboratories Inc. (PS-COOH Mag/Encapsulated, MEDG001, and MEFR001, Fishers, IN). SPION are iron oxide nanospheres encapsulated in an inert polymer with an average particle size of 0.86 diameters and internal fluorescence (Dragon Green [480/520] and Flash Red [660/690]). SPION were prepared in a class 2 biosafety cabinet by gently mixing 3 mL of stock solution and 7 mL of sterile, low endotoxin 1XPBS. A magnet was used to separate the SPION from the liquid and an additional 7 mL of 1XPBS was added for a second wash. This was repeated 7 - 10 times and the SPION were resuspended 1mL of sterile 1XPBS, at a final concentration of 33 mg/mL.

Intracisternal Inoculation Procedure: To avoid an increase in intracranial pressure, 1 mL of cerebrospinal fluid (CSF) was removed from the cisterna magna prior to the inoculation of SPION. Dragon Green SPION (33 mg/mL) were administered 2 weeks post-inoculation at 12 or 14 dpi. Flash Red SPION (33 mg/mL) were injected late during infection prior to euthanasia (Range 3-22 days).

Tissue Collection and Processing: Animals were anesthetized with ketamine-HCl and euthanized with i.v. pentobarbital overdose and exsanguinated. Blood was collected and Heparin Sulfate was administered i.v. and given 5 minutes to diffuse. Sodium pentobarbital was administered via intracardiac stick and CSF was collected. Following CSF collection, animals underwent perfusion with 3L of chilled 1XPBS. Postmortem examination was performed by a veterinary pathologist that confirmed the presence of AIDS-defining lesions as previously described [2, 33-35]. CNS (frontal, temporal, occipital, parietal, and spinal cord) and PNS (cranial nerves, DRG, and spinal nerves) were: i) collected in zinc-buffered formalin and embedded in paraffin and/or ii) fixed with 2% paraformaldehyde for 4-48 hours, sucrose protected and embedded in optimal cutting temperature (OCT) compound for SPION analysis.

Immunohistochemistry: IHC was performed as previously described using the antibodies listed: CD163 (1:250, Leica (Deer Park, IL)), CD68 (1:100, DAKO (Carpinteria, CA)) [2, 34, 35]. Briefly, formalin-fixed paraffin-embedded sections were deparaffinized and rehydrated followed by antigen retrieval with a citrate-based Antigen Unmasking Solution (Vector Laboratories, Burlingame, CA) in a microwave (900 W) for 20 min. After cooling for 20 min, sections were washed with Tris-buffered saline (TBS) containing 0.05% Tween-20 for 5 minutes before incubation with peroxidase block (DAKO, Carpinteria, CA) followed by protein block (DAKO, Carpinteria, CA) for 30 minutes and incubation with primary antibody. Following incubation with a peroxidase-conjugated polymer, slides were developed using a diaminobenzidine chromogen (DAKO, Carpinteria, CA) with Harris Hematoxylin (StatLab, McKinney, TX).

Immunofluorescence: Immunofluorescence for CD163+ and GP41+ macrophages was performed using antibodies and fluorochromes targeting CD163 (NCL-CD163 CE, AF568, Invitrogen (Carlsbad, CA)) and gp41+ (KK41+, 1:100, NIH (Manassas, VA)) on 2% paraformaldehyde (PFA) fixed frozen sections. 2% PFA, fixed frozen sections were thawed for 20 minutes at room temperature, unwrapped, submerged in a citrate-based Antigen Unmasking Solution, and microwaved for one minute and forty-five seconds and cooled to room temperature. Slides were permeabilized in a solution of phosphate-buffered saline with 0.01% Triton X-100 and 0.02% fish skin gelatin (PBS-FSG-TX100) followed by a PBS-FSG wash, transferred to a humidified chamber and blocked with 10% normal goat serum (NGS) diluted in PBS-FSG for 40 minutes, followed by a 60-minute primary antibody incubation, washes, and 40-minute secondary antibody incubation. Routine washes were performed and DAPI nuclear stain added for 10 minutes. Slides were mounted using a custom-formulated anti-bleaching mounting media containing Mowiol (#475904, Calbiochem; San Diego, CA) and DABCO (#D2522, Sigma: St. Louis, MO) and allowed to dry overnight before being digitally imaged with a Zeiss Axio Scan.Z1. HALO software (HALO v3.4, Indica Labs; Albuquerque, NM). The internal fluorescence of SPION was used to detect CD163+SPION+ and GP41+SPION+ macrophages.

QuPATH Analysis for IHC Spinal Cord Macrophage Accumulation: Whole slide brightfield images of IHC with DAB and hematoxylin counterstained sections were scanned using a Zeiss AxioScan Z.1 (Carl Zeiss MicroImaging, Inc., Thornwood, NY). Files were converted (.tiff) and loaded into QuPATH for analysis. Macrophage markers and SPION analysis were performed separately and whole slide images were imported to

the corresponding projects. Stain vector (i.e. color) and background estimates were applied for each IHC analysis project to improve stain separation within QuPath using color deconvolution, by selecting a representative area containing an area of background along with examples of strong hematoxylin and DAB staining, as previously described [39]. Tissue regions in QuPATH were manually annotated by drawing to separate the spinal cord parenchyma from the meninges and DRG with distal nerves into separate regions of interest (ROIs) and tissue area reported as mm². Analysis of CD68+ and CD163+ macrophage was performed using *Fast Cell Count* commands [39]. Briefly, individual cells were identified by separating stains using color deconvolution and identifying peaks in either the hematoxylin channel (CD68 or CD163 negative cells) or the sum of the hematoxylin and DAB channels (CD68 or CD163 positive macrophage) and assigning these as positive or negative cells. The number of positive cells and area detected were used to calculate the average number of positive cells per mm² [39].

Viral RNA: Ultrasensitive SIV-RNAscope with probes for SIVmac251 was used to detect SPION-containing SIV-RNA positive cells in cranial nerves and DRG as previously described [85]. Tissue sections were placed in a target antigen retrieval solution, heated, and treated with protease plus, and a hydrogen peroxide blocker according to the manufacturer's protocol (Advanced Cell Diagnostics, Newark, CA). SIVmac239 RNAscope probes (Advanced Cell Diagnostics, Newark, CA) were hybridized at 40°C in the HyBEZ II Hybridization System. The RNAscope 2.5 HD Assay amplification steps were applied according to the manufacturer's protocol. Target RNA was visualized through the addition of chromogenic Fast Red A and Fast Red B (Advanced Cell Diagnostics, Newark, CA), and sections were counterstained with

hematoxylin (Sigma-Aldrich) and mounted using Vectamount (Vector Laboratories). The internal fluorescence of SPION was used to detect vRNA+SPION+ macrophage.

Detection and quantification of SPION-containing macrophages in tissues: SPION were detected in the central nervous system (CNS) and peripheral tissues by 1) light microscopy by morphology of the amber SPION beads, 2) Prussian blue iron staining (Sigma Aldrich Iron Stain, St. Louis, MO), and 3) internal fluorescence of Dragon Green or Flash Red as previously described (Alvarez, *et al.*, 2024) (Wallis, *et al.*, 2024).

For analysis of early versus late SPION+ macrophages and virally infected SPION+ macrophages, whole slide fluorescent images of stained sections were scanned using a Zeiss AxioScan Z.1 (Carl Zeiss MicroImaging, Inc., Thornwood, NY). Scanned sections were analyzed with HALO modular analysis software (HALO v3.4, Indica Labs; Albuquerque, NM). The spinal cord parenchyma, meninges, and DRG+distal nerve were first annotated into separate ROI/annotation layers. The number of early, late, and dual SPION-containing macrophages and virally infected (SIV-RNA or GP41+) early, late, and dual SPION-containing macrophages were counted using the FISH v.3.2.3 module (HALO v3.4, Indica Labs; Albuquerque, NM) and reported as the number of cells per mm².

Statistical Analysis: Statistical analyses were performed using Prism version 10.0 (GraphPad Software; San Diego, CA). Comparisons between animals with SIVE, ART, and following ART cessation were made using a nonparametric one-way analysis of variance (Kruskal-Wallis, GraphPad Software; San Diego, CA) with Dunn's multiple comparisons. Statistical significance was accepted at $p < 0.05$ and all graphing was done using Prism (GraphPad Software; San Diego, CA).

4.7 Tables, Figures, and Figure Legends

Figure 4.1

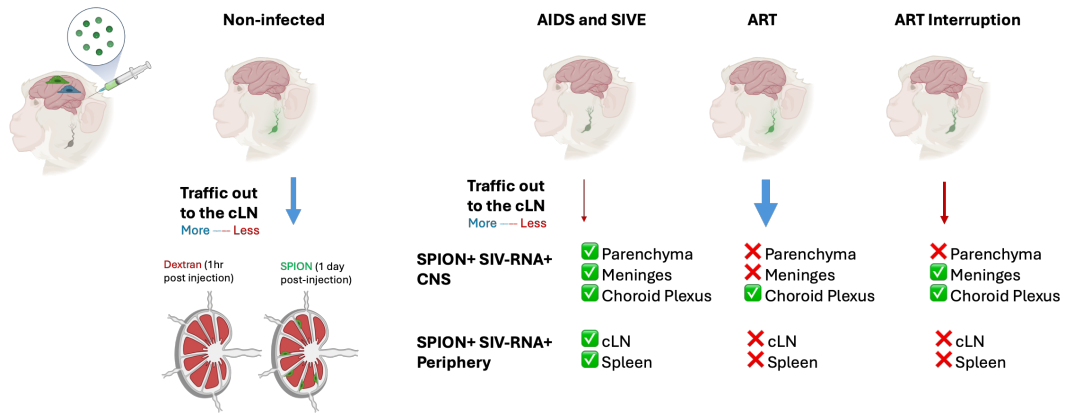


Figure 4.1 ART and CNS Inflammation Resolution: The Role of Macrophage

Traffic. In our previous studies (Alvarez *et al.*, in prep)(Wallis *et al.*, in prep) we performed intracisternal injection (i.c.) of Superparamagnetic iron oxide nanoparticles (SPION) to label macrophage in the CNS and found traffic out to the CNS in non-infected animals that increased over time. We next assessed the effects of AIDS and SIVE and found reduced traffic out of SPION+ macrophage to the deep cervical lymph node (dcLN). We found that SPION+ macrophages within and outside of the CNS were SIV-RNA+. Animals on ART had increased numbers of SPION+ macrophage in the dcLN and no SPION+ SIV-RNA+ perivascular macrophage or macrophage in the periphery. Importantly, following ART cessation, there was a reduction in macrophage traffic to the dcLN and a rebound in SIV-RNA+ SPION+ meningeal and choroid plexus macrophage. Created in BioRender. Wallis, Z. (2024) <https://BioRender.com/f671783>

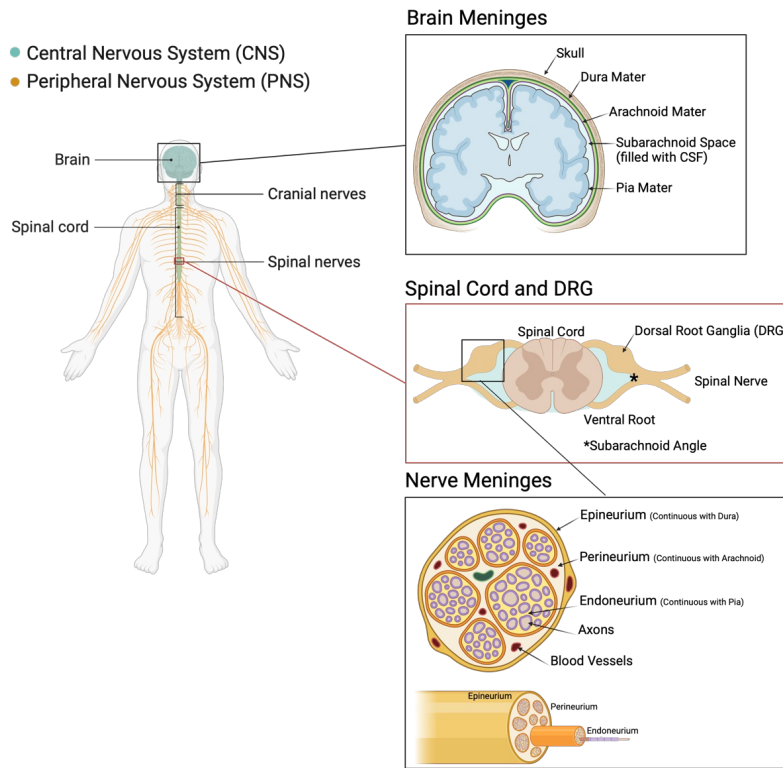
Table 4.1

Cohort	Monkey Group Size	SIV Status & Treatment	Animal Number	Age at Euthanasia	Survival After Infection	Degree of SIV-induced Encephalitis	Days with Green SPIONs	Days with Red SPIONs
SPION Injection Controls	n=1	SIV+, Untreated	HI67	4.97	358	SIVnoE	2hr	none
	n=2	Non-infected	GT17	6.3	n/a	n/a	7	none
			JP34	6.36	n/a	n/a	7	none
	n=2	Non-infected	JE42	7.41	n/a	n/a	14	none
			HE08	10.44	n/a	n/a	14	none
	n=2	Non-infected	IK15	8.46	n/a	n/a	28	none
IC61			4.87	n/a	n/a	28	none	
AIDS and SIVE	n=6	SIV+, Untreated, CD8 Depleted	IK28	10.34	100	Moderate SIVE	86	3
			JE87	9.37	119	Mild SIVE	105	14
			JD29	9.37	126	Mild SIVE	112	7
			KN69	6.32	83	Severe SIVE	69	6
			KT79	6.23	119	Mild SIVE	105	22
			LB12	5.46	115	Mild SIVE	101	10
ART	n=4	SIV+, CD8 Depleted, ART (21-105 dpi)	JJ86	7.87	105	SIVnoE	89	26
			KD67	6.77	105	SIVnoE	89	26
			KM38	5.67	105	SIVnoE	90	27
			LK25	6.18	105	SIVnoE	93	28
ART Off	n=4	SIV+, CD8 Depleted, ART (21-105 dpi), ART Off (105-133 dpi)	KD12	7.47	133	Mild SIVE	119	28
			JV76	7.52	132	SIVnoE	118	27
			JV78	7.53	133	SIVnoE	119	28
			KE98	7.29	133	SIVnoE	119	28

Table 4.1 Animals used in the study. SPION injection controls consisted of one SIV+ rhesus macaque was intracisternally injected (i.c.) with green, fluorescent SPION 2 hours prior to sacrifice and 6 non-infected rhesus macaques were i.c. injected 28 (n=2), 14 (n=2), or 7 days (n=2) prior to sacrifice. Fourteen rhesus macaques were infected with SIVmac251 and CD8 T lymphocytes depleted on 6, 8, and 12 dpi. SIV+ macaques received i.c. SPION injection early (12-14 dpi, green SPION) and late (30 days prior to sacrifice, red SPION false-colored blue). Eight macaques were treated with ART twice daily, starting at 21 dpi until 105 dpi, where animals were sacrificed on ART treatment (n=4) or had 4 weeks of ART interruption prior to sacrifice (n=4). All untreated macaques were sacrificed upon progression to AIDS between 83–126 dpi.

Figure 4.2

(A) A Potential Pathway for Egress of CNS Macrophages to the PNS



(B) Distribution of SPION+ Macrophages in the Spinal Cord and Spinal Cord Meninges

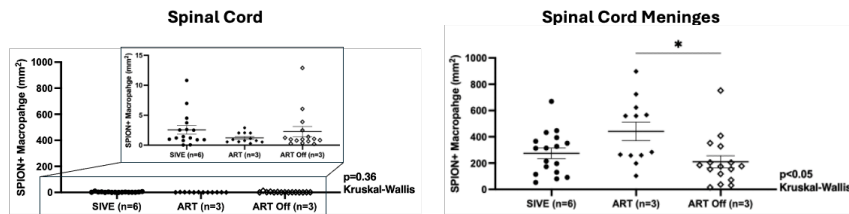


Figure 4.2 Accumulation of SPION in the spinal cord is similar to accumulation in the brain. (A) Diagram of the connection between the CNS and the PNS made with BioRender, highlighting the possible pathway for SPION+ macrophages egress. Created in BioRender. Wallis, Z. (2024) <https://BioRender.com/p44b504> (B) The number of SPION+ macrophages (mm²) in the cervical spinal cord and spinal cord meninges. Each point represents one tissue section counted and each color is a different animal analyzed. The mean \pm SEM are shown and p values were calculated using a Kruskal-Wallis (KW) one-way analysis of variance and Dunn's multiple comparison test. * $P < 0.05$, ** $P < 0.01$, *** $P < 0.001$.

Figure 4.3

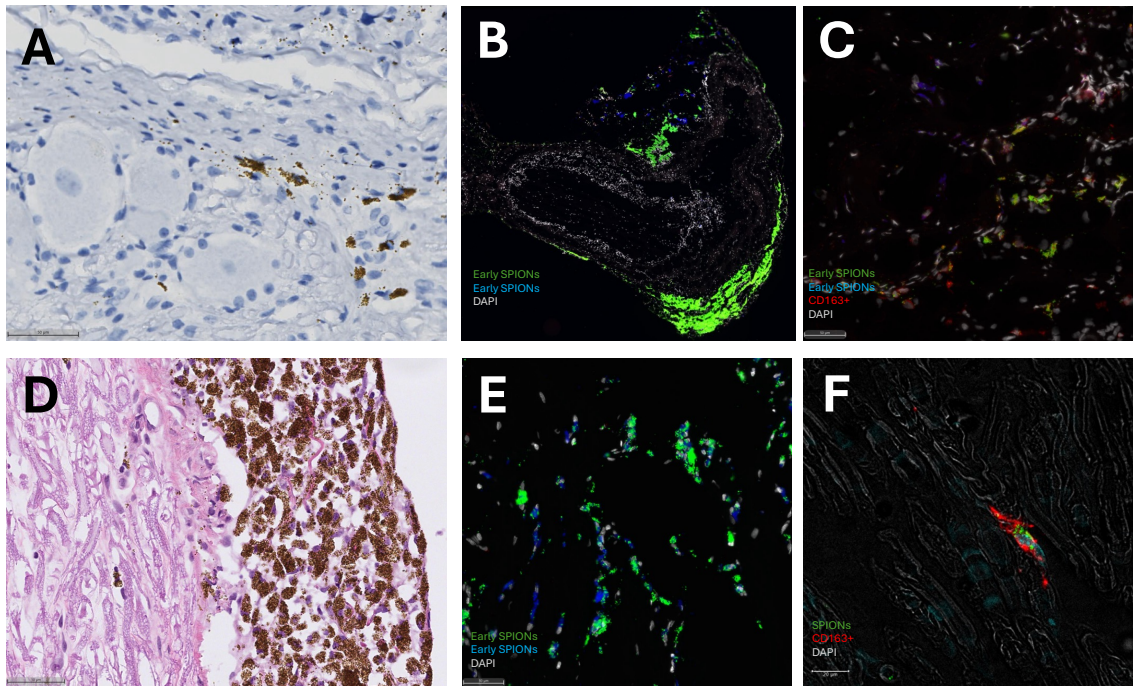
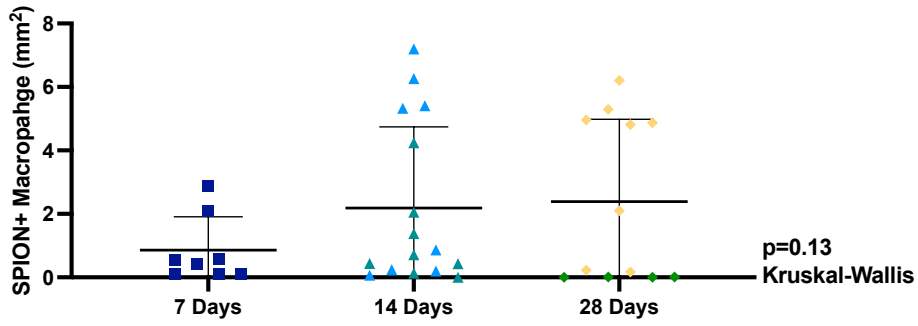


Figure 4.3 SPION+macrophage in the DRG and cranial nerves following i.c. injection. (A) SPION (amber beads) within the perineurium of the DRG. (B) Fluorescent SPION are primarily localized within the perineurium. (C) Green, fluorescent SPION localized to CD163+ macrophage (red) within the perineurium of cranial nerves. (D) SPION (amber beads) within the endoneurium and perineurium of cranial nerves. (E) SPION (green and blue) are cell-associated with (F) CD163+ macrophage (red).

Figure 4.4

(A) SPION+ Macrophages in the DRG of Non-infected Macaques Over Time



(B) Accumulation of SPION+ Macrophages in the DRG

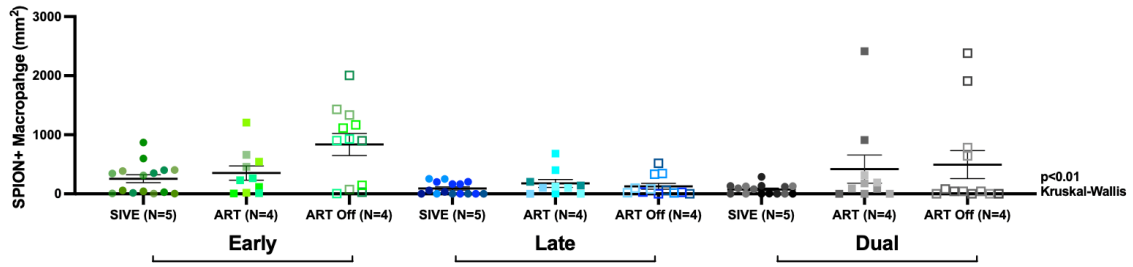


Figure 4.4 SPION+ macrophage accumulates in the DRG over time and is unchanged with ART. (A) The number of SPION+ macrophage (mm²) in the DRG of non-infected macaques 7, 14, and 28 days after i.c. injection of SPION. (B) Distribution of early, late, and dual SPION+ macrophages in the cervical DRG. Each point represents one tissue section counted and each color is a different animal analyzed. The mean \pm SEM are shown and p values were calculated using a Kruskal-Wallis (KW) one-way analysis of variance and Dunn's multiple comparison test. * $P < 0.05$, ** $P < 0.01$, *** $P < 0.001$. **** $P < 0.0001$.

Figure 4.5

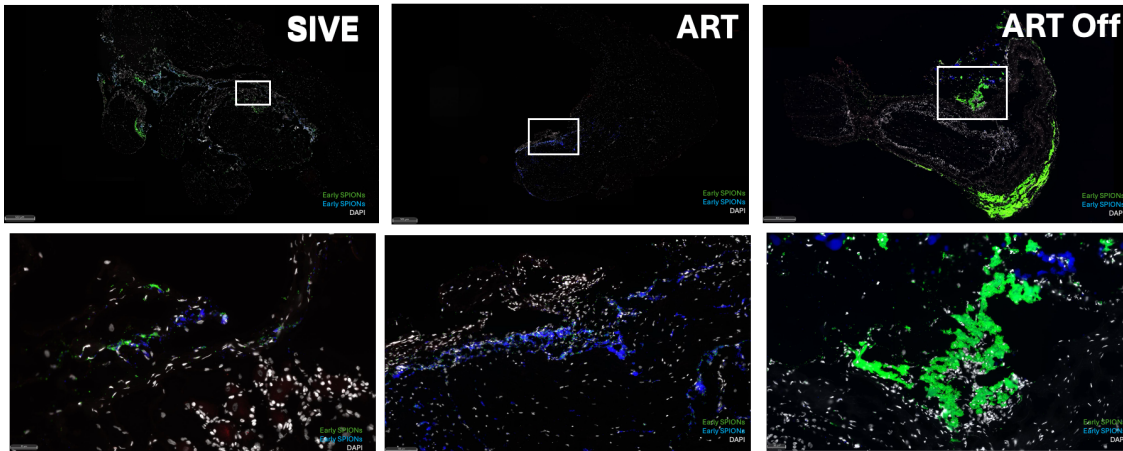
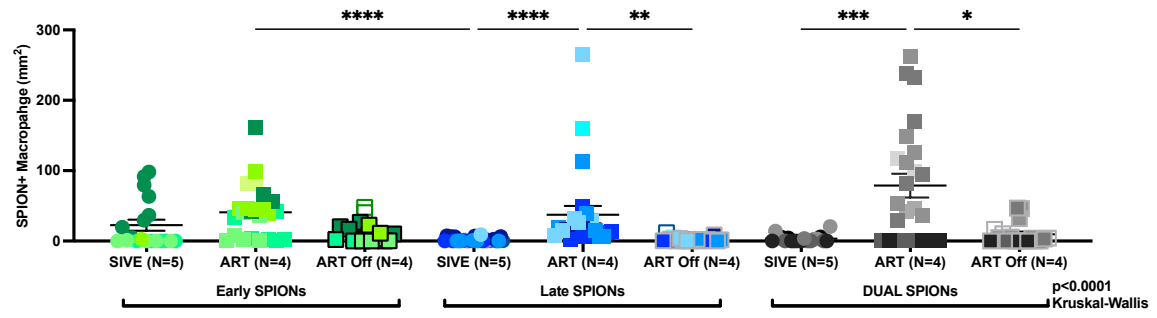


Figure 4.5 Accumulation of SPION+ macrophage in cranial nerves. Accumulation and distribution of early, late, and dual SPION+ macrophage within cranial nerves of non-infected, SIVE, and ART animals. The mean \pm SEM are shown, and p values were calculated using a Kruskal-Wallis (KW) one-way analysis of variance and Dunn's multiple comparison test. A representative image of a cranial nerve section analyzed from each treatment group is shown. * $P < 0.05$, ** $P < 0.01$, *** $P < 0.001$, **** $P < 0.0001$.

Figure 4.6

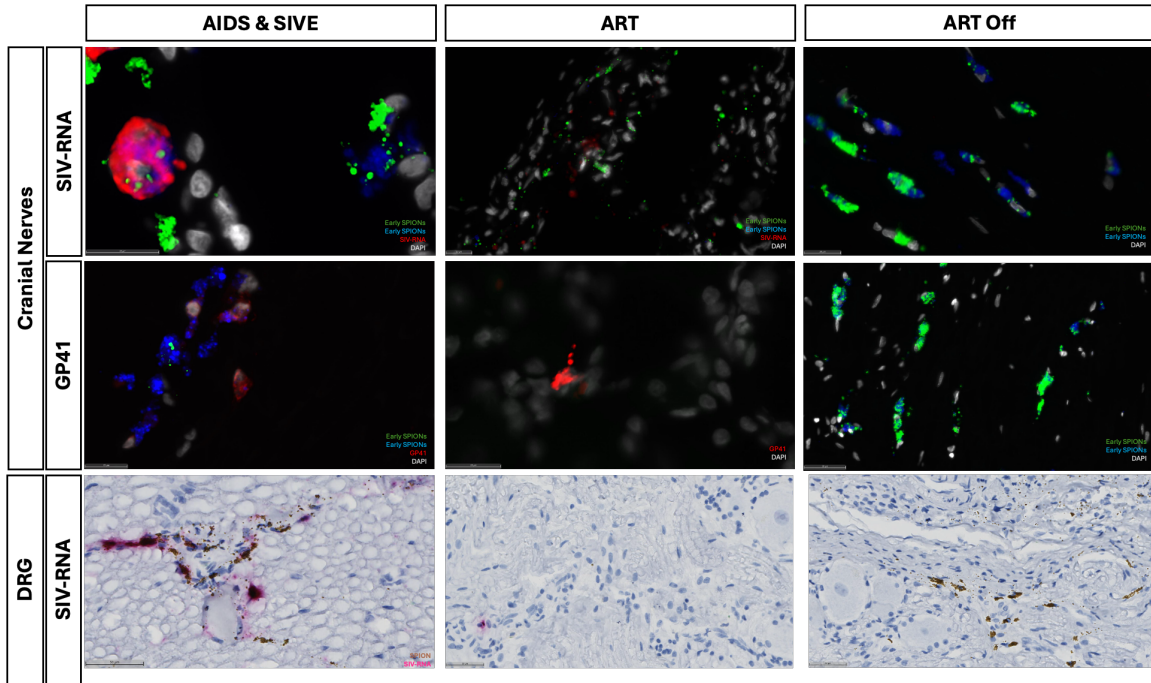


Figure 4.6 ART does not eliminate virally infected SPION+ macrophages in cranial nerves. SPION (green and blue) localized to SIV-RNA+ (red) and SIV-gp41+ (red) macrophages in cranial nerves and DRG. Image captured from scanned cranial nerve and DRG sections.

Table 4.2

	SIV-RNA				GP41			
		Early SPION+	Late SPION+	Dual SPION+		Early SPION+	Late SPION+	Dual SPION+
	SIV-RNA+/mm ²	SIV-RNA+/mm ²	SIV-RNA+/mm ²	SIV-RNA+/mm ²	GP41+/mm ²	GP41+/mm ²	GP41+/mm ²	GP41+/mm ²
SIVE	8.2 ± 7.3	0.6 ± 0.6	0.9 ± 1.2	1.6 ± 2.3	2.5 ± 3.7	0.04 ± 0.09	0.01 ± 0.02	0.0 ± 0.0
Total # of Cells Counted	311	27 ± 20	26	50	50	2	1	0
ART	0.15 ± 0.30	0.03 ± 0.06	0.02 ± 0.04	0.09 ± 0.18	0.23 ± 0.44	0.0 ± 0.0	0.0 ± 0.0	0.0 ± 0.0
Total # of Cells Counted	8	2	1	5	2	0	0	0
ARTOff	0.0 ± 0.0	0.0 ± 0.0	0.0 ± 0.0	0.0 ± 0.0	0.0 ± 0.0	0.0 ± 0.0	0.0 ± 0.0	0.0 ± 0.0
Total # of Cells Counted	0	0	0	0	0	0	0	0

	SPION+	
	SIV-RNA+/mm ²	SIV-RNA+/mm ²
SIVE	214 ± 53	0.03 ± 0.08
Total # of Cells Counted	112333	157
ART	0.1 ± 0.04	0.0 ± 0.0
Total # of Cells Counted	37	0
ARTOff	0.0 ± 0.0	0.0 ± 0.0
Total # of Cells Counted	0	0

Table 4.2 ART eliminates virally infected SPION+ macrophages within the DRG but not cranial nerves. (A) SIV-RNA+ and SIV-GP41+ SPION+ macrophages within cranial nerves of animals with AIDS and SIVE, on ART, and following ART cessation. (B) Number of SIV-RNA+ and SIV-GP41+ SPION+ macrophages within the DRG of animals with AIDS and SIVE, on ART, and following ART cessation. SIVE, SIV encephalitis; cLN, cervical lymph node; DRG, dorsal root ganglia. Early SPION were i.c. injected 12-14 days post-infection; Late SPION were i.c. injected 30 days prior to sacrifice; Dual SPION+ contains both early and late injected SPION. Whole tissue sections were analyzed to obtain the number of positive cells based on the detection of fluorescence. A minimum of 2 cortical CNS tissues were analyzed per animal, and an average of 3 sections were examined per animal, per tissue region. Counts are the means \pm SEM of the number of viral RNA+ cells or GP41+ and SPION+ macrophages with virus.

Figure 4.7

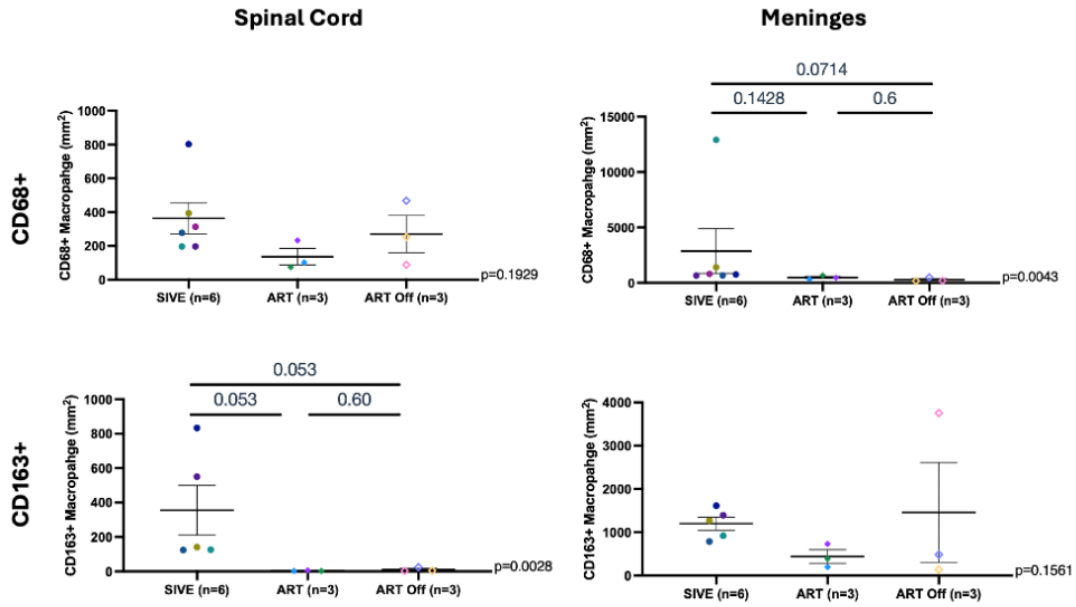


Figure 4.7 Macrophage accumulation in the spinal cord. (A) CD68+ macrophages and (B) CD163+ macrophages. Data are cell numbers (average \pm StDev) counted in whole tissue sections at 20x and expressed as the number of cells per mm². Each color represents a different animal analyzed. Prism was used for graphing and statistical analysis Kruskal-Wallis nonparametric test.

Figure 4.8

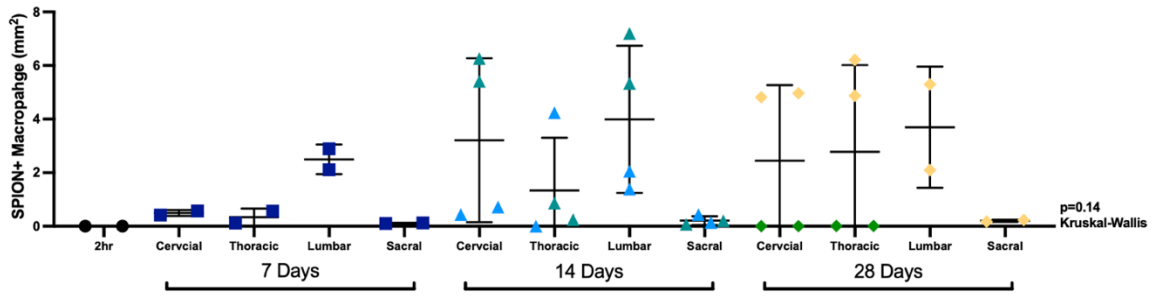


Figure 4.8 SPION+ Macrophage accumulation in each level of the DRG over time.

Data are cell numbers (average \pm StDev) counted in whole tissue sections at 20x and expressed as the number of cells per mm². Each color represents a different animal analyzed. Prism was used for graphing and statistical analysis Kruskal-Wallis nonparametric test.

Figure 4.9

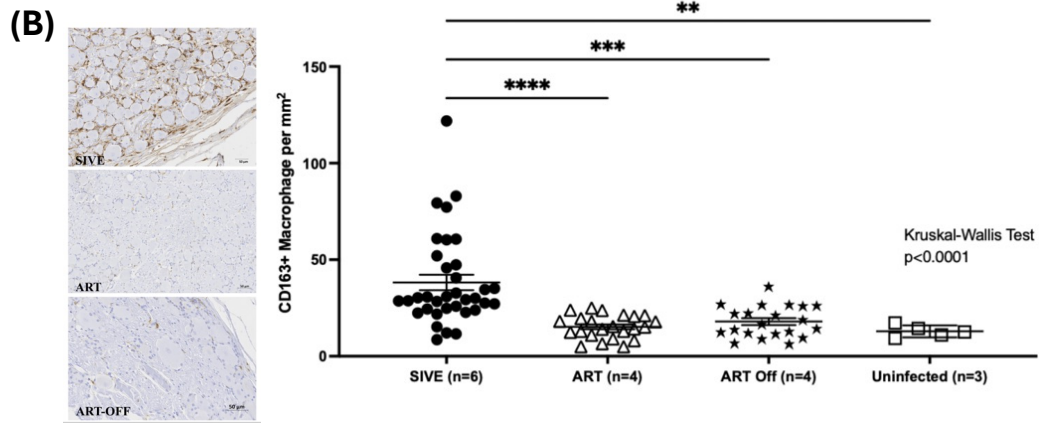
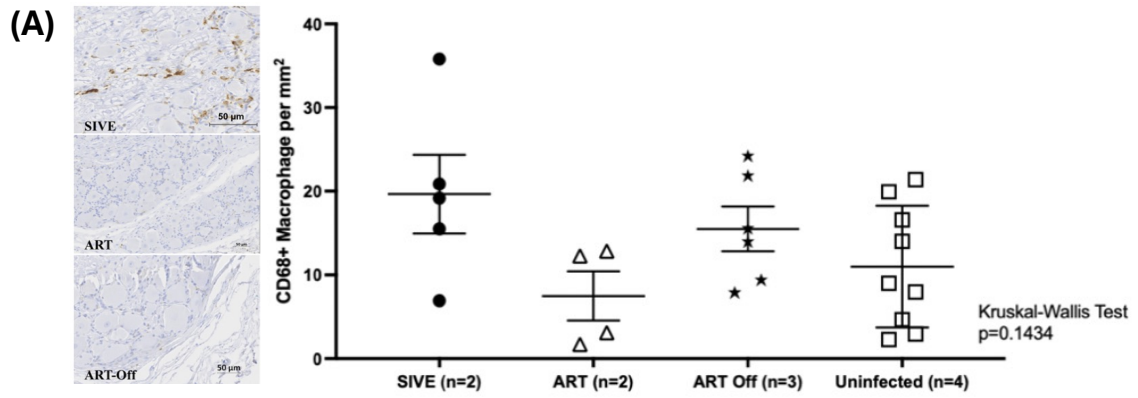


Figure 4.9 Macrophage accumulation in the DRG. (A) CD68+ macrophages and (B) CD163+ macrophages. Data are cell numbers (average \pm StDev) counted in whole tissue sections at 20x and expressed as the number of cells per mm². Prism was used for graphing and statistical analysis Kruskal-Wallis nonparametric test. A representative image for each cohort analyzed is shown on the left.

4.8 References

1. Williams, K.C., et al., *Perivascular Macrophages Are the Primary Cell Type Productively Infected by Simian Immunodeficiency Virus in the Brains of Macaques: Implications for the Neuropathogenesis of AIDS*. Journal of Experimental Medicine, 2001. **193**(8): p. 905-916.
2. Nowlin, B.T., et al., *SIV encephalitis lesions are composed of CD163(+) macrophages present in the central nervous system during early SIV infection and SIV-positive macrophages recruited terminally with AIDS*. Am J Pathol, 2015. **185**(6): p. 1649-65.
3. Fischer-Smith, T., et al., *Monocyte/macrophage trafficking in acquired immunodeficiency syndrome encephalitis: lessons from human and nonhuman primate studies*. J Neurovirol, 2008. **14**(4): p. 318-26.
4. de Vos, A.F., et al., *Transfer of central nervous system autoantigens and presentation in secondary lymphoid organs*. J Immunol, 2002. **169**(10): p. 5415-23.
5. Engelhardt, B., et al., *Vascular, glial, and lymphatic immune gateways of the central nervous system*. Acta Neuropathol, 2016. **132**(3): p. 317-38.
6. Laman, J.D. and R.O. Weller, *Drainage of cells and soluble antigen from the CNS to regional lymph nodes*. J Neuroimmune Pharmacol, 2013. **8**(4): p. 840-56.
7. van Zwam, M., et al., *Brain antigens in functionally distinct antigen-presenting cell populations in cervical lymph nodes in MS and EAE*. J Mol Med (Berl), 2009. **87**(3): p. 273-86.
8. Cserr, H.F., C.J. Harling-Berg, and P.M. Knopf, *Drainage of brain extracellular fluid into blood and deep cervical lymph and its immunological significance*. Brain Pathol, 1992. **2**(4): p. 269-76.
9. Cserr, H.F. and P.M. Knopf, *Cervical lymphatics, the blood-brain barrier and the immunoreactivity of the brain: a new view*. Immunol Today, 1992. **13**(12): p. 507-12.
10. Goldmann, J., et al., *T cells traffic from brain to cervical lymph nodes via the cribroid plate and the nasal mucosa*. J Leukoc Biol, 2006. **80**(4): p. 797-801.
11. Srinivas, M., P. Sharma, and S. Jhunjunwala, *Phagocytic Uptake of Polymeric Particles by Immune Cells under Flow Conditions*. Molecular Pharmaceutics, 2021. **18**(12): p. 4501-4510.

12. Tabata, Y. and Y. Ikada, *Effect of the size and surface charge of polymer microspheres on their phagocytosis by macrophage*. *Biomaterials*, 1988. **9**(4): p. 356-62.
13. Engelhardt, B., P. Vajkoczy, and R.O. Weller, *The movers and shapers in immune privilege of the CNS*. *Nat Immunol*, 2017. **18**(2): p. 123-131.
14. Louveau, A., T.H. Harris, and J. Kipnis, *Revisiting the Mechanisms of CNS Immune Privilege*. *Trends Immunol*, 2015. **36**(10): p. 569-577.
15. Haller, F.R. and F.N. Low, *The fine structure of the peripheral nerve root sheath in the subarachnoid space in the rat and other laboratory animals*. *Am J Anat*, 1971. **131**(1): p. 1-19.
16. Liu, Q., X. Wang, and S. Yi, *Pathophysiological Changes of Physical Barriers of Peripheral Nerves After Injury*. *Frontiers in Neuroscience*, 2018. **12**.
17. Shanthaveerappa, T.R. and G.H. Bourne, *The 'perineural epithelium', a metabolically active, continuous, protoplasmic cell barrier surrounding peripheral nerve fasciculi*. *J Anat*, 1962. **96**(Pt 4): p. 527-37.
18. Weerasuriya, A. and A.P. Mizisin, *The blood-nerve barrier: structure and functional significance*. *Methods Mol Biol*, 2011. **686**: p. 149-73.
19. Jacob, L., et al., *Anatomy and function of the vertebral column lymphatic network in mice*. *Nature Communications*, 2019. **10**(1): p. 4594.
20. Hu, P. and E.M. McLachlan, *Macrophage and lymphocyte invasion of dorsal root ganglia after peripheral nerve lesions in the rat*. *Neuroscience*, 2002. **112**(1): p. 23-38.
21. McCabe, J.S. and F.N. Low, *The subarachnoid angle: An area of transition in peripheral nerve*. *The Anatomical Record*, 1969. **164**(1): p. 15-33.
22. Haberberger, R.V., et al., *Human Dorsal Root Ganglia*. *Front Cell Neurosci*, 2019. **13**: p. 271.
23. Burdo, T.H., et al., *Dorsal root ganglia damage in SIV-infected rhesus macaques: an animal model of HIV-induced sensory neuropathy*. *Am J Pathol*, 2012. **180**(4): p. 1362-9.
24. Lakritz, J.R., et al., *An oral form of methylglyoxal-bis-guanylhydrazone reduces monocyte activation and traffic to the dorsal root ganglia in a primate model of HIV-peripheral neuropathy*. *J Neurovirol*, 2017. **23**(4): p. 568-576.
25. Warfield, R., et al., *Neuroinflammation in the Dorsal Root Ganglia and Dorsal Horn Contributes to Persistence of Nociceptor Sensitization in SIV-Infected*

- Antiretroviral Therapy-Treated Macaques*. The American Journal of Pathology, 2023. **193**(12): p. 2017-2030.
26. Johnston, M., et al., *Evidence of connections between cerebrospinal fluid and nasal lymphatic vessels in humans, non-human primates and other mammalian species*. Cerebrospinal Fluid Res, 2004. **1**(1): p. 2.
 27. Ma, Q., et al., *Clearance of cerebrospinal fluid from the sacral spine through lymphatic vessels*. Journal of Experimental Medicine, 2019. **216**(11): p. 2492-2502.
 28. Hatterer, E., et al., *How to drain without lymphatics? Dendritic cells migrate from the cerebrospinal fluid to the B-cell follicles of cervical lymph nodes*. Blood, 2006. **107**(2): p. 806-12.
 29. Hatterer, E., et al., *Cerebrospinal fluid dendritic cells infiltrate the brain parenchyma and target the cervical lymph nodes under neuroinflammatory conditions*. PLoS One, 2008. **3**(10): p. e3321.
 30. Karman, J., et al., *Initiation of immune responses in brain is promoted by local dendritic cells*. J Immunol, 2004. **173**(4): p. 2353-61.
 31. van Zwam, M., et al., *Surgical excision of CNS-draining lymph nodes reduces relapse severity in chronic-relapsing experimental autoimmune encephalomyelitis*. J Pathol, 2009. **217**(4): p. 543-51.
 32. Yu, X., et al., *Dorsal root ganglion macrophages contribute to both the initiation and persistence of neuropathic pain*. Nature Communications, 2020. **11**(1): p. 264.
 33. Burdo, T.H., et al., *Increased monocyte turnover from bone marrow correlates with severity of SIV encephalitis and CD163 levels in plasma*. PLoS Pathog, 2010. **6**(4): p. e1000842.
 34. Soulas, C., et al., *Recently infiltrating MAC387(+) monocytes/macrophages a third macrophage population involved in SIV and HIV encephalitic lesion formation*. Am J Pathol, 2011. **178**(5): p. 2121-35.
 35. White, K.S., et al., *Simian immunodeficiency virus-infected rhesus macaques with AIDS co-develop cardiovascular pathology and encephalitis*. Front Immunol, 2023. **14**: p. 1240946.
 36. Hansen, S.G., et al., *Profound early control of highly pathogenic SIV by an effector memory T-cell vaccine*. Nature, 2011. **473**(7348): p. 523-7.
 37. Hansen, S.G., et al., *Immune clearance of highly pathogenic SIV infection*. Nature, 2013. **502**(7469): p. 100-4.

38. Lifson, J.D., et al., *Role of CD8(+) lymphocytes in control of simian immunodeficiency virus infection and resistance to rechallenge after transient early antiretroviral treatment*. J Virol, 2001. **75**(21): p. 10187-99.
39. Bankhead, P., et al., *QuPath: Open source software for digital pathology image analysis*. Scientific Reports, 2017. **7**(1): p. 16878.

4.9 Chapter Overview and Next Steps

In this study, we explored a route by which SIV-infected macrophages contribute to viral persistence and reseeded of the CNS viral reservoir, a critical barrier to viral eradication. Using intracisternal injections of SPION in macaques with AIDS, with ART, and following ART interruption, we labeled and tracked CNS macrophages over time. Our results revealed a novel perineural pathway, where SIV-RNA+SPION+ macrophages traffic from the CNS to cranial and peripheral nerves, essentially bypassing the BBB. Importantly, ART significantly reduced but did not eliminate the traffic of these virus-infected macrophages to cranial nerves. Interestingly, while AIDS progression reduced late-stage macrophage traffic out of the CNS, ART restored it, and there was a reduction in traffic following ART interruption. These findings provide new insights into macrophage-mediated viral dissemination outside the CNS, even with ART. As our next step through a comprehensive literature review (Chapter 5), we investigated the effects of HIV on aging, particularly since age is a primary risk factor for HIV-SN.

5.0 Chapter 5

Monocytes in HIV, SIV Infection and Aging: Implications for Inflammaging and Accelerated Aging

Zoey K. Wallis¹

Kenneth C. Williams^{1*}

¹ Department of Biology, Boston College, Chestnut Hill, Massachusetts, 02467, USA.

* Correspondence: kenneth.williams.3@bc.edu

Viruses **2022**, *14*(2), 409; <https://doi.org/10.3390/v14020409>

Submission received: 17 December 2021 / Revised: 4 February 2022 / Accepted: 15 February 2022 / Published: 17 February 2022

Chapter 5 is reproduced with permission and licensed under CC BY 4.0

5.1 Author Contributions

Conceptualization, K.C.W., and Z.K.W.; writing—original draft preparation, K.C.W. and Z.K.W.; writing—review and editing, K.C.W. and Z.K.W.; funding acquisition, K.C.W. All authors have read and agreed to the published version of the manuscript.

5.2 Abstract

Before the antiretroviral therapy (ART) era, people living with HIV (PLWH) experienced complications due to AIDS more so than aging. With ART and the extended lifespan of PLWH, HIV co-morbidities also include aging—most likely due to accelerated aging—as well as cardiovascular, neurocognitive disorders, lung and kidney disease, and malignancies. The broad evidence suggests that HIV with ART is associated with accentuated aging, and that the age-related comorbidities occur earlier, due in part to chronic immune activation, co-infections, and possibly the effects of ART alone. Normally the immune system undergoes alterations of lymphocyte and monocyte populations with aging that include diminished naïve T and B lymphocyte numbers, a reliance on memory lymphocytes, and a skewed production of myeloid cells leading to age-related inflammation, termed “inflamm-aging”. Specifically, absolute numbers and relative proportions of monocytes and monocyte subpopulations are skewed with age along with myeloid mitochondrial dysfunction resulting in increased accumulation of reactive oxygen species (ROS). Additionally, an increase in biomarkers of myeloid activation (IL-6, sCD14, and sCD163) occurs with chronic HIV infection and with age and may contribute to immune-senescence. Chronic HIV infection accelerates aging where ART treatment may slow the age-related acceleration, but it is not sufficient to stop aging or age-related comorbidities. Overall, a better understanding of the mechanisms behind accentuated aging with HIV and the effects of myeloid activation and turnover is needed for future therapies.

Keywords: HIV/SIV; Aging; Monocytes; Macrophage; Inflammaging.

5.3 Introduction

Antiretroviral therapy (ART) has enabled people living with HIV (PLWH) to live longer yet a high risk of developing HIV- and age-associated comorbidities that are cumulative remains. In 2018, the Centers for Disease Control (CDC) reported that over half (51%) of people living with HIV in the United States were age 50 or older [1, 2]. This aging group of PLWH stems from a larger aging population with an estimated 12.5% increase in the number of people over the age of 65 in the next 20 years [1, 2]. Although not well understood, aging leads to alterations in the immune system and responses to HIV infection and co-infections. This review focuses on the biology of monocytes and macrophages with HIV and simian immunodeficiency virus (SIV) infection and HIV infection and aging.

Monocytes and macrophages are important components of the innate immune system that link innate immunity with acquired immunity. They are involved in the first line of defense against pathogens including retroviruses like HIV and SIV and their clearance, as well as toning of the immune response to balance tissue inflammation, tissue injury and repair. Monocytes are derived from the bone marrow (BM) as well as fetal liver, and spleen and can replace tissue macrophages under normal physiologic conditions, during inflammation, and with pathology [3, 4]. Within the central nervous system (CNS) there exist four-to-five macrophage populations normally, and the cardiovascular system and heart have several subpopulations, all of which change with aging, HIV, and disease [5, 6]. Resident macrophages can be replaced by recruitment of inflammatory monocytes from blood as well as repopulation within the organ [5, 6]. Resident tissue macrophage populations are yolk sack derived and present in tissues at the embryonic stage, and at

birth. BM derived-monocytes, monocyte-derived macrophages, and yolk-sack derived macrophages are diverse phenotypically and physiologically in different tissues [3, 4]. These cells are thought to be repopulated in normal physiology at a rate that is augmented with HIV and SIV infection, inflammatory responses, and aging. Monocyte and monocyte/macrophages as well as resident tissue macrophages are critical in immune responses to retroviruses - and by definition can be infected by them—but also play important roles amplifying and toning immune responses, mediating lesion resolution, wound healing and repair [7, 8]. With continued long-term immune stimulation by HIV and SIV in response to cell- and tissue- injury and death signals, and importantly aging, these cells contribute to chronic immune activation termed “inflammaging” seen with aging and HIV [9-12]. This review focuses on the biology of monocytes—and sometimes macrophages—with HIV infection and aging and how these somewhat contradictory responses are not well understood but likely critical in aging populations with HIV and AIDS. Many of the studies described in this review are from the results of SIV infection of rhesus macaques. SIV is the premier model of HIV infection because of the genetic similarity of the virus, SIV’s defined tropism for myeloid, dendritic and lymphocytes, and the similarities on pathogenesis of SIV-infected monkeys with AIDS in lymph nodes, blood, and tissues including the CNS and cardiovascular system [5, 13, 14]. It is interesting to note that SIV has the accessory gene Vpx in place of Vpr in HIV which can result in a higher level of monocyte and macrophage infection [15]. SIV has similar stages of plasma viral expansion in plasma and tissues, and a latent period of infection. Importantly, antiretroviral agents used in HIV-infected humans are used in SIV-infected monkeys where ART leads to non-detectable plasma and tissue virus. Some of the

pioneering work on monocyte and macrophage infection, and their role in viral traffic, and CNS and cardiac pathology, came from studies in SIV-infected monkeys [13, 14, 16-18].

5.4 Monocytes and Macrophages in HIV and SIV

With normal physiology in humans and non-human primates, monocytes comprise 2-10% of total white blood cells (WBC) in blood. They are continually produced by BM hematopoiesis by hematopoietic stem cells (HSC) [19, 20]. The kinetics in blood of the different monocyte populations are distinct [21-24] where the rate of production and turnover are increased with HIV and SIV infection, aging, and HIV and aging [13, 19, 23, 25-28]. He, *et al.* found the production and differentiation of HSCs and monocytes was increased, but the circulating half-life was decreased with age [19]. Although the production of monocytes is increased with age which would seem to imply increased numbers of monocytes in the blood, a decrease in half-life of monocytes results in the total percentage of monocytes in the blood not changing. In addition to the skewed output of monocytes in blood, differentiation of HSCs is altered in BM. With aging, HSCs exhibit an intrinsic myeloid bias thought to result in part due to increased IL-6 production [29, 30].

Historically, monocytes were described by Ehrlich and Metchnikoff [24, 31, 32] where they were originally considered to be two populations based on CD14 and CD16 expression [24]. Currently in humans and non-human primates there are thought to exist three populations that include classical (CD14⁺CD16⁻), non-classical (CD14^{dim/lo}CD16⁺), and intermediate (CD14⁺CD16⁺) monocytes [33-35]. In general, it is considered that classical monocytes in humans—and their equivalents in mice—differentiate and may give rise to some tissue macrophages and dendritic cells (DC) where they are involved in inflammation and repair [32, 34, 36, 37]. Early studies using ³H-Thymidine

demonstrated classical monocytes gave rise primarily to intermediate and non-classical monocytes [38]. We performed similar studies in normal and SIV infected rhesus macaques using bromo-deoxyuridine (BrdU), a thymidine analogue taken-up by myeloid precursor cells that can be detected in classical monocytes within 24 hours, followed by intermediate monocytes (24 hours later), and then non-classical monocytes (found 24 hours later) [13, 26]. These observations are similar to ³H-Thymidine studies in humans that also suggest intermediate and non-classical cells are a continuum of cells originating from classical monocytes that have undergone maturation and/or activation in blood [13, 26, 39]. Using BrdU uptake by monocytes it was found that the magnitude of monocyte expansion in blood and output from BM are good indicators (better than plasma virus and CD4+ T cell nadir) of the rate of AIDS development and the severity of tissue pathogenesis in SIV infected monkeys [13, 19, 26]. Moreover, Kuroda *et al.* found an age-dependent increase in the turnover of monocytes (discussed below). While the continuum of monocytes from classical to non-classical cells in blood is an attractive model, it likely is not absolute, where subsets may also arise from other non-BM compartments including spleen [40]. Overall, the intermediate monocytes are thought to be an activated, more mature phenotype with potential antigen presentation (APC) functions that are susceptible to HIV and more-so SIV infection [34, 37, 41-45]. The percentage of intermediate monocytes increases with HIV and SIV infection and in fact correlates with the incidence of AIDS dementia complex (ADC)(pre ART) [46] and CVD with HIV and SIV infection [5, 14, 47]. Non-classical monocytes are thought to function as patrolling cells that interact with parenchymal tissue endothelium including those involved with viral responses [32]. Changes in the proportion and absolute numbers of

monocyte subsets are seen in HIV and SIV infection, HIV and SIV infection with aging (discussed below). Differences are also observed in the proportion of monocyte subsets between sexes with aging and HIV infection [32, 48-50]. Overall, this general model helps when considering immune phenotype of these cells in normal conditions, and with HIV and SIV infection, with HIV and SIV infection, and aging: it is clear there is a skew towards intermediate monocytes with both, as well as altered monocyte turnover in the blood. Lastly, while the exact signal(s) for monocyte production in BM are not defined, they are likely in part driven by monocyte/macrophage turnover and death in tissues, their response to monokines and trafficking chemokines, HIV and SIV viral antigens, and immune activating factors in plasma, many of which are increased with aging.

It has been shown that the magnitude of BrdU+ monocytes in blood 24 hours after BrdU pulse, correlates with the rate of development of AIDS in SIV infected monkeys where a greater magnitude of BrdU+ labeled monocytes correlated with increased histopathogenesis [13]. Interestingly animals with 10% or greater BrdU+ monocytes, detected as early as 21 days pi, are predicted to develop rapid AIDS [13, 51]. And, the higher the percentage of BrdU+ monocytes correlates with how rapidly animals succumb to AIDS and the severity of brain and cardiac pathology [13]. Additionally, sCD163—a biomarker for myeloid activation—in these monkeys positively correlated with the number of BrdU+ monocytes in a near linear fashion [13]. Soluble CD163 in HIV infected individuals correlated with the degree of neurologic dysfunction and non-calcified vulnerable plaque [17, 52-54] suggesting the degree of monocyte activation and expansion from bone marrow were good biomarkers of HIV and SIV comorbidities. It has been subsequently determined that sCD163 and another marker of activated

monocytes, sCD14, are associated with HIV all cause morbidity and mortality [55, 56]. While the exact signals for this expansion of monocytes and increased sCD163 are not defined, Kuroda *et al.* has shown that macrophage death and turnover in tissues are highly correlated [26]. It is interesting to note these markers are also increased with aging, and aging with HIV. We recently found studying ART interruption, the percentage of BrdU+ monocytes also goes up and down with plasma virus in SIV infected macaques, suggesting plasma virus also plays a role (Williams et al., unpublished data). Additionally, it is reasonable to postulate that monocyte activation and turnover occurs as these cells compensate for loss of the acquired immune response caused by CD4 T memory destruction in early HIV and SIV infection, and perhaps aging [5]. Using math modeling algorithms, Kuroda *et al.* showed that the expansion of monocyte production with SIV infection (based on BrdU) likely occurs with aging [57]. Again, while the signal for such production, in addition to replacing injured and dying macrophages in tissues, are not well defined, they likely also include dying signals in tissues and tissue microenvironments, both of which are likely increased with aging.

5.5 Chronic Monocyte/Macrophage Activation, Inflammation, and "Inflamm-aging"

Numerous groups have found that monocytes isolated from aged individuals have reduced activation, proliferation, or altered signaling and delayed responses that result in increased cytokine production compared to young controls, which is further discussed below [58, 59]. Additionally, at the transcriptomic level, there is an impact of aging on interferon signaling from all monocyte subsets following TLR stimulation [60, 61]. Alterations in monocyte activation and cytokine production with aging and HIV infection results from dysregulation of HSCs production and differentiation leading to chronic inflammation and older immunophenotypes, respectively [48, 62]. Similar changes were found when comparing ART women with HIV versus viremic individuals where the latter were similar to controls who were 12 years older [48]. While overall it is tempting to think ART may reverse immune activation and innate immune responses by decreasing plasma and tissue virus, how long individuals have been on ART and when ART was initiated post infection is an important consideration. We studied the effect of durable ART on plasma sCD163 of individuals with acute infection (ART treatment less than one year of HIV infection) and chronic infection (ART treatment after more than one year of HIV infection) and found plasma sCD163 levels decreased after 3 months to levels found in uninfected controls [52]. This was in contrast to individuals who received ART after more than a year of HIV infection, where after 3 months of ART, sCD163 decreased but not to levels found in acute infection and non-infected controls [52]. It is tempting to speculate these differential responses are informative with regard to the preprogrammed

genetics of the innate immune response to HIV, but also they are as likely linked to the acquired immune response that include antibodies, CD4⁺ T cell depletion by HIV, as well as CD8⁺ T cell responses and HIV-repertoire breadth, all of which importantly are affected by HIV infection and aging [11]. Lastly, it is also important to consider the effects of ART alone, aside from the effects of decreasing plasma and tissue virus, that might also result in premature or accelerated aging, which further complicates the picture [63-66].

Signaling molecules including TLRs, mannose receptors, and scavenging receptors are altered with aging and may contribute to changes in immune populations. Changes in monocyte/macrophage immune phenotype with HIV and SIV infection and accelerated aging are likely also due to increased soluble factors in plasma as well as the effects of translocation of bacteria across the gut, and metabolic effects of this, and co-infections including CMV with aging [67-69]. Additionally, the role of monocyte responses to surface receptor ligation including TLRs to LPS, endocarb and viral antigens should be considered. Recent studies showed changes in the cytokine production of monocytes isolated from aged individuals where following stimulation there was an increase in TNF, IL-1 and IL-6 that are associated with non-AIDS defined comorbidities with PLWHIV [70]. Monocytes isolated from aged individuals have increased cytokine production including IL-6, TNF-alpha, IL-1 alpha and beta that drive alterations in circulating monocyte populations [71-74]. Hearps and colleagues found that plasma cytokines specific to monocyte activation—sCD163 and sCD14—are increased with age [49]. Additionally, wide-spread alterations in expression and function of toll like receptors are impaired with age and contribute to the dysregulation of innate immunity—specifically

production of myeloid cells [75]. It is unknown and more research is necessary to determine whether aging is the cause of alterations in signaling molecules thus resulting in downstream effects on myeloid populations; or, if inherent skewing of HSCs towards a myeloid shift result in changes of myeloid signaling molecules and alterations to myeloid phenotype, or both.

Changes in the proportion of monocyte subsets, their response to immune stimulation by cell surface receptor ligation, and function are reported in PLWHIV and SIV-infected monkeys, but overall, extensive studies have not been done. Hearps and colleagues in a study of HIV infection versus healthy aging, focused on immune phenotype and function in a cross-sectional study, and showed that young viremic HIV+ males had monocyte phenotypes similar to aged controls that include increased CD11b on CD14+CD16+ monocytes and down regulation of CD62L and CD115 [49]. Additionally, they found innate immune markers sCD163 and CXCL10 increased in both young viremic and virologically suppressed individuals to levels similar to that seen in elderly controls. They also found decreased phagocytic function and telomere shortening compared to young controls [49]. Overall, there are similarities in men versus women in age associated changes with increased proportions of intermediate and classical monocytes, but found women were phenotypically different than men [50].

5.6 Monocytes and Macrophage Traffic to Tissues with HIV, SIV, and Aging

Monocytes are produced in the bone marrow in response to colony stimulating factors (CSF) and cytokines and migrate towards specific sites of infection or injury.

Extravasation of monocytes and subsequent differentiation into macrophages is beneficial in normal physiology to assist in clearing infections and promoting tissue repair.

However, chronic accumulation of macrophages leads to inflammation and subsequent tissue damage. “Age-associated inflammation” is thought to be induced by increased inflammatory activated monocytes, IL-6 and higher CCR2 production, which could lead to excess monocyte production and macrophage accumulation [73]. With age, there are increased plasma concentrations of inflammatory mediators (IL-6, IL-10, sICAM-1, sVCAM-1, and MCP-1) that promote monocyte extravasation and subsequent tissue inflammation [76]. Additionally, studies have focused on monocyte and macrophage cytokine dysregulation and NF- κ B pathway activation (discussed below) as drivers of inflammation [77-79] in the context of HIV and SIV, and HIV and SIV and aging.

The NF- κ B pathway is a key mediator of cellular damage and stress response and is impaired with age [79]. A murine bone marrow study identified the largest fraction of cells with increased NF- κ B expression as myeloid cells [80]. Activation of the NF- κ B pathway in macrophages leads to production of proinflammatory cytokines IL-6 and TNF- α . An analysis of monocytes from hospitalized individuals (elderly vs young) showed higher NF- κ B activation but reduced responses to TLR stimulation in elderly populations versus younger controls [79]. Importantly, these studies found that with age continued stimulation of the NF- κ B pathway may lead to immune tolerance and reduced

response to subsequent stimuli. There are multiple stimulatory ligands and factors that signal through the NF- κ B pathway including TLRs via viral ligands, ROS stimulation, and more recently identified miRNA. Grants, *et al.*, attributes one driver of age-related inflammation and myeloid skewing as the loss of miRNA-146a resulting in upregulation of the NF- κ B pathway followed by upregulation of IL-6; yet more research is necessary to determine other contributors to age-related inflammation with chronic HIV infection [77].

5.7 Immunosenescence and Aging

Immunosenescence is the gradual decline of the functionality of the immune system commonly seen in conditions of chronic immune stimulation including HIV-1 infection, and HIV-1 infection and aging, and aging alone [70, 81]. Aging is thought to impair the ability of monocytes and macrophages to clear senescence cells due to reduced phagocytosis, chemotaxis, and accumulation of age-related inflammation. With aging, there is an increase in the expression of markers of senescence including P16^{INK4a}, IL-1 β , and NF-kB [82, 83]. Additionally, adults with HIV+ had increased biomarkers of immune-senescence including TNF-alpha, IL-6, sCD163 and sCD14. The proinflammatory nature of nonclassical monocytes alone—including higher P16^{INK4a}, NK-kB activity, and IL-1 alpha production—are considered markers of cellular senescence [82, 84]. P16^{INK4a} expression is a marker of cellular senescence and is expressed by macrophages from response to external stimuli [84]. Myeloid derived suppressor cells (MDSCs) are thought to be immunosuppressors that act primarily on T and B cells to drive a senescence phenotype. MDSCs are significantly increased with aging and may be potent influencers of immunosenescence, however they are not well understood and their role in aging and disease is unclear [81]. Studies have found that the elimination of senescent cells can extend lifespan by inhibiting pathways of inflammation and senescence [85]; yet, the exact role of myeloid cells in this or the effects of aging and immunosenescence in people living with HIV is not well understood.

5.8 Myeloid Mitochondria Dysfunction and Contribution to Immunosenescence

Dysfunction of macrophage mitochondria with aging can increase oxidative stress, susceptibility to DNA damage and viral infections. This in turn promotes a senescence, proinflammatory microenvironment. Bauer and Fuente describe how aging of macrophage mitochondria leads to dysfunction and expression of proinflammatory cytokines (IL-6, TNF-alpha, and IL-1) resulting in increased inflammation and an overall decline in physiological functions [86]. Specifically, with aging, there is higher production of reactive oxygen species (ROS) from macrophages, mitochondrial dysfunction, increased tissue inflammation, and mutagen susceptibility [87]. Causes of mitochondrial dysfunction with aging are unknown; but believed to be associated with reduced mitochondrial respiratory capacity of myeloid cells [88]. Dysfunction of mitochondrial respiratory chain complexes in macrophages can result in mitochondrial membrane potential changes, which in turn can be used as a determinant of the contribution of a myeloid bias with aging [89]. In addition, there is increasing evidence of mitochondrial dysfunction in PLWHIV [90-92]. This includes treatment for HIV where there are potential adverse effects of nucleoside reverse transcriptase inhibitors (NRTIs) that have been found to induce the accumulation of mutations in mitochondrial DNA (mtDNA) [92]. Alterations to mtDNA can result in changed mitochondrial morphology, energy, and ROS production [91]. Thus, age-related associations in reduced monocyte/macrophage mitochondrial function, the potential effect of HIV treatment on mitochondrial function, and increased oxidative stress with aging and aging with HIV, may be a main contributor to an increased inflammation [93].

Myeloid cells can release ROS in circulation which might be amplified by the inherent HSCs myeloid shift with aging; however, their exact contribution with HIV and HIV and aging is not fully understood [94]. Transmission electron microscopy revealed age-associated changes in the overall number and density of mitochondria in macrophages of aged mice compared to young controls [95]. Additionally, macrophages use tryptophan to generate NAD⁺ de novo through the Kynurenine Pathway (KP). The loss of KP metabolites results in reduced production of NAD⁺ and disrupts macrophage mitochondrial respiration leading to alterations in morphology and phagocytosis [96]. Overall, age-related and HIV and aged related changes in HSCs could affect the number of mitochondria in monocytes/macrophage, mitochondrial function, and regulation of ROS production [29, 97]. Multiple mechanisms link oxidative stress and aging including mitochondrial dysfunction, microRNA dysregulation, and cellular senescence.

5.9 Accelerated Aging with HIV Infection

Chronic immune stimulation caused by HIV-1 infection results in heightened production of pro-inflammatory mediators and likely contributes to accelerated aging [48, 70].

Hearps, *et al.* and others have found that individuals with HIV-1 have similar myeloid immune profiles as elderly individuals with increased CD16⁺ monocyte and activation markers comparable to controls that were 10-14 years older [50]. Specifically, they found elevated CD16⁺ monocytes, sCD163, sCD14, and CXCL10 [48, 50]. Analyzing CD14⁺ monocytes from young HIV⁺ individuals, Hearps *et al.* found impaired phagocytic function consistent with aged CD14⁺ monocytes [50]. In all, HIV infection may contribute to premature and accelerated aging of the immune system likely due to chronic stimulation.

More recently, researchers investigating epigenetic patterns in DNA found increased age-associated methylation in PLWH that is consistent with premature aging [11, 98, 99]. DNA methylation in PLWHIV revealed an accelerated methylation pattern by approximately 14 years [98]. Individuals living with HIV-1 who had over four years of ART treatment did not have significant epigenetic age-related alterations, yet there were still patterns of increased age-associated methylation [100, 101]. HIV-1 infection may accelerate aging where ART treatment may slow the age acceleration but does not stop it. Thus, while ART treatment extends life expectancy of PLWH there remains an increase of age-associated comorbidities like HAND and cardiovascular disease due to overall dysregulation of systemic inflammation.

In a study comparing the mean telomere length of HSCs and monocytes from healthy controls (26 years old) and elderly (65 years old), the telomeres in elderly HSCs and monocytes were significantly shorter than the younger controls [102]. Likewise, individuals with HIV-1 have significantly shorter telomeres in HSCs, monocytes (CD14+), and leukocytes than in noninfected aged-matched controls [50, 103, 104]. Additionally, researchers found an inverse relationship between myeloid activation (sCD163) and telomere length indicating that immune activation may be the cause of telomere shortening [104]. Premature aging is present with apparent telomere shortening even in young individuals with HIV and a study investigating children with HIV-1 (and treated with ART) revealed multiple age-associated alterations including higher percentages of activated cells (CD16+ monocytes), accelerated telomere shortening in HSCs, and higher percentages of senescent cells [103, 105]. Although still not well understood, studies on telomere length show that constant immune stimulation caused by HIV-1 infection may lead to accelerated aging. It is also possible that lack or dysfunction of normal DNA repair within the BM in HSC may also contribute to telomere shortening.

5.10 Conclusion

Changes in the activation, proportion, migration, and phenotype of monocyte subsets are apparent with aging and results in alterations of systemic immune physiology. Similarly, HIV and SIV viral RNA, even if not infectious, contribute to myeloid stimulation and activation. Due to immune senescence and loss of the acquired immune responses to HIV and SIV, as well as other co-infections including CMV, likely require an expanded role of myeloid cells in blood and tissues to aid in pathogen patrol, controlling tissue injury, and repair. It is known with aging augmented hematopoietic production of BM HSC occurs that skews toward increased monocytes and likely preferential phenotypes seen with HIV and SIV and aging, as well as altered functional effects of stimulation of monocytes following ligation of immune molecules including TLR's and phagocytosis. This is including increased monocyte activation, increased inflammatory cytokines and markers of senescence, reduced monocyte/macrophage mitochondrial function, and increased oxidative stress all of which are contributors to chronic inflammation.

5.11 Figure and Figure Legend

Figure 5.1

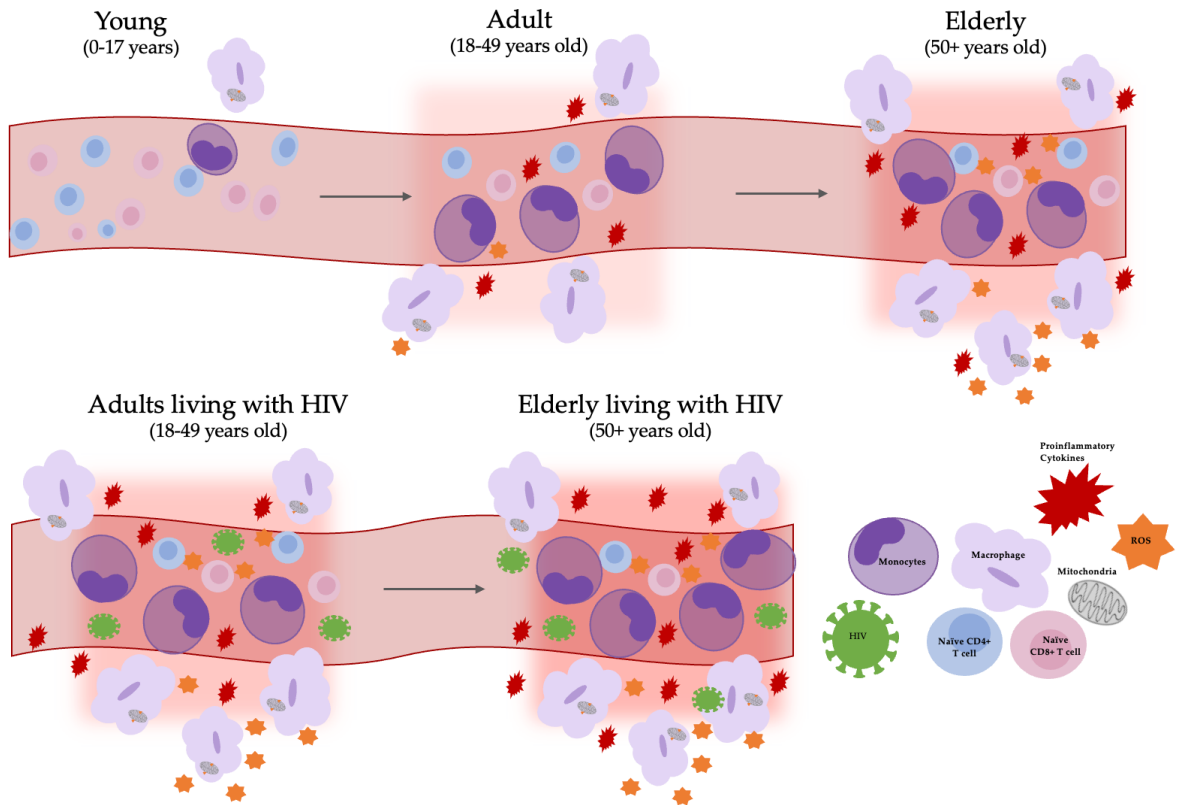


Figure 5.1 Altered myeloid production with aging and HIV infection contributes to chronic inflammation. Aging monocyte populations are skewed towards a proinflammatory phenotype and there is an overall decline in naïve CD4+ and CD8+ lymphocyte production [63,69,72,80]. Additionally, HIV/SIV infection causes an increase in the rate of production and turnover of myeloid cells [19, 28]. Age-induced mitochondrial dysfunction increases reactive oxygen species (ROS) which also contributes to tissue inflammation [84-87]. Elderly adults and adults living with HIV both have persistent inflammation caused by myeloid cells in response to chronic immune activation. Figure reproduced with permission from [Monocytes in HIV and SIV Infection and Aging: Implications for Inflamm-Aging and Accelerated Aging](#) by [Wallis, Z.](#) and [Williams, K.](#) (2022) MDPI. Viruses. 14(2):409 and is licensed under [CC BY 4.0](#).

5.12 References

1. CDC. *Diagnoses of HIV infection in the United States and dependent areas, 2018 (updated)*. HIV Surveillance Report 2020;31 2020 [cited 2021; Available from: <https://www.cdc.gov/hiv/group/age/olderamericans/index.html>].
2. CDC. *Estimated HIV incidence and prevalence in the United States, 2014–2018* HIV Surveillance Supplemental Report 2020;25 2020 [cited 2021; Available from: <https://www.cdc.gov/hiv/pdf/library/reports/surveillance/cdc-hiv-surveillance-supplemental-report-vol-25-1.pdf>].
3. Hoeffel, G. and F. Ginhoux, *Fetal monocytes and the origins of tissue-resident macrophages*. Cell Immunol, 2018. **330**: p. 5-15.
4. Hoeffel, G. and F. Ginhoux, *Ontogeny of Tissue-Resident Macrophages*. Front Immunol, 2015. **6**: p. 486.
5. Williams, K.C. and W.F. Hickey, *Central nervous system damage, monocytes and macrophages, and neurological disorders in AIDS*. Annu Rev Neurosci, 2002. **25**: p. 537-62.
6. Williams, K.C. and W.F. Hickey, *Traffic of hematogenous cells through the central nervous system*. Curr Top Microbiol Immunol, 1995. **202**: p. 221-45.
7. Clayton, K.L., et al., *HIV Infection of Macrophages: Implications for Pathogenesis and Cure*. Pathog Immun, 2017. **2**(2): p. 179-192.
8. Koppensteiner, H., R. Brack-Werner, and M. Schindler, *Macrophages and their relevance in Human Immunodeficiency Virus Type I infection*. Retrovirology, 2012. **9**: p. 82.
9. Oishi, Y. and I. Manabe, *Macrophages in age-related chronic inflammatory diseases*. NPJ Aging Mech Dis, 2016. **2**: p. 16018.
10. Fulop, T., et al., *Immunosenescence and Inflamm-Aging As Two Sides of the Same Coin: Friends or Foes?* Front Immunol, 2017. **8**: p. 1960.
11. Gabuzda, D., et al., *Pathogenesis of Aging and Age-related Comorbidities in People with HIV: Highlights from the HIV ACTION Workshop*. Pathog Immun, 2020. **5**(1): p. 143-174.
12. Mejias, N.H., et al., *Contribution of the inflammasome to inflammaging*. J Inflamm (Lond), 2018. **15**: p. 23.
13. Burdo, T.H., et al., *Increased monocyte turnover from bone marrow correlates with severity of SIV encephalitis and CD163 levels in plasma*. PLoS Pathog, 2010. **6**(4): p. e1000842.

14. Campbell, J.H., et al., *The importance of monocytes and macrophages in HIV pathogenesis, treatment, and cure*. AIDS, 2014. **28**(15): p. 2175-87.
15. Westmoreland, S.V., et al., *SIV vpx is essential for macrophage infection but not for development of AIDS*. PLoS One, 2014. **9**(1): p. e84463.
16. Hickey, W., et al., *Mononuclear phagocyte heterogeneity and the blood-brain barrier: a model for HIV-1 neuropathogenesis*. 1998, New York, NY, Chapman and Hall. p. 61-72.
17. Burdo, T.H., et al., *Elevated sCD163 in plasma but not cerebrospinal fluid is a marker of neurocognitive impairment in HIV infection*. AIDS, 2013. **27**(9): p. 1387-95.
18. Williams, K., A. Lackner, and J. Mallard, *Non-human primate models of SIV infection and CNS neuropathology*. Curr Opin Virol, 2016. **19**: p. 92-8.
19. He, Z., et al., *Rapid Turnover and High Production Rate of Myeloid Cells in Adult Rhesus Macaques with Compensations during Aging*. J Immunol, 2018. **200**(12): p. 4059-4067.
20. van Furth, R., J.A. Raeburn, and T.L. van Zwet, *Characteristics of human mononuclear phagocytes*. Blood, 1979. **54**(2): p. 485-500.
21. Ziegler-Heitbrock, L., *Monocyte subsets in man and other species*. Cell Immunol, 2014. **289**(1-2): p. 135-9.
22. Frankenberger, M., et al., *A defect of CD16-positive monocytes can occur without disease*. Immunobiology, 2013. **218**(2): p. 169-74.
23. Ziegler-Heitbrock, L., *Blood Monocytes and Their Subsets: Established Features and Open Questions*. Front Immunol, 2015. **6**: p. 423.
24. Ziegler-Heitbrock, L., et al., *Nomenclature of monocytes and dendritic cells in blood*. Blood, 2010. **116**(16): p. e74-80.
25. Crowe, S.M. and L. Ziegler-Heitbrock, *Editorial: Monocyte subpopulations and lentiviral infection*. J Leukoc Biol, 2010. **87**(4): p. 541-3.
26. Hasegawa, A., et al., *The level of monocyte turnover predicts disease progression in the macaque model of AIDS*. Blood, 2009. **114**(14): p. 2917-25.
27. Ziegler-Heitbrock, L. and T.P. Hofer, *Toward a refined definition of monocyte subsets*. Front Immunol, 2013. **4**: p. 23.
28. Dutertre, C.A., et al., *Pivotal role of M-DC8⁺ monocytes from viremic HIV-infected patients in TNF α overproduction in response to microbial products*. Blood, 2012. **120**(11): p. 2259-68.

29. Ho, Y.H., et al., *Remodeling of Bone Marrow Hematopoietic Stem Cell Niches Promotes Myeloid Cell Expansion during Premature or Physiological Aging*. Cell Stem Cell, 2019. **25**(3): p. 407-418 e6.
30. Mann, M., et al., *Heterogeneous Responses of Hematopoietic Stem Cells to Inflammatory Stimuli Are Altered with Age*. Cell Rep, 2018. **25**(11): p. 2992-3005 e5.
31. Geissmann, F., S. Jung, and D.R. Littman, *Blood monocytes consist of two principal subsets with distinct migratory properties*. Immunity, 2003. **19**(1): p. 71-82.
32. Kapellos, T.S., et al., *Human Monocyte Subsets and Phenotypes in Major Chronic Inflammatory Diseases*. Front Immunol, 2019. **10**: p. 2035.
33. Kim, W.K., et al., *Monocyte/macrophage traffic in HIV and SIV encephalitis*. J Leukoc Biol, 2003.
34. Kim, W.K., et al., *Monocyte heterogeneity underlying phenotypic changes in monocytes according to SIV disease stage*. J Leukoc Biol, 2010. **87**(4): p. 557-67.
35. Thieblemont, N., et al., *CD14^{low} CD16^{high}: a cytokine-producing monocyte subset which expands during human immunodeficiency virus infection*. Eur J Immunol, 1995. **25**: p. 3418-3424.
36. Weber, C., et al., *Differential chemokine receptor expression and function in human monocyte subpopulations*. J Leukoc Biol, 2000. **67**(5): p. 699-704.
37. Wong, K.L., et al., *Gene expression profiling reveals the defining features of the classical, intermediate, and nonclassical human monocyte subsets*. Blood, 2011. **118**(5): p. e16-31.
38. Patel, A.A., et al., *The fate and lifespan of human monocyte subsets in steady state and systemic inflammation*. J Exp Med, 2017. **214**(7): p. 1913-1923.
39. Nowlin, B., et al., *Monocyte subsets exhibit transcriptional plasticity and a shared response to interferon in SIV-infected rhesus macaques*. The Journal of Leukocyte Biology, 2017. **In Press**.
40. Honold, L. and M. Nahrendorf, *Resident and Monocyte-Derived Macrophages in Cardiovascular Disease*. Circ Res, 2018. **122**(1): p. 113-127.
41. Zawada, A.M., et al., *SuperSAGE evidence for CD14⁺⁺CD16⁺ monocytes as a third monocyte subset*. Blood, 2011. **118**(12): p. e50-61.
42. Zeigler-Heitbrock, H.W.L., M. Strobel, and D. Kieper, *The novel subset of CD14⁺/CD16⁺ blood monocytes exhibits features of tissue macrophages*. Eur J Immunol, 1993. **23**: p. 2053-58.

43. Ellery, P.J., et al., *The CD16+ monocyte subset is more permissive to infection and preferentially harbors HIV-1 in vivo*. J Immunol, 2007. **178**(10): p. 6581-9.
44. Lee, J., et al., *The MHC class II antigen presentation pathway in human monocytes differs by subset and is regulated by cytokines*. PLoS One, 2017. **12**(8): p. e0183594.
45. Zawada, A.M., et al., *SuperSAGE evidence for CD14++CD16+ monocytes as a third monocyte subset*. Blood, 2011. **118**(12): p. e50-e61.
46. Pulliam, L., et al., *Unique monocyte subset in patients with AIDS dementia*. Lancet, 1997. **349**(9053): p. 692-5.
47. Burdo, T., A. Lackner, and K. Williams, *Monocyte/macrophages and their role in HIV neuropathogenesis*. Immunol Rev, 2014. **254**(1): p. 102-13.
48. Angelovich, T.A., et al., *Viremic and Virologically Suppressed HIV Infection Increases Age-Related Changes to Monocyte Activation Equivalent to 12 and 4 Years of Aging, Respectively*. J Acquir Immune Defic Syndr, 2015. **69**(1): p. 11-7.
49. Hearps, A.C., et al., *HIV infection induces age-related changes to monocytes and innate immune activation in young men that persist despite combination antiretroviral therapy*. AIDS, 2012. **26**(7): p. 843-53.
50. Hearps, A.C., et al., *Aging is associated with chronic innate immune activation and dysregulation of monocyte phenotype and function*. Aging Cell, 2012. **11**(5): p. 867-75.
51. Burdo, T.H., A. Lackner, and K.C. Williams, *Monocyte/macrophages and their role in HIV neuropathogenesis*. Immunol Rev, 2013. **254**(1): p. 102-13.
52. Burdo, T.H., et al., *Soluble CD163 made by monocyte/macrophages is a novel marker of HIV activity in early and chronic infection prior to and after anti-retroviral therapy*. J Infect Dis, 2011. **204**(1): p. 154-63.
53. Burdo, T.H., et al., *Soluble CD163, a novel marker of activated macrophages, is elevated and associated with noncalcified coronary plaque in HIV-infected patients*. J Infect Dis, 2011. **204**(8): p. 1227-36.
54. Subramanian, S., et al., *Arterial inflammation in patients with HIV*. Jama, 2012. **308**(4): p. 379-86.
55. Knudsen, T.B., et al., *Plasma Soluble CD163 Level Independently Predicts All-Cause Mortality in HIV-1-Infected Individuals*. J Infect Dis, 2016. **214**(8): p. 1198-204.
56. Sandler, N.G., et al., *Plasma levels of soluble CD14 independently predict mortality in HIV infection*. J Infect Dis, 2011. **203**(6): p. 780-90.

57. Takahashi, N., et al., *Comparison of predictors for terminal disease progression in simian immunodeficiency virus/simian-HIV-infected rhesus macaques*. *Aids*, 2021. **35**(7): p. 1021-1029.
58. Aiello, A., et al., *Immunosenescence and Its Hallmarks: How to Oppose Aging Strategically? A Review of Potential Options for Therapeutic Intervention*. *Front Immunol*, 2019. **10**: p. 2247.
59. Chambers, E.S., et al., *Recruitment of inflammatory monocytes by senescent fibroblasts inhibits antigen-specific tissue immunity during human aging*. *Nature Aging*, 2021. **1**(1): p. 101-113.
60. Metcalf, T.U., et al., *Human Monocyte Subsets Are Transcriptionally and Functionally Altered in Aging in Response to Pattern Recognition Receptor Agonists*. *J Immunol*, 2017. **199**(4): p. 1405-1417.
61. Renshaw, M., et al., *Cutting edge: impaired Toll-like receptor expression and function in aging*. *J Immunol*, 2002. **169**(9): p. 4697-701.
62. Martin, G.E., et al., *Age-associated changes in monocyte and innate immune activation markers occur more rapidly in HIV infected women*. *PLoS One*, 2013. **8**(1): p. e55279.
63. Blas-Garcia, A., N. Apostolova, and J.V. Esplugues, *Oxidative stress and mitochondrial impairment after treatment with anti-HIV drugs: clinical implications*. *Curr Pharm Des*, 2011. **17**(36): p. 4076-86.
64. Lagathu, C., et al., *Some HIV antiretrovirals increase oxidative stress and alter chemokine, cytokine or adiponectin production in human adipocytes and macrophages*. *Antiviral therapy*, 2007. **12**(4): p. 489.
65. Smith, R.L., et al., *Premature and accelerated aging: HIV or HAART?* *Front Genet*, 2012. **3**: p. 328.
66. Torres, R.A. and W. Lewis, *Aging and HIV/AIDS: pathogenetic role of therapeutic side effects*. *Lab Invest*, 2014. **94**(2): p. 120-8.
67. Brechley, J.M., et al., *Microbial translocation is a cause of systemic immune activation in chronic HIV infection*. *Nat Med*, 2006. **12**(12): p. 1365-71.
68. Deeks, S.G., R. Tracy, and D.C. Douek, *Systemic effects of inflammation on health during chronic HIV infection*. *Immunity*, 2013. **39**(4): p. 633-45.
69. Justice, A.C., et al., *Does an index composed of clinical data reflect effects of inflammation, coagulation, and monocyte activation on mortality among those aging with HIV?* *Clin Infect Dis*, 2012. **54**(7): p. 984-94.

70. Desai, S. and A. Landay, *Early immune senescence in HIV disease*. Curr HIV/AIDS Rep, 2010. **7**(1): p. 4-10.
71. Bruunsgaard H, et al., *Predicting death from tumour necrosis factor-alpha and interleukin-6 in 80-year-old people*. Clin Exp Immunol., 2003. **132**: p. 24-31.
72. Bruunsgaard, H., M. Pedersen, and B.K. Pedersen, *Aging and proinflammatory cytokines*. Current Opinion in Hematology 2001. **8**: p. 131-136.
73. Puchta, A., et al., *TNF Drives Monocyte Dysfunction with Age and Results in Impaired Anti-pneumococcal Immunity*. PLoS Pathog, 2016. **12**(1): p. e1005368.
74. Sadeghia, H.M., et al., *Phenotypic and functional characteristics of circulating monocytes of elderly persons*. Experimental Gerontology, 1999. **34**.
75. Shaw, A.C., et al., *Dysregulation of human Toll-like receptor function in aging*. Ageing Res Rev, 2011. **10**(3): p. 346-53.
76. Miles, E.A., et al., *Age-related increases in circulating inflammatory markers in men are independent of BMI, blood pressure and blood lipid concentrations*. Atherosclerosis, 2008. **196**(1): p. 298-305.
77. Grants, J.M., et al., *Altered microRNA expression links IL6 and TNF-induced inflammaging with myeloid malignancy in humans and mice*. Blood, 2020. **135**(25): p. 2235-2251.
78. Rea, I.M., et al., *Age and Age-Related Diseases: Role of Inflammation Triggers and Cytokines*. Front Immunol, 2018. **9**: p. 586.
79. Tavenier, J., et al., *Alterations of monocyte NF-kappaB p65/RelA signaling in a cohort of older medical patients, age-matched controls, and healthy young adults*. Immun Ageing, 2020. **17**(1): p. 25.
80. Flores, R.R., et al., *Expansion of myeloid-derived suppressor cells with aging in the bone marrow of mice through a NF-kappaB-dependent mechanism*. Aging Cell, 2017. **16**(3): p. 480-487.
81. Salminen, A., K. Kaarniranta, and A. Kauppinen, *Immunosenescence: the potential role of myeloid-derived suppressor cells (MDSC) in age-related immune deficiency*. Cell Mol Life Sci, 2019. **76**(10): p. 1901-1918.
82. Ong, S.M., et al., *The pro-inflammatory phenotype of the human non-classical monocyte subset is attributed to senescence*. Cell Death Dis, 2018. **9**(3): p. 266.
83. Ritzel, R.M., et al., *Old age increases microglial senescence, exacerbates secondary neuroinflammation, and worsens neurological outcomes after acute traumatic brain injury in mice*. Neurobiol Aging, 2019. **77**: p. 194-206.

84. Hall, B.M., et al., *p16(Ink4a) and senescence-associated β -galactosidase can be induced in macrophages as part of a reversible response to physiological stimuli*. Aging (Albany NY), 2017. **9**(8): p. 1867-1884.
85. Xu, M., et al., *Senolytics improve physical function and increase lifespan in old age*. Nat Med, 2018. **24**(8): p. 1246-1256.
86. Bauer, M.E. and L. Fuente Mde, *The role of oxidative and inflammatory stress and persistent viral infections in immunosenescence*. Mech Ageing Dev, 2016. **158**: p. 27-37.
87. Batatinha, H.A.P., et al., *Regulation of autophagy as a therapy for immunosenescence-driven cancer and neurodegenerative diseases: The role of exercise*. J Cell Physiol, 2019.
88. Pence, B.D. and J.R. Yarbrow, *Aging impairs mitochondrial respiratory capacity in classical monocytes*. Exp Gerontol, 2018. **108**: p. 112-117.
89. Mansell, E., et al., *Mitochondrial Potentiation Ameliorates Age-Related Heterogeneity in Hematopoietic Stem Cell Function*. Cell Stem Cell, 2021. **28**(2): p. 241-256 e6.
90. Hulgan, T. and M. Gerschenson, *HIV and mitochondria: more than just drug toxicity*. J Infect Dis, 2012. **205**(12): p. 1769-71.
91. Hunt, M. and B.A.I. Payne, *Mitochondria and ageing with HIV*. Curr Opin HIV AIDS, 2020. **15**(2): p. 101-109.
92. Payne, B.A., et al., *Mitochondrial aging is accelerated by anti-retroviral therapy through the clonal expansion of mtDNA mutations*. Nat Genet, 2011. **43**(8): p. 806-10.
93. Saare, M., et al., *Monocytes present age-related changes in phospholipid concentration and decreased energy metabolism*. Aging Cell, 2020. **19**(4): p. e13127.
94. Cannizzo, E.S., et al., *Oxidative stress, inflamm-aging and immunosenescence*. J Proteomics, 2011. **74**(11): p. 2313-23.
95. Minhas, P.S., et al., *Restoring metabolism of myeloid cells reverses cognitive decline in ageing*. Nature, 2021. **590**(7844): p. 122-128.
96. Minhas, P.S., et al., *Macrophage de novo NAD(+) synthesis specifies immune function in aging and inflammation*. Nat Immunol, 2019. **20**(1): p. 50-63.
97. Ho, T.T., et al., *Autophagy maintains the metabolism and function of young and old stem cells*. Nature, 2017. **543**(7644): p. 205-210.

98. Rickabaugh, T.M., et al., *Acceleration of age-associated methylation patterns in HIV-1-infected adults*. PLoS One, 2015. **10**(3): p. e0119201.
99. Sehl, M.E., et al., *The Effects of Anti-retroviral Therapy on Epigenetic Age Acceleration Observed in HIV-1-infected Adults*. Pathog Immun, 2020. **5**(1): p. 291-311.
100. Esteban-Cantos, A., et al., *Longitudinal Changes in Epigenetic Age Acceleration in Aviremic Human Immunodeficiency Virus-Infected Recipients of Long-term Antiretroviral Treatment*. J Infect Dis, 2022. **225**(2): p. 287-294.
101. Esteban-Cantos, A., et al., *Epigenetic age acceleration changes 2 years after antiretroviral therapy initiation in adults with HIV: a substudy of the NEAT001/ANRS143 randomised trial*. Lancet HIV, 2021. **8**(4): p. e197-e205.
102. Spyridopoulos, I., et al., *Accelerated telomere shortening in leukocyte subpopulations of patients with coronary heart disease: role of cytomegalovirus seropositivity*. Circulation, 2009. **120**(14): p. 1364-72.
103. Alcaraz, M.a.J., et al., *Subclinical atherosclerosis and immune activation in young HIV- infected patients with telomere shortening*. Aging 2021. **13**(14): p. 18094-18105.
104. Srinivasa, S., et al., *Soluble CD163 is associated with shortened telomere length in HIV-infected patients*. J Acquir Immune Defic Syndr, 2014. **67**(4): p. 414-418.
105. Dalzini, A., et al., *Biological Aging and Immune Senescence in Children with Perinatally Acquired HIV*. J Immunol Res, 2020. **2020**: p. 8041616.

6.0 Discussion and Summary

6.1 Discussion

This thesis aimed to define the role of macrophage traffic from the CNS and its contribution to the spread of HIV and SIV to peripheral tissues. The central hypothesis of this thesis is that macrophage traffic from the CNS results in viral dissemination and recrudescence in peripheral tissues such as cervical lymph nodes, the spleen, cranial nerves, DRGs, and peripheral nerves. To investigate this hypothesis, we utilized a novel method to label CNS macrophages *in vivo*. We identified the migration of macrophages out of the CNS and evaluated the impact of ART and ART interruption on the traffic of virally infected macrophages to peripheral tissues. In this study we examined: i) whether macrophage traffic out of the CNS in non-infected (normal) non-human primates and the effects of SIV infection (Chapter 2), ii) the impact of AIDS, ART, and following ART interruption on traffic of virally infected macrophage out of the CNS (Chapter 3), and iii) explored a understudied pathway for CNS macrophage to traffic out and redistribute virus to the periphery with AIDS, on ART, and following ART interruption (Chapter 4).

Since the introduction of combination ART in 1996, there have been significant improvements in both the quality of life and lifespan of PLHIV, yet comorbidities such as HAND and HIV-SN remain prevalent [1-6]. In the ART era, HAND persists in over half of PLHIV on ART [7], with the most severe form (HAD) less prevalent, while less severe forms (MND and ANI) are more prevalent than pre-ART [7]. HIV-SN remains the most common neurologic disorder linked to HIV infection [8, 9]—caused by chronic innate immune activation—affecting over one-third of PLHIV on ART, even with viral load suppression and improved CD4+ T cell counts [8, 9]. With age being one of the primary

risk factors associated with HIV-SN, the growing population of older individuals with HIV is likely to face increasing rates of this condition. These HIV-associated comorbidities are a direct result of chronic immune activation driven by monocytes and macrophages. In this thesis, we briefly explored the aging population of PLHIV and the numerous health challenges they encounter due to chronic myeloid activation (Chapter 5). Importantly, many diseases and conditions typically associated with advanced age appear earlier in people with HIV, as their immune systems undergo accelerated aging, even though they are living longer than ever before [10]. With currently 50% of PLHIV over 50, this percentage is only expected to increase over the next 20 years [11, 12]. Understanding the role of macrophage traffic, CNS viral dissemination and recrudescence, and the role of chronic myeloid activation in PLHIV on ART is essential to addressing chronic neurocognitive disorders and neuropathy to bridge the health gap between PLHIV and the general population.

6.2 What immune cells can traffic out of the CNS?

In this thesis, we showed for the first time (Chapter 2) that macrophages can traffic out of the CNS normally in non-human primates and SIV-infected macaques; however, this is not the first evidence of immune cells trafficking out of the brain. Limited work performed in rodents has shown that myeloid-DCs migrate from the brain to cervical lymph nodes to trigger an immune response [13, 14]. Subsequent work has shown that DCs injected into the CSF migrate to the cervical lymph nodes while injection of DCs directly into the brain parenchyma remained confined to the brain [15, 16]. As we labeled all CNS macrophages *in vivo* with SPION, our study does not distinguish which

macrophages are leaving the CNS (perivascular or meningeal), but we hypothesize that perivascular macrophages must first migrate to the meninges to leave via meningeal lymphatics or perineural pathways, as perivascular pathways are too small for macrophages to leave the CNS [17]. In rodents, CD4⁺ T cells injected into a lesion site—even T cells injected into a non-lesioned parenchyma—migrate to the deep cervical lymph node via the cribriform plate and nasal mucosa [18]. Thus, regardless of the injection site, T cells can migrate through the cribriform plate and accumulate primarily in the dCLN, whereas only DCs in the CSF migrate out [18]. Even B cells injected into the CSF have been shown to migrate to the dCLN node via dural lymphatics [19]. Recent evidence using single-cell sequencing has implied that microglia-like cells are found in the CSF and may traffic out via dural lymphatics [20]; we did not study this as SPION are not taken up by microglia. In a spinal cord injury model, it has been suggested that microglia exit the spinal root to the periphery, where they clear debris at the injury site and then carry that debris back into the CNS [21]; however, there has been limited research on this topic. Building on previous rodent research, we were the first to demonstrate macrophage traffic out of the CNS in a non-human primate model (Chapter 2), to better understand the dynamics of macrophage traffic out of the CNS with AIDS, on ART, and following ART interruption (Chapter 3), and potential pathways of this migration out of the CNS (Chapter 4).

6.3 What evidence supports viral traffic out of the CNS?

In this study, for the first time, we have provided direct evidence that with AIDS, SIV-RNA⁺ CNS macrophage can traffic out to reseed virus in the dCLN and spleen

(Chapter 2) and cranial and peripheral nerves (Chapter 3), potentially resulting in viral recrudescence. Importantly, we found that ART eliminates the traffic of virally infected macrophages to the dCLN and spleen (Chapter 2) but does not eliminate the traffic of virally infected macrophages via cranial nerves (Chapter 3). This is in parallel with molecular work done by our lab (unpublished data) and others to demonstrate the reseeding of the CNS viral reservoir in the periphery [22, 23]. It is well known that CNS compartmentalization emerges within the first years after HIV infection and persists [24-26]. In addition, it has been eloquently demonstrated that macrophages in the brain harbor latent HIV and SIV capable of reactivation and possible infection of new cells [27, 28]. Using phylogenetic analysis, we identified significant differences in sequence diversity across peripheral tissues, meninges, and even within distinct brain regions [29]. Viral Env and Pol sequences from cortical brain regions showed significantly lower diversity than those in the meninges ($p < 0.05$) [29]. In turn, the meninges exhibited significantly lower diversity ($p < 0.001$) than the combined peripheral tissues and cell populations [29]. The lower diversity of viral Env and Pol sequences in cortical regions—compared to the meninges—suggests limited viral traffic to and from these cortical regions. However, the meninges exhibit higher diversity than the cortical tissues, indicating some degree of continual viral traffic, though less extensive than that observed in peripheral tissues. This suggests that while cortical areas are relatively isolated, the meninges have moderate viral exchange, likely an intermediate for viral dissemination with limited but notable viral migration relative to the periphery. Our findings in Chapter 3 show a rebound of SIV in the meninges following ART interruption, which is in agreement with previous work [29] and supports a viral rebound from the blood that

disseminates in the CNS meninges. Others have found and suggested that the choroid plexus is a distinct viral reservoir in the CNS, harboring viral strains that were a mixture of those found in the brain and spleen [30], suggestive of viral migration from the blood to the brain. In our study (Chapter 3), we also found persistence of SIV in the choroid plexus with ART and a rebound following ART interruption, further supporting viral dissemination in the CNS from the blood. An in-depth analysis of viral populations revealed that CSF viral escape stems from continuously replicating viral populations—likely macrophages—within the CNS over 3 years of ART [31]. This underscores the likelihood that infected cells continue to traffic between the CNS and other viral reservoirs, even with durable ART [25, 31]. Recently using barcoded virus, the Ling lab has found that mesentery lymph nodes, inaugural lymph nodes, and the spleen shared viral populations with plasma, suggesting these tissues may contribute to viral reactivation and rebound after ART interruption [32]. Although the authors only found low numbers of barcoded virus in the brain (and thus no similar clonal types detected in peripheral tissues), this does not rule out the possibility of viral migration from the brain to the periphery (and known vice versa phenomenon), especially considering these animals did not develop SIVE and only had a short period of ART interruption (3 weeks) [32].

In this study, we provide the first direct evidence in the context of AIDS that virally infected CNS macrophages migrate out and reseed peripheral tissues and remain persistent within cranial and peripheral nerves with ART (Chapters 2-4). Our findings demonstrate that while ART effectively stops the traffic of virally infected macrophages to the dCLN and spleen (Chapter 3), it does not prevent their migration via cranial nerves

(Chapter 4). Although we did not sequence the virus in our study to confirm its origin, our results align with molecular data from our lab (unpublished) and other studies that support the reseeding of the CNS viral reservoir in the periphery. This work strengthens our understanding of the interactions between the CNS and peripheral tissues in the contribution to viral persistence.

6.4 What is the effect of ART on CNS macrophage and rebound following ART Off?

In Chapter 3—and in agreement with our previous work [33, 34]—we found that with AIDS and SIVE, there is an increase in the number of CD163+ PVM in the brain and a significant decrease with ART. Importantly, we found that with ART interruption, there was a significant increase in CD163+ PVM compared to durable ART (Chapter 3). As CD163+ PVM are bone marrow-derived, this increase in CD163+ PVM in the brain correlated with an increase in the percent of newly produced monocytes in the blood (data not shown). In our study, animals began ART on day 21 post-infection, and all animals had over 10% of newly produced monocytes in the blood at this time (data not shown). We previously determined this timepoint (21 dpi) to be an accurate predictor of CNS disease severity, with these newly produced monocytes migrating to the brain, resulting in accumulation and inflammation if left untreated [35]. We propose that the resolution of inflammation in the brain could be a result of macrophage traffic out as animals on ART had increased numbers of macrophages that trafficked out of the CNS to the periphery, and fewer SPION-labeled PVM remained in the brain. As these animals were predisposed to develop CNS disease, this novel finding underscores the role of macrophage traffic out of the CNS and the resolution of CNS inflammation.

In our previous work using dextran dye, we found that SIVE lesions are composed primarily of macrophages present early in infection [34], supporting the early establishment of the CNS viral reservoir. Similarly, in this study, we found that SIV-RNA+ PVM were primarily labeled with early injected SPION, consistent with the early establishment of the CNS viral reservoir (Chapter 3). Interestingly, in Chapter 3, we found only a slight decrease in the number of CD163+ meningeal macrophages with ART compared to animals with AIDS and no change following ART interruption. We found with AIDS that SIV-RNA+ meningeal macrophages were primarily labeled with dual- and late-SPION, more so than early alone. Moreover, SPION+ SIV-RNA+ meningeal macrophages in animals on ART and following ART interruption only contained late-SPION, further supporting the rebound of SIV from the blood with chronic infection. With AIDS, we found that SIV-RNA+ macrophages trafficked out of the CNS to peripheral tissues primarily containing late-injected SPION, underscoring the role of macrophage traffic out of the CNS and viral dissemination during chronic infection. Importantly, we found that ART eliminated the traffic of SIV-RNA+ macrophages from the CNS to the dCLN, spleen, and DRG but did not eliminate the traffic of SIV-RNA+ macrophages to cranial nerves, primarily labeled with dual SPION. This suggests that these macrophages were in the CNS early during infection but did not traffic out to cranial nerves until late infection, further underscoring the role of viral dissemination during chronic infection, even with ART. Our study highlights the importance of better understanding the contribution of macrophage traffic out of the CNS in viral dissemination and the resolution of CNS inflammation.

6.5 What is the effect of CNS macrophage traffic on immune activation, tolerance, and pathogenesis?

Macrophage traffic out of the CNS may play a crucial role in immune activation, tolerance, and pathogenesis by bridging the CNS and the peripheral immune responses. When macrophages migrate from the CNS to peripheral tissues, they can present antigens—such as HIV and SIV—to other immune cells to stimulate local immune responses and drive immune activation. Rodent studies using antigen-loaded (ovalbumin, OVA) DCs injected into the CSF found traffic out to the dCLN to induce activation of CD8⁺ T cells with subsequent migration of Ag-specific T cells to the brain [13]. Surprisingly, intravenously injected GFP-labeled DCs did not trigger the accumulation of antigen-specific T cells in the brain [13]. This suggests that intravenous administration is ineffective at inducing an immune response within the brain, likely due to CNS entry barriers or differences in antigen presentation, highlighting the critical role of CSF and cellular traffic from the brain in activating CNS immune responses. The recruitment of T cells into the CNS occurs only when brain-derived DCs migrate to the peripheral lymphoid tissues, suggesting that migration of brain-resident DCs is absolutely necessary to initiate antigen-specific T cell homing to the CNS [13]. This is consistent with the initiation of immune responses in peripheral tissues where APCs capture, process, and present antigens via MHC molecules to naïve T cells in secondary lymphoid organs, triggering their activation, proliferation, and differentiation into effector T cells such as cytotoxic (CD8⁺) or helper (CD4⁺) T cells [14, 36]. Although the CNS is immune-privileged, engagement in immune surveillance and responses by traffic of CNS myeloid-DCs and macrophages out of the CNS results in T cell activation to HIV and SIV.

The migration of macrophages from the CNS to the periphery can also potentially induce disease and/or tolerance, as macrophages present antigens and modulate immune responses in peripheral tissues. A series of eloquent studies by Laman, Weller, and others have detailed the drainage of soluble antigens from the CNS to the dCLN [37-39]. Much of this drainage of soluble antigen out of the CNS is along the perivascular pathway through basement membranes of capillaries and arteries, a pathway too small for APCs to traffic out [40]. Importantly, the perivascular pathway has been described to drain amyloid-beta out of the brain which builds up in perivascular spaces of aging individuals with Alzheimer's disease (see *Alzheimer's disease* section for more details) [41, 42]. Within 15–20 hours of injecting serum albumin into the rabbit brain, it drains to the dCLN [43]. Likewise, when human serum albumin is injected into the rat brain or CSF, antibodies are produced in the CLNs and spleen [44-46]. Importantly, ablation of lymphatic drainage from the CNS to the CLNs fails to produce a humoral response [44-46]. Drainage of soluble antigens and/or traffic of antigen-loaded APCs suggests that the CLNs play a key role in initiating B cell and T cell-mediated immune responses to CNS antigens. A better understanding of the balance between immune activation and tolerance by macrophage traffic out of the CNS is crucial to understanding CNS disease pathogenesis, especially in chronic conditions like HIV and other neuroinflammatory disorders.

6.6 Can macrophage traffic out of the CNS play a role in neurodegenerative diseases such as HAND, HIV-SN, Multiple sclerosis, Alzheimer's disease, and normal aging?

Macrophage traffic out of the CNS could have important implications for HAND, HIV-SN, Multiple Sclerosis, Alzheimer's disease, and even the effects of normal aging [10, 47-51]. Understanding how macrophages traffic out of the CNS is crucial, as it could lead to new treatments that target their activation and movement, offering better ways to manage these diseases.

HAND

The term HAND encompasses the spectrum of neurocognitive impairments linked to HIV infection (HAD, MND, and ANI), with affected individuals often experiencing issues in executive function and memory [7, 52, 53]. This spectrum includes notable disruptions in attention, multitasking, impulse control, judgment, and memory and retrieval [7, 52, 53]. HAND can also involve motor impairments, such as bradykinesia, coordination loss, and gait instability [7, 52, 53]. While motor skill and psychomotor speed deficits were the primary HAND symptoms before ART, today, in the ART era, impairments in learning, memory, and executive function are more frequently observed [7, 52, 53]. The processes leading to neuronal injury as a result of HIV and SIV infection remain poorly understood; however, the presence of activated and productively infected macrophages in the CNS is the strongest correlate of neurocognitive decline and further supports the role of monocytes and macrophages in driving CNS pathogenesis [35, 54-56]. We have found that soluble CD163—produced by activated CD163+ monocytes and macrophages—correlates better with neurocognitive decline than traditional predictors

(CD4+ T cell count or viral load) [54, 55]. Additionally, increased production of bone marrow-derived monocytes with HIV and SIV infection is correlated with neuronal injury [35, 57]. Importantly, with HIV and SIV infection, there is an increased rate of the traffic of bone marrow-derived monocytes to the CNS and subsequent accumulation and retention [34, 58, 59], supported by our SPION studies (Chapters 2-4). Similar to previous discussions, we hypothesize that the resolution of inflammation is influenced by macrophage traffic out, and with AIDS and SIVE, there is a reduction of macrophage traffic out, resulting in an accumulation of CNS macrophages and subsequent neuronal damage. Our findings indicate that the resolution of CNS inflammation may be mediated by macrophage traffic out of the CNS. In conditions such as AIDS, SIVE, and potentially HAND, reduced traffic out of CNS macrophages leads to their accumulation within the CNS, exacerbating neuronal injury and contributing to neurocognitive decline.

HIV-SN

Macrophage accumulation in the DRG and peripheral nerves contributes to HIV-SN by promoting local inflammation and neuronal damage, exacerbating sensory dysfunction and pain [60, 61]. Importantly, it was found that macrophage accumulation in the DRG, but not at the injury site, was required to initiate the nerve-induced mechanical hypersensitivity [62]. In our study (Chapter 4), we found that CNS macrophages migrate to the DRGs normally and at a rate that is unchanged with AIDS, in animals on ART, and with ART interruption. We hypothesize that this macrophage migration from the CNS to the DRGs may contribute to HIV-SN. Following nerve injury, there is an influx of CCR2+ macrophages to the injury site, some of which result from

local proliferation [62] but also could result from macrophage traffic from the CNS. Previously, we observed that rhesus macaques infected with SIV had a significant increase of CD68+, CD163+, and MAC387+ macrophages in the DRG compared to non-infected macaques [61, 63, 64]. Recently, Burdo *et al.* found that substantial neuroinflammation persisted in the DRG and the dorsal horn of SIV-infected macaques, even while on ART [65]. The ongoing inflammation in these regions was associated with the sustained sensitization of nociceptors, which may account for the ongoing neuropathic pain experienced despite ART treatment [65]. Our results indicate that the persistent activation of myeloid cells in the DRG during ART might be due to the continuous migration of macrophages out of the CNS through the perineural pathway.

Multiple Sclerosis

Multiple Sclerosis (MS) is a chronic autoimmune disease where the immune system targets the protective myelin sheath covering nerve fibers in the CNS [50, 66]. This leads to inflammation, nerve damage, and symptoms such as muscle weakness, impaired coordination, vision problems, and fatigue [66]. Experimental autoimmune encephalomyelitis (EAE) is a common rodent model used to study MS pathogenesis with similar pathological features: CNS inflammation, demyelination, axonal loss, and gliosis [67]. When EAE is induced by injecting antigen (such as myelin basic protein or adoptive transfer of pathogenic, myelin-specific CD4 T cells) into the footpad of rats or mice, inflammation primarily affects the spinal cord, causing hind limb paralysis in about two weeks while the brain remains less affected, unlike in cyrolesion-induced EAE where the brain is primarily affected [50, 68, 69]. In rodent studies examining the traffic of DCs

from the CNS, it was found that DCs migrated to the CLNs and enhanced the response against myelin oligodendrocyte glycoprotein, a major immunogenic myelin antigen [15]. Ablation of CLNs in EAE animals reduces brain inflammation by up to 40% and likewise, the removal of lumbar lymph nodes reduces EAE symptoms in the spinal cord [68, 70]. Although the CNS is considered immunologically privileged, cervical and lumbar lymph nodes play a significant role in initiating immune responses in MS and EAE. Understanding the mechanisms underlying antigen drainage and APC traffic to these lymph nodes could improve therapeutic strategies for MS.

Alzheimer's disease

Alzheimer's disease (AD) is a neurodegenerative disorder, with the main pathological hallmark being the accumulation of amyloid-beta ($A\beta$) deposits in the brain [51, 71]. This results in cognitive decline, memory loss, confusion, and difficulty with daily tasks over time [51, 71]. AD is the leading cause of dementia, affecting an estimated 6 million Americans aged 65 and older [72]. In older adults, $A\beta$ is deposited as insoluble plaques in the brain and accumulates in the walls of cerebral arteries and capillaries [51]. $A\beta$ is cleared from the brain through several mechanisms, including degradation by neprilysin and insulin-degrading enzymes [73], absorption into the blood via the low-density lipoprotein receptor protein-1 pathway [74, 75] and P-glycoprotein [76], and elimination through the perivascular lymphatic drainage pathway [40, 42, 77]. Importantly, PVM play a major role in clearing vascular $A\beta$ deposited from the brain parenchyma [78]. Ablation of PVM in AD mice leads to worsened $A\beta$ plaque deposition, while increasing PVM turnover (with chitin) reduces plaque accumulation [79, 80].

Others found that the CCR2 is required for CNS homing of PVM and that this CNS homing is essential for brain A β removal [81]. In AD mice, nonspecific deletion of CCR2 led to increased accumulation of A β plaques, fewer microglia and macrophages around these plaques, worsened cognitive deficits, and a reduced lifespan [81-83]. The drainage of A β and its clearance by PVM are crucial for eliminating plaques and mitigating AD pathology; however, whether these macrophages in AD migrate from the CNS to the CLNs remains unknown but could potentially worsen disease.

Macrophage Traffic and Aging

Meningeal lymphatics are important for draining antigens and traffic of immune cells out of the CNS; however, recent studies have found that with age, these lymphatic vessels' efficiency declines, resulting in reduced clearance of waste and antigens from the CNS [84, 85]. This diminished drainage can lead to a buildup of neurotoxic substances, potentially worsening neurocognition, such as those seen in AD [84, 85]. Additionally, individuals living with HIV age faster than aged-matched non-infected individuals [10, 86-89], yet the impact of HIV on meningeal lymphatic function remains unknown. In our study, we found that with AIDS, there is an accumulation of SPION+ PVMs in the brain compared to animals treated with ART (Chapter 2). This accumulation of PVM with AIDS and SIVE could be a result of impaired meningeal lymphatic function to clear virally infected PVMs whereas with ART there is clearance from the parenchyma. Importantly, there is no difference in the number of SPION+ meningeal macrophages with AIDS compared to ART-treated animals, whereas in non-infected macaques, there is gradual clearance over time. This suggests impairment in clearance via meningeal

lymphatics with SIV infection that is not restored with ART. Further research is needed to understand how HIV (and SIV) affects the function of meningeal lymphatics, especially considering that individuals living with HIV experience accelerated aging, which is known to contribute to the impairment of these lymphatic vessels. The impaired function of meningeal lymphatics can restrict immune cell movement, hindering response to disease and inflammation in the brain and leading to accumulation [90-94].

Understanding how HIV and aging affect meningeal lymphatics could help develop treatments that improve lymphatic function and clear adverse pathogens and proteins in the brain with aging and neurodegenerative diseases.

6.7 Signals that could initiate or prevent macrophage traffic out of the CNS.

Chemokines and cytokines are signaling molecules that may regulate immune cell migration out of the CNS. CC-chemokine receptor 7 (CCR7)—expressed by various immune cells—is involved in the homing of various subpopulations of T cells and APCs to the lymph nodes, which highly express its ligands, C-C motif chemokine ligand 19 (CCL19) and C-C motif chemokine ligand 21 (CCL21) [95]. Louveau and Herz *et al.* found that the loss of CCR7 significantly impaired T cells and DCs' ability to migrate to both the dural lymphatics and the dCLN [94]. Others have also shown that sphingosine-1-phosphate receptor (S1PR) is required for the egress of DCs from the brain [96]. The process by which monocytes and macrophages reach the CLNs from the CNS and the receptors they use are not fully understood, though they may rely on a CCR7-mediated mechanism similar to T cells and DCs. A recent study on nasal inflammation showed that antigen-loaded monocytes lacking CCR7 can use the C-C motif chemokine receptor 5

(CCR5)- C-C motif chemokine ligand 5(CCL5) signaling pathway to reach lymph nodes [97]. The authors found that a CCL5 gradient from CCR7+ migratory DCs guides CCR5+ monocytes through the lymphatic system [97]. It's unclear whether this pathway also plays a role in monocyte/macrophage trafficking out of the CNS and meninges, but if so, it could be a mechanism used to enhance antigen clearance from the CNS [97]. Investigating the molecular signals that regulate the clearance of CNS immune cells—such as monocytes and macrophages—and their interactions in initiating antigen-specific responses is crucial for better understanding CNS disease pathogenesis.

6.8 How to target macrophage activation and traffic out of the CNS?

Despite the use of ART, HIV-SN and HAND remain prevalent due to chronic immune activation. Our lab has found that monocyte activation and increased monocyte production are better predictors of neurocognitive disorders than CD4+ T cell count or viral load [35, 54, 55, 98]. This underscores the need for therapies that specifically target the activation and traffic of monocytes and macrophages. By reducing chronic activation, it may be possible to reduce the neuroinflammation associated with HAND and HIV-SN. While ART is essential for managing viral loads, the underlying causes of chronic inflammation needs to be addressed through therapies aimed at monocyte and macrophage activation could improve cognitive function, pain relief, and an overall better quality of life for PLHIV.

Monocyte and macrophage activation drives inflammation, thus therapies to target myeloid activation, in conjunction with ART, may aid in reducing inflammation in the CNS and peripheral nerves. Using an oral form of the polyamine biosynthesis inhibitor

methylglyoxal-bis-guanylhydrazone (MGBG) alone, we have reduced the percentage of monocyte turnover and prevented the development of SIVE (unpublished data). MGBG, in conjunction with ART, reduced the percentage of monocyte turnover, reduced monocyte activation, and macrophage accumulation in the CNS, but there is no additive effect (unpublished data). Importantly, despite treatment interruption, the number of SIV-RNA⁺ cells in the brain was reduced with MGBG in conjunction with ART compared to the interruption of ART alone (unpublished data). MGBG treatment significantly reduced histopathological damage in the DRG and lowered the number of CD68⁺ and CD163⁺ macrophages [64], essential to reducing neuropathic pain [62, 99]. Additionally, MGBG significantly decreased the number of newly trafficked BrdU⁺ cells in the DRG [64]. However, despite the reduced DRG pathology, intraepidermal nerve fiber density did not recover following MGBG treatment [64]. When combined with ART, MGBG's ability to limit macrophage infiltration and reduce DRG inflammation may help lower the incidence of HIV-SN, although further research is needed.

Bone marrow-derived monocytes traffic to the CNS normally and at an increased rate with viral infection and inflammation [1, 4, 48]. Targeting monocyte and macrophage traffic to the CNS could not only prevent the establishment of the CNS viral reservoir but also reduce inflammation in the CNS. An anti- α 4 β 1 antibody (natalizumab) can be used to block the trafficking of lymphocytes to the CNS by preventing interaction with its ligand, vascular cell adhesion molecule-1 (VCAM-1), which is expressed on the endothelial cells of the BBB [100]. We have previously used an anti-A4B1 antibody at the time of infection to block the traffic of monocytes and macrophages to the CNS, prevent the establishment of the CNS viral reservoir, and reduce neurological injury

[101]. Additionally, we have highlighted the role of monocyte traffic and activation in HIV-SN, as histopathology showed that natalizumab treatment reduced DRG inflammation and pathology, including fewer BrdU+, MAC387+, CD68+, and SIVp28+ macrophages, while CD3+ T lymphocyte numbers remained unchanged and VCAM-1 levels were decreased [63]. These data indicate that blocking monocyte—but not T cell—traffic to the DRG is key to reducing inflammation [63]. Regarding the traffic of SPION+ macrophages, we find large numbers of SPION+ macrophages in the choroid plexus (Chapter 3), but the origin is not well known whether the traffic of SPION+ macrophages is from the CSF, diffusion of SPIONs across the epithelium, or recirculation of SPION+ macrophages. As the A4 integrin is expressed on both sides of the choroid plexus, treatment with anti- $\alpha 4\beta 1$ antibody would prevent cellular traffic via both sides of the choroid plexus to elude how macrophages became labeled with SPIONs and implications for recirculation of monocytes/macrophages to the CNS.

Fingolimod is an FDA-approved drug for MS that prevents the egress of immune cells from lymphoid tissues by downregulating the sphingosine-1 phosphate receptor (S1PR) [102, 103]. S1PR and its ligand, S1P, modulate immune cells in circulation by controlling the exit of immune cells from lymphoid tissue. S1PR is expressed on all immune cells, including T cells, macrophages and monocytes, and DCs. It has been demonstrated that roughly 77% of MS patients using Fingolimod had reduced relapses, and over 90% did not experience disability progression [104]. Other studies have found that with Fingolimod there are reduced brain lesions and reduced brain atrophy in MS patients [105] indicating a direct role for immunomodulation and development of CNS disease. It has also been shown that DCs rely on S1PR to migrate from the CNS to CLNs

[96]. In a mouse model of EAE, administering Fingolimod into the ventricles led to the buildup of CD11c⁺ cells in the olfactory bulbs near the cribriform plate, which impaired drainage to the CLNs [96]. Similarly, when DCs were treated with Fingolimod before being injected into the brain, their migration to the CLNs was reduced [96]. As S1PR is involved with DC migration from the CNS to CLNs, we propose that blocking S1PR signaling could also inhibit the traffic of monocytes and macrophages out of the CNS in HIV infection, potentially reducing peripheral immune activation, similar to what has been observed in models of EAE and MS.

Despite ART, chronic immune activation persists, contributing to HAND and HIV-SN. We have demonstrated that monocyte activation and production are stronger predictors of neurocognitive decline than traditional markers, highlighting the need for therapies targeting monocyte and macrophage activation and traffic. Specifically, the polyamine inhibitor MGBG, in combination with ART, reduced monocyte turnover, CNS macrophage accumulation, and DRG inflammation, lowering neuropathy indicators in SIV models (unpublished). Additionally, therapies like the anti- $\alpha 4\beta 1$ and Fingolimod show promise by limiting macrophage trafficking into the CNS, blocking monocyte migration, and reducing inflammation. This suggests that targeting CNS macrophage and monocyte activation and traffic could improve HAND symptoms, reduce HIV-SN, and prevent CNS viral reservoir reseeding and dissemination, though further research is needed.

6.9 Summary

This thesis examines the persistence of macrophage viral reservoirs in the CNS and how infected macrophages contribute to viral recrudescence and dissemination by migrating from the CNS to peripheral tissues, even with durable ART. Using a novel *in vivo* labeling method, we studied and tracked CNS macrophages and found that, under normal conditions, macrophages migrate to the dCLN, but during SIV infection, they accumulate in the CNS, and virally infected macrophages migrate out, contributing to inflammation. With ART, there was increased traffic of CNS macrophages out to the periphery, resulting in the resolution of CNS inflammation. ART was shown to clear infected perivascular macrophages and virally infected macrophages that traffic out to the dCLN and spleen but not meningeal and choroid plexus macrophages. Following ART interruption, virus rebounded in meningeal and choroid plexus macrophages, plasma, and the spleen, supporting viral rebound from the blood. The thesis also identified an understudied pathway for infected macrophages to exit the CNS via cranial and spinal nerves with AIDS and SIVE that persists despite ART. Additionally, we explored how HIV and ART influence accelerated aging and contribute to neurocognitive disorders. Overall, our findings highlight that CNS macrophages play a critical role in viral persistence, dissemination, and resolution of inflammation in the CNS by trafficking out to peripheral tissues.

6.10 References

1. Burdo, T.H., A. Lackner, and K.C. Williams, *Monocyte/macrophages and their role in HIV neuropathogenesis*. Immunol Rev, 2013. **254**(1): p. 102-13.
2. Campbell, J.H., et al., *The importance of monocytes and macrophages in HIV pathogenesis, treatment, and cure*. AIDS, 2014. **28**(15): p. 2175-87.
3. Ding, A., et al., *Galectin-3, galectin-9, and IL-18 are associated with monocyte activation and turnover more so than SIV-associated cardiac pathology or encephalitis*. AIDS Res Hum Retroviruses, 2024.
4. Kim, W.K., X. Alvarez, and K. Williams, *The role of monocytes and perivascular macrophages in HIV and SIV neuropathogenesis: information from non-human primate models*. Neurotox Res, 2005. **8**(1-2): p. 107-15.
5. Williams, K.C. and W.F. Hickey, *Central nervous system damage, monocytes and macrophages, and neurological disorders in AIDS*. Annu Rev Neurosci, 2002. **25**: p. 537-62.
6. White, K.S., et al., *Simian immunodeficiency virus-infected rhesus macaques with AIDS co-develop cardiovascular pathology and encephalitis*. Front Immunol, 2023. **14**: p. 1240946.
7. Saylor, D., et al., *HIV-associated neurocognitive disorder — pathogenesis and prospects for treatment*. Nature Reviews Neurology, 2016. **12**(4): p. 234-248.
8. Gabbai, A.A., A. Castelo, and A.S. Oliveira, *HIV peripheral neuropathy*. Handb Clin Neurol, 2013. **115**: p. 515-29.
9. Keswani, S.C., et al., *HIV-associated sensory neuropathies*. AIDS, 2002. **16**(16): p. 2105-2117.
10. Wallis, Z.K. and K.C. Williams, *Monocytes in HIV and SIV Infection and Aging: Implications for Inflamm-Aging and Accelerated Aging*. Viruses, 2022. **14**(2): p. 409.
11. CDC. *Diagnoses of HIV infection in the United States and dependent areas, 2018 (updated)*. HIV Surveillance Report 2020;31 2020 [cited 2021; Available from: <https://www.cdc.gov/hiv/group/age/olderamericans/index.html>].
12. CDC. *Estimated HIV incidence and prevalence in the United States, 2014–2018* HIV Surveillance Supplemental Report 2020;25 2020 [cited 2021; Available from: <https://www.cdc.gov/hiv/pdf/library/reports/surveillance/cdc-hiv-surveillance-supplemental-report-vol-25-1.pdf>].

13. Karman, J., et al., *Initiation of immune responses in brain is promoted by local dendritic cells*. J Immunol, 2004. **173**(4): p. 2353-61.
14. Carson, M.J., et al., *Disproportionate recruitment of CD8+ T cells into the central nervous system by professional antigen-presenting cells*. Am J Pathol, 1999. **154**(2): p. 481-94.
15. Hatterer, E., et al., *Cerebrospinal fluid dendritic cells infiltrate the brain parenchyma and target the cervical lymph nodes under neuroinflammatory conditions*. PLoS One, 2008. **3**(10): p. e3321.
16. Hatterer, E., et al., *How to drain without lymphatics? Dendritic cells migrate from the cerebrospinal fluid to the B-cell follicles of cervical lymph nodes*. Blood, 2006. **107**(2): p. 806-12.
17. Iliff, J.J., et al., *A paravascular pathway facilitates CSF flow through the brain parenchyma and the clearance of interstitial solutes, including amyloid β* . Sci Transl Med, 2012. **4**(147): p. 147ra111.
18. Goldmann, J., et al., *T cells traffic from brain to cervical lymph nodes via the cribriform plate and the nasal mucosa*. J Leukoc Biol, 2006. **80**(4): p. 797-801.
19. Brioschi, S., et al., *Heterogeneity of meningeal B cells reveals a lymphopoietic niche at the CNS borders*. Science, 2021. **373**(6553).
20. Farhadian, S.F., et al., *Single-cell RNA sequencing reveals microglia-like cells in cerebrospinal fluid during virologically suppressed HIV*. JCI Insight, 2018. **3**(18).
21. Green, L.A., J.C. Nebiolo, and C.J. Smith, *Microglia exit the CNS in spinal root avulsion*. PLoS Biol, 2019. **17**(2): p. e3000159.
22. Salemi, M., et al., *Phylogenetic analysis of human immunodeficiency virus type 1 in distinct brain compartments provides a model for the neuropathogenesis of AIDS*. J Virol, 2005. **79**(17): p. 11343-52.
23. Lamers, S.L., et al., *HIV-1 phylogenetic analysis shows HIV-1 transits through the meninges to brain and peripheral tissues*. Infect Genet Evol, 2011. **11**(1): p. 31-7.
24. Schnell, G., et al., *Compartmentalization and clonal amplification of HIV-1 variants in the cerebrospinal fluid during primary infection*. J Virol, 2010. **84**(5): p. 2395-407.
25. Bednar, M.M., et al., *Compartmentalization, Viral Evolution, and Viral Latency of HIV in the CNS*. Curr HIV/AIDS Rep, 2015. **12**(2): p. 262-71.

26. Chan, P. and S. Spudich, *HIV Compartmentalization in the CNS and Its Impact in Treatment Outcomes and Cure Strategies*. Curr HIV/AIDS Rep, 2022. **19**(3): p. 207-216.
27. Abreu, C., et al., *Brain macrophages harbor latent, infectious simian immunodeficiency virus*. Aids, 2019. **33 Suppl 2**(Suppl 2): p. S181-s188.
28. Avalos, C.R., et al., *Quantitation of Productively Infected Monocytes and Macrophages of Simian Immunodeficiency Virus-Infected Macaques*. Journal of virology, 2016. **90**(12): p. 5643-5656.
29. Rife, B.D., et al., *Evolution of Neuroadaptation in the Periphery and Purifying Selection in the Brain Contribute to Compartmentalization of Simian Immunodeficiency Virus (SIV) in the Brains of Rhesus Macaques with SIV-Associated Encephalitis*. J Virol, 2016. **90**(13): p. 6112-6126.
30. Chen, H., C. Wood, and C.K. Petito, *Comparisons of HIV-1 viral sequences in brain, choroid plexus and spleen: potential role of choroid plexus in the pathogenesis of HIV encephalitis*. J Neurovirol, 2000. **6**(6): p. 498-506.
31. Joseph, S.B., et al., *Human Immunodeficiency Virus Type 1 RNA Detected in the Central Nervous System (CNS) After Years of Suppressive Antiretroviral Therapy Can Originate from a Replicating CNS Reservoir or Clonally Expanded Cells*. Clin Infect Dis, 2019. **69**(8): p. 1345-1352.
32. Solis-Leal, A., et al., *Lymphoid tissues contribute to plasma viral clonotypes early after antiretroviral therapy interruption in SIV-infected rhesus macaques*. Sci Transl Med, 2023. **15**(726): p. eadi9867.
33. Soulas, C., et al., *Recently infiltrating MAC387(+) monocytes/macrophages a third macrophage population involved in SIV and HIV encephalitic lesion formation*. Am J Pathol, 2011. **178**(5): p. 2121-35.
34. Nowlin, B.T., et al., *SIV encephalitis lesions are composed of CD163(+) macrophages present in the central nervous system during early SIV infection and SIV-positive macrophages recruited terminally with AIDS*. Am J Pathol, 2015. **185**(6): p. 1649-65.
35. Burdo, T.H., et al., *Increased monocyte turnover from bone marrow correlates with severity of SIV encephalitis and CD163 levels in plasma*. PLoS Pathog, 2010. **6**(4): p. e1000842.
36. Murphy, K., et al., *Janeway's immunobiology*. Tenth edition. / Kenneth Murphy, Casey Weaver, Leslie J. Berg. ed. Immunobiology. 2022, New York: W.W. Norton and Company.

37. de Vos, A.F., et al., *Transfer of central nervous system autoantigens and presentation in secondary lymphoid organs*. J Immunol, 2002. **169**(10): p. 5415-23.
38. Laman, J.D. and R.O. Weller, *Drainage of cells and soluble antigen from the CNS to regional lymph nodes*. J Neuroimmune Pharmacol, 2013. **8**(4): p. 840-56.
39. van Zwam, M., et al., *Brain antigens in functionally distinct antigen-presenting cell populations in cervical lymph nodes in MS and EAE*. J Mol Med (Berl), 2009. **87**(3): p. 273-86.
40. Carare, R.O., et al., *Solutes, but not cells, drain from the brain parenchyma along basement membranes of capillaries and arteries: significance for cerebral amyloid angiopathy and neuroimmunology*. Neuropathol Appl Neurobiol, 2008. **34**(2): p. 131-44.
41. Preston, S.D., et al., *Capillary and arterial cerebral amyloid angiopathy in Alzheimer's disease: defining the perivascular route for the elimination of amyloid beta from the human brain*. Neuropathol Appl Neurobiol, 2003. **29**(2): p. 106-17.
42. Weller, R.O., et al., *Lymphatic drainage of the brain and the pathophysiology of neurological disease*. Acta Neuropathol, 2009. **117**(1): p. 1-14.
43. Yamada, S., et al., *Albumin outflow into deep cervical lymph from different regions of rabbit brain*. Am J Physiol, 1991. **261**(4 Pt 2): p. H1197-204.
44. Cserr, H.F., C.J. Harling-Berg, and P.M. Knopf, *Drainage of brain extracellular fluid into blood and deep cervical lymph and its immunological significance*. Brain Pathol, 1992. **2**(4): p. 269-76.
45. Cserr, H.F. and P.M. Knopf, *Cervical lymphatics, the blood-brain barrier and the immunoreactivity of the brain: a new view*. Immunol Today, 1992. **13**(12): p. 507-12.
46. Harling-Berg, C., et al., *Role of cervical lymph nodes in the systemic humoral immune response to human serum albumin microinfused into rat cerebrospinal fluid*. J Neuroimmunol, 1989. **25**(2-3): p. 185-93.
47. Kim, W.K., et al., *Monocyte/macrophage traffic in HIV and SIV encephalitis*. J Leukoc Biol, 2003. **74**(5): p. 650-6.
48. Fischer-Smith, T., et al., *Monocyte/macrophage trafficking in acquired immunodeficiency syndrome encephalitis: lessons from human and nonhuman primate studies*. J Neurovirol, 2008. **14**(4): p. 318-26.
49. Lamers, S.L., et al., *The meningeal lymphatic system: a route for HIV brain migration?* J Neurovirol, 2016. **22**(3): p. 275-81.

50. Lassmann, H., *Models of multiple sclerosis: new insights into pathophysiology and repair*. *Curr Opin Neurol*, 2008. **21**(3): p. 242-7.
51. Murphy, M.P. and H. LeVine, 3rd, *Alzheimer's disease and the amyloid-beta peptide*. *J Alzheimers Dis*, 2010. **19**(1): p. 311-23.
52. Letendre, S., *Central nervous system complications in HIV disease: HIV-associated neurocognitive disorder*. *Top Antivir Med*, 2011. **19**(4): p. 137-42.
53. Heaton, R.K., et al., *HIV-associated neurocognitive disorders before and during the era of combination antiretroviral therapy: differences in rates, nature, and predictors*. *J Neurovirol*, 2011. **17**(1): p. 3-16.
54. Burdo, T.H., et al., *Soluble CD163 made by monocyte/macrophages is a novel marker of HIV activity in early and chronic infection prior to and after anti-retroviral therapy*. *J Infect Dis*, 2011. **204**(1): p. 154-63.
55. Burdo, T.H., et al., *Elevated sCD163 in plasma but not cerebrospinal fluid is a marker of neurocognitive impairment in HIV infection*. *AIDS*, 2013. **27**(9): p. 1387-95.
56. Campbell, J.H., et al., *Minocycline Inhibition of Monocyte Activation Correlates with Neuronal Protection in SIV NeuroAIDS*. *PLOS ONE*, 2011. **6**(4): p. e18688.
57. Soulas, C., et al., *Genetically modified CD34+ hematopoietic stem cells contribute to turnover of brain perivascular macrophages in long-term repopulated primates*. *Am J Pathol*, 2009. **174**(5): p. 1808-17.
58. Lane, J.H., et al., *Neuroinvasion by simian immunodeficiency virus coincides with increased numbers of perivascular macrophages/microglia and intrathecal immune activation*. *J Neurovirol*, 1996. **2**(6): p. 423-32.
59. Crowe, S., T. Zhu, and W.A. Muller, *The contribution of monocyte infection and trafficking to viral persistence, and maintenance of the viral reservoir in HIV infection*. *J Leukoc Biol*, 2003. **74**(5): p. 635-41.
60. Aziz-Donnelly, A. and T.B. Harrison, *Update of HIV-Associated Sensory Neuropathies*. *Curr Treat Options Neurol*, 2017. **19**(10): p. 36.
61. Burdo, T.H., et al., *Dorsal root ganglia damage in SIV-infected rhesus macaques: an animal model of HIV-induced sensory neuropathy*. *Am J Pathol*, 2012. **180**(4): p. 1362-9.
62. Yu, X., et al., *Dorsal root ganglion macrophages contribute to both the initiation and persistence of neuropathic pain*. *Nature Communications*, 2020. **11**(1): p. 264.

63. Lakritz, J.R., et al., *alpha4-Integrin Antibody Treatment Blocks Monocyte/Macrophage Traffic to, Vascular Cell Adhesion Molecule-1 Expression in, and Pathology of the Dorsal Root Ganglia in an SIV Macaque Model of HIV-Peripheral Neuropathy*. Am J Pathol, 2016. **186**(7): p. 1754-1761.
64. Lakritz, J.R., et al., *An oral form of methylglyoxal-bis-guanylhydrazone reduces monocyte activation and traffic to the dorsal root ganglia in a primate model of HIV-peripheral neuropathy*. J Neurovirol, 2017. **23**(4): p. 568-576.
65. Warfield, R., et al., *Neuroinflammation in the Dorsal Root Ganglia and Dorsal Horn Contributes to Persistence of Nociceptor Sensitization in SIV-Infected Antiretroviral Therapy-Treated Macaques*. The American Journal of Pathology, 2023. **193**(12): p. 2017-2030.
66. Lassmann, H., J. van Horssen, and D. Mahad, *Progressive multiple sclerosis: pathology and pathogenesis*. Nat Rev Neurol, 2012. **8**(11): p. 647-56.
67. Constantinescu, C.S., et al., *Experimental autoimmune encephalomyelitis (EAE) as a model for multiple sclerosis (MS)*. Br J Pharmacol, 2011. **164**(4): p. 1079-106.
68. Phillips, M.J., M. Needham, and R.O. Weller, *Role of cervical lymph nodes in autoimmune encephalomyelitis in the Lewis rat*. J Pathol, 1997. **182**(4): p. 457-64.
69. Phillips, M.J., et al., *Focal brain damage enhances experimental allergic encephalomyelitis in brain and spinal cord*. Neuropathol Appl Neurobiol, 1995. **21**(3): p. 189-200.
70. van Zwam, M., et al., *Surgical excision of CNS-draining lymph nodes reduces relapse severity in chronic-relapsing experimental autoimmune encephalomyelitis*. J Pathol, 2009. **217**(4): p. 543-51.
71. Selkoe, D.J., *Alzheimer's disease: genes, proteins, and therapy*. Physiol Rev, 2001. **81**(2): p. 741-66.
72. *Alzheimer's Disease Fact Sheet*. [Web] 2023 October 2024]; Available from: <https://www.nia.nih.gov/health/alzheimers-and-dementia/alzheimers-disease-fact-sheet#:~:text=Estimates%20vary%2C%20but%20experts%20suggest,of%20dementia%20among%20older%20adults>.
73. Miners, J.S., et al., *SYMPOSIUM: Clearance of A β from the Brain in Alzheimer's Disease: A β -Degrading Enzymes in Alzheimer's Disease*. Brain Pathology, 2008. **18**(2): p. 240-252.
74. Bell, R.D., et al., *Transport pathways for clearance of human Alzheimer's amyloid beta-peptide and apolipoproteins E and J in the mouse central nervous system*. J Cereb Blood Flow Metab, 2007. **27**(5): p. 909-18.

75. Shibata, M., et al., *Clearance of Alzheimer's amyloid-ss(1-40) peptide from brain by LDL receptor-related protein-1 at the blood-brain barrier*. J Clin Invest, 2000. **106**(12): p. 1489-99.
76. Cirrito, J.R., et al., *P-glycoprotein deficiency at the blood-brain barrier increases amyloid-beta deposition in an Alzheimer disease mouse model*. J Clin Invest, 2005. **115**(11): p. 3285-90.
77. Weller, R.O., et al., *Cerebral amyloid angiopathy: amyloid beta accumulates in putative interstitial fluid drainage pathways in Alzheimer's disease*. Am J Pathol, 1998. **153**(3): p. 725-33.
78. Lai, A.Y. and J. McLaurin, *Clearance of amyloid- β peptides by microglia and macrophages: the issue of what, when and where*. Future Neurol, 2012. **7**(2): p. 165-176.
79. Hawkes, C.A. and J. McLaurin, *Selective targeting of perivascular macrophages for clearance of beta-amyloid in cerebral amyloid angiopathy*. Proc Natl Acad Sci U S A, 2009. **106**(4): p. 1261-6.
80. Yokoyama, M., et al., *Mouse Models of Alzheimer's Disease*. Front Mol Neurosci, 2022. **15**: p. 912995.
81. Mildner, A., et al., *Distinct and non-redundant roles of microglia and myeloid subsets in mouse models of Alzheimer's disease*. J Neurosci, 2011. **31**(31): p. 11159-71.
82. El Khoury, J., et al., *Ccr2 deficiency impairs microglial accumulation and accelerates progression of Alzheimer-like disease*. Nat Med, 2007. **13**(4): p. 432-8.
83. Naert, G. and S. Rivest, *CC chemokine receptor 2 deficiency aggravates cognitive impairments and amyloid pathology in a transgenic mouse model of Alzheimer's disease*. J Neurosci, 2011. **31**(16): p. 6208-20.
84. Da Mesquita, S., et al., *Ageing-associated deficit in CCR7 is linked to worsened glymphatic function, cognition, neuroinflammation, and β -amyloid pathology*. Sci Adv, 2021. **7**(21).
85. Da Mesquita, S., et al., *Functional aspects of meningeal lymphatics in ageing and Alzheimer's disease*. Nature, 2018. **560**(7717): p. 185-191.
86. Dalzini, A., et al., *Biological Aging and Immune Senescence in Children with Perinatally Acquired HIV*. J Immunol Res, 2020. **2020**: p. 8041616.
87. Smith, R.L., et al., *Premature and accelerated aging: HIV or HAART?* Front Genet, 2012. **3**: p. 328.

88. Torres, R.A. and W. Lewis, *Aging and HIV/AIDS: pathogenetic role of therapeutic side effects*. Lab Invest, 2014. **94**(2): p. 120-8.
89. Zanni, M.V., et al., *Effects of Antiretroviral Therapy on Immune Function and Arterial Inflammation in Treatment-Naive Patients With Human Immunodeficiency Virus Infection*. JAMA Cardiol, 2016. **1**(4): p. 474-80.
90. Bolte, A.C., et al., *Meningeal lymphatic dysfunction exacerbates traumatic brain injury pathogenesis*. Nat Commun, 2020. **11**(1): p. 4524.
91. Frederick, N. and A. Louveau, *Meningeal lymphatics, immunity and neuroinflammation*. Curr Opin Neurobiol, 2020. **62**: p. 41-47.
92. Hsu, M., et al., *Neuroinflammation creates an immune regulatory niche at the meningeal lymphatic vasculature near the cribriform plate*. Nat Immunol, 2022. **23**(4): p. 581-593.
93. Louveau, A., S. Da Mesquita, and J. Kipnis, *Lymphatics in Neurological Disorders: A Neuro-Lympho-Vascular Component of Multiple Sclerosis and Alzheimer's Disease?* Neuron, 2016. **91**(5): p. 957-973.
94. Louveau, A., et al., *CNS lymphatic drainage and neuroinflammation are regulated by meningeal lymphatic vasculature*. Nat Neurosci, 2018. **21**(10): p. 1380-1391.
95. Förster, R., A.C. Davalos-Misslitz, and A. Rot, *CCR7 and its ligands: balancing immunity and tolerance*. Nature Reviews Immunology, 2008. **8**(5): p. 362-371.
96. Mohammad, M.G., et al., *Immune cell trafficking from the brain maintains CNS immune tolerance*. J Clin Invest, 2014. **124**(3): p. 1228-41.
97. Rawat, K., et al., *CCL5-producing migratory dendritic cells guide CCR5+ monocytes into the draining lymph nodes*. J Exp Med, 2023. **220**(6).
98. Burdo, T.H., et al., *Soluble CD163, a novel marker of activated macrophages, is elevated and associated with noncalcified coronary plaque in HIV-infected patients*. J Infect Dis, 2011. **204**(8): p. 1227-36.
99. Laast, V.A., et al., *Macrophage-mediated dorsal root ganglion damage precedes altered nerve conduction in SIV-infected macaques*. Am J Pathol, 2011. **179**(5): p. 2337-45.
100. Baker, D.E., *Natalizumab: overview of its pharmacology and safety*. Rev Gastroenterol Disord, 2007. **7**(1): p. 38-46.
101. Campbell, J.H., et al., *Anti-alpha4 antibody treatment blocks virus traffic to the brain and gut early, and stabilizes CNS injury late in infection*. PLoS Pathog, 2014. **10**(12): p. e1004533.

102. Rommer, P.S., et al., *Immunological Aspects of Approved MS Therapeutics*. *Frontiers in Immunology*, 2019. **10**.
103. Chiba, K., *FTY720, a new class of immunomodulator, inhibits lymphocyte egress from secondary lymphoid tissues and thymus by agonistic activity at sphingosine 1-phosphate receptors*. *Pharmacol Ther*, 2005. **108**(3): p. 308-19.
104. Zecca, C., et al., *Real-life long-term effectiveness of fingolimod in Swiss patients with relapsing-remitting multiple sclerosis*. *Eur J Neurol*, 2018. **25**(5): p. 762-767.
105. Kappos, L., et al., *A placebo-controlled trial of oral fingolimod in relapsing multiple sclerosis*. *N Engl J Med*, 2010. **362**(5): p. 387-401.